

Dynamic technique analysis of the female equestrian rider

Céleste A. Wilkins

Thesis submitted in partial fulfilment of the requirements of the
University of the West of England for the degree of Doctor of Philosophy

Faculty of Health and Applied Sciences/Hartpury University

June 2021

Abstract

INTRODUCTION Advances in both measurement and analysis techniques offer the opportunity to assess the dynamics of the rider's position in the saddle. As previous studies have used discrete measures to summarise the kinematics of the rider over the movement cycle or compared riders grouped by their experience level, many questions remain on the characteristics of the rider's dynamic technique and the influence of dressage competition level. This thesis aimed to examine the competitive dressage rider's pelvis, progressing from its static posture to analyses of the dynamic pelvic technique, and the rider's coordination in a controlled environment using a riding simulator.

METHODS Fifty-two nationally or internationally competitive female dressage riders volunteered and were measured by motion capture in simulated walk, trot, and canter, using a riding simulator and optical motion capture. Simulator-rider coordination was measured using the continuous relative phase (CRP) and CRP variability. The effect of rider competition level on CRP variability was assessed using statistical parametric mapping. The characteristics of simulator-pelvis harmony were analysed using principal component analysis (PCA) on the CRP. Finally, riders were grouped by their trunk and pelvis coordination strategies using a self-organising map (SOM) and *k*-means clustering.

RESULTS There were no significant correlations between static and dynamic pelvic tilt. Simulator-pelvis coordination was significantly less variable than simulator-trunk, simulator-left foot or simulator-head in medium trot. In extended trot, simulator-trunk coordination variability decreased significantly ($p < 0.001$) on the downward phase of the riding simulator's vertical displacement. The PCA showed differences in how riders achieve in-phase coordination between their pelvis pitch to the vertical displacement of the riding simulator in medium and extended trot. Measures of coordination and coordination variability were not significantly different between competition levels. The SOM identified three large clusters of rider trunk-pelvis coordination in medium trot and eight smaller clusters described coordination characteristics in detail.

CONCLUSION The results of this thesis underline that riders should be measured using dynamic techniques and that competition level should not be used to group riders during passive riding on the riding simulator. The rider's independent seat is evident in medium trot, but independence may decrease as the challenge to the rider's balance increases in extended trot. Rider movement strategies can be identified by the temporal features of the trunk-pelvis pitch, which may relate to individual factors inherent to the rider, and potentially their horse. Further studies should explore these strategies and their influence on performance.

Acknowledgements

Thanks are owed to many who supported my thesis over the last three years. I am grateful that COVID-19 did not have a significant impact on my data collection, but it had significant impacts on many aspects of my project and life. The importance of mentorship, friendship, networks and family was underscored, and I am so grateful that many significant people ensured I wasn't taking this journey on my own.

First, I would like to thank my parents and Ivy for their support, without which I would not have been able to overcome every obstacle and follow my dreams back to the UK... and back to Canada during the height of the pandemic.

Thank you to my supervisory team: Dr Stephen Draper, Dr Laurence Protheroe and especially Dr Kathryn Nankervis, who provided immense moral support especially during the COVID year. Thanks are owed to the Margaret Giffen Trust, who have invested in the facilities at Hartpury University, including the Racewood Eventing Simulator, which has been a significant asset to my studies.

Professor Jonathan Wheat was instrumental in helping me to discover how to correctly calculate the continuous relative phase and coordination variability. His help and mentorship not only saved me many hours, but his example of collaboration and kindness will stay with me for my career.

The support of the other PGRs at Hartpury has been a great asset and I hope that the community will grow in the years to come. Thank you, John and Amelia, for coming through with the coffee chats and gym sessions. Isabeau Deckers, I hope we will be asking each other 'what's the craic, how's the science going' for many years to come.

Finally, I would like to dedicate this thesis to my late friend Samantha Calzone. She supported every data collection in her time at Hartpury with moral and practical support. Her love of horses reminded me why I started in the first place.

Publications

Wilkins, Celeste A., Nankervis, Kathryn, Protheroe, Laurence, Draper, Stephen B. (2020) Static pelvic posture is not related to dynamic pelvic tilt or competition level in dressage riders. *Sports Biomechanics*. DOI: 10.1080/14763141.2020.1797150

Conference proceedings

Wilkins, Celeste A., Nankervis, Kathryn, Protheroe, Laurence, Draper, Stephen B. (2019) Static pelvic posture is not related to dynamic pelvic tilt or competition level in dressage riders. *Journal of Sports Sciences*. 37(suppl. 1), pp 39.

Table of Contents

| | |
|--|-----------|
| Abstract..... | 2 |
| Acknowledgements..... | 3 |
| Publications | 4 |
| Conference proceedings..... | 4 |
| Table of Contents..... | 5 |
| List of Figures..... | 10 |
| List of Tables..... | 13 |
| 1.0 Introduction | 15 |
| 2.0 Literature Review | 23 |
| 2.1 The kinematics of the rider during riding | 23 |
| 2.1.1 The kinematics of high-level riders | 26 |
| 2.1.2 Active techniques of high-level dressage riders in sitting trot | 29 |
| 2.1.3 Comparison of kinematics measured by optical motion capture and inertial measurement units | 30 |
| 2.1.4 Performance aspects of the rider's technique | 38 |
| 2.1.5 Future directions for measuring the kinematics of riders using motion capture..... | 41 |
| 2.2 The influence of skill on rider kinematics | 42 |
| 2.2.1 Horse-rider coordination | 47 |
| 2.2.2 Future directions to analyse the effect of rider skill on riding performance..... | 51 |
| 2.3 The use of simulators in equestrian research..... | 52 |
| 2.4 Dynamical systems in sport | 54 |
| 2.4.1 Coordination variability | 55 |
| 2.4.1.1 The role of coordination variability in sport performance | 56 |
| 2.4.2 Methods to analyse coordination and coordination variability | 58 |
| 2.4.2.1 Discrete relative phase..... | 58 |
| 2.4.2.2 Continuous relative phase | 59 |
| 2.4.2.3 Vector coding | 64 |
| 2.4.2.4 Cross-correlation..... | 64 |
| 2.5 Quantifying and making inferences on kinematic time-series | 65 |
| 2.5.1 Statistical parametric mapping | 66 |
| 2.5.2 Principal component analysis | 67 |
| 2.5.3 Self-organising maps..... | 69 |
| 2.6 Summary | 70 |
| 3. General Methods | 72 |
| 3.1 Participants | 76 |
| 3.1.1 Participant inclusion and exclusion criteria | 76 |

| | |
|---|------------|
| 3.1.2 Participant characteristics..... | 81 |
| 3.2 Experimental set-up..... | 82 |
| 3.2.1 Motion capture equipment | 82 |
| 3.2.2 Motion capture calibration | 83 |
| 3.2.3 Marker placement | 85 |
| 3.2.4 Riding simulator | 87 |
| 3.2.5 Data capture | 91 |
| 3.3 Data processing..... | 92 |
| 3.3.1 Rigid body definition | 92 |
| 3.3.2 Filtering | 94 |
| 3.3.3 Time-normalisation..... | 95 |
| 4. Development of dynamic methods of analysis in the equestrian rider | 96 |
| 4.1 Introduction | 96 |
| 4.2 Estimation of soft tissue artefact and influence of clothing on motion capture accuracy during simulated riding | 97 |
| 4.2.1 Methods..... | 98 |
| 4.2.1.2 Data processing..... | 99 |
| 4.2.1.2 STA characterisation | 100 |
| 4.2.1.3 Rigid body calculations..... | 100 |
| 4.2.1.4 Statistical analysis | 100 |
| 4.2.2 Results..... | 101 |
| 4.2.3 Discussion..... | 106 |
| 4.2.4 Conclusion..... | 109 |
| 4.3 Comparison between continuous and discrete coordination analysis in the rider..... | 111 |
| 4.3.1 Methods..... | 112 |
| 4.3.1.1 Selection of signals..... | 112 |
| 4.3.1.1 Discrete relative phase..... | 114 |
| 4.3.1.2 Continuous Relative Phase..... | 115 |
| 4.3.1.2.1 Inspection..... | 115 |
| 4.3.1.2.2 Normalisation..... | 117 |
| 4.3.1.2.3 Calculation of CRP using the Hilbert Transform..... | 118 |
| 4.3.1.3 Statistical Analysis | 120 |
| 4.3.2 Results..... | 120 |
| 4.3.3 Discussion..... | 121 |
| 4.3.4 Conclusion..... | 123 |
| 5. Static pelvic posture is not related to dynamic pelvic tilt or competition level in dressage riders | 125 |
| 5.1 Introduction | 125 |
| 5.2 Methods..... | 127 |
| 5.2.1 Participants | 127 |
| 5.2.2 Data acquisition | 127 |
| 5.2.3 Data processing..... | 127 |
| 5.2.4 Statistical analysis | 128 |
| 5.3 Results..... | 128 |
| 5.3.1 Mean pelvic tilt | 128 |

| | |
|---|------------|
| 5.3.2 Pelvis range of motion | 130 |
| 5.3.3 Minimum and maximum tilt values | 130 |
| 5.4 Discussion and Implications | 133 |
| 5.4.1 Comparison between halt pelvic posture and mean pelvic posture in motion..... | 133 |
| 5.4.2 Competition level..... | 135 |
| 5.4.3 Range of motion..... | 136 |
| 5.4.4 Minimum and maximum pelvic tilt values..... | 137 |
| 5.4.5 Study limitations | 138 |
| 6.0 Conclusions | 139 |
| 6. Coordination variability in skilled riders on the riding simulator in medium and extended trot | 140 |
| 6.1 Introduction | 140 |
| 6.2 Methods..... | 143 |
| 6.2.1 Study design | 143 |
| 6.2.2 Participant characteristics..... | 143 |
| 6.2.3 Data collection | 143 |
| 6.2.4 Data Analysis..... | 143 |
| 6.2.5 Statistical analysis | 145 |
| 6.4 Results..... | 146 |
| 6.5 Discussion..... | 149 |
| 6.5 Conclusions | 155 |
| 7. Principal component analysis of the coordination between rider and riding simulator in medium and extended trot | 156 |
| 7.1 Introduction | 156 |
| 7.2 Methods..... | 159 |
| 7.2.1 Participants | 159 |
| 7.2.2 Data processing..... | 160 |
| 7.2.3 Continuous relative phase | 160 |
| 7.2.4 Principal component analysis | 161 |
| 7.2.5 Statistical analysis | 162 |
| 7.3 Results..... | 162 |
| 7.3.1 Qualitative analysis of group principal component scores..... | 162 |
| 7.3.2 Effect of competition level on PC scores | 166 |
| 7.4 Discussion..... | 169 |
| 7.5 Conclusions | 174 |
| 8. Defining functional groups of rider trunk-pelvis technique in simulated medium trot using self-organising maps and <i>k</i>-means clustering..... | 175 |
| 8.1 Introduction | 175 |
| 8.2 Methods..... | 177 |
| 8.2.1 Participants | 177 |
| 8.2.2 Data processing..... | 177 |
| 8.3 Results..... | 180 |

| | |
|--|------------|
| 8.4 Discussion..... | 186 |
| 8.4.1 Functional Groups and movement interpretation | 186 |
| 8.4.2 Limitations and future directions..... | 189 |
| 8.5 Conclusions | 191 |
| 9. Summary and implications | 192 |
| 9.1 Summary and implications of individual chapters..... | 196 |
| 9.1.2 Chapter 4..... | 196 |
| 9.1.1 Chapter 5..... | 198 |
| 9.2.3 Chapter 6..... | 199 |
| 9.2.4 Chapter 7..... | 201 |
| 9.2.5 Chapter 8..... | 202 |
| 9.3 Limitations..... | 203 |
| 10. Conclusion | 205 |
| References..... | 207 |
| Appendix A | 223 |
| Ethics application and approval | 223 |
| A1 Letter of approval from Hartpury University Ethics Committee | 223 |
| A2 Participant informed consent and rider questionnaire | 223 |
| A2.2 Participant informed consent form | 223 |
| A2.2 Rider questionnaire | 223 |
| A2 – Letter of Approval from Hartpury University Ethics Committee | 224 |
| A2.1 Participant informed consent form | 225 |
| A2.1 Rider questionnaire | 226 |
| Appendix B – Participant characteristics and inclusion in studies | 228 |
| Appendix C – Statistical Outputs..... | 230 |
| C1 – Chapter 4..... | 230 |
| C1.1 Section 4.2 | 230 |
| C1.1.1 Descriptive statistics | 230 |
| C1.1.2 Normality tests..... | 230 |
| C1.1.3 Mann-Whitney U Test outputs | 230 |
| C1.1.4 Spearman’s Correlation Test output..... | 230 |
| C1.2 Section 4.3 | 230 |
| C1.2.1 Descriptive statistics | 230 |
| C1.2.2 Normality tests..... | 230 |
| C1.2.3 Pearson’s correlation test outputs | 230 |
| C1.2.4 T-test outputs..... | 230 |
| C2 – Chapter 5..... | 230 |
| C2.1 Descriptive statistics | 230 |
| C2.2 Normality tests..... | 230 |
| C2.3 ANOVA output | 230 |

| | |
|--|------------|
| C2.3.1 Post-hoc t-tests | 230 |
| C2.4 Kruskal-Wallis test outputs | 230 |
| C2.4.1 Range of motion..... | 230 |
| C2.4.2 Minimum pelvic tilt..... | 230 |
| C2.4.3 Maximum pelvic tilt | 230 |
| C2.5 Spearman correlation test outputs..... | 230 |
| C2.5.1 Halt posture – range of motion | 230 |
| C2.5.2 Halt posture – mean pelvic tilt..... | 230 |
| C2.5.3 Halt posture – minimum and maximum pelvic tilt | 230 |
| C3 – Chapter 7..... | 230 |
| C3.1 Descriptive statistics | 230 |
| C3.2 Normality tests..... | 230 |
| C3.3 Linear mixed model output | 230 |
| C1.1 Section 4.2 | 231 |
| C1.1.1 Descriptive statistics | 231 |
| C1.1.2 Normality tests..... | 232 |
| C1.1.3 Mann-Whitney U test outputs..... | 233 |
| C1.1.4 Spearman’s Correlation Test outputs | 234 |
| C1.2 Section 4.3 | 235 |
| C1.2.1 Descriptive statistics | 235 |
| C1.2.2 Normality tests..... | 235 |
| C1.2.3 Pearson’s correlation test outputs | 236 |
| C1.2.4 Paired t-test outputs..... | 236 |
| C2 – Chapter 5..... | 237 |
| C2.1 Descriptive statistics | 237 |
| C2.2 Normality tests..... | 238 |
| C2.3 ANOVA output | 238 |
| C2.3.1 Post-hoc t-tests..... | 239 |
| C2.4 Kruskal-Wallis test outputs | 239 |
| C2.4.1 Range of motion..... | 239 |
| C2.4.2 Minimum pelvic tilt..... | 240 |
| C2.4.3 Maximum pelvic tilt | 240 |
| C2.5 Correlation test outputs | 241 |
| C2.5.1 Halt posture – mean pelvic tilt..... | 241 |
| C2.5.2 Halt pelvic tilt – range of motion | 241 |
| C2.5.3 Halt pelvic tilt – minimum and maximum pelvic tilt | 241 |
| C3 – Chapter 7..... | 242 |
| C3.1 Descriptive statistics | 242 |
| C3.2 Normality test | 242 |
| C3.3 Linear mixed model output | 243 |
| Appendix D: MATLAB script used to calculate CRP | 245 |
| Appendix E: Rider level, assessment rate (% of cycles in the same cluster) and cluster with the greatest assessment rate..... | 246 |

List of Figures

| Figure | | Page |
|-------------------|---|------|
| Figure 2.1 | The correct rider position as described by the British Horse Society (2011). When seated in the saddle, the rider should adopt a position that aligns their ear, shoulder, hip and heel. | 42 |
| Figure 2.2 | Phase-plane to describe the pitch rotation of an example rider's pelvis over several cycles of simulated medium trot, sitting. The angular displacement is plotted on the x-axis and the angular velocity on the y-axis. | 59 |
| Figure 3.1 | Camera set-up with nine motion capture cameras and two video cameras (labelled) around the riding simulator with rider sitting in the saddle. Large axes represent the global coordinate system which were established during calibration under the saddle. | 82 |
| Figure 3.2 | Marker placement depicted on the standing rider. Markers are denoted by circles. Blue circles indicate markers affixed to clothing or the elasticated strap around the rider's mid-section (in white). Orange circles indicate rigid clusters of markers. Purple circles indicate markers affixed directly to the skin. | 85 |
| Figure 3.3 | The riding simulator in Arena Mode with standard saddle and motion capture cameras. Not pictured: motion capture cameras placed to the rear and left side of the simulator. | 87 |
| Figure 3.4 | The riding simulator screens in Instruction Mode. The circle depicts the data from the four pressure sensors located under the saddle. Other bars indicate the leg pressure and rein pressures from the pressure sensors embedded into the side of the riding simulator and at the end of the reins. | 87 |
| Figure 3.5 | Three-dimensional displacement of the riding simulator (millimeters) in collected, medium and extended walk, trot, left canter, and right canter. | 89 |
| Figure 3.6 | Depiction of the rigid bodies of the head, trunk, pelvis and riding simulator (left) and the foot (right) with the local coordinate systems shown relative to the large global coordinate system axes. | 92 |
| Figure 3.7 | The effect of various cut-off values on the attenuation of noise when a fourth-order recursive Butterworth filter was applied to an example signal. The 10 Hz cut-off was chosen as it was deemed to effectively attenuate noise, while maintaining the characteristics of the signal. | 93 |
| Figure 4.1 | Spatial orientation of the rmsdc vectors in mm for the four markers: left/right anterior superior iliac spines (ASIS), left/right posterior superior iliac spines (PSIS), plotted relative to the pelvis coordinate system in walk, trot, and left canter. | 104 |
| Figure 4.2 | Time-normalised and filtered trunk (left) and pelvis (right) pitch waveforms for one subject over 34 cycles of the vertical displacement of the riding simulator in medium trot, sitting. | 115 |

| | | |
|-------------------|---|-----|
| Figure 4.3 | An example of phase-planes for a sinusoidal signal (top) and the filtered, but not normalised trajectory of an example rider's pelvis pitch in medium trot, sitting. | 115 |
| Figure 4.4 | Illustration of the Gibbs phenomenon in an example cycle for the simulator-pelvis CRP. The CRP was calculated from raw signals interpolated over 101 points (black) or 1001 points (red). | 119 |
| Figure 5.1 | Riders' minimum and maximum pelvic tilt by halt pelvic posture category in (a) walk, (b) trot, (c) left canter, and (d) right canter, and by competition level category in (e) walk, (f) trot, (g) left canter, and (h) right canter. Posture categories were defined by the rider's pelvic tilt value at halt. Anterior was defined as values of -1° or less, neutral as between 0.99° and -0.99° and posterior as 1° or greater. Competition level categories were defined by the level of their last three results in competition as novice (British Dressage Novice, Preliminary or Elementary), intermediate (British Dressage Medium, Advanced Medium or Advanced) and advanced (FEI Prix St Georges, Inter I or II or Grand Prix). | 131 |
| Figure 6.1 | Characteristics of the riding simulator's displacement and displacement frequency in medium and extended trot. As evident in the plot of the anterior-posterior displacement relative to the vertical displacement (top), extended trot results in greater anterior-posterior but not vertical displacement or vertical displacement frequency than medium trot. | 143 |
| Figure 6.2 | Results of three-way repeated measures SPM1D ANOVA on simulator-segment CSD ϕ by segment (pelvis, trunk, head and foot), by level (national, international) and gait (medium and extended trot). F(t) trajectory (black) and corresponding critical thresholds calculated using random field theory (horizontal red dashed lines) for main effect of level, main effect of segment and interactions. NB: critical threshold values vary as they represent the critical threshold at which α % (in this case, 5%) of smooth random curves would be expected to cross. | 146 |
| Figure 6.3 | Results of the post-hoc Bonferroni-corrected SPM1D paired t-tests in medium (left) and extended (right) trot. Group mean and error cloud CSD ϕ trajectories for the paired segments (legend to far right) to the left of corresponding SPM1D T(t) trajectories. Red dotted lines indicate corresponding critical thresholds on SPM1D plots, while shaded areas indicate supra-threshold clusters with significance at the level of $p < 0.001$. | 147 |
| Figure 6.4 | Multiple SPM1D paired t-tests to analyse the difference between simulator-segment CSD ϕ values within a segment between medium and extended trot. Red dotted lines indicate corresponding critical thresholds. | 148 |
| Figure 7.1 | Plots to describe the principal components of the continuous relative phase between the riding simulator and the rider's pelvis in medium trot that explained at least 90% of the variance. A-C: Loading vectors for each PC score. D-F: Trajectories corresponding to the 5th and 95th percentile of the PC score plotted (red and blue dotted lines) with all trials (grey) and mean (bold black line). G-I: Single component reconstruction of the PC score for the 5th and 95th percentile scores and the mean time-series. | 163 |

| | | |
|-------------------|--|-----|
| Figure 7.2 | Plots to describe the principal components of the continuous relative phase between the riding simulator and the rider's pelvis in extended trot that explained at least 90% of the variability. A-C: Loading vectors for each PC score. D-F: Trajectories corresponding to the 5th and 95th percentile of the PC score plotted (red and blue dotted lines) with all trials (grey) and mean (bold black line). G-I: Single component reconstruction of the PC score for the 5th and 95th percentile scores and the mean time-series. | 164 |
| Figure 7.3 | Group means \pm standard deviation for (A) simulator-pelvis CRP in medium trot and (B) simulator-pelvis CRP in extended trot. | 166 |
| Figure 7.4 | Box plots of the three PC scores needed to account for 90% of the variation in medium (top) and extended (bottom) trot by cycle, grouped by competition level category. | 167 |
| Figure 8.1 | Davies-Bouldin Index calculated for clusters 1-10. The score for cluster 3 is 0.8401 and cluster 8 is 0.8420. | 178 |
| Figure 8.2 | Time-normalised and scaled trajectories for the trunk (red) and pelvis (blue) pitch for the three functional groups for all (n = 389) cycles. | 170 |
| Figure 8.3 | Time-normalised and scaled trajectories for the trunk (red) and pelvis (blue) pitch for the eight clusters for all (n = 389) cycles. | 181 |
| Figure 8.4 | Mean (bold red or blue lines) and error clouds of unscaled, normalised pelvis (blue) and trunk (red) pitch trajectories within each cluster. Black line indicates the timing of the maximal vertical displacement of the riding simulator. | 183 |

List of Tables

| Table | | Page |
|------------------|--|------|
| Table 2.1 | Comparison of pelvic ranges of motion (ROM) reported in studies measuring riders on live horses. | 36 |
| Table 3.1 | Simplified aims, hypotheses and analysis methods for each experimental chapter. Full details to describe and justify the rationale, methods and results are available in each chapter, indicated by the page number in the far-right column. | 72 |
| Table 3.2 | Participant inclusion and exclusion criteria for factors that would potentially influence the rider's kinematics. | 76 |
| Table 3.3 | Simplified aims (refer to study for full details), inclusion criteria, number of participants included and additional information for the six experimental studies contained within this thesis. | 79 |
| Table 3.4 | Participant characteristics for each study. Age in years, mass in kilograms and height in metres are the mean \pm SD | 80 |
| Table 3.5 | Description of standard marker placement. Markers were affixed to either skin, clothing, rigid cluster or elasticated bandage depending on placement, as indicated. | 86 |
| Table 3.6 | Periods (seconds) and amplitudes (millimetres) of the displacement of the riding simulator in the anterior-posterior, lateral, and vertical directions. | 90 |
| Table 4.1 | Anthropometric characteristics of each BMI-matched pair of participants. | 98 |
| Table 4.2 | Results of the statistical tests for the comparison between parameters measured in riders with markers affixed directly to skin versus to their tight-fitting trousers. | 100 |
| Table 4.3 | Root mean square amplitude (<i>rmsd</i>) and peak-to-peak amplitude (Δ_{pmax}) of the soft tissue artefact (STA) for each pair of participants. The S prefix in the participant column denotes skin-affixed markers and the T denotes trouser-affixed markers. <i>rmsd</i> is reported in mm and BMI is reported in kg/m ² . | 102 |
| Table 4.4 | Pitch range of motion (degrees) and rigid body residual range (millimetres) for participants with skin-affixed markers (S prefix) and trouser-affixed markers (T prefix). | 103 |
| Table 4.5 | Angular displacement values for the rigid body of the riding simulator in each gait and variation obtained from an example rider. All values reported in degrees. | 112 |

| | | |
|------------------|---|-----|
| Table 4.6 | Means \pm standard deviation of the circular standard deviation of the discrete relative phase and continuous relative phase for the simulator-pelvis and simulator-trunk couplings in simulated medium trot. Grey shading indicates means that were significantly different ($p < 0.05$). | 120 |
| Table 5.1 | Mean pelvic tilt values \pm standard deviations in halt, walk, left canter and right canter by competition level. | 128 |
| Table 5.2 | Mean range of motion \pm standard deviation by competition level category. | 129 |
| Table 5.3 | As riders progressed through the gaits individuals exhibited unique pelvic tilt strategies. The rider's dynamic pelvic strategy was determined by their minimum and maximum pelvic tilt values. Riders were anterior if their minimum and maximum pelvic tilt values were less than 0° , anterior/posterior if their minimum was less than 0° and maximum greater than 0° , and posterior if their minimum and maximum values were both greater than 0° . | 130 |
| Table 7.1 | Estimates of fixed effects for each mixed-effects models conducted to examine the influence of competition level on the PC scores in each gait. | 168 |
| Table 8.1 | Parameter selection for the self-organising map. | 177 |
| Table 8.2 | Percentage (%) of each of the eight clusters within each functional group and of the total number of cycles. N is the percentage of the functional group of the overall number of cycles ($n = 389$). | 182 |
| Table 8.3 | Characteristics and qualitative interpretation of clusters representing sub-groups of the functional groups of rider trunk-pelvis movement in sitting trot. Mean peak timing given as a percentage of the period of the movement cycle of the riding simulator. | 184 |

1.0 Introduction

The equestrian sport of dressage is a test of the rider's ability to train and coordinate with the horse (Fédération Internationale Équestre, 2021a). The name comes from the French word '*dresser*', which translates directly as 'training'. It is a subjectively judged sport where the rider pilots the horse through a series of movements (known as the 'test'). The movements increase in complexity in the demands on the horse's athleticism as the pair progress through the levels of competition. The levels of dressage and the prescribed tests within each level are set by the national governing body of dressage. In the United Kingdom, this is British Dressage (known as BD). As per BD rules (British Dressage, 2021c), the lowest levels (Intro, Prelim and Novice) feature transitions between gaits, changes in direction, circles and three-loop serpentines: an 'S'-shaped figure that crosses the arena (British Dressage, 2021a). As horse and rider move up to the intermediate levels of BD Elementary and Medium, the test can include transitions within gaits (e.g. medium and extended trot), lateral movements (side stepping) and smaller figures, including pirouettes (British Dressage, 2021c). At the highest levels of national competition (BD Advanced Medium and Advanced) and at the international levels of competition, where the tests are prescribed by the Fédération Internationale Équestre (Fédération Internationale Équestre, 2021b), the tests can include lateral movements, trotting in place or with limited forward displacement (piaffe and passage), pirouettes, and flying changes (jumping from left to right canter in a single stride). In addition to increasing the complexity of the movements in a test, they also occur in more rapid succession as the difficulty increases (British Dressage, 2021c).

The quality of performance is typically judged by a single judge, however in championship competition (e.g. British Dressage Area Festivals) or international competition, (e.g. Olympics) up to five judges may judge the horse-rider combination from separate stations around the arena (British Dressage, 2021e; Fédération Internationale Équestre, 2020). As the horse's gait quality can be identified from an early age (Barrey *et al.*, 2002), progression in a dressage competition is biased to the horse's natural talent. However, while the quality of the gait is certainly important to the overall impression, the rider must

train the horse to perform the movements and increase the 'collection' in the gaits, which refers to the impression of taking more weight on the hindlimbs (British Dressage, 2021d). In the collected gaits, including collected trot, passage and piaffe, the horse increases the stance time (Clayton and Hobbs, 2019a), increases hock and stifle flexion during stance (Holmström, Fredericson and Drevemo, 1995), and increases the propulsive contribution of the hindlimbs (relative to the forelimbs) to the vertical oscillation of the horse's centre of mass (Clayton, Schamhardt and Hobbs, 2017). The rider must also cue the horse to accurately execute the test. The test occurs inside an arena, with markers placed at 12-16 metre intervals. Accuracy in the dressage test refers to the execution of the element of the test relative to the marker and the precision of the movement. For example, during a circle, the judge scores the circle's placement in the arena, its shape and the horse's gait as it performs the circle. Therefore, the role of the rider is threefold: (1) to train the horse to express the movements of the dressage test; (2) to accurately direct the horse to complete the movements during the test; (3) and to ride in such a way that allows and encourages the horse to move with balance and cadence.

As the horse is the primary focus of judging, there is much focus in research and practice on the attributes of elite horses (Barrey *et al.*, 2002; Morales *et al.*, 1998; Holmström and Drevemo, 1997; Holmstrom, Fredericson and Drevemo, 1994) and on competition demands on the horse: how they influence performance (Walker *et al.*, 2013; Clayton, 1994, 1995; Holmström, Fredericson and Drevemo, 1995; Deuel and Park, 1990) and the common injuries that affect dressage horses due to the demands of competition (Murray *et al.*, 2006, 2010). Undoubtedly, the focus on the horse's performance is warranted for welfare; using an animal for sporting competition has myriad ethical implications. However, in contrast to the abundance of research on equine biomechanics (for review see: Clayton and Hobbs, (2017b)), equine performance (Clayton and Hobbs, 2019b; Dyson, 2017; Williams and Tabor, 2017; Zsoldos and Licka, 2015; Valle *et al.*, 2013; Barrey *et al.*, 2002; Back *et al.*, 1995; Holmstrom *et al.*, 1994), welfare (Peeters *et al.*, 2013; McGreevy *et al.*, 2011), and veterinary interventions (Contino, 2018; Girodroux, Dyson and Murray, 2009; Caron, 2005; Engeli, Haussler and Erb, 2004), relatively little attention has been paid to the rider. The rider certainly considers the horse

as an athlete, however, may not extend the same consideration to themselves, even at the Olympic level (Bye and Chadwick, 2018). It should be argued that the rider is indeed an athlete as they incur significant muscular (Elmeua González and Šarabon, 2020; Terada *et al.*, 2017; Terada, 2000) and cardio-metabolic demands (Sainas *et al.*, 2016; Beale *et al.*, 2015; Douglas, Price and Peters, 2012; Wright and Peters, 2008; Westerling, 1983) during riding. Approaching the rider as an athlete would support sport-specific rider training and interventions, coaching the fundamental movements and demands of the sport with consideration of the rider's development, and understanding of the aetiology of rider-specific injuries. However, to achieve this paradigm shift, significant empirical evidence of the demands of equestrianism must be amassed to support training, coaching and injury reduction.

Data collection to support the shift in the perception of the rider as an athlete is a key challenge in equestrian sport. The performance of the horse and rider are interdependent; the rider can influence the horse's gait variability (Peham *et al.*, 2004), but horse movement variability can also influence the rider (Wolframm, Bosga and Meulenbroek, 2013). Therefore, relatively few studies have analysed the rider in isolation in static conditions, although these do exist (Guire *et al.*, 2017; Hobbs *et al.*, 2014). Instead, many more field studies (Baillet *et al.*, 2017; Eckardt and Witte, 2017; Engell *et al.*, 2016; Alexander *et al.*, 2015; Byström *et al.*, 2009, 2010, 2015; Münz, Eckardt and Witte, 2014; Wolframm, Bosga and Meulenbroek, 2013; Symes and Ellis, 2009; Terada, Clayton and Kato, 2006; Lagarde *et al.*, 2005; Lovett, Hodson-Tole and Nankervis, 2005; Peham *et al.*, 2001; Schils *et al.*, 1993) have examined the rider's movements and the horse-rider movement interaction on live horses. Two study designs have been frequently used to investigate the equestrian rider. Several studies have tested hypotheses regarding the effect of the rider's experience level on their kinematics (Baillet *et al.*, 2017; Eckardt and Witte, 2017; Olivier *et al.*, 2017; Münz, Eckardt and Witte, 2014; Kang *et al.*, 2010; Lagarde *et al.*, 2005; Peham *et al.*, 2001; Schils *et al.*, 1993). Other studies have analysed a group of competent or elite riders, and reported specific kinematic measures as the mean of the individuals (Engell *et al.*, 2016; Byström *et al.*, 2009, 2010, 2015; Gandy *et al.*, 2014; Lovett, Hodson-Tole and Nankervis, 2005).

Due to the complexity of analysing a horse and rider in motion, studies that compared groups of riders had small samples of riders ranging from two (Lagarde *et al.*, 2005; Peham *et al.*, 2001) to 20 riders (Eckardt and Witte, 2017; Münz, Eckardt and Witte, 2014). This is a statistical issue, as the studies that compare two (or more) small groups of riders may be underpowered (Abt *et al.*, 2020), but also results in inferences about riders drawn from a small, homogenous sample that may not represent the full spectrum of riders. Besides, the complexities of collecting rider data have led to several studies that make inferences from the same data set (e.g. Byström *et al.* (2009, 2010, 2015); Engell *et al.* (2016)). Therefore, there is a need to increase the number and diversity of riders analysed when groups of riders are compared.

The studies currently published examining the rider's biomechanics have described how the rider moves during riding, focussing on competent (Gandy *et al.*, 2014; Terada, Clayton and Kato, 2006; Lovett, Hodson-Tole and Nankervis, 2005) or elite (Engell *et al.*, 2016; Byström *et al.*, 2009, 2010, 2015) individuals. Movement data have been summarised as group means, or as the mean trajectory (e.g. pelvis pitch) with error bars to indicate the standard deviation. As such, intra- and inter-rider variability is treated as noise. Reporting elite athlete data (as per Byström *et al.*, 2009, 2010; Engell *et al.*, 2016) as a group assumes that all athletes at the elite level demonstrate a similar technique. However, as there can be significant variability between riders and their horses, it could be argued that the average does not accurately represent any horse-rider combination at all, and that interesting information could be gleaned from individual-based analysis of elites (Glazier and Mehdizadeh, 2019). Alternatively, grouping riders based on shared characteristics using statistical methods, such as clustering analysis or feature detection methods for kinematic time-series data, may be more advantageous than macroscopic grouping and microscopic single-subject analyses to identify classes of rider technique.

Horse-rider interaction is an important aspect of research and practice in equestrian sport. The rider aims to achieve a high level of coordination with the horse, known as 'harmony' (Fédération

Internationale Équestre, 2020). The horse-rider coordination should give the judge the impression that there is '*always a harmonious cooperation between Horse and Athlete*' (p. 24, Fédération Internationale Équestre, 2020). For the rider's part, their ability to achieve coincident movement to the horse is important to give the overall impression of 'harmonious cooperation'. However, achieving the necessary balance to anticipate and adapt to the horse's movement while also controlling the speed and direction of travel of the horse cannot be understated. As such, several studies have sought to understand how riders learn to achieve harmony by comparing expert and novice riders. The seminal study of horse-rider coordination dynamics by Lagarde *et al.* (2005) reported significant differences between a novice and professional rider's coordination to a horse in a sitting trot. Subsequent studies have presented a diverse range of methods to analyse horse-rider coordination, predominately comparing novice and expert populations.

Many of these studies used discrete methods, analysing the coordination between horse and rider at a given point in the horse's gait cycle. For example, Münz, Eckardt and Witte (2014) and Eckardt and Witte (2017) analysed the horse-rider coordination by cross-correlation, which analyses the latency between the occurrence of peaks in two cycles (Nelson-Wong *et al.*, 2009). These studies have assessed horse-rider coordination at one point in the stride, although the movement and forces incurred by the rider change as the horse moves from stance to swing phases. Continuous horse-rider coordination has been analysed by Wolframm, Bosga and Meulenbroek (2013), however, they presented the mean of the continuous relative phase (a measure of coordination between two moving parts throughout the movement cycle (Wheat and Glazier, 2006)) for the horse-rider trial. Studies in other sports using the continuous relative phase have profiled how the coordination between two moving parts changes throughout a movement cycle, and attributed differences to skill level (Mazurek *et al.*, 2020; Busquets *et al.*, 2013). Similar studies of the rider using continuous methods could help to elucidate how the rider achieves harmony throughout the horse's stride.

Finally, given the paucity of data to support hypothesis generation for rider studies, many studies have assumed the determinants of rider performance from conventions in equestrian practice. The most common of these is the influence of rider competition or experience level and the influence of the rider's pelvic posture on their performance. The influence of rider competition or experience level on riding tasks has been tested by several studies that have examined its influence on horse- or simulator-rider coordination (Baillet *et al.*, 2017; Eckardt and Witte, 2017; Münz, Eckardt and Witte, 2014; Lagarde *et al.*, 2005; Peham *et al.*, 2001), rider intersegmental coordination (Olivier *et al.*, 2017), and kinematics (Biau *et al.*, 2013; Kang *et al.*, 2010; Schils *et al.*, 1993). Several definitions of rider experience are used in these studies, ranging from the years of rider experience (Baillet *et al.*, 2017; Eckardt and Witte, 2017; Münz, Eckardt and Witte, 2014; Kang *et al.*, 2010), their competition level (Olivier *et al.*, 2017), their involvement on a spectrum from recreational to professional (Biau *et al.*, 2013; Lagarde *et al.*, 2005; Peham *et al.*, 2001), and finally, an assessment of their riding judged by a panel (Schils *et al.*, 1993). The skill in equestrian sport is the rider's physical ability to match the horse's movement, as well as to anticipate and adapt to changes in the horse's gait and behaviour to maintain consistent horse-rider coordination. Therefore, it is logical to assume that horse-rider coordination increases with the rider's experience.

The small number of studies that have examined the effect of rider experience on horse-rider coordination (Baillet *et al.*, 2017; Eckardt and Witte, 2017; Münz, Eckardt and Witte, 2014; Lagarde *et al.*, 2005; Peham *et al.*, 2001) found significant differences between horse-rider coordination measurements of beginner and experienced riders until rider experience exceeded three years. Eckardt and Witte (2017) compared riders with an average of 3.6 years of experience to professional riders and could not identify any significant differences in horse-rider coordination. If coordination is established through the complex interaction of participant, environmental and task constraints (Newell, 1986), the perception of the task of riding may be different between competitive and non-competitive riders. Therefore, differences between recreational and competitive riders may be compounded by differences in the perception of the task. Compared to their recreational

counterparts, competitive dressage riders follow the 'scales of training' (German National Equestrian Federation, 2005) that prescribes a systematic progression of training goals for the horse. Comparisons of kinematics and horse-rider coordination in a cohort of competitive riders may reveal the effect of rider skill. Also, insights gained from studies of competitive riders may be more relevant to recommendations to increase rider performance than comparisons of non-competitive and competitive riders (e.g. Baillet *et al.* (2017)).

The rider's pelvic posture has been directly assessed by Engell *et al.* (2018) and Walker *et al.* (2020). Several other studies have also reported pelvic kinematics (Engell *et al.*, 2016; Alexander *et al.*, 2015; Byström *et al.*, 2009, 2010, 2015; Gandy *et al.*, 2014) and the coordination between the horse and the rider's pelvis during riding (Eckardt and Witte, 2017; Münz, Eckardt and Witte, 2014). The rider's pelvis is considered the movement interface between horse and rider. Its movement has a joint influence on horse-rider performance: the rider's pelvis influences the pressure distribution in the saddle which can be altered to cue changes in the horse's gait tempo (Engell *et al.*, 2016; Byström *et al.*, 2015), but the orientation of the pelvis influences the rider's sagittal spinal curves (Boulay *et al.*, 2006). There is a common belief in equestrian sport that a neutral pelvis is a prerequisite to achieving a high level of coordination with the horse (Mackechnie-Guire, 2020; Gandy *et al.*, 2018). By extension, competitive riders that can achieve harmony better than novice counterparts should then exhibit a neutral pelvis. However, Hobbs *et al.* (2014) observed increased deviations from a neutral standing posture as riders' competition level increased. Also, as the rider's pelvis rotates during riding, characterising the rider's pelvic posture during the dynamic activity of riding could be challenging. Therefore, further clarity is needed to understand how to assess rider pelvic posture and whether there is any relationship between rider pelvic posture and competition level.

This thesis aimed to (1) use continuous methods to analyse the rider's technique; and (2) understand whether competition level influenced measures of simulator-rider coordination and coordination variability. To meet the first aim, the objectives of this thesis were to: (1) analyse the influence of

riding clothing on motion capture error during simulated riding; (2) analyse the difference between the variability calculated from the discrete and continuous relative phase; and (3) to analyse the characteristics of the continuous relative phase and variability using continuous methods, including statistical parametric mapping, principal component analysis and self-organising maps. The second aim of the thesis was met by using a standardised riding test on a riding simulator to compare competitive dressage riders, grouped by their competition level according to the aims of each study.

The hypotheses of this thesis were that: (1) affixing the markers on the trousers and increased rider body mass index will increase the error compared to affixing markers directly to skin; (2) that there would be significant differences between the coordination variability of the simulator-trunk and simulator-pelvis quantified by the continuous relative phase and discrete relative phase; (3) that riders would show common patterns of pelvic tilt related to competition level; (4) that there would be differences due to international or national competition level on the coordination variability between the rider's head, trunk, pelvis or foot in pitch, relative to the vertical displacement of the riding simulator in simulated medium and extended trot; (5) that there would be differences between the features of the simulator-pelvis coordination due to competition level and gait; and (6) that riders could be grouped by the characteristics of the kinematics of their trunk and pelvis pitching movements.

2.0 Literature Review

2.1 The kinematics of the rider during riding

Horse and rider performance are inextricably tied. Traditionally, research has focussed on the horse, however, an increasing interest in the rider has emerged in the past two decades. Evidence from studies, including Peham *et al.* (2004), position the rider as more than a passive passenger during riding as they can have an active influence on the determinants of performance in dressage, including the rhythm and regularity of the horse's gait. The growing interest in the rider as an athlete (Douglas, Price and Peters, 2012) has accompanied an increase in technology available to measure horse and rider in field and lab settings (MacKechnie-Guire and Pfau, 2021; Pfau and Reilly, 2020; Bosch *et al.*, 2018; Gandy *et al.*, 2018). As equestrian sports science and rider biomechanics are in their infancy, there is a distinct lack of standardisation of protocols and methods of analysis for the rider, which has resulted in a diverse range of research outcomes. However, the development of standardisation in this area is warranted for several reasons. Firstly, to improve riders' performance, regardless of riding discipline, the most relevant features of the movements that constitute the skill must be known (Lees, 2010). Secondly, while back pain (Deckers *et al.*, 2020; Hobbs *et al.*, 2014; Kraft *et al.*, 2009) and head and spinal injuries from falls (Gates and Lin, 2020) are prevalent, the contribution of specific rider movements to injury is unknown. Finally, as the horse-rider interaction during dressage constitutes coordination of many degrees of freedom inherent to both horse and rider, the structure and variability of coordination are important to performance (Austin, 2001).

Coordination can be quantified by computational tools in the dynamical systems theory framework (Kurz and Stergiou, 2004). To date, research investigating horse-rider coordination has sought to determine the influence of rider skill (Baillet *et al.*, 2017; Eckardt and Witte, 2017; Olivier *et al.*, 2017; Münz, Eckardt and Witte, 2014; Lagarde *et al.*, 2005; Peham *et al.*, 2001). The advent of pattern recognition tools, including principal component analysis (Daffertshofer *et al.*, 2004) and self-

organising maps (Bauer and Schöllhorn, 1997) offers the potential to discover new relationships between variables influencing rider performance.

Kinematics describes the motion of a body without regard to the causes of the motion (Robertson *et al.*, 2014). The systematic measurement and description of the rider's movements during riding and the movement interaction between horse and rider can inform coaching, performance, and the aetiology of riding-related injury (Hobbs *et al.*, 2014). However, performing a kinematic analysis of the rider is fraught with challenges. The gold standard of kinematic analysis is optical motion capture, as it measures the displacement of markers that represent underlying bones with high accuracy in a calibrated volume (Buganè *et al.*, 2014). The optical motion capture system is comprised of two or more cameras that are synchronised to record the position of reflective markers affixed to a moving subject (Robertson and Caldwell, 2014). Infrared cameras, such as those manufactured by Qualisys (Qualisys AB, Gothenburg, Sweden) or Vicon (Vicon Motion Systems Ltd, Oxford, UK), are equipped with a ring of infrared lights around the camera lens. These lights pulse at a frequency predetermined by the operator based on the frequency of the movement of interest (Winter, 2009). Multiple cameras are used to capture a subject's kinematics. Each camera captures the scene in two dimensions, but when they are synchronised and calibrated (full details on p. 31), they use triangulation to determine the position of the visible markers in three dimensions (Chèze, 2014). Accordingly, each marker must be seen by at least two cameras (Winter, 2009).

Accurate three-dimensional motion capture of horse and rider requires a large capture volume and many cameras. For this reason, only a few studies have published three-dimensional kinematic measurements of the rider riding a live horse captured using optical motion capture (Engell *et al.*, 2016; Alexander *et al.*, 2015; Byström *et al.*, 2009, 2010, 2015; Terada, Clayton and Kato, 2006; Lagarde *et al.*, 2005; Peham *et al.*, 2001; Schils *et al.*, 1993). Several studies have established approaches using inertial measurement units (IMUs) (Eckardt and Witte, 2017; Gandy *et al.*, 2014;

Münz *et al.*, 2013), although no known study has published validation of IMUs against optical motion capture during riding.

Briefly, IMUs combine tri-axial accelerometers, gyroscopes and magnetometers to quantify angular velocity, the sum of gravitational and inertial linear accelerations and the local magnetic field vector components, respectively (Camomilla *et al.*, 2018). These allow the researcher to obtain information about the orientation of the body and its three-dimensional movements. The signals from the components of the IMU are fused to estimate orientation and position (sensor fusion) (Sabatini, 2011). Processing can integrate errors into the data, known as sensor drift, that can increase over time when the acceleration is integrated once, to obtain orientation, or twice to obtain position (Camomilla *et al.*, 2018). In addition, as the magnetometer is crucial to the estimate of orientation, ferromagnetic disturbances from appliances or, in the case of horse and rider, the walls of an indoor arena, may influence the magnetic field detected by the magnetometer and therefore increase orientation error (Ahmad *et al.*, 2013). Therefore, validation of the measurements of the rider's kinematics in the saddle obtained with an IMU versus motion capture is hardly trivial.

Much of the current understanding of three-dimensional rider kinematics during riding on a live horse is based on a single data collection of the three-dimensional kinematics, using optical motion capture, of a group of FEI-level riders mounted on their own horses in walk or trot on a treadmill (Byström *et al.*, 2009, 2010, 2015; Engell *et al.*, 2015). These data have contributed to the understanding of how high-level riders move during collected walk (Byström *et al.*, 2010), collected trot (Byström *et al.*, 2009), different speeds of collected trot (Byström *et al.*, 2015), and sitting trot techniques described as 'active' or 'passive' (Engell *et al.*, 2016). These studies (Byström *et al.*, 2009, 2010, 2015; Engell *et al.*, 2015) took a three-dimensional approach, analysing the position and orientation of the body in three-dimensional (3D) space (e.g. from all angles). Other studies describing the rider's kinematics have taken a two-dimensional approach, examining riders in the sagittal plane only (Walker *et al.*, 2020; Kang *et al.*, 2010; Terada, Clayton and Kato, 2006; Lagarde *et al.*, 2005; Lovett, Hodson-Tole and

Nankervis, 2005; Schils *et al.*, 1993) or IMU-based approach (Gandy *et al.*, 2014, 2018; Eckardt and Witte, 2017; Münz, Eckardt and Witte, 2014). Finally, a subset of these studies has investigated questions relating to the rider's functional symmetry in the frontal plane (Symes and Ellis, 2009), the influence of an athletic taping intervention on a three-dimensional assessment of rider asymmetry using three-dimensional optical motion capture (Alexander *et al.*, 2015) and the influence of pelvic tilt control on a measure of horse-rider interaction (Walker *et al.*, 2020). Based on the questions posed by each of these studies, the current body of research describing the rider's kinematics can be grouped as (1) describing the kinematics of high-level riders; (2) assessing the influence of rider skill by comparing the kinematics of experienced and novice riders; and (3) performance aspects of the rider's technique, including functional asymmetries.

2.1.1 The kinematics of high-level riders

In dressage riding, the rider remains fully seated in the saddle during walk and canter. In trot, the rider may sit ('sitting trot') or sit and rise out of the saddle on alternate diagonal support phases ('rising trot'). At the highest levels of dressage, the trot is always performed sitting, although riders may use rising trot in training. Seven high-level dressage riders mounted on their own horses on an equine treadmill were assessed by Byström *et al.* (2009, 2010, 2015) and Engell *et al.* (2016) in walk and sitting trot. They described the kinematics of the rider in terms of the Euler rotations of the rider's pelvis and trunk, whereby pitch refers to the anterior-posterior rotation, roll refers to the mediolateral rotation, and yaw refers to the transverse rotation. In walk and trot, there are two pitching cycles of the rider's pelvis and the saddle in each stride (Byström *et al.*, 2009, 2010). The characteristics of the roll, pitch and yaw are influenced by the pattern of footfalls and the vertical height of the hindquarters of the horse relative to the withers (Hilary M. Clayton and Hobbs, 2017). The walk is a four-beat gait with a lateral sequence of footfalls. The maximal anterior pitch of the rider's pelvis at the walk, as reported by Byström *et al.* (2010), occurred at the beginning and end of left forelimb stance and maximal posterior pitch at the beginning and end of left hindlimb stance. Trot has a two-beat rhythm: diagonal pairs of fore- and hindlimbs are synchronised, with an intervening suspension phase between each

diagonal support phase (Clayton and Hobbs, 2017). In sitting trot, Byström *et al.* (2009) reported that maximal anterior pitch occurred at the beginning of the diagonal support phase and maximal posterior pelvic tilt during late-stance, just before the onset of the suspension phase. It is interesting to note that walk had less pelvis pitch range of motion (ROM) than trot (mean \pm standard deviation (SD) difference trot-walk: $-28 \pm 20\%$). Relative to the size of the mean, there were no appreciable differences between the variability of walk (mean \pm SD: $9.7 \pm 2.0^\circ$) and trot pitch ROM ($13.9 \pm 2.2^\circ$).

Comparing the rider's trunk pitch between walk and trot yields interesting insights into the rider's strategy. In walk, Byström *et al.* (2010) reported pitch values fluctuating around 0° throughout the stride (ROM: $6.0 \pm 2.0^\circ$) in a group of high-level riders, however, the error cloud representing the standard deviation suggests that there are large between-rider differences that perhaps indicate different movement patterns even between high-level riders. In trot, Byström *et al.* (2009) reported a much larger trunk pitch ROM ($10.7 \pm 3.4^\circ$) with what looks like an approximately anti-phase (opposite direction of rotation) relationship to the pelvis. The trunk reached maximal anterior pitch during early diagonal stance and maximal posterior pitch at diagonal mid-stance. Therefore, in walk, the rider primarily moves their pelvis in pitch to follow the anterior-posterior movement of the horse (and by extension, saddle), while keeping their trunk around neutral. In trot, these riders sequenced their pelvis and trunk to pitch in opposite directions to absorb the movement in sitting trot when initiated by the stance and swing phases of the horse's stride. In roll, the pelvis rotates in opposite direction to the horse's trunk in walk and trot. The roll ROM of the pelvis was similar between walk ($5.6 \pm 0.6^\circ$) and trot ($5.1 \pm 1.1^\circ$) (Byström *et al.*, 2009, 2010). The rider's pelvis reached maximal roll to their right side at the beginning of left fore- and hindlimb stance in walk and maximum left roll at the beginning of right fore- and hindlimb stance. Notably, the pelvis roll pattern in trot is not as symmetrical as in walk. Riders reached maximum right roll at the beginning of the left forelimb/right hindlimb diagonal stance phase and maximum left roll during mid-stance of the same diagonal support phase. The rider's trunk had similar roll ROMs in walk ($5.0 \pm 1.8^\circ$) and trot ($4.9 \pm 1.8^\circ$). The roll trajectories were observably less biased to left or right in walk than a trot, where greater peak trunk roll was observed

during the left forelimb/right hindlimb diagonal support phases, and likely relates to the asymmetries observed in the pelvis during the same limb phase.

Discrete measurements, sampled at one point within the stride cycle, have been used to describe the rider's position in an experienced-matched population. Terada, Clayton and Kato (2006) described the rider's position during one half of the trot gait cycle. They placed markers on the rider's right side, on the lateral epicondyle of the humerus, forearm, upper arm and greater trochanter of the hip. Inspection of data reported for individual riders indicated that the angle of the trunk to the vertical during sitting trot was individual. Mean values ranged from 12.9° to 24.2° for the six riders assessed. They reported that the rider's trunk tilted backwards in early stance and forward tilt at the end of stance. This agrees with Byström *et al.* (2009), who reported that maximal posterior trunk pitch occurred in early stance. However, it should be noted that Terada, Clayton and Kato (2006) measured the trunk tilting angle as the angle formed between the hip and shoulder marker, which assumes the trunk acts as a rigid segment during sitting trot. As shown by Byström *et al.* (2009), the trunk and pelvis can move approximately opposite due to flexion-extension of the spine during riding, therefore, it is unlikely that the trunk acts as a rigid segment for many riders. Additionally, Terada, Clayton and Kato (2006) assumed that as the trot is a symmetrical gait; that riders replicate a similar pattern in sitting trot between left and right diagonal support phases. Incidentally, Lovett *et al.* (2005) found significant differences between the rider's trunk, thigh and ankle angles between diagonal stance phases in trot defined by the hindlimb (left: left hindlimb/right forelimb; right: right hindlimb/left forelimb). The riders' trunk was significantly closer to the vertical during the left stance than the right. This corresponds with Byström *et al.* (2009) who reported a right bias of the rider's pelvis roll and likely relates to asymmetries in the rider's pelvic ROM. Therefore, while discrete statistics may reveal interesting insights regarding the rider's technique, it cannot be assumed that the rider will produce the same pattern between diagonal support phases in trot.

2.1.2 Active techniques of high-level dressage riders in sitting trot

Collected and extended gaits feature in dressage tests at the higher levels. Collection is a variation of the gait where the horse shortens their stride length while maintaining the same stride duration and energy. Extended gaits are those where the horse increases the stride length while maintaining the same stride duration, resulting in greater speed and increased suspension phase (Clayton and Hobbs, 2019a). As the stance duration during extended trot is shorter than collected trot, a greater vertical impulse is produced in extended than collected trot, particularly by the hind limbs (Clayton and Hobbs, 2019b). The horse's normal gait without any influence from the rider is referred to as the 'working' walk, trot or canter. To increase or decrease the stride length, the rider must actively cue the horse, using their seat, legs, and hands on the reins. Alternatively, the rider may also allow the horse to travel freely in their working gait to promote stretching and relaxation of the horse. For clarity, the rider's technique was defined as per Engell *et al.* (2016) as 'active' if they cue the horse to perform a collected or extended gait.

Sitting trot is always performed at the high levels of dressage competition, and thus, the seven high-level riders assessed by both Byström *et al.* (2009, 2015) and Engell *et al.* (2016) performed sitting trot exclusively. Byström *et al.* (2015) and Engell *et al.* (2016) studied the influence of variations of the gait on the kinematics of the aforementioned seven high-level riders on their own horses on the treadmill. Byström *et al.* (2015) examined differences between the rider's kinematics during higher and lower speeds of collected trot and during passage, a slower variation of collected trot with a shorter stride length and duration (Clayton and Hobbs, 2019a). As the horse's speed was controlled by the treadmill, the results of this study indicate three different rider techniques; (1) a passive position: free trot, where the rider allows the horse to travel without interference in sitting trot; (2) increased speeds within collected trot; and (3) passage. In free trot, riders anteriorly rotated their pelvis and posteriorly rotated their trunk. The distance between the rider's neck and the horse's lumbar spine increased compared to other techniques, suggesting that although they rotated their trunk posteriorly, they also pitched their whole body forward to allow the horse to travel freely. To achieve a higher speed in

collected trot, riders posteriorly rotated their pelvis but anteriorly rotated their trunk, increasing spinal flexion. To achieve passage, riders increased posterior pitch of their pelvis and anterior pitch of the trunk compared to collected trot. It is interesting to note that there was higher variation between riders' pelvis pitch in passage versus collected trot indicating that high-level riders may employ individual and horse-specific techniques to achieve the advanced movement of passage.

A similar analysis was performed by Engell *et al.* (2016) on the same group of riders. Inspection of the time series describing the pitch of the group of high-level riders' pelvis, trunk and head for the free trot and one speed of the collected trot illustrate the stride-specific changes in the rider's technique. These data elaborate on previous findings by showing significantly greater head ROM in the active rider posture. A pressure mat was used to capture the effect of the rider's seat during the active and passive technique. In the active rider posture, the number of loaded saddle mat cells was significantly decreased, which suggests that riders concentrate their seat pressure to a smaller area as they increase the coupling between their pelvis and the horse.

2.1.3 Comparison of kinematics measured by optical motion capture and inertial measurement units

Measurement of the rider's kinematics poses some unique challenges. As the horse's stride length can exceed two metres in trot (Clayton, 1994) and canter (Clayton *et al.*, 2018), capturing the movement of the horse and rider over a sequence of strides requires a large area. Two systems are commonly used to analyse horse and rider kinematics: optical motion capture and inertial measurement units (IMUs), each with its advantages and disadvantages. Optical motion capture is considered the criterion measurement of kinematics, as a series of synchronised and calibrated cameras track the displacement of markers affixed to specific points on the body with small (less than 1 millimetre depending on camera and calibration) error (van der Kruk and Reijne, 2018). The displacement of the rider's body segments is tracked, and higher derivatives can be calculated. The field of vision of each camera varies by model, but for larger three-dimensional capture volumes, such as those required to capture horse and rider in the field, many cameras are needed. For example, an 824 m² capture

volume was achieved by Spörri *et al.* (2016) with 24 cameras to track the movement of a ski jumper. Additionally, many optical motion capture systems may not be suitable for use in large-volume, outdoor settings (van der Kruk and Reijne, 2018). The accuracy between modern motion capture camera models was assessed by Topley and Richards (2020). Their results indicate that the maximum error of modern camera systems from a range of manufacturers (Qualisys, Vicon, OptiTrack and Motion Analysis) does not exceed 1.0 mm. Therefore, the camera and hardware errors between systems are quite small, and the biggest challenge to accuracy of analysis remains the number of cameras required to adequately capture the volume and consideration of marker placement (Topley and Richards, 2020).

To circumvent these challenges Byström *et al.* (2009, 2010, 2015) and Engell *et al.* (2016) captured the three-dimensional kinematics of riders mounted on their horses in walk and trot on a high-speed treadmill. Twelve optical motion capture cameras were positioned around the treadmill. Similarly, Baillet *et al.* (2017) used 10 cameras, positioned around a riding simulator to measure riders' kinematics. Three-dimensional capture of the rider's kinematics in a riding arena is less common, although Alexander *et al.* (2015) measured riders' trunk and pelvis kinematics in trot with four optical motion capture cameras positioned on each side of a straight track. More commonly, two-dimensional kinematics measuring the rider in the sagittal plane has been reported when optical motion capture is used (Terada, Clayton and Kato, 2006; Lagarde *et al.*, 2005; Peham *et al.*, 2001).

In contrast, IMUs can measure the horse and rider without the constraints of remaining within the field of view of a set of cameras, with similar sampling frequencies to optical motion capture (Camomilla *et al.*, 2018). IMUs contain accelerometers, gyroscopes and often magnetometers, therefore, measure acceleration, rotation and magnetic field, respectively. IMU placement varies, and unless specifically indicated, they typically represent the movement of the segment on which they are placed, rather than a specific bony prominence (e.g. anterior superior iliac spine of the pelvis). For example, Wolframm *et al.* (2013) measured the rider's trunk with an accelerometer placed on the skin

overlying the sternum and Münz *et al.* (2014) and Münz *et al.* (2013) measured the interaction between the rider's pelvis (IMU placed on the dorsal aspect of the pelvis) and the horse's trunk (IMU affixed to horse's girth strap).

Except for Wolframm *et al.* (2013) who reported acceleration-based measures using a single IMU, all other studies reported displacement-based measures including roll and pitch of the rider's segments (Münz, Eckardt and Witte, 2014; Eckardt and Witte, 2017) or hip angles (Gandy *et al.*, 2018, 2014). As IMUs do not measure displacement or orientation directly, the data must be processed to elicit displacement measures, such as Euler rotations or joint angles of the underlying segments. The accuracy of these processing routines can vary, particularly when the signals are integrated twice to obtain the position (Camomilla *et al.*, 2018), which can cause errors known as sensor drift. Therefore, the resulting displacement measures from IMUs are estimations of the rider's kinematics.

Several studies have used a 17-sensor Xsens MVN motion capture suit (XSens, Enschede, Netherlands) to analyse the rider's kinematics (Gandy *et al.*, 2014, 2018; Eckardt and Witte, 2016, 2017; Eckardt, Münz and Witte, 2014). This suit measures signals from 17 IMUs that are mounted to the body with adjustable straps or onto a Lycra suit (depending on the exact model). Post-processing in the XSens proprietary software (MVN Analyze, XSens, Enschede, Netherlands) combines the signals from the IMUs to estimate joint angles, segment kinematics and positions, and other kinematic data. The proprietary software aims to filter out sensor drift (as described above) by using sensor fusion that combines the accelerometer, gyroscope and magnetometer signals to estimate orientation while correcting for error (XSens, 2021). Although the algorithms may improve the accuracy of the orientation measures, as these must be calculated from the IMU data, these data also remain estimates of the rider's kinematics.

Several sources of error can occur that influence the accuracy of motion capture systems including errors relating to the motion capture system itself or the markers (Cappozzo *et al.*, 2005). To minimise measurement errors, the measurement area is calibrated using a wand and calibration frame (Chiari

et al., 2005). Calibration serves to determine the internal (optical characteristics of the individual cameras) and external (position and orientation of the cameras relative to each other and the scene) parameters for each camera, given a specific camera set-up and scene (Chiari *et al.*, 2005). The calibration then allows the three-dimensional volume to be reconstructed in the motion capture camera's software.

Calibrations are performed per the camera manufacturer's guidelines. For example, Qualisys and Vicon prescribe dynamic calibration procedures whereby an L-shaped frame with embedded markers is placed at a static location within the desired capture volume and a T-shaped wand of a known length with markers at its extremities is moved through the capture volume in three dimensions for several seconds or more, depending on the size of the area. The L-shaped frame defines the origin and orientation of the global coordinate system, while the wand generates data that determines the location and orientation of the cameras (Qualisys AB, 2020). The motion capture software then determines the quality of the calibration. In Qualisys Track Manager (Qualisys AB, Gothenburg, Sweden), this is the residual in millimetres of the distance between the origin of the coordinate system (described by the static L-shaped frame) in the anterior-posterior, lateral, and vertical axes and the optical centre of the individual camera. In Vicon Nexus (Vicon Motion Systems Ltd, Oxford, UK), this is the root mean square distance in camera pixels of the 3D reconstruction of the markers. Thresholds of accuracy depend on factors such as the size of the capture volume and camera lens type (Vicon Ltd, 2015).

Instrumental errors are considered random and are attenuated by filtering and smoothing processes (Chiari *et al.*, 2005). This appears as noise within the resulting kinematic signals, which can be selectively minimised with specially designed filters or smoothing processes. Filtering and smoothing may be accomplished in the motion capture software (e.g. Qualisys Track Manager or Vicon Nexus) or post-processing using biomechanics software such as Visual 3D (C-Motion Inc, Germantown, MD, USA) or with custom filters designed in MATLAB (The MathWorks, Inc, Natick, Mass., USA). Consideration

of the movement of interest and the characteristics of the signal will determine the approach to filtering or smoothing. Components of the signal that are not due to the process itself are considered noise (Winter, 2009). The components of the signal that relate to non-biological noise can be assessed using tools such as a fast Fourier transform (Winter, 2009). Smoothing high-frequency 'spikes' in the kinematic time-series, such as by a low-pass filter is an important step before data analysis (Robertson and Caldwell, 2014). A low-pass filter is that which selectively eliminates high-frequency noise in the data while leaving the low-frequency signal unchanged (Winter, 2009). This is the common approach for human movement data (Winter, 2009).

Measurement accuracy is also contingent on the placement of the reflective markers used for optical motion capture as well as IMU placement. Reflective markers affixed to the individual's skin represent the underlying bones. Together, individual markers can be integrated to represent the movement of segments, such as the pelvis or trunk by rigid body analysis (Söderkvist and Wedin, 1993). Accuracy, therefore, relates to the precision in which the markers track the intended bony prominences. Misplacement of markers can occur; intra- and inter-examiner variability in marker placement for pelvis and lower extremity bony prominences are described by Della Croce *et al.* (2005). The greatest inter- and intra-examiner variability in marker placement were reported for the pelvis landmarks (left and right anterior and posterior superior iliac spines), ranging up to 25mm. This is particularly pertinent for studies of the rider, as the three-dimensional kinematics of the pelvis are relevant to many questions regarding the rider's performance and horse-rider coordination.

Another source of error in motion capture and IMU is known as soft tissue artefact (STA). As previously stated, the markers affixed to the skin represent underlying bones. Therefore, STA is considered as the movement between the marker or IMU and the bone, caused by the displacement of the soft tissue during the trial (Camomilla, Bonci and Cappozzo, 2017). STA has a frequency content similar to the actual bone movement, therefore, is not attenuated by filtering, and should be considered within the context of the analysed movement (Leardini *et al.*, 2005). The extent of STA relates to the

movements analysed and the anthropometric characteristics of the participants, particularly, body mass index (BMI) (Camomilla and Bonci, 2020), and in the case of IMUs, the task-specific accelerations (Buganè *et al.*, 2014). The BMI is used as a measure of body composition, calculated as the quotient of the individual's weight (in kilogram) and the square of their height (in metres) (Nuttall, 2015). STA is a pertinent consideration for the measurement of pelvis kinematics. Reported STA for pelvis markers affixed directly to skin can range up to 17 mm in static positions and influence the pitch of the pelvis by up to 7.5°, depending on the subject's body mass index (BMI) (Camomilla, Bonci and Cappozzo, 2017). However, this error has not been quantified in the equestrian rider.

Only Engell *et al.* (2018) has assessed pelvic kinematics of riders with markers affixed to the skin, although their assessment was conducted on a static balance chair, rather than a live horse or simulator. Byström *et al.* (2009, 2010, 2015), Engell *et al.* (2016), Alexander *et al.* (2015) and Baillet *et al.* (2017) affixed markers to tight-fitting clothing. Alexander *et al.* (2015) reported that the tight-fitting leotards that the riders wore helped to reduce errors due to skin displacement. However, no current study has assessed this claim. The extent of STA during riding and the influence of clothing on marker accuracy is yet unknown, but could potentially influence the clinical relevance and application of evidence. The same is true for IMU placement; it is unknown whether suits with embedded IMUs (e.g. Xsens MVN suit) are considerably less accurate in their estimation of the rider's segmental kinematics than IMUs affixed directly to the skin during riding.

Measures from studies examining ranges of motion of the rider's pelvis are presented in Table 2.1. Each of these studies attempted to mitigate instrumental error with a filter and STA by instructing riders to wear tight-fitting clothing. Therefore, although the precision of the markers or IMU tracking of the underlying bony prominence or segment can be questioned, all studies employed strategies to mitigate the propagation of these sources of error and the data may be compared. It is worth noting that Eckardt *et al.* (2014) and Eckardt and Witte (2017) described pitch as left-right rotation over the sagittal axis and roll as forward-backwards rotations over the mediolateral axis. This is opposite to the

convention that defines pitch as the rotation about the mediolateral axis (nose up-down motion), and roll as the rotation about the sagittal axis (left-right rotation) (Robertson *et al.*, 2014). Therefore, caution must be exercised in the interpretation and comparison of these studies to others. To aid comparison of results between studies, angular displacement values that refer to anterior-posterior rotation will be referred to as pitch and left-right rotation will be referred to as roll in Table 2.1 and in this literature review.

Table 2.1. Comparison of pelvic ranges of motion (ROM) reported in studies measuring riders on live horses.

| Study | Subjects | Measurement | Gait | | Pitch (°) | Roll (°) |
|------------------------------|--|--|--|------|------------|-----------|
| Byström <i>et al.</i> (2010) | | | Collected walk | | 9.7 ± 2.0 | 5.6 ± 0.6 |
| Byström <i>et al.</i> (2009) | Seven high-level riders on a treadmill | Optical motion capture | Sitting trot | | 13.9 ± 2.2 | 5.1 ± 1.1 |
| Engell <i>et al.</i> (2016) | | | Actively cueing collected trot (sitting) | | 12.2 ± 1.5 | - |
| | | | Free trot (sitting) | | 10.8 ± 1.6 | - |
| Eckardt <i>et al.</i> (2014) | 10 professional dressage riders | IMU (17-sensor Xsens MVN suit) | Sitting trot | Pro: | 11.5 ± 0.9 | 4.0 ± 1.6 |
| | | | | Pro: | 11.5 ± 0.9 | 4.0 ± 1.6 |
| Eckardt and Witte (2017) | 20 riders: 10 professional dressage riders; 10 beginners | IMU (17-sensor Xsens MVN suit) | Sitting trot | Beg: | 12.3 ± 3.4 | 5.2 ± 3.1 |
| | | | | Pro: | 24.0 ± 5.9 | 5.5 ± 1.9 |
| | | | Left canter | Beg: | 23.1 ± 6.1 | 6.2 ± 1.7 |
| | | | | Pro: | 11.1 ± 3.6 | 3.1 ± 3.7 |
| | | | Walk | Beg: | 8.1 ± 4.1 | 3.6 ± 2.1 |
| Münz <i>et al.</i> (2014) | 20 riders: 10 professional dressage riders; 10 beginners | Two IMUs: one on the dorsal aspect of rider's pelvis, one on horse's girth strap | Sitting trot | Pro: | 14.8 ± 7.5 | 4.1 ± 1 |
| | | | | Beg: | 13.5 ± 4.1 | 6.5 ± 2.3 |
| | | | Right canter | Pro: | 18.5 ± 5 | 5.9 ± 1.9 |
| | | | | Beg: | 22.2 ± 7.8 | 5.4 ± 1.9 |

Legend: Beg: beginner; Pro: professional. All values reported in degrees.

These data suggest that the measures of pelvic pitch are similar between IMUs and motion capture. It is plausible that both Münz *et al.* (2014) and Eckardt and Witte (2014, 2016) used the same population of professional riders as identical population demographics are provided for the professional population in both studies (8 females, 2 males, full-time professional riders of their national federation, with a mean \pm SD age of 23.4 ± 5.3 years). Eckardt and Witte (2017) used the 17-sensor Xsens MVN suit, while Münz *et al.* (2014) measured pelvic pitch with only one IMU affixed to the dorsal aspect of the rider's pelvis. The pelvic pitch ROM in sitting trot measured with one sensor (Münz, Eckardt and Witte, 2014) was larger ($14.8 \pm 7.5^\circ$) than the ROM measured by the Xsens MVN suit ($11.5 \pm 0.9^\circ$). However, both ROMs were similar to those reported by Byström *et al.* (2009) in sitting trot ($13.9 \pm 2.2^\circ$) measured using optical motion capture. As seen in walking studies, a single sensor may overestimate pelvic tilt, due to soft-tissue artefact (Teufl *et al.*, 2019), or differences in placement and the initial inclination of the sensor (Buganè *et al.*, 2014). Certainly, further studies are needed to compare motion capture and IMU accuracy during riding. Finally, the same considerations for interpreting pelvic orientation should be given to studies using IMUs as those using motion capture: caution should be taken in the interpretation of the pelvic inclination, particularly when making inferences to the aetiology of back pain in the rider. The anterior or posterior pelvic tilt is clinically defined as the absolute anterior or posterior rotation of the pelvis relative to the neutral orientation (O'Sullivan *et al.*, 2006). As the sensors are calibrated on the subject and represent the rotation of the local coordinate system of the pelvis formed by the sensor(s), anterior tilt is not necessarily analogous to the clinical definition of anterior pelvic tilt, as is also true for posterior tilt.

2.1.4 Performance aspects of the rider's technique

Performance analysis in biomechanics seeks to define the position and orientation of body segments during the performance of a sport task to perform it effectively (Lees, 2010). In dressage, performance analysis can focus on the horse, rider, or both. Given the unique nature of equestrian sport, where the rider must consider the ethical implications of their riding and equipment use on the horse's welfare, and additionally, under the premise that improving the horse's welfare may lead to enhanced

performance, much of the focus of research investigating the rider's performance has analysed its effect on the horse. Central to this area of research has been the investigation of so-called 'rider asymmetries' (Symes and Ellis, 2009), which refer to frontal plane (left-right) imbalances in the rider's technique.

A commonly reported rider asymmetry is known as 'collapsing at the hip' (Gunst *et al.*, 2019; Blokhuis *et al.*, 2008), which refers to the side-bending of the rider's trunk in a given direction. Gunst *et al.* (2019) studied 80 riders on their own horses and reported that collapsing at the hip in sitting trot resulted in greater pressure on the side of the saddle contralateral to the side-bend, but if the rider shifted their trunk to one side without side bend, greater pressure was recorded on the side to which the rider shifted. They noted that there was a shift of the rider's force distribution to the left side of the saddle throughout and that there were significant differences in force measurements when taken in riders on the left and right reins. The left force bias was even stronger when the riders were performing sitting trot on the right rein. This indicates that the presentation and extent of rider asymmetry may be task-dependent. For example, in rising trot, Gandy *et al.* (2014) found greater right hip external rotation in 12 riders during the sit phase of rising trot.

In a rising trot, the rider alternately rises out of and sits into the saddle during successive diagonal stance phases. In a follow-up study, of 18 riders, Gandy *et al.* (2018) did not find significant differences between left and right hip flexion at the halt or during left rein rising trot but did find significantly greater flexion of the right hip on the right rein. Greater hip external rotation and hip flexion on the right would suggest that the rider is rising and sitting down and to the right during the rising trot. This agrees with Alexander *et al.* (2015) who reported that, before a taping intervention, 6/10 riders displayed right bias in pelvic obliquity (frontal tilt) and 9/10 riders had left trunk lateral flexion. This would reflect collapsing at the hip on the left and likely greater saddle pressure to the right, which contradicts the left bias observed by Gunst *et al.* (2019), although they did not assess saddle pressures directly. Similarly, Symes and Ellis (2009) reported a greater median range of motion for the right

shoulder in the walk, sitting trot and left canter and greater left axial rotation measured with video analysis. Individual factors may also contribute to asymmetry. Hobbs *et al.* (2014) assessed 122 riders on a static saddle horse and found significant decreases in left lateral bending ROM as competition level increased, as well as significant decreases as rider age increased.

There is potential for the rider to have an effect on the horse's movement pattern (Peham *et al.*, 2004) and to influence the horse's spinal loading and gait (Mackechnie-Guire *et al.*, 2018). There is undoubtedly a mutual interaction between horse and rider asymmetries (Gunst *et al.*, 2019). It is therefore difficult to ascertain the influence of the rider's own asymmetries on the horse-rider performance as well as their impact on the welfare of the horse. Individual factors, such as age, previous injuries and competition level may influence the manifestation of asymmetries in the rider. However, educated and competitive riders display asymmetries in their posture (Alexander *et al.*, 2015; Hobbs *et al.*, 2014) and movement of their pelvis (Engell *et al.*, 2018), yet successfully compete in dressage competitions. No known study has examined the influence of specific movement asymmetries on competition outcomes in the rider. Given that competitive riders can be asymmetrical in their movement, yet still compete in judged sports such as dressage, riders can possibly learn to manage their asymmetries to limit their effect on the outcomes of performance. As the measures, protocols and populations of the studies assessing rider asymmetries are so diverse, it is imprudent to make any definitive conclusions about the prevalence, and indeed, potential performance effects, of rider asymmetries on the horse. Consensus on a consistent methodology and protocol to assess rider asymmetries is needed.

Back pain is frequently reported in riders (Deckers *et al.*, 2020; Hobbs *et al.*, 2014; Greve and Dyson, 2013; Nevison and Timmis, 2013; Kraft *et al.*, 2009; Bird, 1996). Studies on the aetiology of low back pain (LBP) suggest that muscle endurance and weakness are greater influences of the development of pain than pelvic tilt or the degree of lumbar lordosis (Nourbakhsh and Arab, 2002). Indeed, dynamic assessments of the rider indicate that riders with back pain may have poor movement control of the

low back (Deckers *et al.*, 2020) and lower functional movement screen scores than the general population (Lewis *et al.*, 2019). Few studies have examined pelvic and spinal characteristics of riders in the sagittal plane, and even fewer have assessed the rider during dynamic tasks or directly during riding. Hobbs *et al.* (2014) assessed 122 riders' standing posture and a chartered physiotherapist characterised their sagittal spinal posture depending on its deviation from neutral. Most riders (59%) were either kyphotic/lordotic (31%) or normal (28%). When asked, only 32% of riders reported no pain. Of the 68% of riders that did report pain, the most prominent site was 'various' (25%), followed by the lumbar area (23%). Certainly, back pain could be a performance-limiting factor for riders. Two studies have seen successful increases in horse and rider performance outcomes following rider core (Hampson and Randle, 2015) and resistance band (Lee *et al.*, 2015) training programmes. Neither study assessed rider motor control or back pain directly, however, the increase in muscle strength and endurance measured by Lee *et al.* (2015) following the resistance band training programme is promising. Further studies should aim to develop dynamic rider assessment protocols and investigate factors that relate to the rider's movement proficiency and motor control on the incidence of back pain as well as performance outcomes during riding.

2.1.5 Future directions for measuring the kinematics of riders using motion capture

Data reporting kinematic measurements using motion capture on high-level riders mounted on horses in walk or trot on a treadmill (Engell *et al.*, 2016; Byström *et al.*, 2009, 2010, 2015) and a straight line (Terada, Clayton and Kato, 2006) give a basis for comparison of subsequent rider kinematic studies. However, when comparing to other results, the methods used to collect these data must be considered. The seven high-level riders analysed in three dimensions by (Byström *et al.* (2015, 2009, 2010) and Engell *et al.* (2016) were subjected to rigid body analysis as described by Söderkvist and Wedin (1993). Their pelvis rigid body was formed by the markers on the rider's sacrum and the left/right greater trochanters of the femur. Their trunk rigid body was formed by the markers on the sacrum, shoulder joints, and seventh cervical vertebra. The International Society of Biomechanics recommended pelvis coordinate system is formed by markers placed on the left/right anterior

superior iliac spines and virtual markers formed by lines intersecting these markers (Wu *et al.*, 2002). There may be significant inter-subject variability in the placement of the marker on the greater trochanter of the femur, which may cause undetected error propagation in the joint angle time-series, particularly when the total range of motion is $<10^\circ$ (Della Croce, Cappozzo and Kerrigan, 1999). Markers covering pelvis bony landmarks can be integrated into a rigid body representing the three-dimensional movement of the pelvis (Söderkvist and Wedin, 1993). The local coordinate system of the rigid body is assumed to be located at the centre of the points describing the centre of the rigid body and the pitch rotation relative to this coordinate system. As such, these rotations describe the relative anterior or posterior pitch of pelvis, but as previously mentioned, in the case of the pelvis they do not represent the clinical definition of anterior or posterior pelvic tilt. Therefore, the clinical relevance of the movements of high-level riders described by these studies must be taken with care. It is recommended that future studies use the standard pelvis coordinate system (Wu *et al.*, 2002) and thoroughly report data processing procedures to improve replicability.

2.2 The influence of skill on rider kinematics

The rider position, described in coaching texts produced by the British Horse Society (2011), describes the correct rider position in the saddle as the vertical alignment of the rider's ear, shoulder, hip and heel (shown in Figure 2.1). In theory, this position would place the rider's centre of gravity within the base of support, between their feet in the stirrups. In practice, this performance indicator of the rider is based on a static position and does not consider how the rider moves to absorb the movement of the horse during riding while steering and controlling the horse. It is acknowledged in these texts that the rider's position is developed with practice, however, little evidence exists of the rider's learning process. Only one study (Kang *et al.*, 2010) has examined the rider's skill acquisition, while several other studies have made inferences on the effects of rider experience by comparing riders of varying experience levels (Baillet *et al.*, 2017; Eckardt and Witte, 2017; Olivier *et al.*, 2017; Münz, Eckardt and Witte, 2014; Biau *et al.*, 2013; Lagarde *et al.*, 2005; Peham *et al.*, 2001).

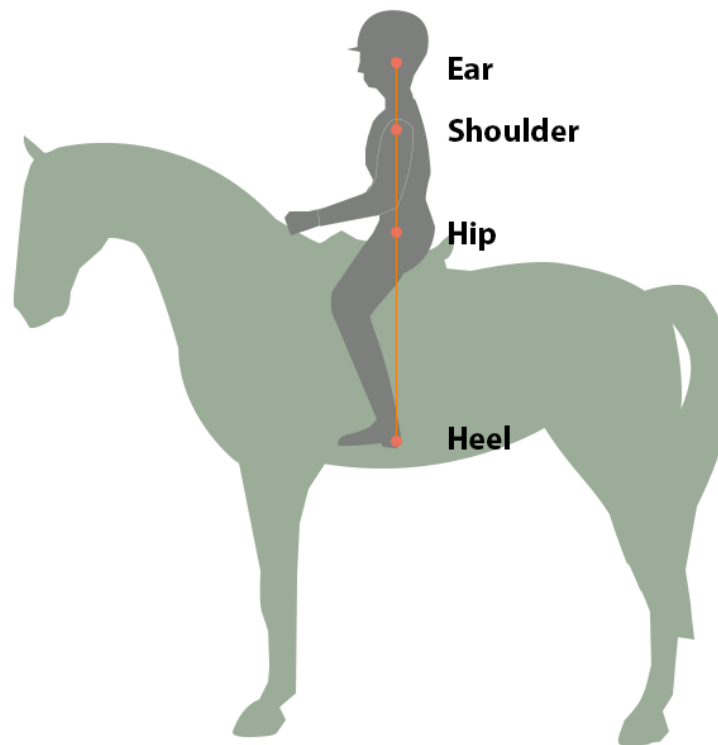


Figure 2.1. The correct rider position as described by the British Horse Society (2011). When seated in the saddle, the rider should adopt a position that aligns their ear, shoulder, hip and heel.

In equestrian sport, as the horse-rider combination is judged in performance, the rider's position should be functional and aesthetically pleasing. The rider must maintain control of the horse but also adopt an upright trunk, balanced, supple seat, straight (not hunched) shoulders, and still hands (German National Equestrian Federation, 2006). These attributes are thought to contribute to the rider's ability to achieve harmony with the horse, but also to give an elegant impression to the judge. It is accepted that the rider must develop their technique with experience. In addition, judges may identify the rider's experience level based on the aesthetics of their technique. For example, when judges categorised riders as beginner, intermediate or advanced riders, significant differences in the hip, knee and lower leg angles during riding were found (Schils *et al.*, 1993). Schils *et al.* (1993) found a significant interaction between the riders' hip angle and their skill level. Advanced riders had significantly greater hip angles than their beginner counterparts, indicating they sat closer to the vertical. When Schils *et al.* (1993) tested the interaction between ability and gait, advanced riders had

a significantly greater thigh angle (calculated as the angle between the thigh and a horizontal line bisecting the knee) in walk and rising trot only. They also found that advanced riders had significantly greater trunk angles in the rising trot and sitting trot. Advanced riders had significantly greater trunk angles than intermediate riders in sitting trot only. No significant interactions were found between ability and gait for the hip or knee angles. Schils *et al.* (1993) indicate that this identifies the thigh angle's influence on producing significantly greater hip angles between skill levels. In their study Schils *et al.* (1993) did not give information about the participant demographics including years of riding experience, so it is not known whether the riders categorised as beginners adopted riding positions categorised as such due to inexperience.

Only Kang *et al.* (2010) has undertaken a longitudinal study of riders from their first lesson to 24 weeks of riding tuition twice a week. The evidence presented by this study, and supported by others, suggests that the development of the rider's position and technique is gait dependent. The beginners' trunk orientation became more upright at walk throughout their lessons. By the 24th week of riding, beginner riders' trunk angles were not significantly different from those of their instructors at the walk. This agrees with Schils *et al.* (1993), who also did not find any significant differences between beginner, intermediate or advanced riders' trunk angles at the walk. In rising trot, however, both Kang *et al.* (2010) and Schils *et al.* (1993) found that beginner riders' had smaller hip angles compared to advanced (Schils *et al.*, 1993) or instructor (Kang *et al.*, 2010) riders. Riders may learn to conform to the desired trunk position at different stages in their learning for each gait; likely due to the differences in the horse's trunk oscillations, speed and ground reaction forces between the gaits.

The adaptations that facilitate the rider's upright trunk during riding are yet unclear, however, they are likely to relate to the ability of the rider's lumbopelvic-hip region to dissipate the inertial and passive forces induced by the horse's trunk movement during the gait cycle (de Cocq *et al.*, 2013). Riders may adapt their seat to the horse's movement at an early stage in their riding to keep their upper body and arms stable. Münz, Eckardt and Witte (2014) found no significant differences in the

pelvic range of motion of beginner (riding once per week for six years) and professional riders captured with an inertial measurement unit (IMU) placed on their pelvis. However, they did find significant differences in riders' minimum and maximum values, and these varied by gait. Riders moved through the same range of motion, but with significantly different start and end positions. There were significant differences between the riders' minimum value in walk (beginner: $8.3 \pm 10.4^\circ$; pro: $-3.1 \pm 10.3^\circ$), minimum and maximum in trot (beginner: min: $5.7 \pm 7.4^\circ$; max: $19.2 \pm 7.6^\circ$; pro: min: $-5.2 \pm 11.6^\circ$; max: $9.6 \pm 9.9^\circ$) and maximum in right canter (beginner: $20.9 \pm 8.2^\circ$; pro: $10.6 \pm 10.1^\circ$). Interestingly, these values suggest that professional riders sit more centrally in the saddle, while novice riders tilted their pelvis posteriorly, which is opposite to findings by Schils *et al.* (1993) and Kang *et al.* (2010), who found that novice riders had smaller hip angles and a forward trunk posture. It is possible that these differences resulted from the measurement technique, although they may be indicative of divergent participant characteristics, or even influenced by the saddle.

The hip angles are influenced by the position of the thigh, which may be dictated by the type of saddle (e.g. dressage or general-purpose) and its configuration (stirrup bar position, blocks, and flap configuration), as well as stirrup length (Bondi *et al.*, 2020; Roost *et al.*, 2020; Clayton *et al.*, 2018; Mackechnie-Guire *et al.*, 2018; Harman, 1999). Many riders purchase a saddle that is specifically constructed for their discipline of choice, for example, dressage or jumping. Specific dressage or jumping saddles are configured to allow the rider to assume the prescribed position for their discipline. Dressage saddles are constructed with a deep seat and long, straight flaps, which facilitate the rider's position that aligns the hip, shoulder and ankle vertically when the stirrup leather hangs vertically (Bondi *et al.*, 2020). The jumping saddle facilitates the rider's ability to stand in the stirrups with a longer, flatter seat so that they can follow the horse's movement over a fence by closing their hip angle when the horse reaches the peak of its flight arc over the jump (Bondi *et al.*, 2020). Common issues arising from improper saddle fit with regards to the rider include insufficient saddle seat area to accommodate the rider (Roost *et al.*, 2020), and imbalance of the legs due to stirrup bars that place the stirrups ahead or behind the vertical line connecting the rider's hip and ankle (Harman, 1999). The

former can influence the peak pressures underneath the saddle that are applied to the horse's back (Roost *et al.*, 2020) and cause discomfort to the rider.

Incorrect stirrup positioning can unbalance the rider, leading to a 'chair seat' (stirrups too far forward), where the rider's ankle is ahead of the vertical line from the hip, or cause the rider's legs to slip back (stirrups too far back) over a jump (Harman, 1999). Other factors such as the configuration of the saddle's panels (Clayton *et al.*, 2018) and the saddle's knee or thigh blocks (Bondi *et al.*, 2020) can influence the position of the rider, contributing or detracting from their stability and ability to follow the horse's movement. However, the saddle design and its dimensions must be considered on an individual basis to fit the horse and rider (Bondi *et al.*, 2020; Harman, 1999). Optimal saddle fit is subjective (Russell Guire *et al.*, 2017), and requires the balance of considerations of the horse's performance and comfort, and the rider's anatomy and their discipline specific-requirements (Harman, 1999).

The rider's shoulder and arm position are integral for maintaining a consistent bit contact through the reins. Schils *et al.* (1993) found that overall, advanced riders positioned their arm furthest away from the body; however, shoulder angle did not reach significance for the interaction between gait and ability. Kang *et al.* (2010) did not find significant differences between rider elbow or shoulder angles in the walk. In trot, beginner riders had significantly greater shoulder angle, but significantly smaller elbow angles in the rising trot at 12- and 24-weeks' tuition. The reciprocal relationship between the rider's shoulder and elbow angle, rein length and horse head and neck posture may be an influential factor in skill-linked differences (Terada, Clayton and Kato, 2006; Peham *et al.*, 2001).

Indeed, riders at the high levels of dressage aim to control the horse's head and neck position, so that the poll (the point between the horse's ears) is the highest point of the neck and a line subtended from the poll to the horse's nose to the horizontal is slightly greater than 90° (nose slightly in front of the vertical) (Fédération Internationale Equestre, 2017). The rider achieves stability of the horse's head position by exerting tension on the reins, however, the horse may respond with corresponding

movements of their head and mouth that vary individually (Eisersiö *et al.*, 2013). Therefore, the rider must be able to interpret the horse's behavioural cues and react accordingly to stabilise the horse's head and neck position (Eisersiö *et al.*, 2013), while also maintaining a consistent tension on the reins (Egenvall *et al.*, 2015) despite perturbations to their seated stability that occur during locomotion (Terada, Clayton and Kato, 2006). Given the complexities of the rider's ability to achieve and maintain a consistent head and neck position, it is unsurprising that Peham *et al.* (2001) found significant differences between novice and expert horse-rider coordination defined by the angle formed by the rider's trunk to the horse's bit. The expert rider coordinated their trunk-bit movements more consistently than the novice rider (Peham *et al.*, 2001). Therefore, the rider's arm technique may change with skill from simply controlling the horse at a basic level, to influencing the horse's head-neck posture.

2.2.1 Horse-rider coordination

Achieving a high level of coordination, known as 'harmony', between horse and rider is a key objective in dressage training (Kottas-Heldenburg and Fitzpatrick, 2014) and competition (Fédération Internationale Équestre, 2020). Although harmony is subjectively assessed in the dressage test, several studies have sought to quantify harmony using measures of horse-rider coordination. The approaches used to quantify harmony and populations used to compare rider skill level vary greatly between studies. Baillet *et al.* (2017) and Olivier *et al.* (2017) measured coordination as the discrete relative phase (DRP) between horse and rider or between the rider's segments. This measure quantifies the latency (in degrees) between the peaks of a segment's displacement in relation to another, such as the rider's trunk angle to an angle formed by the horse's sacrum and the vertical. The resulting DRP values can be qualitatively described as anti-phase if peaks occur in opposite timing, in-phase if they occur together, and out-of-phase if occurring between anti-phase and in-phase. When segments are oscillating together, they are most strongly attracted to in-phase or anti-phase relationships as these constitute the most stable spatiotemporal relationships between two moving parts (oscillators) (Scott Kelso *et al.*, 1981).

Olivier *et al* (2017) measured differences in inter-segmental coordination between the rider's cervical and lumbar spinal segments between Club (10.23 ± 6.02 years experience) and professional riders on a riding simulator in gallop, exposed to various visual conditions. Differences observed between Club and professional riders suggested that skilled riders develop out-of-phase cervical-lumbar coordination that deviates from pure anti-phase or in-phase coordination. Therefore, this suggests that riders' trunk coordination is developed with practice. This study did not include a measure of the relative phase between the rider's segments and the riding simulator, so it is unclear whether the professional riders' strategy resulted in greater harmony.

Their finding was similar to Lagarde *et al.* (2005), who presented the continuous angle of a novice and professional rider's trunk to the vertical during the sitting trot. The professional rider's trunk-vertical angle followed a consistent sinusoidal pattern, indicating they oscillated their trunk in time with the horse's stride. The novice rider maintained a consistent trunk-vertical angle for the first second of the trial, however, as it progressed, the pattern showed inconsistencies, indicating they did not adapt their trunk to the horse's stride. Indeed, experience may result in better coordination between the rider's trunk and the horse. Similarly, Baillet *et al.* (2017) measured the DRP between naïve and experienced riders' trunk on a riding simulator. They also concluded that riders, compared to non-riders, had better postural coordination as they maintained an anti-phase rider trunk-simulator phase relationship at all frequencies of oscillation tested, while non-riders changed from anti-phase at lower frequencies to out-of-phase at the maximal frequency.

Lagarde *et al.* (2005) is the only study to date that compared full-body (head, shoulder, elbow, wrist, hip, heel and toe) coordination between a professional and novice rider's segments and a horse (right hind hoof, fetlock, hock, forehoof, fore fetlock, carpal joint, cranial and caudal aspect of the sacrum, nasal bone and frontal bone) in sitting trot. The mean relative phase for all markers was compared with an analysis of variance between riders, which indicated that the mean relative phase was significantly different between riders ($p < 0.05$). Both riders aligned their hip, knee and toe with the

horse, however, the professional rider dissociated their heel and toe movement. This relates to an ankle strategy to accommodate the horse's movement. The professional rider also displayed greater consistency in their trunk movement across trials, and their trunk movement was frequency-matched to the vertical displacement of the horse's sacrum. The professional rider had significantly less relative phase variability than the novice. Greater variability of the novice's movements was observed during the extension phase of the stride, which corresponded with increased variability of the time interval between limb extensions.

When ridden by the professional rider, the horse was significantly less variable; however, it is unclear which aspect of the rider's technique influenced variability most. Mean relative phase and variability increased from the novice rider's shoulder to wrist. Contact with the horse's mouth acts as a feedback loop: inconsistencies in the rider's contact with the bit may increase the variability of the horse's head-neck position, which has a corresponding influence on the flexion-extension, lateral bending and axial rotation of the horse's lumbar spine (Rhodin *et al.*, 2005). In addition, variability of rein tension can influence the horse's behaviour when ridden, resulting from or leading to less rideability (the ease and comfort with which a horse can be ridden) (König von Borstel and Glißman, 2014). However, a lack of technique to adequately dissipate the horse's movement within the rider's legs and lower back may have influenced the trunk variability, which in turn precludes consistency in the bit contact.

Similar results were presented by Peham *et al.* (2001), who compared a professional and novice rider riding the same 20 horses in sitting trot. Horse-rider coordination was assessed as the resultant vector of the angular displacement of the angle formed by the rider's head and back to the horse's head and its first two derivatives plotted in phase space. The length of the resultant vector was not significantly different between the professional and novice rider, indicating no significant differences in the relationship between the angular displacement, velocity and acceleration. There was a significant difference between the angular deviation, which describes the variability of the movement (pro: $11.5 \pm 1.4\%$; novice: $13 \pm 2.8\%$). The score given to each trial by a dressage judge was correlated to the

angular deviation (pro: $r = 0.63$; novice: $r = 0.87$). A stronger correlation between judges scores and the angular deviation for the novice, rather than the professional, may reflect the judges' ability to identify performances with less harmony more consistently when they are produced by a novice rider, but difficulty identifying smaller deviations in harmony produced by a professional rider. This is similar to the findings of Blokhuis *et al.* (2008), who found that judges were equivocal in their assessment of the nuances of experienced riders' riding position. The smaller angular deviations between the rider's trunk and the horse's mouth produced by the professional rider (Peham *et al.*, 2001) may have been more difficult to perceive, which underlines the subjectivity of dressage judging. The angle chosen by Peham *et al.* (2001) conceivably defines the stability of the rider's trunk and the rider's connection with the horse's bit. Competitive or professional riders aim to train the horse with a fixed head-neck position; however, this may not be the goal of the novice rider. Moreover, the novice rider rode the horse significantly slower than the speed the horse selected when it was trotted without a rider, which indicates that the novice rider rode the horse below its optimal stride frequency. Conversely, a professional rider may be required to ride many different horses and may more easily adapt to the horse's preferred stride frequency to decrease the overall variability of the performance.

Finally, Eckardt and Witte (2017) and Münz, Eckardt and Witte (2014) used cross-correlation to quantify horse-rider coordination. Eckardt and Witte (2017) compared the cross-correlation of the pitch and roll of the horse's trunk to the rider's pelvis between 10 professional (33.9 ± 11.9 years experience, 33.9 hours of practice per week) and 10 beginner riders (3.2 ± 1.9 years experience, 2.6 ± 1.4 hours of practice per week). They found no significant interaction between gait and skill level for the measure of cross-correlation, which describes the time lag between the maximal value of the angular displacement of the horse's trunk relative to the rider's pelvis.

Significant differences in skill level for roll and pitch between the rider's segments and between horse and rider are intuitive: each gait has a unique series of footfalls and forces that the rider must accommodate. Münz, Eckardt and Witte (2014) observed time lags between the rider's pelvis and the

horse's trunk quantified by cross-correlation. The highest time lag between the rider's pelvis and the horse's trunk was 23% of the stride duration in lateral rotation at the trot. However, they also observed significant differences between the lateral rotation range of motion (ROM) of the novice and expert riders' horses and corresponding differences in the riders' pelvis ranges of motion. The horses ridden by the beginner riders had a mean lateral rotation ROM of $6.3 \pm 1.8^\circ$ in trot, while the professionals' horses had a mean lateral rotation ROM of $4.6 \pm 1.3^\circ$. Accordingly, the mean lateral rotation ROM for the beginner riders' pelvis was $6.5 \pm 2.3^\circ$ and $4.1 \pm 1.0^\circ$ for the professional riders. As riders aim to follow the movement of the horse, and given the significant differences between the population of horses ridden by the beginners and professionals in trot, the significant differences in lateral rotation ROM reported by Münz, Eckardt and Witte (2014) may reflect horse variability rather than skill-linked differences.

2.2.2 Future directions to analyse the effect of rider skill on riding performance

Deriving actionable performance indicators in equestrian sport is complicated by the inherent variability of horse and rider performance. The body of evidence suggests that professional or expert riders are more aligned with the horse's movement (Lagarde *et al.*, 2005), less variable (Peham *et al.*, 2001), display consistent movement patterns in changing frequencies (Baillet *et al.*, 2017), adapt their technique to changing visual conditions (Olivier *et al.*, 2017), and ride the horse nearer to its natural gait rhythm than novice or beginner riders (Peham *et al.*, 2001). They also sit up straighter in the saddle (Schils *et al.*, 1993), and use their ankle as a damper, to move their trunk coincidentally to the horse (Lagarde *et al.*, 2005).

The literature has presented several techniques to compare riders in field and simulation settings. Many of the studies (Gandy *et al.*, 2014, 2018; Eckardt and Witte, 2017; Münz, Eckardt and Witte, 2014) described in the previous sections used video or IMUs to capture data and presented a scalar value to describe the rider's position in the saddle. Accordingly, many studies describe the rider's 'posture' (Kang *et al.*, 2010; Lovett, Hodson-Tole and Nankervis, 2005; Schils *et al.*, 1993), although the mean value may not adequately describe how the rider moves to accommodate the horse's

movement. For example, the novice rider studied by Lagarde *et al.* (2005) achieved an upright trunk angle in a sitting trot but overall lacked resonance with the horse. Therefore, there should be an important distinction in equestrian sport, between rider posture and technique. The term posture relates to the '*appropriate vertical relationship between body segments to counteract the forces of gravity and thus allow the maintenance of upright stance*' (p. 1, Massion and Woollacott (2004)). The term *technique* is related to the pattern and sequence of movements and is often used to describe sports performance (Lees, 2010). It follows that the technique is comprised of technical skills that must be learned and developed with experience. The body of evidence supports progression in technical proficiency with riding technique; however, once riders reach a certain level of proficiency, differences between individuals in some segments may be insignificant. Indeed, judges agreed less frequently on the classification of intermediate riders (67% agreement) than a beginner (81%) and advanced (95%) (Schils *et al.*, 1993). Therefore, future studies of rider technique should be assessed with continuous methods, relative to a performance outcome, such as horse-rider coordination.

2.3 The use of simulators in equestrian research

Research into specific questions about the rider is challenging given the high level of interaction between horse and rider and variability between horses. Several studies of the rider have examined riders on their own horses (e.g. Byström *et al.* (2009) and Münz, Eckardt and Witte (2014)), while others use one horse for all riders (e.g. Alexander *et al.* (2015) and Terada, Clayton and Kato (2006)). There can be significant variability between horses ridden by different groups of riders, for example, the horses ridden by beginner riders studied by Münz, Eckardt and Witte (2014) had significantly less anterior-posterior trunk rotation than those ridden by professionals. Therefore, the forces and oscillations that the two groups were exposed to were not consistent. While mounting all riders on the same horse can help to standardise the task, there can be significant differences between a given horse's gait when ridden by different riders, as seen by Peham *et al.* (2001). In addition, there are ethical implications of using a single horse for repeated trials that may limit the number of riders that can be studied at a time.

To overcome some of these issues, riding simulators have been used to answer specific research questions pertaining to the rider (Kim *et al.*, 2018; Baillet *et al.*, 2017; Clayton, Smith and Egenvall, 2017; Olivier *et al.*, 2017; Prin-Conti *et al.*, 2017; Cha, Lee and Lee, 2016; Park, Lee and Lee, 2015; Temcharoensuk *et al.*, 2015; Biau *et al.*, 2013). Questions regarding the rider's inter-segmental coordination during simulated riding (Olivier *et al.*, 2017) and differences in coordination and energy expenditure between naïve and experienced riders (Baillet *et al.*, 2017) have been probed with simulators. In addition, the three-dimensional kinematics of the rider's back (Biau *et al.*, 2013), the effect of simulated riding on low back pain (Yoo *et al.*, 2014), the effect of simulated riding on balance and gait (Cha, Lee and Lee, 2016; Lee, Lee and Park, 2014), the effect of the rider's weight on a specific riding simulator (Prin-Conti *et al.*, 2017), and symmetry of rein tension during simulated riding (Clayton, Smith and Egenvall, 2017).

Various riding simulators are commercially available with different characteristics and features. Simulators aim to produce a consistent oscillation that mimics the gait-specific trunk movements of a live horse. One study to date has illustrated significant and specific differences between a galloping horse and a specific model of a racing simulator (Walker *et al.*, 2016). There are significant differences between the locomotion of a live horse and the movement of a riding simulator. For one, the riding simulator produces a looped oscillation on a stable, fixed base, while the live horse moves forward with ground reaction forces produced each stance phase (Clayton and Hobbs, 2019a). These limitations notwithstanding, the use of riding simulators has distinct advantages, including reduced concerns regarding the ethical and safety implications of exposing novice and naïve (Baillet *et al.*, 2017; Clayton, Smith and Egenvall, 2017) or aged (Kim *et al.*, 2018; Mitani *et al.*, 2008) populations to a horse. Similarly, questions about the rider's field of vision can be addressed using a simulator without concern for safety (Olivier *et al.*, 2017; Cha, Lee and Lee, 2016). Finally, the use of simulators permits a wide use of lab-based measurements, such as respiratory gas exchanges (Baillet *et al.*, 2017). There are inherent limitations of the use of simulators in research. First, the simulator produces a more consistent oscillation than a live horse, thereby reducing the variability of the oscillation that to which

the rider must adapt. Second, when studying the interaction between rider and riding simulator, one must be cognizant of the absence of the mutual interaction between rider and simulator. This is particularly relevant when assessing rein pressure or leg cues. Like studies using a treadmill rather than overground running, there may be many advantages that support the use of a riding simulator to answer specific research questions about the rider, although further comparative studies are needed to fully understand their limitations and advantages with relation to a live horse.

2.4 Dynamical systems in sport

Coordination is a crucial aspect of horse-rider performance. On the most basic level, a total lack of coordination between horse and rider can unseat the rider, leading to injury and even death. Conversely, higher levels of coordination are associated with better marks awarded by a dressage judge (Lagarde *et al.*, 2005). Therefore, the study of horse-rider coordination is intertwined in both rider safety and equestrian competition performance. Horse and rider can be described individually and collectively as complex, dynamical systems: they have many interacting parts on multiple scales that can be unpredictable and can self-organise into stable or unstable states (Davids, Button and Bennett, 2008). Both horse and rider have a multitude of options of joints, limbs, muscles and motor units that can be integrated to perform a given motor task. These are known as biomechanical degrees of freedom (DoF). In most cases, the number of DoF available exceeds the number required to perform a given task which makes many redundant (Bernstein, 1967). Therefore, to perform a movement, the elements of the dynamic system assemble into functional groups, called synergies (Button, Wheat and Lamb, 2014). The functional groups are co-dependent; they constantly exchange information to create an order that is context-specific and can change when necessitated by critical fluctuations in the system (Passos, Araújo and Davids, 2013). Each system has a tendency towards preferred, stable states, called attractor states (Scott Kelso, 2009a). Systems typically have multiple stable states and instability is observed as the system transitions between them (Button, Wheat and Lamb, 2014). Transitions can occur spontaneously in response to changes in the constraints imposed on the system. Constraints that influence coordinative structures can be classed as relating to the participant,

environment and task (Davids, Button and Bennett, 2008). As the rider's perception of the environment (e.g. competition, arena) and task (e.g. a circle in collected canter, jumping) can be drastically different between individuals, perceptual information shapes the coordination outcomes to meet the unique demands of the performance. The participant's perceptions of the constraints and possibilities of movement for a given task ('affordances' (Jones, 2003)) can change with development and experience (Orth, Davids and Seifert, 2016). Therefore, learning can alter the organisation of the DoFs to meet the task.

Bernstein (1967) viewed motor learning as the mastery of redundant degrees of freedom. As they learn to produce a given movement, humans first rigidly fix DoF to limit segmental rotation and translation and reduce the dimensionality of the system (Kay, 1988). In the second stage, more DoF is incorporated, and in the third stage, the performer utilises and exploits (rather than resists) the passive forces that result from the interaction between the performer and the environment (Ko, Challis and Newell, 2003). Changes in the coordination patterns with experience reflect the task goals and constraints, therefore, there can be considerable variability between individuals in skill acquisition (Ko, Challis and Newell, 2003) and between the characteristics of coordination employed by experienced performers to meet a given task (Busquets *et al.*, 2013).

Over the last two decades, an abundance of research has examined aspects of coordination, coordination variability and skill acquisition from a dynamical systems perspective in a variety of sports (for a review see Button, Wheat and Lamb (2014)). Comparatively fewer studies have focussed on the horse and rider. Therefore, the evidence presented here to explain the concepts of coordination, coordination variability and the computational methods used to quantify both will expand outside of the equestrian disciplines.

2.4.1 Coordination variability

The traditional view of variability as either detrimental to performance or as insignificant noise has been challenged in recent years (Newell *et al.*, 2006). Variability can be measured between individuals

or within an individual and between trials. The expert-novice research paradigm and prevalence of pooling data to report means and standard deviations suggests that the average trial of a skilled individual represents the optimal performance. However, the existence of an optimal performance across individuals and the practice of pooling data, particularly among expert athletes, is disputed (Glazier and Mehdizadeh, 2019; Button, Wheat and Lamb, 2014; Hamill *et al.*, 2006; Davids *et al.*, 2003). Instead, recent studies have sought to understand the role of coordination variability as either functional or detrimental to performance and its relationship to skill level (Mo and Chow, 2019; Cazzola, Pavei and Preatoni, 2016; Wilson *et al.*, 2008; Scholz, Schoner and Latash, 2000), and the association between measures of coordination variability and injury (Hamill, Palmer and Van Emmerik, 2012; Seay, Van Emmerik and Hamill, 2011).

2.4.1.1 The role of coordination variability in sport performance

In sport coaching, repetitive practice is traditionally viewed as a way of reducing the athlete's technique variability. Through corrections, the athlete is driven towards an 'optimal' model (Davids, Button and Bennett, 2008). Certainly, if the athlete displays high variability in their successful completion of a sporting task (e.g. variability in the number of successful shots on goal), this can be viewed as determinantal to performance. From a metabolic perspective, high variability can be more costly (Billat *et al.*, 2001). However, from a dynamical systems perspective, investigation of the structure and nature of coordination variability and its contribution to the success of the task can reveal interesting insights that describe how individuals integrate unique and changing constraints to meet a performance goal.

Coordination variability measures can describe how an athlete accomplishes a task goal and adapts to fluctuating constraints. This concept is illustrated nicely by the seminal work of Arutyunyan, Gurfinkwl and Mirskii (1968), who found that skilled marksmen conserved the accuracy of their shot by increasing coordination variability in their upper arm joints. Several other studies have reported similar findings, in pistol shooting (Scholz, Schoner and Latash, 2000) and javelin throwing (Morriss, Bartlett and Fowler, 1997). In these cases, the coordination variability observed in skilled individuals

was functional, allowing the athlete to adapt to ever-changing constraints to meet the performance goal. Different between-athlete coordination variability profiles of World Championship javelin medallists observed by Morriss, Bartlett and Fowler (1997) is an indication that world-class performances may not adhere to an 'optimal' template and that measures of between-individual coordination variability can yield results that explain how the athletes manage their individual and environmental constraints to meet a specific task goal. Additionally, athletes may not reproduce the exact same technique on every repetition, showing varying degrees of inter-trial variability (Bauer and Schöllhorn, 1997). Indeed, how athletes respond to variations in the internal and external constraints to meet a task demand relates to the concept of degeneracy (Edelman and Gally, 2001). Degeneracy describes how individuals with many differences in their constraints and affordances can produce equivalent outcomes. To summarise, functional variability can be defined as coordination variability that is associated with high or consistent achievement of a performance outcome. Individual analyses (Lamb and Pataky, 2018; Schöllhorn *et al.*, 2002; Button *et al.*, 2000) can elucidate functional coordination variability which is important to understand how talented individuals produce their peak performances.

Functional coordination variability may help elite athletes to maintain accuracy throughout the performance or adapt to changing environments, but for the novice individual qualifying, the role of variability as functional or detrimental is nuanced. Increased coordination variability at the early stages of learning may occur due to inadequate adaptations to the task constraints (Davids *et al.*, 2003). Several studies have observed higher coordination variability in novice, compared to experienced athletes in running (Mo and Chow, 2019), basketball shooting (Button *et al.*, 2003), gymnastic longswing (Busquets *et al.*, 2013) and during sitting trot on a horse (Lagarde *et al.*, 2005; Peham *et al.*, 2001). However, other studies have observed less coordination variability in unskilled versus skilled athletes in the triple jump (Wilson *et al.*, 2008). According to Newell's (1985) motor learning framework, based on Bernstein's (1967) DoF proposition, coordination variability should increase with practice. In the first stage of learning, novices form rigid intersegmental coordination

patterns to 'freeze' DoF, but with practice, they learn to incorporate more DoF into their movement and eventually exploit the passive inertial forces generated by the movement (Davids, Button and Bennett, 2008). Differential effects of skill level on coordination variability suggest that it is task-specific, and the value of coordination variability depends on the segments analysed. In tasks requiring high accuracy or stability but with higher levels of environmental variability, such as bouncing a ball or standing on an oscillating platform, coordination variability is decreased in the segments closest to the ball (Broderick and Newell, 1999) or platform (Ko, Challis and Newell, 2003) with experience. Athletes adapt coordination variability to the task and environment, and the positive influence of this adaptation on the performance outcomes or rank in competition increases with experience. Therefore, the role of variability in sport performance should be interpreted with a task-specific lens.

2.4.2 Methods to analyse coordination and coordination variability

The interaction between two moving parts, for example, between thigh and shank or indeed between horse and rider, can be assessed using quantitative measures of coordination. These can be characterised as discrete or continuous techniques. The selection of the ideal technique depends on the aims and hypothesis of the research and the nature of the signals to be analysed. Several techniques have been used, including the discrete relative phase, continuous relative phase, vector coding and cross-correlation.

2.4.2.1 Discrete relative phase

The discrete relative phase (DRP) is a point estimate of the latency between an event in one segment relative to another (Wheat and Glazier, 2006). It is the most commonly used coordination measure in equestrian studies (Baillet *et al.*, 2017; Olivier *et al.*, 2017; Lagarde *et al.*, 2005). In these cases, the DRP measured the difference in degrees of the relative timing between the maximal displacement of a horse segment to a rider segment in the motion cycle of a riding simulator (Baillet *et al.*, 2017; Olivier *et al.*, 2017) or stride cycle of a horse (Lagarde *et al.*, 2005). This technique is most appropriate when the relative timing at a key event is functionally important. For example, the relationship between subtalar inversion-eversion and knee flexion-extension during stance phase in a human running stride

is commonly assessed using DRP (Dierks and Davis, 2007; Hamill, Bates and Holt, 1992), as when the knee reaches maximal flexion, the subtalar joint should have reached eversion (Hamill, Palmer and Van Emmerik, 2012). As the DRP is an angle in the range of $0^\circ \leq \varphi \leq 360^\circ$ it is a circular variable and circular statistics are needed to compute the mean or a measure of variance (Batschelet, 1981).

The advantage of DRP is that the signals of interest do not need to be manipulated beyond standard processing (e.g. filtering and time-normalisation) before calculation. The prevailing assumptions of the DRP are that the signals of interest are sinusoidal and have a one-to-one frequency (Wheat and Glazier, 2006). Calculation of the DRP when the signals contain multiple peaks or in signals without well-defined peaks is not advised (Van Emmerik, Miller and Hamill, 2014).

2.4.2.2 Continuous relative phase

Many signals deriving from biomechanical analyses do not meet the assumptions of the DRP; they may not have a distinct peak, or they have multiple peaks per cycle. In this case, the DRP is not a suitable estimate of the coordination over the entire cycle. There are many cases where the state of the coordination over the entire cycle is of interest. The continuous relative phase (CRP) quantifies the coordination of two oscillators over the entire stride cycle or predefined period of movement. Many studies have used the CRP to assess intersegmental coordination during sporting movements including ice skating (Mazurek *et al.*, 2020), lifting (Zehr, Howarth and Beach, 2018), golfing (Lamb and Pataky, 2018), riding (Wolframm, Bosga and Meulenbroek, 2013), race walking (Cazzola, Pavei and Preatoni, 2016), and the gymnastic longswing (Busquets *et al.*, 2013). It is also a common measure used to assess coordination during gait (Van Emmerik and Wagenaar, 1996) and to discriminate between injured and healthy individuals during gait and movement (Hamill, Palmer and Van Emmerik, 2012). As the coordination variability increases before a transition to a more stable state, assessing the coordination throughout a cycle or movement can provide insight on stability and transitions in a movement (Scott Kelso, 1995).

The CRP is not free from assumptions; it too assumes that the signals are sinusoidal (Lamb and Stöckl, 2014). Many biomechanical signals defy this assumption, therefore additional steps must be taken to produce an accurate calculation of the CRP. The CRP is calculated as the difference between phase angles calculated from the phase-plane. The phase plane is a plot with the displacement angle on the horizontal axis and the angular velocity on the vertical axis (an example plot shown in Figure 2.2). The phase angle for each segment is then calculated by obtaining the four-quadrant inverse tangent angle relative to the right horizontal for each time point and the CRP is calculated as the difference in phase angle between the two segments at each point within the cycle (Van Emmerik, Miller and Hamill, 2014).

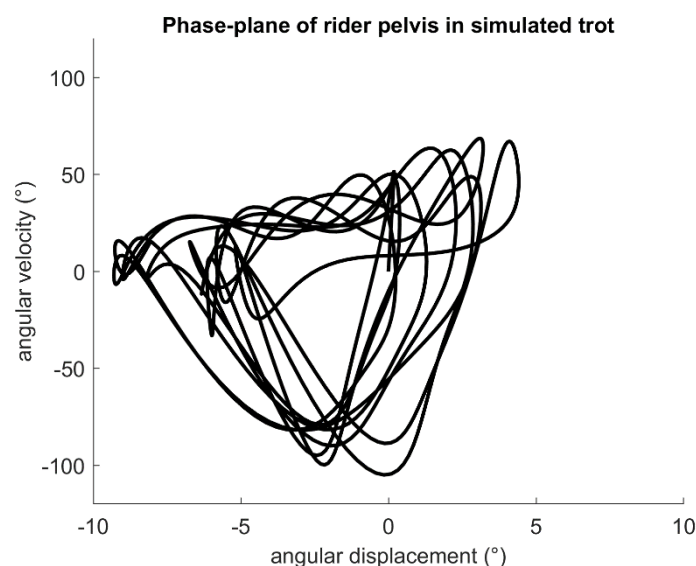


Figure 2.2. Phase-plane to describe the pitch rotation of an example rider's pelvis over several cycles of simulated medium trot, sitting. The angular displacement is plotted on the x-axis and the angular velocity on the y-axis.

If the data are not sinusoidal Lamb and Stöckl (2014) suggest the following steps to reduce error in the calculation of the CRP:

1. Normalisation to centre the data around zero.

2. Instead of directly calculating the CRP from the phase plane (displacement and velocity), transforming of the signal (typically the displacement) into a complex analytical signal with the Hilbert transform (Lamb and Stöckl, 2014).
3. Calculation of the CRP from the phase angles calculated in the complex plane.

The process of normalisation has been discussed thoroughly in the literature (Lamb and Stöckl, 2014; Van Emmerik, Miller and Hamill, 2014; Kurz and Stergiou, 2004; Hamill *et al.*, 1999; Burgess-Limerick, Abernethy and Neal, 1993). Whether the CRP is calculated from the phase-plane or by the Hilbert transform, several authors advocate for some normalisation of the data before calculation (Lamb and Stöckl, 2014; Van Emmerik, Miller and Hamill, 2014; Hamill *et al.*, 1999; Burgess-Limerick, Abernethy and Neal, 1993). However, others (Kurz and Stergiou, 2004) oppose it, as it changes the original topology of the data. When the CRP is calculated from the phase-plane, van Emmerik, Miller and Hamill (2014) argue that normalisation is necessary as the amplitude of the velocity data is much greater than the displacement, which would bias the subsequent calculation of the phase angle. Lamb and Stöckl (2014) suggest that normalisation is necessary to remove frequency artefacts, and centring the data so that zero represents the midpoint between the minimum and maximum values so that the data are centred around the origin of the phase-plane (or complex plane if calculated with Hilbert transform).

Two common equations are used for normalisation, one where the angular position and velocity are normalised to the unit circle using the minimum and maximum values (Van Emmerik and Wagenaar, 1996), and the other where the descriptive value of 0 is maintained by allowing the angular velocity to float below or above -1 or +1 on the vertical axis (Lamb and Stöckl, 2014; Burgess-Limerick, Abernethy and Neal, 1993). If zero has a qualitative meaning in the signal of interest, then the second normalisation technique is preferable (Hamill, Haddad and McDermott, 2000). If the CRP is calculated from the complex plane, using the Hilbert transform, normalisation is recommended (Lamb and Stöckl, 2014).

The CRP is commonly calculated over several cycles within a trial. As the data are normalised to the minimum and maximum values, an inspection of the data is important to determine whether the data can be normalised to the trial minimum and maximum or normalised cycle-by-cycle, using the local minimum and maximum. Hamill, Haddad and Mcdermott (2000) suggest that normalising the data to the trial minimum and maximum may help to preserve the original data. However, if the trial contains outliers, this process may distort the other cycles within the trial. If the outliers are deemed valid, the data can be normalised on a cycle-by-cycle basis to retain the outlier cycles but protect against distortion. This decision is particularly relevant if the coordination variability is of interest to the research question. Cycle-by-cycle normalisation does not influence the coordination variability (Hamill, Haddad and McDermott, 2000). It is evident that the normalisation process is not trivial, and the nature of the signals and research question must be considered when choosing the appropriate method.

Signals deriving from human biomechanical data are seldom sinusoidal. Several studies have described the potential error when calculating the CRP based on the phase-plane with non-sinusoidal data (Lamb and Stöckl, 2014; Peters *et al.*, 2003). To circumvent the sinusoidal assumptions of the CRP, alternative methods for calculating the CRP have been proposed, including the relative Fourier phase (Lamoth *et al.*, 2009) and the Hilbert transform (Lamb and Stöckl, 2014). The Hilbert transform has become commonplace in the analysis of coordination in sport (Lamb and Pataky, 2018; Lames, 2006; Palut and Zanone, 2005). The Hilbert transform shifts the phase of the signal by 90° using the fast Fourier transform, to create a complex signal where the imaginary component is analogous to an estimate of the velocity of the original signal (Boashash, 2016; Lamb and Stöckl, 2014). Therefore, the original signal is transformed into a complex analytical signal. The phase angle is then calculated from the complex plane as previously described as the four-quadrant inverse tangent angle relative to the right horizontal, and the CRP as the difference between the two phase angles at each time point (Lamb and Stöckl, 2014).

If calculating the CRP with the four-quadrant inverse tangent, the phase angles and resulting CRP values take on values in the range of $-360^\circ \leq 0^\circ \leq 360^\circ$. Values near 0° and $\pm 360^\circ$ indicate in-phase movement (moving together), those near $\pm 180^\circ$ indicate anti-phase movement (moving opposite) (Van Emmerik, Miller and Hamill, 2014). As the CRP is a circular variable and because values between $\pm 180^\circ$ and $\pm 360^\circ$ have the same qualitative meaning, circular statistics must be used to calculate descriptive statistics (Batschelet, 1981). Alternatively, the CRP can be limited to the range between 0° and 180° after calculation (Van Emmerik, Miller and Hamill, 2014) to permit the use of linear statistics. However, by limiting the range of the CRP values to positive values, the descriptive value of the sign to indicate the lead or lag of the signals is lost. Experts are equivocal as to whether the CRP describe lead or lag. van Emmerik, Miller and Hamill (2014) argue that as the data are normalised and the CRP is derived from two phase angles, the lead-lag interpretation is potentially invalid. Kurz and Stergiou (2004) submit that a lead-lag relationship can indeed be inferred as the phase angles are subtracted from one another. No conclusive evidence exists to support or deny either stance. Therefore, if quantifying the lead-lag relationship between oscillators is the primary aim of the research, other methods that analyse this directly, such as cross-correlation (Van Emmerik, Miller and Hamill, 2014) should be employed.

Coordination variability is frequently calculated from the CRP for sporting movements (Mazurek *et al.*, 2020; Lamb and Pataky, 2018; Cazzola, Pavei and Preatoni, 2016; Wolframm, Bosga and Meulenbroek, 2013). The coordination variability can be calculated as the standard deviation of the mean CRP between several trials or cycles (Wolframm, Bosga and Meulenbroek, 2013). However, this is only valid if the CRP does not have large fluctuations throughout the cycle. Instead, it is proposed that the CRP variability be maintained as a continuous variable, by calculating the circular standard deviation between each sample of the cycles contained within the trial (Van Emmerik, Miller and Hamill, 2014). This is particularly relevant if the CRP variability is used to investigate the stability of the coordination, or transitions between stable states indicated by increased variability within a cycle.

2.4.2.3 Vector coding

The relative motion between two joints or segments can be plotted as angle-angle diagrams and quantitative measures of the coordination derived using a technique called vector coding. Angle-angle diagrams have been used to illustrate horse-rider coordination (Münz, Eckardt and Witte, 2014) although they did not employ vector coding. Other studies have quantified pelvis-thorax coupling (Zehr, Howarth and Beach, 2018), running mechanics (Dierks and Davis, 2007) and the triple jump (Wilson *et al.*, 2008) using vector coding. The angle-angle plots present the angular displacement for one segment on the x-axis and another on the y-axis. From these plots, the coupling angle can be determined by the angle subtended from a vector adjoining two successive time points (Van Emmerik, Miller and Hamill, 2014). This results in a coupling angle that can range from 0° to 360°. The angles can be assigned to bins, each with a specific qualitative interpretation such as in-phase, anti-phase, segment extension and flexion (Chang, Van Emmerik and Hamill, 2008). The interpretation proposed by Chang, Van Emmerik and Hamill (2008) seems intuitive, particularly for anatomically coupled segments like the leg and could produce insights that are easier for clinicians to understand than the CRP or DRP (Wheat and Glazier, 2006). The disadvantages of vector coding are; (1) the data must be evenly spaced and the trajectories must contain the same number of data points; (2) it cannot capture the coordination between multiple trajectories at a time, meaning only pair-wise comparisons of the cycle is possible; (3) only spatial information is provided; temporal information is not considered; (4) vector coding is more sensitive to slight changes in displacement, particularly that caused by closer data points during transitions and artefacts in the assessment of variability might ensue (Wheat and Glazier, 2006).

2.4.2.4 Cross-correlation

Cross-correlation has been used to assess coordination between horse and rider (Eckardt and Witte, 2017; Münz, Eckardt and Witte, 2014) and for coordination between events in human gait (Nelson-Wong *et al.*, 2009). The strength of this technique is in its ability to characterise the spatiotemporal similarity of two signals without the need for normalisation processes. To perform cross-correlation

on two signals, one signal is shifted iteratively and the Pearson's correlation coefficient calculated at each step (Nelson-Wong *et al.*, 2009). This produces a time-series of Pearson r values to represent the relationship between the two signals. Cross-correlation is a suitable technique to investigate lead-lag relationships between two signals (Van Emmerik, Miller and Hamill, 2014).

2.5 Quantifying and making inferences on kinematic time-series

Kinematic data collection using IMUs and optical motion capture can produce a large amount of data for a single trial. The researcher must then choose an appropriate method to group, reduce and test these data to the relevant parameters to meet the aims and objectives of the study. Studies of the equestrian rider typically reduce variables to a trial mean or a separate mean of stance and swing phases of the horse's gait (Walker *et al.*, 2020; Lovett, Hodson-Tole and Nankervis, 2005; Schils *et al.*, 1993). Hypotheses are then tested using linear statistics. Reducing continuous time-series to zero-dimensional (0D) scalar values (example: mean, maximum, minimum, standard deviation) can make group comparisons straightforward. However, if the objective of the study is to compare the techniques of riders between groups, such as experience level, one-dimensional (1D) analyses that consider the entire time series is more suitable for several reasons. Firstly, from a pattern recognition perspective, it is easier to recognise a person when walking, rather than standing still (Schöllhorn *et al.*, 2006), which means that the single value does not capture the dynamic qualities of the movement. Additionally, discrete values only represent the rider's technique at a pre-determined point in time or a mean value, rather than capturing the fluctuations throughout the stride that may serve as the crucial differentiating factor between groups.

Secondly, from a statistical perspective, reduction of complex time series to discrete values and performing multiple tests on the same dataset introduces significant biases (Knudson, 2017). Also, many studies do not make hypotheses relating specifically to these regions of interest, instead, reducing the scope of the null hypothesis after seeing the data, leading to an increased risk of incorrectly rejecting the null hypothesis (Pataky, Robinson and Vanrenterghem, 2013). Linear statistics

assume the independence of data; however, continuous time series are highly correlated, and thus discrete measures sampled from a continuous time series violate the assumption of independence (Pataky, Robinson and Vanrenterghem, 2013). This is particularly relevant when correcting for multiple comparisons. Common corrections such as the Bonferroni adjustment assume independence between multiple tests, which is violated by OD measures of 1D data and can increase the likelihood of false negatives (Naouma and Pataky, 2019). To overcome these challenges, several options for 1D hypothesis testing and exploratory data analysis have risen to prominence in biomechanics literature in the last two decades. These include statistical parametric mapping (SPM1D), principal component analysis (PCA), and self-organising maps (SOM). Each procedure has its unique strengths and potential applications within equestrian research are discussed in turn.

2.5.1 Statistical parametric mapping

As highlighted, bias and error can be introduced when reducing continuous data to scalar values or testing hypotheses with multiple data samples from a single trial. An alternative approach is to test hypotheses by comparing full waveforms. One-dimensional statistical parametric mapping (SPM1D) is conceptually like conventional linear statistics, with options to perform analyses of variance (ANOVA), t-tests and regressions on continuous data. SPM1D uses Random Field Theory to generate inferences on a particular dataset (Pataky, Robinson and Vanrenterghem, 2013). It has been used in sport to assess golfers' kinematics (Lamb and Pataky, 2018) and handball (Serrien *et al.*, 2015), among others. Although this technique has vast potential for horse-rider analyses, no known study has used SPM1D for hypotheses focussed on the rider, although several studies have used SPM1D for hypotheses focussed on the horse (Hobbs *et al.*, 2018; Hobbs, Robinson and Clayton, 2018; Oosterlinck *et al.*, 2013; Oomen *et al.*, 2012).

Before analysis, continuous data must be normalised so that all the trajectories are the same length. Trajectories should be smoothed appropriately; there is some suggestion that data with non-uniform smoothness (e.g. noise that varies between trials) may have a small influence on the resulting p-value but not the null hypothesis rejection decision (Pataky *et al.*, 2019). When considered in the context of

a t-test (although the F statistic of an ANOVA is analogous), the SPM1D analysis procedure can be described as: (1) a t-value is computed at each time point separately, to give a continuous t trajectory (SPM{t}); (2) the critical test statistic (threshold) is computed by Random Field Theory; (3) if the SPM{t} trajectory crosses the critical threshold due to differences in waveform smoothness, the null hypothesis is rejected (Robinson, Vanrenterghem and Pataky, 2015). The null hypothesis for SPM1D tests relates to the probability that supra-threshold clusters could have been produced by a random field process with the same temporal smoothness (Pataky, Robinson and Vanrenterghem, 2018). Supra-threshold clusters relate to areas of the continuous data where the null hypothesis is rejected. These can be visualised in SPM1D plots, which has great functional utility to biomechanical studies: the timing of the supra-threshold clusters may be interpreted functionally.

SPM1D has great potential use in horse and rider studies, specifically for hypothesis testing. As previously stated, a major limitation of previous rider studies is the use of means and other discrete measures to summarise the dynamic movement or coordination across the horse's gait cycle. SPM1D codes are available open-source, for MATLAB and Python (spm1d.org), and the graphical interpretation of the results (see Chapter 6) should facilitate future whole-curve analysis for horse and rider.

2.5.2 Principal component analysis

Kinematic analyses can produce many continuous time series, which can be segmented into a set of n trials or movement cycles for n participants. Studies often aim to characterise the key features of a movement or differences in features between groups. This involves reducing these large data sets to a smaller number of variables that capture the variation within or between individuals, depending on the research question at hand. Principal component analysis (PCA) can determine the features of the time series that explain the greatest amount of variation (Deluzio and Astephen, 2007). The data points within a given continuous data set are correlated. PCA transforms these correlated variables into uncorrelated principal components (PCs) that represent the features of variation within the original dataset (Deluzio *et al.*, 2014). It has been used extensively in biomechanical analyses of many

sporting movements and inter-segmental coordination (Mazurek *et al.*, 2020; Cushion *et al.*, 2019; Mears, Roberts and Forrester, 2018; Forner-Cordero *et al.*, 2005; Ko and Newell, 2001). Several studies have used PCA to analyse continuous time-series of horse or rider movement. Witte, Schobesberger and Peham (2009) analysed the gait of 13 horses using PCA, comparing walk, trot and canter when ridden with a side-saddle or English saddle. Engell *et al.* (2018) used PCA to analyse the frontal plane trunk and pelvis movement of riders rocking on a static balance chair. Solé *et al.* (2013) analysed the kinematic features of trot strides in three different Iberian horse breeds. Finally, Elmeua González and Šarabon (2020) analysed the muscle activation patterns in recreational and professional riders during the walk, rising trot and canter.

PCA is a useful statistical tool to reduce the high complexity of biomechanical datasets to a small number of variables for further statistical analysis and interpretation. The study aims and objectives determine the structure of the PCA analysis. For example, an analysis of multiple segments may perform the PCA on each segment individually (Deluzio and Astephen, 2007) or incorporate all segments into the PCA (Forner-Cordero *et al.*, 2005). Similarly, the entire groups' trials may be analysed together, or individual PCAs may be performed (Cushion *et al.*, 2019). Regardless of the approach, the PCA procedure is the same. PCA transforms the data into a new coordinate frame with an orthonormal basis, defined by the data itself (Cushion *et al.*, 2019). The PCA results in principal component (PC) scores, which are the transformed variables that represent the features of the original data, loading vectors (also called 'coefficients'), which are the basis vectors of the data, and the percentage of variance explained by each PC score (Deluzio *et al.*, 2014). As PCA retains the spatiotemporal characteristics of the data, the loading vectors and PC scores can be plotted for qualitative interpretation of the functional characteristics described by each feature, depending on the study aims (Brandon *et al.*, 2013). As PC scores are uncorrelated variables, they may be used in further statistical analyses. For example, Mazurek *et al.* (2020) assessed whether the features of the continuous relative phase of hockey players' lower limbs were related to their skill level using hierarchical linear models on the PC scores.

In many cases, only a small number of (<5) PC scores are needed to quantify greater than 90% of the variation in the dataset (Engell *et al.*, 2018; Lamothe *et al.*, 2009; Witte, Schobesberger and Peham, 2009). However, some evidence suggests that PC scores that account for smaller amounts of variance may have clinical significance in human lower extremity kinematics (Phinyomark *et al.*, 2015). Phinyomark *et al.* (2015) suggest that sorting PC scores by effect size, rather than by variance explained, could be more sensitive when determining the effect of an intervention on running gait mechanics. Further studies are needed to analyse the difference between these two methods of determining PC score retention for subsequent statistical analysis.

2.5.3 Self-organising maps

Statistical parametric mapping and PCA are useful for scenarios where the groups are known or to test hypotheses. As previously stated, much of the equestrian research has used the novice-expert paradigm. This methodology assumes that all expert riders exhibit similar, more optimal techniques within the group than novices. This approach is limited; it is based on expected behaviours, therefore, no new classifications can be obtained (Schöllhorn *et al.*, 2006). Several studies have shown that equestrian coaches do not agree on classifications of the rider's technique (Blokhuys *et al.*, 2008; Schils *et al.*, 1993), which is a testament to the high dimensionality of the horse-rider interaction during riding. Exploratory approaches for kinematic data include those that group data based on its features, rather than an *a priori* grouping or hypothesis. Self-organising Kohonen maps (SOM) are a type of artificial neural network that take high-dimensional data and plot them into a low-dimensional map of neurons that are clustered together based on their similarity (Bauer and Schöllhorn, 1997). The raw waveforms are mapped onto the neurons; therefore, similar patterns can be grouped. Visualisation of the SOM itself can be useful to determine movement patterns (Lamb *et al.*, 2007). Subsequent cluster analysis of the SOM can separate trials or individuals into functional groups (Hoerzer *et al.*, 2015).

Only one known study has applied a SOM approach to a horse or rider question. Schöllhorn *et al.* (2006) applied a SOM to investigate a group of horse's movement patterns with a professional and novice rider. Their findings suggest that SOMs can quantify how the rider influences the horse. Their

study did not investigate the rider's movements, however, there is much potential to explore, or; not only the influence of the rider on the horse but how riders adapt to different horses, the effect of skill and many equipment-related questions.

2.6 Summary

This literature review has identified that, while there have been significant advances in the study of the equestrian rider over the last two decades, many questions remain. Particularly, the influence of skill or competition level on the rider's kinematics is questioned. Inherent to the performance of the horse-rider combination in equestrian dressage is the concept of harmony, which is defined as the coordination between horse and rider. Harmony has been analysed using the dynamical systems theory framework. From this perspective, coordination and coordination variability is influenced by constraints, which can arise from the individual, their environment and their perception of the task. Coordination and coordination variability can be measured in myriad ways, however, the suitability of the method to the research question itself must be considered. These methods can give rise to rich information describing the continuous coordination over a movement cycle. The features of these continuous time-series may have functional relevance, however, typically studies choose to analyse discrete variables which may introduce bias and neglect important features. Several options for continuous data analysis exist to facilitate hypothesis testing or to discover new classifications by pattern recognition.

Based on the previous literature highlighted in this review, the thesis will employ methods to analyse the kinematics of the rider using motion capture and a riding simulator. The thesis will consider potential error incurred when using motion capture by analysing the difference between markers affixed to clothing or directly to skin using the approach outlined by Camomilla and Bonci (2020). Each study will hone in on questions that remain in the field of equestrian rider research. As riders have been assessed in static (Guire *et al.*, 2017; Hobbs *et al.*, 2014) and dynamic (Eckardt and Witte, 2017; Terada *et al.*, 2017; Alexander *et al.*, 2015; Münz, Eckardt and Witte, 2014; Wolfram, Bosga and

Meulenbroek, 2013; Byström *et al.*, 2009, 2010; Lagarde *et al.*, 2005; Peham *et al.*, 2001) conditions, the relationship between these measures as they pertain to the rider's pelvis and pelvic posture will be assessed. Many studies (Eckardt and Witte, 2017; Alexander *et al.*, 2015; Münz, Eckardt and Witte, 2014; Byström *et al.*, 2009, 2010) have focussed on the rider's pelvis, therefore, this approach is justified. Coordination between horse and rider has been identified as a key aspect of the dressage judging criteria (e.g. harmony) (British Dressage, 2021d).

This review has identified several studies that have reported measures of horse-rider coordination (Baillet *et al.*, 2017; Eckardt and Witte, 2017; Münz, Eckardt and Witte, 2014; Lagarde *et al.*, 2005; Peham *et al.*, 2001). However, as covered in the review, key questions remain as to the influence of competition level on horse-rider coordination. The underlying concepts defining coordination and coordination variability are outlined in Section 2.4, alongside several approaches to analyse coordination. In keeping with the theme of dynamic analysis of the female equestrian rider that unites the studies within this thesis, the coordination between the riding simulator and the rider will be analysed throughout the cycle using the continuous relative phase. Pertinent considerations for this analysis presented by Lamb and Stöckl (2014) will be incorporated into the methods of the study. The continuous relative phase produces a time-series to describe the coordination throughout the movement cycle (Wheat and Glazier, 2006). As outlined in Section 2.5, reducing the time-series to a discrete value may result in loss of information (Knudson, 2017). Statistical parametric mapping, principal component analysis and self-organising maps are tools that may be used to analyse continuous data. The application of these methods is discussed in detail in Section 2.5. Each of these approaches will be used to answer key questions relating to the rider's coordination to the riding simulator, variability of the coordination between the simulator and rider and the trunk-pelvis kinematics during simulated riding. Together, the studies in this thesis will give a comprehensive understanding of the rider's pelvis during simulated riding, the influence of competition level, and the characteristics of simulator-rider coordination throughout the cycle.

3. General Methods

The data used in the analysis of each study was collected for five data collection sessions held between November 2018 and October 2019. Data analysis was ongoing throughout this period. Ethical approval was granted by the University Ethics Committee. The application and approval are contained within Appendix A. Riders provided signed informed consent and filled out a general questionnaire. These are contained within Appendix A and further details are described in subsequent sections of this chapter. The data collection was performed in the Margaret Giffen Rider Performance Centre at Hartpury University, Gloucester, UK. Riders were tested on a riding simulator (Event Simulator, Racewood, Tarporley, UK) using motion capture cameras (Miquis M3, Qualisys AB, Gothenburg, Sweden). The full procedure is described in this chapter and analysis of the data is described within each experimental chapter.

The data from the five data collections were used to answer the specific hypotheses posed by each study. As stated in Chapter 1, the overarching aim of the thesis was to investigate the dynamic technique of the female equestrian rider. Within this overall aim, specific questions were asked of the data set using methods rationalised by the research question and detailed in Table 3.1. The studies were structured from a preliminary static analysis of the rider on the riding simulator (Chapter 5) to three dynamic analyses, using tools to analyse continuous data (Chapter 6-8). Coincidentally, the analysis procedures were developed to investigate the practical consideration of motion capture with tight-fitting clothing on the riding simulator (Section 4.2) and continuous compared with discrete analysis of the relative phase between the simulator and rider (Section 4.3).

Table 3.1. Simplified aims, hypotheses and analysis methods for each experimental chapter. Full details to describe and justify the rationale, methods and results are available in each chapter, indicated by the page number in the far-right column.

| Study | Study aims | Hypothesis | Analysis methods | Page |
|--------------------|--|---|--|------|
| Chapter 4 | | | | 95 |
| Section 4.2 | <ul style="list-style-type: none"> - To investigate the effect of affixing markers to clothing, compared to directly on the skin overlying the rider's pelvis on: <ul style="list-style-type: none"> - Marker position error. - Rigid body error. - To investigate the influence of rider body mass index (BMI) on the marker position error and rigid body residual. | It was hypothesised that affixing the markers on the trousers and increased rider BMI will increase the error compared to affixing markers directly to the skin. | <p>Marker position error quantified as:</p> <ul style="list-style-type: none"> - The root mean square amplitude and amplitude components, and the peak-to-peak amplitude of the three-dimensional marker trajectories. <p>Rigid body error quantified as:</p> <ul style="list-style-type: none"> - The residual of the rigid body. <p>Statistical test:</p> <ul style="list-style-type: none"> - Mann-Whitney U tests: <ul style="list-style-type: none"> - Condition (skin/trouser) on marker position error and rigid body residual. - BMI on marker position error and rigid body residual. | 96 |
| Section 4.3 | <ul style="list-style-type: none"> - To detail the steps required for accurate continuous relative phase (CRP) calculation as per Lamb and Stöckl (2014). - To compare the measures of simulator-pelvis and simulator-trunk coordination variability obtained by CRP and the discrete relative phase (DRP) in simulated medium trot, sitting. | It was hypothesised that there would be significant differences between the coordination variability of the simulator-trunk and simulator-pelvis quantified by the CRP and DRP. | <p>CRP:</p> <ul style="list-style-type: none"> - Calculated using the Hilbert Transform as described by Lamb and Stöckl (2014). <p>DRP:</p> <ul style="list-style-type: none"> - Calculated as the latency between the rider's peak trunk or pelvis pitch and the vertical displacement of the riding simulator. <p>Coordination variability:</p> <ul style="list-style-type: none"> - Quantified as the mean circular standard deviation of these measures. <p>Statistical test:</p> <ul style="list-style-type: none"> - Paired-samples <i>t</i>-tests: <ul style="list-style-type: none"> - CRP and DRP variability for simulator-pelvis and simulator-trunk couplings, respectively. | 110 |
| Chapter 5 | <ul style="list-style-type: none"> - To explore whether patterns of pelvic tilt were related to rider competition level. - To examine whether the association between the rider's pelvic tilt in their static, seated position and during riding. | It was hypothesised that riders would show common patterns of pelvic tilt related to competition level. | <p>Pelvic variables:</p> <ul style="list-style-type: none"> - Mean pelvic tilt, ROM, minimum and maximum pitch. <p>Statistical tests:</p> <ul style="list-style-type: none"> - One-way ANOVA: <ul style="list-style-type: none"> - Mean pelvic tilt by gait and competition level. - Independent Samples Kruskal-Wallis tests: | 124 |

| | | | | |
|------------------|--|--|--|------------|
| | <ul style="list-style-type: none"> - To describe the characteristics of the rider's range of pelvic pitching motion (ROM), including. total mean ROM, minimum and maximum - To compare mean pelvic tilt assessed in walk, sitting trot, left canter and right canter. | | <ul style="list-style-type: none"> - Competition level by pelvis ROM, pitch minimum and maximum, respectively. - Spearman's Rank-Order correlation tests: <ul style="list-style-type: none"> - Halt pelvic posture, minimum pitch, maximum pitch, and ROM. | |
| Chapter 6 | <ul style="list-style-type: none"> - To investigate the influence of segment, competition level and gait (medium or extended trot) on the coordination variability of the rider's segments (head, trunk, pelvis and foot) to the vertical displacement of the riding simulator. | <p>It was hypothesised that there would be differences due to international or national competition level on the coordination variability between the rider's head, trunk, pelvis or foot in pitch, relative to the vertical displacement of the riding simulator in simulated medium and extended trot.</p> | <p>Coordination variability</p> <ul style="list-style-type: none"> - The CRP was calculated up to 10 simulator cycles as per Section 4.3 for the couplings between the vertical displacement of the riding simulator and the pitch of the rider's head, trunk, pelvis, and foot. - The circular standard deviation for the simulator-segment CRP was calculated between cycles at each time node to yield a continuous measure of coordination variability within the riding simulator's movement cycle in medium and extended trot. <p>Statistical tests:</p> <ul style="list-style-type: none"> - Statistical parametric mapping (SPM) repeated measures ANOVA: <ul style="list-style-type: none"> - Coordination variability by segment, competition level, and gait. - SPM <i>t</i>-tests <ul style="list-style-type: none"> - Coordination variability by segment. - Coordination variability by gait. | 139 |
| Chapter 7 | <ul style="list-style-type: none"> - To quantify and explain the functional significance of the features of the simulator-pelvis coordination in medium and extended trot. - To assess whether differences in the features of the coordination occurred due to competition level - To investigate whether the rider's coordination patterns significantly changed between simulated medium and extended trot. | <p>It was hypothesised that there would be differences between the features of the simulator-pelvis coordination due to competition level and gait.</p> | <p>CRP:</p> <p>The simulator-pelvis coordination was quantified as the CRP of the pitch of the pelvis relative to the vertical displacement of the simulator as per Lamb and Stöckl (2014).</p> <p>Statistical tests:</p> <ul style="list-style-type: none"> - Principal component analysis (PCA): <ul style="list-style-type: none"> - The features of the simulator-pelvis coordination were quantified using PCA. Scores were extracted for principal components needed to quantify 95% of the variability. - Linear mixed model: <ul style="list-style-type: none"> - Significant differences between the features of coordination quantified by principal component scores were tested using a linear mixed model with a fixed effect for competition level and a random effect for gait. | 155 |

| | | | | |
|---|---|---|---|-------------------|
| <p>Chapter 8</p> | <ul style="list-style-type: none"> - To identify different strategies in the pitch displacement of the rider's trunk and pelvis in simulated medium trot using self-organising maps (SOM) and <i>k</i>-means clustering. | <p>It was hypothesised that several groups would exist with characteristic kinematic profiles that could be described quantitatively.</p> | <ul style="list-style-type: none"> - Trunk and pelvis pitch trajectories: <ul style="list-style-type: none"> - Rider trunk and pelvis pitch trajectories were extracted for up to 10 cycles of medium trot (sitting) on the riding simulator. - Statistical tests: - Self-organising map (SOM): <ul style="list-style-type: none"> - The SOM was trained on the normalised and scaled cycles of trunk and pelvis pitch trajectories. - K-means clustering: <ul style="list-style-type: none"> - Rider movement cycles were clustered based on their proximity in the SOM using <i>k</i>-means clusters. | <p>174</p> |
| <p>Legend: CRP: continuous relative phase, DRP: discrete relative phase, SPM: statistical parametric mapping, PCA: principal component analysis, SOM: self-organising map.</p> | | | | |

Inclusion and exclusion criteria were developed to meet the aims and objectives of each study. These are detailed in Section 3.2.1. In addition, where the influence of competition level was tested in Chapters 5-7, the definition of the competition level categories used, the number of participants, and participant characteristics are detailed in Table 3.4 and Section 3.1.2. Finally, the data collection and processing steps are detailed in Section 3.2 and Section 3.3.

3.1 Participants

Volunteers were solicited for five data collection sessions held between November 2018 and October 2019 at the Rider Performance Centre at Hartpury University, Gloucester, UK.

3.1.1 Participant inclusion and exclusion criteria

The inclusion/exclusion criteria for the overall dataset are defined in Table 3.2. The participant inclusion and exclusion criteria were developed to meet the aims of the study questions, which broadly pertained to the riders' pelvic kinematics and the influence of competition level, among other factors. A convenience sampling strategy was used, whereby participants volunteered for one of the five data collection sessions and were included if they met the inclusion criteria. Using a convenience sample can introduce bias; generalisation to the greater population of female competitive dressage riders is undertaken with caution, relative to a random sample, as it is not known whether the convenience sample adequately represents the larger population (Cresswell and Cresswell, 2018). In the present study, riders needed to be able to attend the Hartpury Rider Performance Centre for the data collection, while meeting the inclusion criteria. While the introduction of bias is inherent to convenience sampling, this sampling strategy is common in biomechanical studies, given the cost and logistical implications of seeking a truly random sample (Vagenas, Palaiothodorou and Knudson, 2018).

Table 3.2. Participant inclusion and exclusion criteria for factors that would potentially influence the rider's kinematics.

| | Inclusion | Exclusion |
|---------------------------------|---|---|
| Age | Adults over 18 years of age | Minors under 18 years of age |
| Biological sex | Biological females | Biological males |
| Competitive history in dressage | At least three results in British Dressage or international (FEI) competitions within the last 12 months before data collection | Less than three results in British Dressage or international (FEI) dressage competitions within the last 12 months before data collection |
| Injury | No current injury that precluded participation in normal riding activities | A current injury that precluded participation in normal riding activities |

It should be noted that previous studies of competitive riders, such as Münz, Eckardt and Witte (2014) and Eckardt and Witte (2017) sampled riders from a single riding school, or riders participating in a training camp (Guire *et al.*, 2017; Hobbs *et al.*, 2014). As the data collection for the studies in this thesis took part over a series of dates over 11 months, a variety of different riders, with different histories, backgrounds and competitive experiences, training under different coaches and riding different horses volunteered for the study. Therefore, while the generalisation of these results to the general population must be taken with care, it is also possible that the present sampling strategy allowed greater diversity of riders than sampling on one occasion from a single source.

The participant inclusion/exclusion criteria were comprised of age, biological sex, competitive history in dressage and injury (Table 3.2). Volunteers were included if they were adults, aged 18 years or older so that they could give their own informed consent (sample informed consent in Appendix A). As the rider's pelvis was measured in each study, and given potential anatomical and functional differences between the male and female pelvis (Lewis *et al.*, 2017), including greater anterior pelvic tilt in females, relative to males during gait (Cho *et al.*, 2004), only biological female riders were included in the data collection. In addition, as Chapter 5, 6 and 7 address questions about the rider's competition

level, riders were included if they had at least three results in British Dressage (BD) or international (FEI) competitions within the last 12 months before data collection.

At least three results in affiliated dressage competition the last 12 months preceding data collection was deemed as the minimum inclusion criteria to solicit riders whose main discipline was dressage and to generate a sample population of riders who regularly competed in dressage. It must be noted that the initial study (Chapter 5) and first data collection categorised riders based on three results in the last six months before data collection, however, this was expanded to 12 months in subsequent studies/data collections for greater inclusivity. Riders self-reported their competition results and these were verified on the British Dressage database (British Dressage, 2021b).

The aims of studies 5, 6 and 7 pertained to the effect of competition level on the rider's kinematics, therefore, assessing the rider's competition level was important to the participant inclusion/exclusion criteria. Riders self-reported their competition level in a questionnaire (Appendix A) as the highest level in which they had at least three results in the last 12 months preceding the data collection. Hobbs *et al.* (2014) is the only known biomechanics study to categorise riders based on their competition level; other studies that have analysed competitive riders (e.g. Byström *et al.* (2010, 2009); Münz, Eckardt and Witte (2014); Eckardt and Witte (2017) and Olivier *et al.*, (2017)) did not split riders into groups based on their competition levels, rather they analysed the group of riders as a whole (e.g. Grand Prix riders analysed by Byström *et al.* (2010, 2009)) or split riders based on their riding experience rather than competition level (e.g. beginner and professional analysed by Münz, Eckardt and Witte (2014); Eckardt and Witte (2017); and Olivier *et al.* (2017)). Hobbs *et al.* (2014) also used self-reported competition level via a questionnaire to group riders into competition level groups, however, they did not require a minimum number of results at that level. As competition level is a factor analysed in studies 5, 6 and 7, assigning riders based on the highest level with three results would ensure that riders were assigned to the competition level group that most accurately represented their current level.

Riders were included if they did not have any current injury that would prevent them from riding. Some details regarding the rider's previous injury history and prevalence of pain were obtained in the pre-data collection questionnaire, however, the questionnaire was developed before the first data collection (November 2018). In the year following the first data collection, the research questions were developed and narrowed down to those described in the Introduction (Section 1.0) that focussed solely on the influence of competition level on the rider's kinematics. In addition, the visual analogue scale used to determine the severity of pain was not deemed to be clinically relevant or specific to accurately assess back pain in riders; off-horse movement tests such as those described in Deckers *et al.* (2021) should be used to assess rider back pain and dysfunction. Questionnaire data that was deemed irrelevant to the data analyses contained within the studies of this thesis were securely deleted from the participant records and only data that was used in the study was kept for further analysis.

Riders signed informed consent and ethical approval was granted by the Hartpury University Ethics Committee. All riders completed a participant information form with information regarding their competition history, exercise regime, previous injuries and other demographic information. Example copies of informed consent and participant information sheets can be found in Appendix A. In total, 52 riders volunteered and met the inclusion criteria (overall mean \pm SD age 32 ± 12 years, height 1.66 ± 0.07 m, and mass 61.5 ± 8.1 kg). Participants from the overall dataset were used within the five studies according to the inclusion criteria set out in each study, availability of the riders' data at the point of data analysis, and upon inspection of the quality of the kinematic measurements. In-depth description of the aims of the studies relative to the inclusion criteria are described in Table 3.3.

Table 3.3. Simplified aims (refer to study for full details), inclusion criteria, number of participants included and additional information for the six experimental studies contained within this thesis.

| Chapter | Aims (refer to study for full details) | Inclusion criteria | Number of participants included | Additional information |
|---------------------------|--|--|---------------------------------|------------------------------|
| Chapter 4: Section 4.1 | To compare the measures of coordination variability obtained by CRP and DRP. | Three results at British Dressage Medium or higher in last 12 months preceding data collection. | 28 | Same population as Chapter 6 |
| Chapter 4: Section 4.2 | To investigate whether markers affixed to clothing, compared to directly on the skin, significantly increases the marker position error and its influence on the calculation of pelvic tilt | Four riders captured with markers affixed directly to the skin covering the pelvis matched by body mass index with four riders from the overall dataset. | 8 | |
| Chapter 5 | To explore whether patterns of pelvic tilt are related to competition level, to examine whether there is a relationship between pelvic tilt in their static seated position and during riding and describe the kinematics of the pelvis during simulated walk, trot and canter (left/right). | Three results at any British Dressage or FEI level in the last six months preceding data collection. | 35 | |
| Chapter 6 | To investigate the influence of segment, competition level and gait (medium or extended trot) on the coordination variability of the rider's segments to the riding simulator. | Three results at British Dressage Medium and above, including FEI levels. Competition level groups must be balanced in number for ANOVA. | 28 | |
| Chapter 7 | To quantify and explain the functional significance of the features and changes of coordination between medium and extended trot; assess whether differences in the features of coordination occurred due to competition level. | Three results at British Dressage Preliminary and higher, including FEI levels. | 40 | Same population as Chapter 8 |
| Chapter 8 | To use self-organising maps and <i>k</i> -means clustering to separate riders' trunk and pelvis angular displacement in the sagittal plane into functional groups during simulated medium trot, sitting. | Three results at British Dressage Preliminary and higher, including FEI levels. | 40 | |

3.1.2 Participant characteristics

The participant characteristics for each experimental chapter are outlined in Table 3.4.

Table 3.4. Participant characteristics for each study. Age in years, mass in kilograms and height in metres are the mean \pm SD.

| Chapter | Participants | Age (years) | Mass (kg) | Height (m) |
|-----------------------------------|---|------------------|----------------|-----------------|
| Chapter 4: Section 4.1 | 28 riders (BD Medium to FEI Grand Prix) | 33.9 \pm 11.8 | 63.0 \pm 7.8 | 1.67 \pm 0.07 |
| Chapter 4: Section 4.2 | Markers affixed to trousers (n = 4) | 27.3 \pm 4.1 | 66.5 \pm 5.7 | 1.69 \pm 0.05 |
| | Markers affixed directly to skin (n = 4) | 30.5 \pm 6.9 | 63.0 \pm 5.4 | 1.65 \pm 0.09 |
| Chapter 5 | Advanced riders at any FEI level (n = 9) | 28.8 \pm 11.5 | 66.1 \pm 8.2 | 1.64 \pm 0.06 |
| | Intermediate (BD Medium, Advanced Medium or Advanced) (n = 15) | 31.9 \pm 11.6 | 61.6 \pm 8.6 | 1.56 \pm 0.04 |
| | Novice (BD Novice, Prelim and Elementary) (n = 11) | 27.8 \pm 11.2 | 58.2 \pm 7.6 | 1.63 \pm 0.05 |
| Chapter 6 | National level (BD Medium, Advanced Medium, Advanced) (n = 14) | 35.7 \pm 13.1 | 62.3 \pm 8.1 | 1.69 \pm 0.07 |
| | International level (Any FEI level) (n = 14) | 32.1 \pm 10.1 | 63.8 \pm 7.3 | 1.65 \pm 0.06 |
| Chapter 7 | Intermediate level (BD Prelim, Novice, Elementary) (n = 15) | 32.7 \pm 11.1 | 63.7 \pm 7.9 | 1.68 \pm 0.07 |
| | Advanced level (BD Medium, Advanced Medium, Advanced; any FEI level) (n = 25) | 30.9 \pm 12.8 | 60.8 \pm 7.6 | 1.64 \pm 0.08 |
| Chapter 8 | 40 riders (BD Prelim to FEI Grand Prix) | 32.02 \pm 11.8 | 62.6 \pm 7.9 | 1.67 \pm 0.07 |

BD: British Dressage, FEI: Fédération Internationale Équestre,

3.2 Experimental set-up

3.2.1 Motion capture equipment

All kinematic data were collected using an eleven-camera motion capture system sampling at 200 Hz. Nine cameras were optical motion capture cameras (Miquis M3, Qualisys AB, Gothenburg, Sweden), while two cameras captured video (Miquis Video, Qualisys AB, Gothenburg, Sweden) to aid in labelling the markers during analysis. The spatial resolution of the individual cameras was two megapixels to capture 1824 by 1088 pixels at 340 frames per second. The 3D resolution of the cameras was 0.11 mm. Briefly, the motion capture lenses emit stroboscopic radiation that is red to infrared, and this light reflects onto strategically placed retroreflective markers (explained in detail in Section 3.2.3). If the markers are seen by two or more cameras coincidentally, the position of the markers in the calibrated volume is calculated by triangulation (Chèze, 2014). The cameras were positioned around the riding simulator (Eventing Simulator, Racewood Ltd., Tarporley, Cheshire, United Kingdom) as in Figure 3.1 so that all markers on the rider and the riding simulator could be seen by at least two cameras, and therefore, captured in three dimensions.

Data collection occurred from November 2018 to July 2019. Throughout this period, small changes in the camera set-up were made to ensure that the crucial markers were captured without significant gaps in measurement. In particular, the video cameras that were synchronised to the optical motion capture system were added during the second data collection session onward. In addition, the position of cameras 10 and 11, depicted in Figure 3.1 were altered from the first to the second data collection as the markers placed over the rider's anterior superior iliac spines initially proved challenging to obtain 100% measured fill during riding as some riders occluded the markers from view with their hands. Figure 3.1 depicts the final camera set-up, including the video cameras.

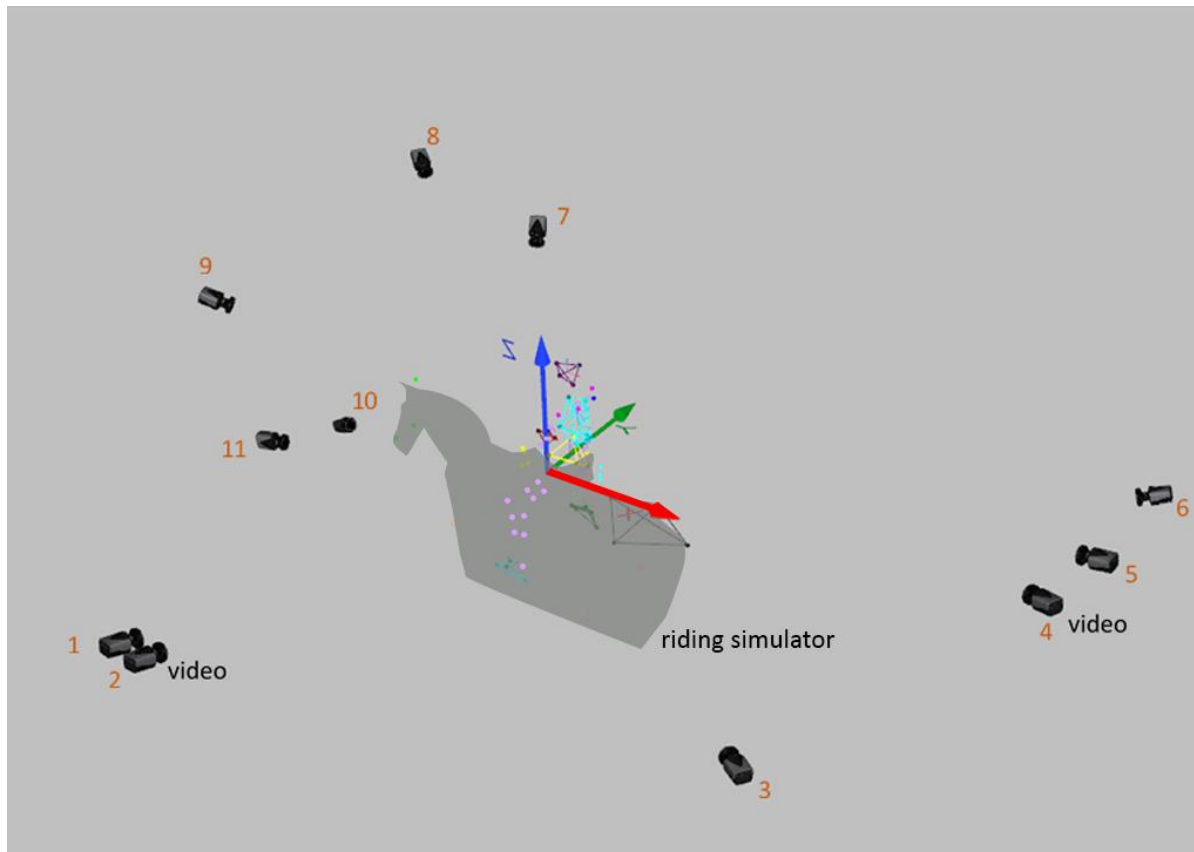


Figure 3.1. Camera set-up with nine motion capture cameras and two video cameras (labelled) around the riding simulator with a rider sitting in the saddle. Large axes represent the global coordinate system that was established during calibration under the saddle.

3.2.2 Motion capture calibration

The concept of calibration for motion capture is covered in Section 2.1.3. To achieve a calibrated three-dimensional motion capture volume an L-shaped calibration frame and wand (601.3 mm) were used. The position of the L-frame during calibration determines the position of the global coordinate system. As the cameras were set up to capture the riding simulator and rider on the simulator optimally, the most ideal placement of the calibration frame was on the riding simulator itself. The saddle was removed for the calibration and the L-frame was placed on the simulator's 'back', where the saddle sits. The saddle was removed so that the calibration frame could be levelled, as assessed by the built-in spirit levels within the L-frame itself.

The calibration process was as follows: (1) the saddle on the riding simulator was removed, (2) the calibration frame was positioned on the simulator's back, where the saddle would sit, with the long

arm pointing to the rear of the simulator and the short arm to the right to follow the right-hand rule (Robertson and Caldwell, 2014) (3) the frame was levelled to the precision of the built-in spirit levels, (4) a calibration measurement was taken with the same sampling frequency as the data collection itself (200 Hz). The wand was moved for 45 seconds in three dimensions through the capture volume. Finally, the calibration was processed in Qualisys Track Manager (version 2020.1, Qualisys AB, Gothenburg, Sweden) and the quality was assessed. The calibration quality is given in a report in Qualisys Track Manager, which details the distance in millimetres between the origin of the coordinate system of the motion capture (e.g. the L-frame) to the optical centre of each camera, the number of points used in the calculation of the distance between the origin and camera centre, and the average residual in millimetres for the points used to calculate the distance between the origin and camera centres (Qualisys AB, 2020).

An additional measure of the standard deviation of the wand length in millimetres is given. Based on these parameters, Qualisys Track Manager either passes or rejects a calibration. The number of points and the average residual should be similar in size for all cameras, and for the average residual, as low as possible (Qualisys AB, 2020). At least 1000 points per camera should be found and the average residual should be less than 1 mm (Qualisys AB, 2020). The standard deviation of the wand length should be ideally less than 1 mm, although this can vary depending on the measurement volume (Qualisys AB, 2020). For the current set-up, the calibration was accepted if the standard deviation of the wand length was less than 1.5mm. Recalibration was performed every time a camera was moved. For day-long data collection sessions exceeding 5 hours, recalibration was performed every 4 hours as directed by Qualisys Track Manager.

3.2.3 Marker placement

Riders wore tight-fitting riding trousers or tights, a vest top, their normal long or short riding boots and their own riding helmet which met the British Dressage standards (British Dressage, 2021d) for data collection. Forty-one markers were affixed to the rider in total, including rigid clusters. Anatomical references for each marker are described in Table 3.5. Figure 3.2 depicts marker placement from the front and back on a standing participant. The markers were spherical, 14 mm in diameter, and covered with retroreflective material. Three and four marker rigid clusters (19 mm diameter spherical reflective markers) were also used. Markers were a combination of commercially produced clusters and marker sets (Qualisys AB, Gothenburg, Sweden) and custom-made markers and clusters with identical marker diameters. Markers were affixed directly to the rider's skin and their clothing, depending on placement (detailed in Figure 3.2 and Table 3.5), with double-sided tape or with elasticated bandages if rigid clusters.

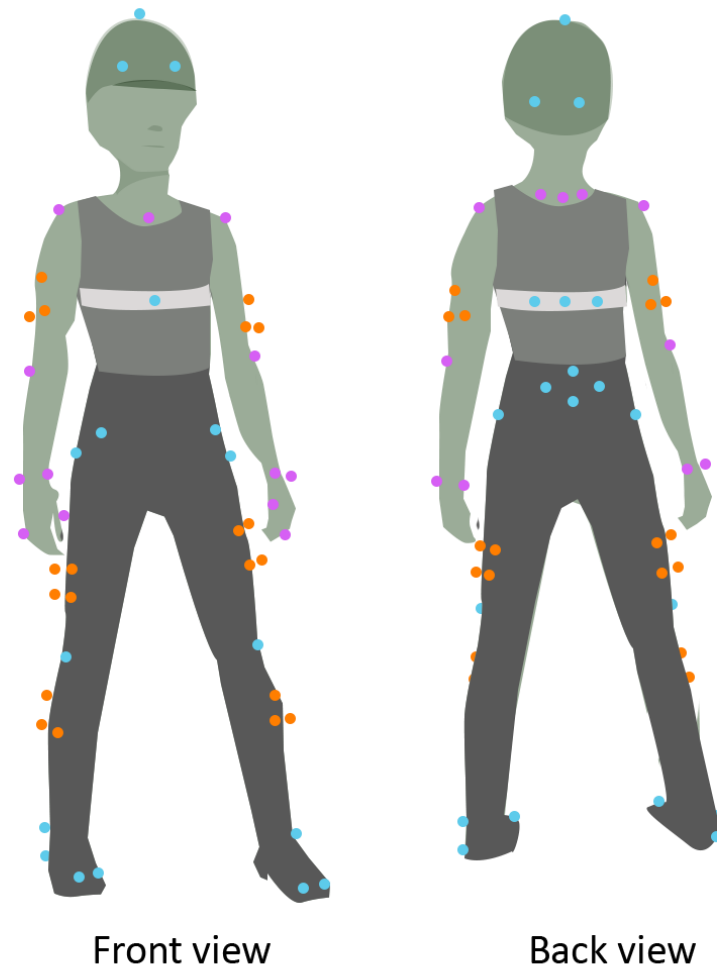


Figure 3.2. Marker placement depicted on the standing rider. Markers are denoted by circles. Blue circles indicate markers affixed to clothing or the elasticated strap around the rider's mid-section (in white). Orange circles indicate rigid clusters of markers. Purple circles indicate markers affixed directly to the skin.

Table 3.5. Description of standard marker placement. Markers were affixed to either skin, clothing, rigid cluster or elasticated bandage depending on placement, as indicated.

| Segment | Markers |
|--------------------|--|
| Head | Five markers attached to the riding helmet: two anterior, four posterior, one on top of head. |
| Trunk | Eleven markers: Left/right acromion process (skin), C7 and left/right of C7 (skin), sternum, elasticated bandage strapped around mid-back with three posterior markers and one anterior marker, L5 (clothing). |
| Pelvis | Five markers: left/right anterior and posterior iliac spines, body of sacrum (all affixed to clothing, with the exception of the specific study in Section 4.2). |
| Left and right leg | Twelve markers: greater trochanter of femur (clothing), rigid cluster mid-thigh with four markers, lateral tibial tuberosity (clothing), rigid cluster with 3 markers mid-shank, lateral malleolus (clothing – riding boot), two markers on the toe of the riding boot and one on the heel (clothing – riding boot). |
| Left and right arm | Eight markers: Rigid cluster with three markers on upper arm, medial elbow, distal ulna and radius (skin), knuckle of thumb and fifth digit (skin). |

3.2.4 Riding simulator

The riding simulator is pictured in Figure 3.3. The riding simulator is equipped with three screens. The simulator can be operated in Arena Mode, where the screens show a simulated riding arena (Figure 3.3) or Instruction Mode, where data from pressure sensors under the saddle, in the reins and on the sides of the riding simulator is projected (Figure 3.4). The riders rode the riding simulator in Instruction Mode (Figure 3.4) for the data collection sessions. The pressure sensors were not calibrated for the data collection sessions as none of the studies aims required data extraction from the riding simulator itself, and riders were advised that the data appearing on screen were not accurate. While it is acknowledged that the information displayed on the screen during data collection may have given visual feedback to the riders, with a potential effect on the rider's kinematics, the operator of the riding simulator needed to be able to see the current gait of the simulator.



Figure 3.3. The riding simulator in Arena Mode with standard saddle and motion capture cameras. Not pictured: motion capture cameras placed to the rear and left side of the simulator.



Figure 3.4. The riding simulator screens in Instruction Mode. The circle depicts the data from the four pressure sensors located under the saddle. Other bars indicate the leg pressure and rein pressures from the pressure sensors embedded into the side of the riding simulator and at the end of the reins.

The riding simulator moves in three dimensions to simulate the horse's gaits of walk, trot and left/right canter. Each gait has a repeatable rhythm of oscillations that mimic the horse's trunk displacements during the walk (four beats), trot (two beats) and canter (three beats). Within each gait, there are three variations: collected, medium and extended. The frequencies and amplitudes of each gait variation can be found in Table 3.6. The three-dimensional displacements of the riding simulator within each gait and gait variation are depicted graphically in Figure 3.5. From this figure and the supporting data presented in Table 3.6, it is evident that there are large differences between the movement of each gait, but smaller differences between the gait variations.

A standard dressage saddle (Devoucoux, Biarritz, France) with a 17.5-inch seat was used for all participants. The saddle was visually inspected in the sagittal and lateral planes before each participant to ensure it was level. As a standard saddle was used for all participants, the only variable that the riders could adjust to customise the fit was the stirrup length. Few studies outline how this is standardised between riders, however, similar to Gunst *et al.* (2019), riders adjusted the stirrup leathers to the length of their preference. The riders held the reins as normal, at their desired length. While other authors have specifically assessed the rein tension generated by riders on a riding simulator (Clayton, Smith and Egenvall, 2017), none of the objectives of the current studies pertained to the rider's rein tension. Therefore, instructing the riders to hold their reins 'as normal' and at their desired length aimed to contribute to the rider's ability to ride the simulator as they would a normal horse.

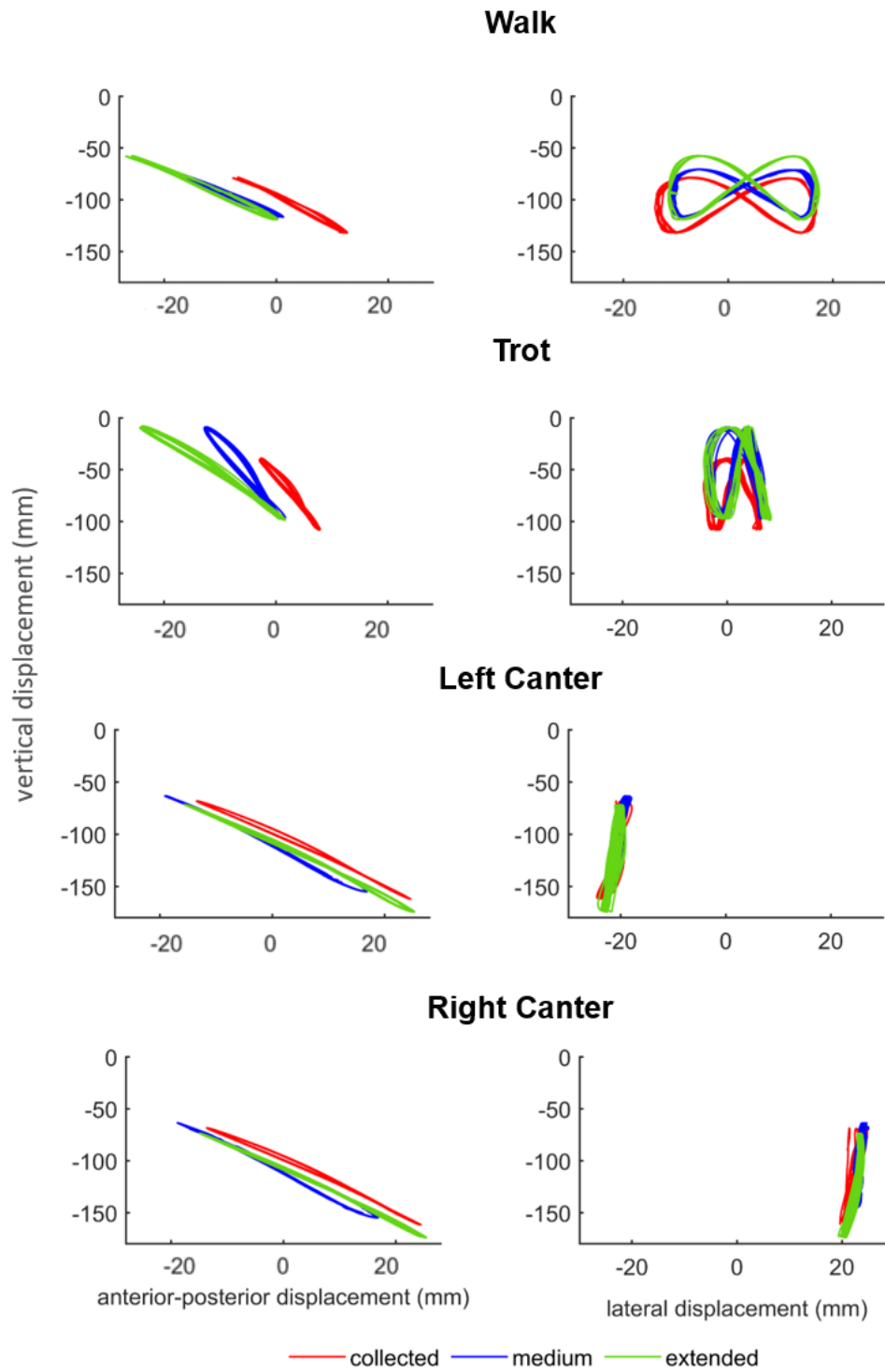


Figure 3.5. Three-dimensional displacement of the riding simulator (millimeters) in collected, medium and extended walk, trot, left canter, and right canter.

Table 3.6. Frequencies (seconds) and amplitudes (millimetres) of the displacement of the riding simulator in the anterior-posterior (A-P), lateral, and vertical directions.

| | | Period (s) | | | Amplitude (mm) | | |
|-------------------------|-----------|------------|---------|----------|----------------|---------|----------|
| | | A-P | Lateral | Vertical | A-P | Lateral | Vertical |
| Walk | Collected | 0.815 | 1.62 | 0.815 | 45.44 | 24.26 | 52.95 |
| | Medium | 0.815 | 1.47 | 0.735 | 53.34 | 33.93 | 44.64 |
| | Extended | 0.815 | 1.52 | 0.745 | 61.26 | 23.39 | 60.33 |
| Trot | Collected | 0.577 | 1.17 | 0.575 | 25.10 | 8.99 | 70.72 |
| | Medium | 0.577 | 1.13 | 0.575 | 33.61 | 14.14 | 71.44 |
| | Extended | 0.577 | 1.15 | 0.575 | 64.35 | 13.57 | 83.89 |
| Left canter | Collected | 0.769 | 0.768 | 0.769 | 93.07 | 3.86 | 93.17 |
| | Medium | 0.699 | 0.701 | 0.699 | 91.22 | 6.03 | 91.19 |
| | Extended | 0.629 | 0.636 | 0.629 | 101.76 | 6.03 | 101.93 |
| Right canter | Collected | 0.777 | 0.784 | 0.777 | 92.44 | 3.68 | 92.52 |
| | Medium | 0.699 | 0.699 | 0.699 | 90.87 | 5.80 | 90.79 |
| | Extended | 0.629 | 0.630 | 0.692 | 99.70 | 4.23 | 99.80 |

3.2.5 Data capture

Riders were given at least five minutes to acclimate to the riding simulator in all gaits. When the rider felt comfortable that they could ride each gait, the data collection commenced. Riders could stop the protocol at any time if they felt unbalanced or did not wish to continue. The gait of the riding simulator was controlled by a trained attendant during data capture.

The data capture protocol consisted of capture (sampling at 200 Hz) at a halt for two seconds, then ten seconds each of collected, medium and extended walk, trot, and canter, in that order. Ten seconds was chosen as it offered at least 10 cycles in each gait to capture the rider's kinematics without the potential effects of fatigue. A similar protocol with eight seconds of data capture on a riding simulator was followed by Clayton, Smith and Egenvall (2017). The only instruction given to every participant was to "ride as normal". Riders were not given any verbal feedback before or during the capture protocol that could have influenced their riding style or intent on the simulator. The lead (left or right)

of the canter was randomised between participants. The data selected to meet the aims of each study is detailed within the relevant chapter.

3.3 Data processing

Following data capture, markers were labelled in Qualisys Track Manager (version 2020.1, Qualisys AB, Gothenburg, Sweden). Trials were accepted for further processing if they did not contain continuous gaps of more than 0.4 s for the markers used to form the rigid bodies. As the cameras were sampling at a rate of 200 Hz, 0.4 s would be equivalent to a gap of 133 samples. As gaps in the measurement can result in poor accuracy of the data (Robertson and Caldwell, 2014), this threshold was chosen to ensure the quality of the kinematic data. Gaps smaller than 0.4 s were filled in Qualisys Track Manager using a polynomial technique. A similar approach was used by Cereatti *et al.* (2017) with regards to the threshold for gap filling. If riders did not meet the threshold for further analysis due to gaps in their data, their trials were discarded securely. In addition, if any of the pelvic markers were not captured completely or missing from the capture, the capture was not included. As a result, four riders were eliminated and one rider was excluded from further analysis of the left canter in Section 4.2 only. Further details of the inclusion of the riders can be obtained in Appendix B.

Several processing steps were applied for all studies: the creation of rigid bodies, export into MATLAB (version R2020b, The MathWorks, Natick, Mass., USA), filtering, and splitting the time-series into motion cycles. Further study-specific processing steps are described in the relevant chapters.

3.3.1 Rigid body definition

The rigid body of the riding simulator (3 markers placed on the rear of the simulator), head (all head markers), pelvis (all pelvis markers), trunk (left/right acromion process, C7, middle posterior mid-back marker, sternum and anterior mid-back marker) and foot (lateral malleolus, markers on the toe, marker on the heel) were created in Qualisys Track Manager. The local coordinate system was translated to the centre of the body points with the same orientation as the global coordinate system and following the right-hand rule, as can be seen in Figure 3.4. A data file with the linear and angular

displacement time-series for each rigid body was exported from Qualisys Track Manager into MATLAB (R2020a, The MathWorks, Natick, Mass., USA) for further processing. The thigh and shank segments were not relevant to the research questions posed in this thesis; therefore, they were not included in the rigid body analysis, however, they were collected for completeness of the kinematic data and, in the case of Section 4.2, to meet the aims of the study that informed the wider data collection.

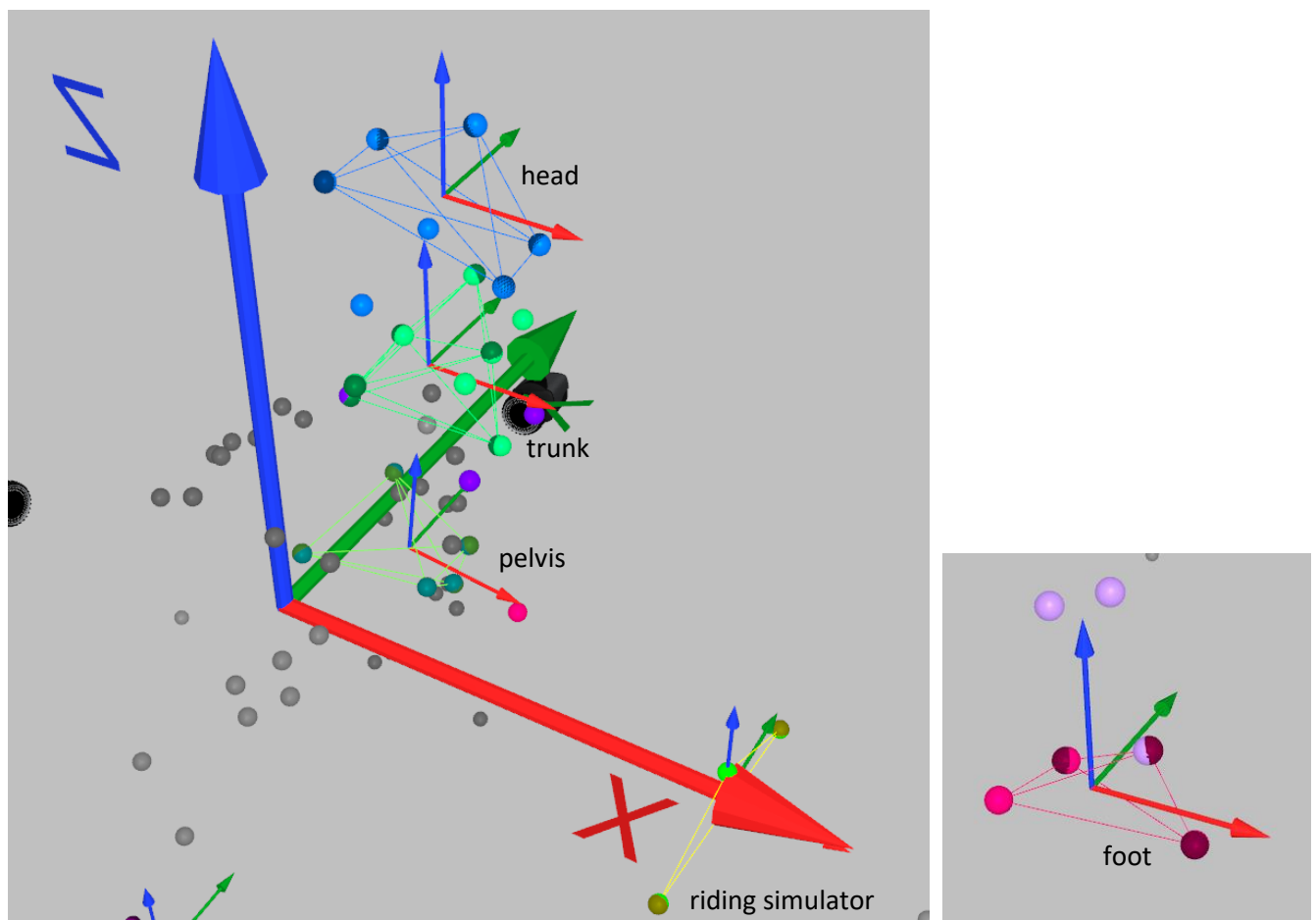


Figure 3.6. Depiction of the rigid bodies of the head, trunk, pelvis and riding simulator (left) and the foot (right) with the local coordinate systems shown relative to the large global coordinate system axes.

3.3.2 Filtering

A fourth-order recursive Butterworth filter was applied to all time series in MATLAB. A range of cut-off values was trialled and visually inspected to determine their effect on the data (Figure 3.7). The ideal cut-off value is that which attenuates the high-frequency noise but preserves the low-frequency signals that characterise the movement of interest (Winter, 2009). The cut-off was chosen as 10 Hz upon visual inspection of a range of cut off values. This cut-off preserved the features of the time series while attenuating small amounts of noise (measurement error) that were present.

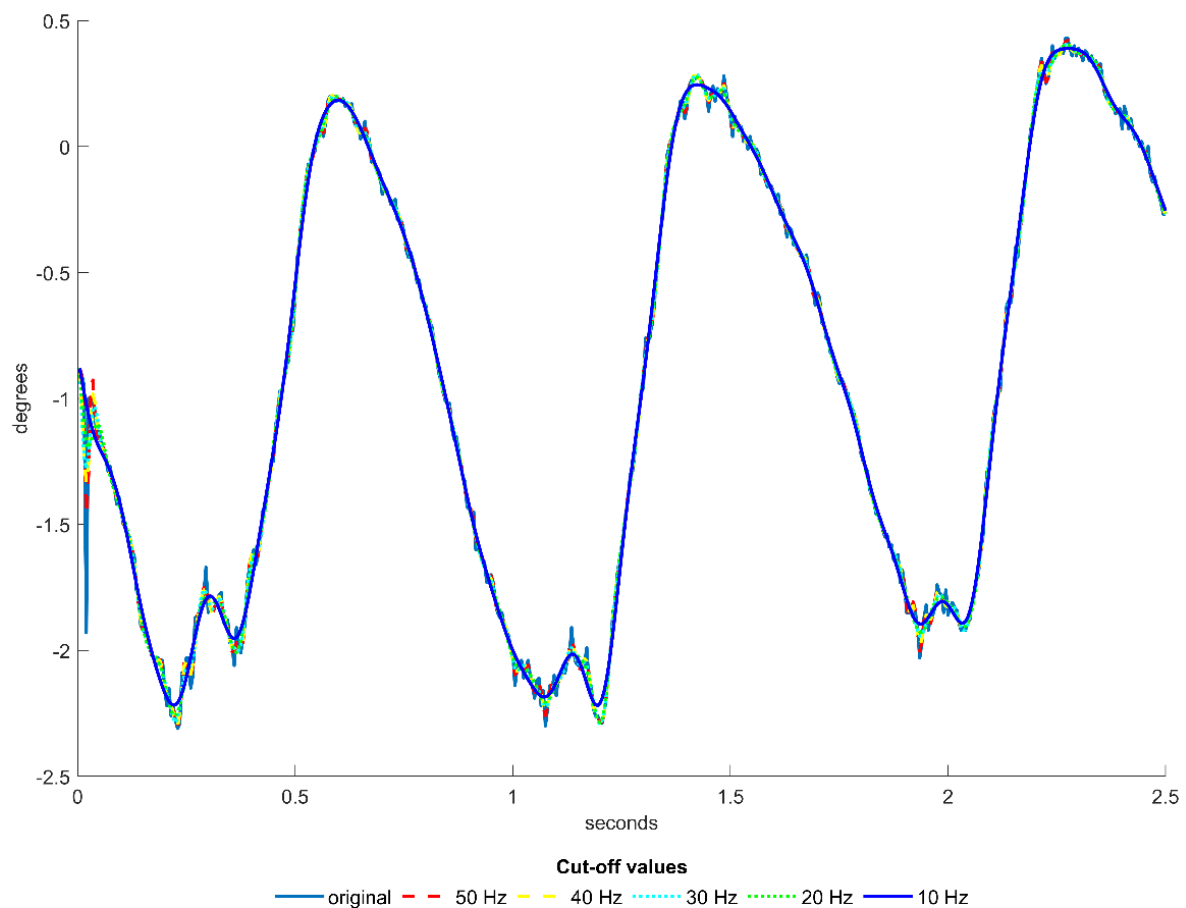


Figure 3.7. The effect of various cut-off values on the attenuation of noise when a fourth-order recursive Butterworth filter was applied to an example signal. The 10 Hz cut-off was chosen as it was deemed to effectively attenuate noise, while maintaining the characteristics of the signal.

3.3.3 Time-normalisation

All rider time series were split into motion cycles based on the period between the minimum-to-minimum vertical displacement of the rigid body of the riding simulator using a script in MATLAB. Time series were then interpolated using linear interpolation to a predetermined number of points depending on the study. It is important to note that this definition of a movement cycle is not necessarily analogous to the horse's gait. In trot, each complete stride features two cycles of peak vertical displacement of the horse's hindquarters, therefore, the cycles analysed within this thesis represent only one half of the live horse's trot. This approach was chosen as the riding simulator has a cyclic pattern of movement in trot that does not allow the identification of the left or right diagonal stance phases, therefore, it would be difficult to consistently determine the start and end of a two-beat stride. Similar difficulties with a riding simulator were described by Clayton, Smith and Egenvall (2017), who adopted a similar approach of identifying riding simulator movement cycles based on a cycle of troughs in the data.

4. Development of dynamic methods of analysis in the equestrian rider

4.1 Introduction

In the current body of equestrian rider performance analysis literature two common themes emerge: analysis of the kinematics of the rider's body segments during riding (Engell *et al.*, 2016; Byström *et al.*, 2009, 2010, 2015), and analysis of horse-rider coordination, also known as 'harmony' (Baillet *et al.*, 2017; Lagarde *et al.*, 2005; Peham *et al.*, 2001). These themes relate directly to the demands of the sport: as the rider is sitting in the saddle, their seat should reciprocate the movement of the horse's trunk, allowing the rider to remain stable and use their weight to influence the horse's speed and direction (German National Equestrian Federation, 2005). The kinematics of the rider's pelvis is frequently analysed, as its movement is integral to achieving horse-rider coordination (as described in Section 2.2.1). The accuracy of measures of the rider's kinematics and horse-rider coordination is critical to support their use to inform interventions or performance analysis of the rider. Scrutiny of the previous literature has identified two potential sources of error: (1) error in the kinematic measurements of the rider due to analysing riders with motion capture markers affixed to riding clothing and (2) miscalculation of the coordination variability between horse and rider when using a discrete versus a continuous measure of coordination.

Therefore, this two-part study aimed to: (1) quantify and compare the error accrued during optical motion capture with markers affixed to the skin or onto tight-fitting trousers, and (2) compare the coordination variability measured by discrete and continuous relative phases. The objectives of these studies were to; (1) measure the kinematics of the rider's pelvis in a range of female competitive riders during a simulated walk, sitting trot and canter and to compare the error between the two approaches, and (2) to calculate the discrete and continuous relative phase between the vertical displacement of the riding simulator and the pitch rotation of the rider's pelvis and trunk, separately, and to analyse the difference between the coordination variability between these two approaches.

4.2 Estimation of soft tissue artefact and influence of clothing on motion capture accuracy during simulated riding

Accuracy in the kinematic assessment of the rider poses some unique challenges (see Section 2.1.3). Previous studies have analysed the angular kinematics of the rider's pelvis as a rigid body formed by several markers affixed on their riding trousers over various bony reference points (Byström *et al.*, 2009, 2010, 2015; Engell *et al.*, 2016). The measurement of the rider's pelvis kinematics is highly relevant due to its role in horse-rider coordination (Blokhuys *et al.*, 2008). As the pelvis influences spinal curves, uncontrolled pelvic movement may influence back pain, which is prevalent in the rider (Deckers *et al.*, 2020; Alexander *et al.*, 2015; Comerford and Mottram, 2012). Accuracy of the measurement of the rider's pelvis kinematics is therefore pertinent. When optical motion capture is used to measure the rider's kinematics, accuracy refers to the precision of the optical motion capture markers' in track the underlying bony prominences.

One common source of error in human motion analysis is soft tissue artefact (STA). It is particularly prevalent for pelvic markers and can propagate errors when calculating pelvic orientation (Camomilla and Bonci, 2020; Camomilla, Bonci and Cappozzo, 2017). The extent of STA can depend on the movement analysed and the subject's characteristics, including body mass index (BMI). Skin-affixed pelvic markers STA can range up to 17 mm in static positions and influence the pitch of the pelvis by up to 7.5° (Camomilla, Bonci and Cappozzo, 2017). However, all studies of the rider mounted on a horse or simulator have affixed optical motion capture markers to tight-fitting clothing, rather than directly to the skin. As skin and soft tissue have a high propensity to introduce error to kinematic measurements, it is also possible that the additional layer of clothing may increase the measurement error. However, riding with markers affixed to the skin is impractical as it requires the rider to expose areas of skin that may come in contact with the saddle, which is likely to be uncomfortable for the rider during riding.

As the accuracy of the orientation of the pelvis measured in Chapter 5 depends on the accuracy of the markers placed on the pelvic landmarks, the difference between measurements of the rider's pelvis obtained with markers affixed to clothing and the skin directly is pertinent. Therefore, analysis of the difference between the error accrued during simulated riding with markers affixed to the skin and affixed to tight-fitting clothing is warranted.

The effect of clothing on motion capture error is a consideration for the pelvis in particular. As stated, it is impractical to affix passive markers to the skin overlying the bony prominences of the pelvis during riding. However, by wearing a vest top (as per Engell *et al.* (2018)), the majority of the trunk and arm markers may be affixed directly to the rider's skin. In the subsequent chapters of this thesis, the markers used to form the rider's head segment were affixed to their riding helmet. In this case, no consideration of the soft tissue artefact or effect of clothing is necessary as the helmet is a rigid body and would not move relative to the rider's head unless improperly fitted. Cereatti *et al.* (2017) proposed a standardised characterisation of STA by calculation of the root mean square amplitude of the markers' displacement relative to its mean position. Understanding the potential error introduced by clothing, anthropometry and the movements performed during riding will increase the accuracy of the data in equestrian studies. Therefore, this study aims to investigate whether markers affixed to clothing, compared to directly on the skin, significantly increases the marker position error and its influence on the calculation of pelvic tilt when markers are incorporated into a six degrees of freedom (6DOF) rigid body. It is hypothesised that affixing the markers on the trousers will increase the error compared to affixing the markers directly to the skin.

4.2.1 Methods

Kinematic measurements were collected as per the standard protocol using motion capture (Miquis M3, Qualisys AB, Gothenburg Sweden) and the riding simulator (Eventing Simulator, Racewood Ltd., Tarporley, Cheshire, UK), described in Section 3.2. Four riders rode the riding simulator wearing a sports bra and shorts that left the skin covering the left and right anterior superior iliac spines (ASIS) and posterior superior iliac spines (PSIS) free of any interference from clothing ('skin-affixed')

condition). Riders' height and mass were taken with scales and a measuring tape on the day of data collection. Participants' body mass index (BMI) was calculated as:

$$\frac{\text{mass (kg)}}{\text{height (m)}^2} \quad (5.1)$$

These riders were then paired for analysis with the closest match to their BMI from the overall dataset of riders whose data were available at the time of data analysis. Markers were affixed to these riders as per the protocol described in Section 3.2.3. The pelvic markers were affixed, as standard, to tight-fitting trousers ('trouser-affixed' condition). Anthropometric characteristics of each participant are given in Table 4.1, and group means of participant characteristics presented in Table 3.4.

Table 4.1. Anthropometric characteristics of each BMI-matched pair of participants.

| | Skin-affixed markers | | | Trouser-affixed markers | | |
|---------------|----------------------|-----------|------|-------------------------|-----------|------|
| | Height (m) | Mass (kg) | BMI | Height (m) | Mass (kg) | BMI |
| Pair 1 | 1.80 | 65 | 20.1 | 1.77 | 63 | 20.1 |
| Pair 2 | 1.58 | 55 | 22.0 | 1.65 | 59 | 21.8 |
| Pair 3 | 1.62 | 62 | 23.6 | 1.67 | 69 | 23.9 |
| Pair 4 | 1.58 | 70 | 28.0 | 1.67 | 72 | 25.8 |

Legend: BMI: Body mass index.

4.2.1.2 Data processing

Displacement of the individual markers and the angular displacement of the rigid body of the pelvis were exported from each trial, filtered and time normalised as per the standard protocol described in Section 3.3. Trials were checked for the quality of their data as per the criteria defined in Section 3.3. The skin-affixed rider in Pair 4 had significant gaps in the pelvic markers in left canter only that necessitated exclusion.

4.2.1.2 STA characterisation

Soft tissue artefact was calculated for both groups as the root mean square amplitude ($rmsd$), peak-to-peak amplitude (Δp_{\max}), and root mean square amplitude components ($rmsd_c$) in MATLAB (R2020b, The MathWorks Inc., Natick, Mass., USA) with a script developed by Cereatti *et al.* (2017). The $rmsd$ and Δp_{\max} describe the trial mean and maximum STA amplitude encompassing all three planes of movement, while $rmsd_c$ provides information about the direction of the STA (Cereatti *et al.*, 2017). As these parameters are calculated as the root mean square of the pelvic markers' instantaneous displacement relative to their mean position in the global coordinate system, they do not depend on the definition of the pelvis' local coordinate system, which allows comparison of riders, regardless of differences in pelvis size.

4.2.1.3 Rigid body calculations

The pitch rotation of the pelvis rigid body relative to the global coordinate system is frequently used in kinematic analysis of the rider's technique. Therefore, the influence of STA on the resulting six degrees of freedom (6DOF) rigid body was of interest. The rigid body was created for the pelvis segment for each participant as per the standard protocol described in Section 3.3.1. The pitch range of motion (ROM) was calculated as the difference between the trial maximum and minimum pitch values. The effect of marker STA on the resulting rigid body was defined as the rigid body residual: the average error in millimetres of the marker position in the rigid body compared to their initial position defined during the static capture. This parameter was calculated by Qualisys Track Manager (version 2020.1, Qualisys AB, Gothenburg, Sweden) and exported into MATLAB. The amplitude of the residual was calculated as the difference between the trial minimum and maximum values.

4.2.1.4 Statistical analysis

STA variables were calculated within each gait. These variables were then imported into SPSS (version 26, IBM Corp., Armonk, N.Y., USA) for statistical analysis. All statistical outputs can be found in Appendix C. The variables were assessed for normality using a Shapiro-Wilk test. All ROM, residual,

$rmsd$, $rmsd_c$, and Δp_{max} variables were not normally distributed, therefore the median \pm interquartile range are reported as descriptive statistics and non-parametric tests were carried out.

The difference between the median $rmsd$ and Δp_{max} of markers affixed to skin or trousers was assessed with an independent samples Mann-Whitney U test in each gait. The difference between pelvis pitch ROM and pelvis rigid body residual amplitude between marker groups was also assessed by a Mann-Whitney U test. The relationship between BMI and the STA parameters was tested by Spearman's rank-order correlation. Only significant correlations were reported in these results, however, full details are available in Appendix C. Effect sizes were calculated for each test as per the test-specific protocol outlined by Tomczak and Tomczak (2014). Significance for all tests was set at $p = 0.05$.

4.2.2 Results

Results of the statistical tests are presented in Table 4.2. The independent samples Mann-Whitney U tests did not find significant differences between skin or trouser affixed group $rmsd$, Δp_{max} , rigid body residual, or pelvis range of motion medians in the walk, trot or left canter.

Table 4.2. Results of the statistical tests for the comparison between parameters measured in riders with markers affixed directly to skin versus to their tight-fitting trousers.

| Parameter | | Walk | | | Trot | | | Left Canter | | |
|------------------------|------------|-------|----------|----------|-------|----------|----------|-------------|----------|----------|
| | | U | <i>r</i> | <i>p</i> | U | <i>r</i> | <i>p</i> | U | <i>r</i> | <i>p</i> |
| <i>rmsd</i> | Left ASIS | 9.00 | 0.10 | 1.00 | 15.00 | 0.71 | 0.57 | 4.00 | -0.25 | 0.629 |
| | Right ASIS | 9.00 | 0.10 | 1.00 | 7.00 | 0.27 | 0.866 | 4.00 | 0.17 | 0.629 |
| | Left PSIS | 6.00 | -0.20 | 0.686 | 4.00 | -0.41 | 0.343 | 6.00 | 0.00 | 1.00 |
| | Right PSIS | 11.00 | 0.31 | 0.486 | 8.00 | 0.00 | 1.00 | 8.00 | 0.17 | 0.629 |
| Δp_{\max} | | 12.00 | 0.41 | 0.343 | 9.00 | 0.10 | 1.00 | 4.00 | -0.25 | 0.629 |
| Rigid body residual | | 10.00 | 0.20 | 0.686 | 8.00 | 0.00 | 1.00 | 10.00 | 0.40 | 0.229 |
| Pelvis range of motion | | 2.00 | -0.61 | 0.114 | 8.00 | 0.00 | 1.00 | 1.00 | -0.63 | 0.114 |

Legend: U: Mann-Whitney U test statistic. *r*: effect size. *p*: level of statistical significance. ASIS: anterior superior iliac spine. PSIS: posterior superior iliac spine.

The *rmsd* and Δp_{\max} values for each participant are reported in Table 4.3. The *rmsd* values were similar for the markers within each gait. In walk, median *rmsd* for the posterior markers (L PSIS: 28.74 mm \pm 10.05; R PSIS: 29.33 mm \pm 7.39) were slightly less than the anterior markers (L ASIS: 31.27 mm \pm 6.93; R ASIS: 30.13 mm \pm 4.73), however, in trot and left canter, similar median *rmsd* values were observed for all markers. There were no significant correlations between *rmsd* values and BMI (results presented in Appendix C). The root mean square amplitude vectors (*rmsd_e*) presented in Figure 5.1 shows the changes in direction of STA amplitude due to changes in gait. These values aligned with the predominant direction of movement of the riding simulator (movement of simulator described in Section 3.2.1) to produce the simulated gait, which suggests that the STA is largely influenced by inertial forces.

The pelvis rigid body residual amplitude (Table 4.4) did not differ significantly between the skin and trouser marker groups. Large ranges of motion were found for riders S3 and S4, however, motion capture and video files were visually inspected, and these values were deemed to be genuine representations of the riders' pelvis movement.

Table 4.3. Root mean square amplitude (*rmsd*) and peak-to-peak amplitude (Δp_{\max}) of the soft tissue artefact (STA) for each pair of participants. The S prefix in the participant column denotes skin-affixed markers and the T denotes trouser-affixed markers. The *rmsd* is reported in millimetres and BMI is reported in kg/m².

| | Participant | BMI | <i>rmsd</i> | | | | Δp_{\max} |
|-------------------------------------|-------------|-------|---------------|---------------|--------------|---------------|-------------------|
| | | | Left PSIS | Right PSIS | Left ASIS | Right ASIS | |
| Walk | S1 | 20.06 | 29.03 | 29.33 | 31.27 | 30.13 | 89.47 |
| | T1 | 20.11 | 28.74 | 28.55 | 28.84 | 29.55 | 84.61 |
| | S2 | 22.03 | 33.13 | 31.02 | 33.62 | 31.24 | 89.72 |
| | T2 | 21.78 | 24.60 | 24.30 | 26.69 | 26.51 | 131.65 |
| | S3 | 23.62 | 22.58 | 18.67 | 17.48 | 22.31 | 68.45 |
| | T3 | 23.88 | 32.63 | 31.69 | 31.55 | 31.23 | 90.70 |
| | S4 | 28.04 | 26.47 | 27.94 | 30.07 | 30.78 | 98.20 |
| | T4 | 25.82 | 31.85 | 32.30 | 31.14 | 30.54 | 116.94 |
| <i>Median ± interquartile range</i> | | | 28.74 ± 10.05 | 29.33 ± 7.39 | 31.27 ± 6.93 | 30.13 ± 4.73 | 89.72 ± 32.33 |
| Trot | S1 | 20.06 | 45.72 | 43.67 | 39.17 | 38.71 | 115.90 |
| | T1 | 20.11 | 39.17 | 35.93 | 39.50 | 35.35 | 105.98 |
| | S2 | 22.03 | 43.84 | 41.42 | 40.25 | 46.01 | 134.02 |
| | T2 | 21.78 | 37.89 | 37.75 | 45.51 | 44.93 | 131.65 |
| | S3 | 23.62 | 44.25 | 29.55 | 30.90 | 45.39 | 142.75 |
| | T3 | 23.88 | 40.65 | 39.53 | 42.96 | 39.50 | 127.23 |
| | S4 | 28.04 | 27.22 | 26.84 | 36.46 | 35.07 | 105.71 |
| | T4 | 25.82 | 39.45 | 39.56 | 47.53 | 43.44 | 152.24 |
| <i>Median ± interquartile range</i> | | | 40.65 ± 5.08 | 39.53 ± 5.49 | 40.25 ± 6.34 | 43.44 ± 6.68 | 131.65 ± 26.85 |
| Left Canter | S1 | 20.06 | 48.26 | 44.63 | 43.47 | 48.96 | 143.44 |
| | T1 | 20.11 | 42.12 | 41.12 | 39.49 | 40.83 | 123.99 |
| | S2 | 22.03 | 54.39 | 48.52 | 48.95 | 52.55 | 170.18 |
| | T2 | 21.78 | 37.91 | 37.92 | 37.81 | 37.44 | 116.99 |
| | S3 | 23.62 | 35.72 | 29.21 | 39.53 | 28.92 | 96.89 |
| | T3 | 23.88 | 49.48 | 49.05 | 44.03 | 45.09 | 140.67 |
| | S4 | 28.04 | - | - | - | - | - |
| | T4 | 25.82 | 52.62 | 52.69 | 48.01 | 37.36 | 127.06 |
| <i>Median ± interquartile range</i> | | | 48.26 ± 14.71 | 44.63 ± 11.13 | 43.47 ± 8.52 | 40.83 ± 11.60 | 127.06 ± 26.45 |

Legend: BMI: body mass index, PSIS: posterior superior iliac spine, ASIS: anterior superior iliac spine

Table 4.4. Pitch range of motion (ROM) in degrees and rigid body residual amplitude (millimetres) for participants with skin-affixed markers (S prefix) and trouser-affixed markers (T prefix).

| Participant | Walk | | Trot | | Left Canter | |
|-------------|-----------|--------------------|-----------|--------------------|-------------|--------------------|
| | Pitch ROM | Residual amplitude | Pitch ROM | Residual amplitude | Pitch ROM | Residual amplitude |
| S1 | 7.02 | 5.70 | 7.38 | 3.09 | 13.79 | 2.93 |
| T1 | 4.88 | 2.85 | 9.41 | 2.63 | 13.24 | 4.13 |
| S2 | 5.76 | 3.02 | 6.65 | 2.30 | 18.96 | 4.98 |
| T2 | 7.93 | 3.01 | 9.72 | 1.61 | 14.92 | 3.34 |
| S3 | 12.94 | 2.15 | 18.30 | 1.97 | 24.62 | 3.17 |
| T3 | 4.63 | 2.58 | 7.03 | 2.58 | 10.11 | 6.08 |
| S4 | 12.72 | 2.16 | 10.54 | 2.98 | - | - |
| T4 | 5.58 | 1.97 | 10.58 | 5.74 | 8.60 | 6.78 |

Legend: ROM: range of motion

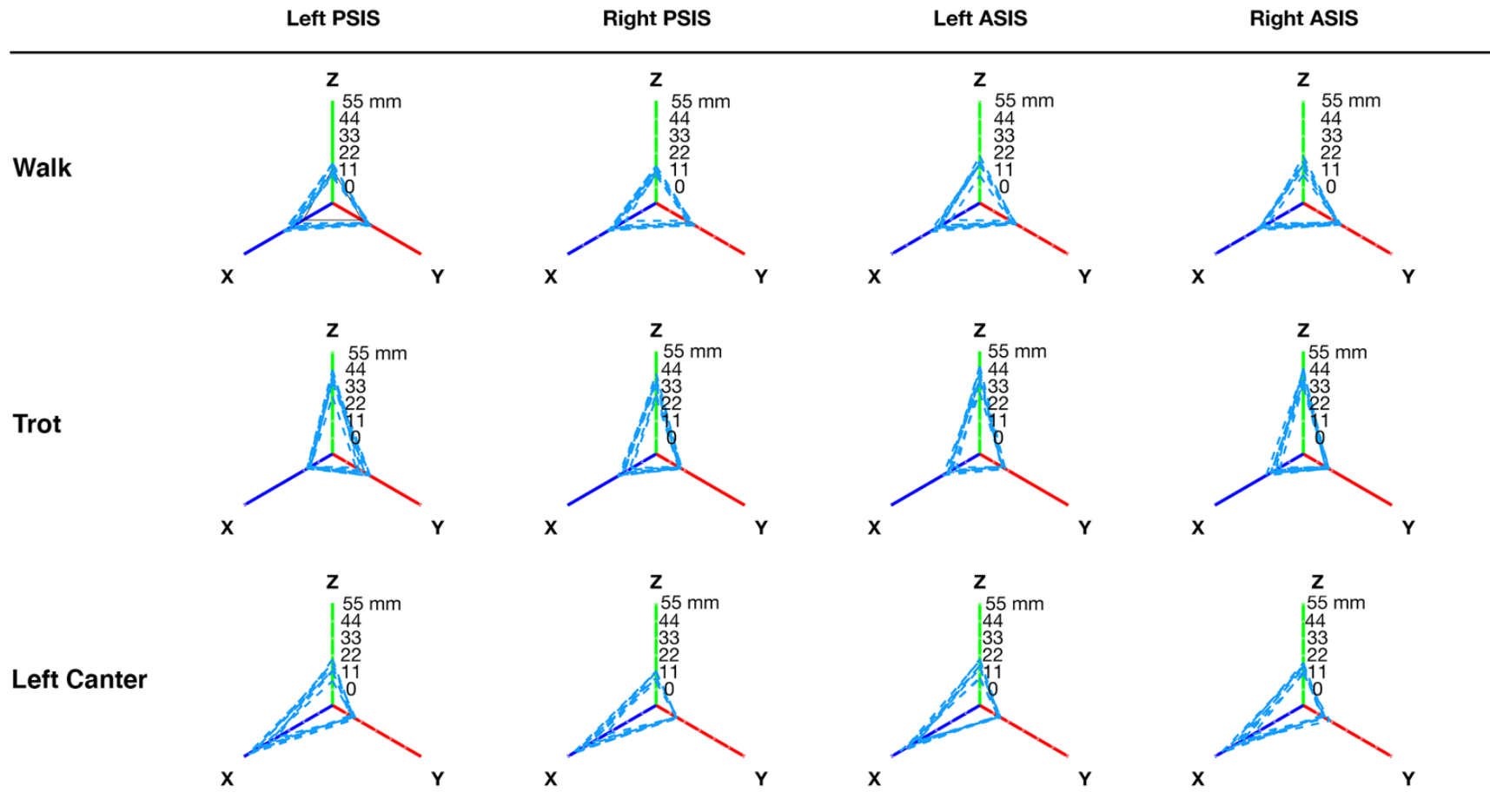


Figure 4.1. Spatial orientation of the $rmsd_c$ vectors in mm for the four markers: left/right anterior superior iliac spines (ASIS), left/right posterior superior iliac spines (PSIS), plotted relative to the pelvis coordinate system in walk, trot, and left canter.

4.2.3 Discussion

This chapter compared the effect of affixing markers to skin or tight-fitting trousers on the soft tissue artefact (STA) of tracking of anatomical landmarks on the riders' pelvis during a simulated walk, trot, and left canter. This was an important step in the development of the methods to validate whether riders could be assessed wearing tight-fitting riding trousers or tights for the subsequent chapters within this thesis. STA was quantified with metrics proposed by Cereatti *et al.* (2017), including the root mean square amplitude of the markers (*rmsd*), peak-to-peak amplitude (Δp_{\max}), and root mean square amplitude components (*rmsd_c*). The hypothesis that affixing markers to tight-fitting trousers or tights would increase error was not accepted as no metrics were significantly different between marker attachment groups.

The STA metrics indicate that the errors in the estimation of the pelvic orientation are systematic and repeatable within the population. The direction of the error, given by the *rmsd_c* (Figure 4.1) indicates that the error is most influenced by the movement of the riding simulator. For example, in trot, the riding simulator primarily moves up and down and in left canter, it rocks back and forth. Accordingly, the STA was largest for all markers in the frontal plane in trot and the sagittal plane in left canter. Therefore, as the riding simulator produces repeatable movement between all participants, the direction of the error is consistent between all participants and the error will not affect the variability between riders. Equally, similar values were observed for *rmsd* of anterior and posterior markers (Table 4.2) in trot and canter, but slightly greater *rmsd* of anterior markers in walk (median \pm IQR: L PSIS: 28.74 mm \pm 10.05; R PSIS: 29.33 mm \pm 7.39 L ASIS: 31.27 mm \pm 6.93; R ASIS: 30.13 mm \pm 4.73). Camomilla and Bonci (2020) reported greater STA for anterior than posterior markers, particularly in individuals with a larger BMI. No differences between anterior and posterior markers were observed regardless of gait, which underlines the influence of the movement of the riding simulator on STA over and above the rider's BMI or marker location.

Differences in the direction of the STA of the markers would result in a high residual of the rigid body due to rigid body deformation. Several studies report the rider's pelvis kinematics calculated as a rigid body (Engell *et al.*, 2016; Byström *et al.*, 2009, 2010, 2015). The rigid body assumes that the distance between the markers will not change during movement (Robertson *et al.*, 2014). The amount of deformation of the rigid body of the pelvis can be determined by calculating its residual: the difference between the position of the markers during movement and the initial definition of the rigid body determined, in this study, from the rider's static capture. The residual amplitude was calculated for each participant in each gait (Table 4.3). The residual amplitude ranged from 1.97 mm to 5.70 mm in walk, 1.61 mm to 5.74 mm in trot, and 2.93 mm to 6.78 mm in left canter. It was not correlated with BMI and there were no significant differences observed between marker attachment groups. Some deformation does indeed occur due to the movement of the riding simulator, however, individual factors that influence the residual amplitude are unknown. As the STA of all markers is predominately in the same direction, there is likely only a small impact on the rigid body calculations.

The median of the markers' *rmsd* ranged from 28.74 mm to 30.13 mm in walk, 39.5 mm to 43.44 mm in trot, and 40.83 mm to 48.26 mm in left canter. These values are much larger than those reported in static positions of varying degrees of hip flexion by Camomilla, Bonci and Cappozzo (2017). In their study, the static position most resembling the hip flexion assumed by the rider seated in the saddle (SA2) had STA amplitudes in left/right anterior superior iliac spines (ASIS) and posterior superior iliac spines (PSIS) ranging from 1.9 mm to 52.1 mm. In their study, STA amplitudes were related to the participants' BMI (range:14.6), with higher values observed with greater BMI. In this study, BMI was not significantly correlated to any STA metric or the residual of the rigid body. Camomilla, Bonci and Cappozzo (2017) considered a BMI greater than 25 as overweight, and in this study, only one pair exceeded this (skin: 28.04; trouser: 25.82). Similar effects of BMI on STA during riding on the static hip flexion positions measured by Camomilla, Bonci and Cappozzo (2017) are probable, however, data was not available to confirm this as

riders rode through an entire range of motion, rather than holding a static position. It is important to note that the rider's BMI does not describe the distribution of the soft tissue; a higher BMI does not necessarily mean that the rider will have greater adipose tissue around the pelvis region. Notwithstanding, the results of this study are most valid for non-obese riders, and further study of the effect of STA on riders with a BMI greater than 28 or quantification of the soft tissue around the pelvis region are needed.

It was surprising that attaching the markers to tight-fitting riding trousers or tights did not significantly increase error compared to affixing markers directly to the skin. In human biomechanics studies, it is standard protocol to affix markers directly to the skin, particularly where a single marker represents the underlying anatomical landmark (AL) as in the ASIS and PSIS. Accordingly, there is information on the characteristics of error due to STA and the accuracy of the markers confirmed with imaging or pins inserted into the bone (Leardini *et al.*, 2005). Large STA amplitudes for all markers in both conditions and lack of an assessment of the accuracy of the marker's position relative to the AL in this study leads to the conclusion that for non-obese riders' pelvis markers during simulated riding, affixing the markers directly to the skin does not result in significant decreases in error. Although the importance of the rider's pelvic orientation and kinematics during riding have been underlined by many studies from a technique and injury perspective (Walker *et al.*, 2020; Engell *et al.*, 2016, 2018; Guire *et al.*, 2017; Alexander *et al.*, 2015; Hobbs *et al.*, 2014), no studies have assessed the accuracy of the measures used to estimate these variables. Requiring riders to wear shorts in the saddle is impractical and potentially unsafe for in-field assessment. Furthermore, no currently published studies have used motion capture to assess riders on live horses or a riding simulator with pelvis markers affixed directly to the skin. Therefore, it is encouraging that there are no significant differences in error obtained from tracking markers affixed to the skin compared to tight-fitting riding trousers. However, further studies are needed to assess whether these measures accurately track the AL in riders.

Finally, the marker set used to measure the rider's pelvis should be considered. Previous studies using motion capture to analyse the rider's kinematics during riding have measured the pelvis using markers affixed to the rider's trousers overlying the sacrum and left/right trochanters of the femur (Byström *et al.*, 2009, 2010, 2015), lumbosacral joint and left/right greater trochanters of the femur (Engell *et al.*, 2016, 2018), and anterior superior iliac spines, posterior superior iliac spines, iliac crests, and greater trochanters of the femur (Alexander *et al.*, 2015). Terada, Clayton and Kato (2006) describe the movement of the rider's pelvis based on the displacement of a marker on the rider's hip. Only Engell *et al.* (2018) captured riders' pelvic kinematics with markers affixed directly to skin over the anterior and posterior superior iliac spines and greater trochanter of the femur, although riders were assessed in a balance chair rather than on a live horse. Marker placement over the greater trochanter of the femur can be highly variable, potentially more so than markers placed over ASIS/PSIS (Della Croce, Cappozzo and Kerrigan, 1999). Additionally, the values of the measures obtained from the rigid body analysis depend on the definition of the rigid body itself. Therefore, comparison between studies is hampered by the variety of definitions of the pelvis. To overcome these challenges, this study recommends that further studies of the equestrian rider follow the International Society of Biomechanics recommended pelvis coordinate system, formed by markers placed on the bony prominences of the left and right anterior and posterior superior iliac spines (ASIS and PSIS, respectively) (Wu *et al.*, 2002).

4.2.4 Conclusion

In conclusion, affixing pelvic markers to the rider's skin does not significantly decrease the potential soft tissue artefact (STA) compared to affixing the markers to tight-fitting trousers or tights. However, the accuracy of these markers to track anatomical landmarks of the pelvis is not understood as the movement between the skin and the underlying anatomical landmarks during riding is not known. During simulated riding, the marker error is related to the movement of the riding simulator as the largest amplitudes of error are in the direction of the predominant movement of the riding simulator within the specific gait.

As the riding simulator's movement is reproducible, so is the magnitude of the error in each direction between participants. The effect of the clothing or affixing markers to skin on the resulting calculation of rigid body angular kinematics is equivocal and small (1.97-5.74 mm) residual values were recorded for the pelvis rigid body in a simulated walk, trot and left canter. Therefore, affixing markers to the rider's skin offers no significant improvements in marker tracking or rigid body error compared to affixing markers to tight-fitting trousers. This study provides an important first step to understanding the accuracy of motion capture applied to riders, with practical considerations for the comfort and safety of the rider, and the similarity of the testing protocol to real-life riding. However, the absolute accuracy of the motion capture markers is still unknown, as it is unclear how the skin moves relative to the bony landmarks during riding. Therefore, further studies are needed for a greater understanding of the threats to accuracy in capturing the rider's kinematics.

4.3 Comparison between continuous and discrete coordination analysis in the rider

A second consideration in the accuracy of quantitative measurements of the rider's technique is the measurement of horse-rider harmony. Harmony is an ideal outcome due to its importance to performance, and as such, several studies have tested the differences in levels of harmony between rider experience levels (Baillet *et al.*, 2017; Lagarde *et al.*, 2005; Peham *et al.*, 2001). These authors used analyses founded in dynamical systems theory to describe the self-organisation of horse and rider as the similarity of the timing between the movements of the rider's segments and reference markers on the horse. The discrete relative phase (DRP) has been used extensively to characterise the temporal similarity between horse and rider movement (Baillet *et al.*, 2017; Lagarde *et al.*, 2005) or between the rider's segments (Olivier *et al.*, 2017). The DRP describes the timing between two events, such as the maximum vertical displacement of horse and rider movements during a stride. The continuous relative phase (CRP) describes the phase relationship between two oscillators, such as horse and rider, over the entire cycle of movement (Wheat and Glazier, 2006). Only Wolframm, Bosga and Meulenbroek (2013) have calculated the CRP between horse and rider, using an IMU approach.

Calculation of the DRP is straightforward, while the CRP requires time and amplitude normalisation and correction if the time series are non-sinusoidal (Lamb and Stöckl, 2014). The mean CRP or DRP provides relevant information on the phase relationship between the two oscillators, describing in-phase, out-of-phase or anti-phase, the cycle-to-cycle variability is particularly relevant for the equestrian, as it indicates the stability of the coordination relationship (Oullier *et al.*, 2006). The regularity of the horse's gait is judged in all levels of dressage competition (Fédération Internationale Équestre, 2020), and variability of the rider's technique may influence the horse's gait (Peham *et al.*, 2004). Therefore, coordination variability is a relevant performance metric for quantitative assessment of performance. This study aims

to detail the steps required for accurate CRP calculation as per Lamb and Stöckl (2014) and to compare the measures of coordination variability obtained by CRP and DRP.

4.3.1 Methods

The riders used in this study were the same subset of the overall dataset used in Chapter 6. Therefore, riders were included in this study if they met the inclusion criteria for Chapter 6 (described in detail in Table 3.3). Twenty-eight 28 female riders were included. The participant characteristics are listed in Table 3.4.

Kinematic data were collected as per the protocol described in Chapter 3. The data were collected using the experimental set-up and data collection protocol described in Section 3.2. The rigid bodies of the trunk, pelvis and riding simulator were exported from Qualisys Track Manager (version 2020.2, Qualisys AB, Gothenburg, Sweden) as per the standard protocol described in Section 3.3.1 and exported to MATLAB (R2020b, The MathWorks, Inc., Natick, Mass., USA). Data were filtered as per the standard protocol described in Section 3.3.2. Cycles were then interpolated to 101 samples for the DRP calculations and 1001 samples for the CRP calculations due to the rationale described in Section 4.3.1.2.3. Ten cycles per rider were accepted for further analysis.

4.3.1.1 Selection of signals

The pitch of the rigid body of the rider's pelvis and the vertical displacement of the riding simulator was chosen as the signals for coordination analysis. No previously known study has analysed the coordination between the angular displacement of the rider's segments and a riding simulator. Previous studies have analysed coordination between a live horse and rider, comparing the roll and pitch of the rider's segments to the roll and pitch of the horse's trunk (Eckardt and Witte, 2017; Münz, Eckardt and Witte, 2014). While it may seem intuitive to compare the pitch of the rider's pelvis to the pitch of the riding simulator, the values listed in Table 4.4 illustrate that the riding simulator does not rotate about an axis in a walk or trot. For example, the riding simulator only rotates around 3° in a medium trot. It is clear from the small ranges

of motion (ROM) for the angular displacement of the riding simulator presented in Table 4.5, that the riding simulator is not mechanically driven to rotate about any axis in walk and trot. For example, the pitch ROM of the riding simulator in a medium trot is 2.95° (Table 4.5). Evidence from Münz, Eckardt and Witte (2014) and Byström *et al.* (2010, 2009) suggest that the ranges of motion of the rider's segments, particularly those of the pelvis, are influenced by the ROMs of the horse's trunk and the saddle.

Table 4.5. Angular displacement values for the rigid body of the riding simulator in each gait and variation obtained from an example rider. All values reported in degrees.

| Gait | Variation | | Roll (°) | Pitch (°) | Yaw (°) |
|-------------|-----------|-----|----------|-----------|---------|
| Walk | Collected | Min | -0.61 | -0.25 | -0.29 |
| | | Max | 2.41 | 1.22 | 0.08 |
| | | ROM | 3.02 | 1.47 | 0.37 |
| | Medium | Min | -2.51 | -3.54 | -0.29 |
| | | Max | 0.19 | 0.29 | 0.62 |
| | | ROM | 2.70 | 3.83 | 0.91 |
| | Extended | Min | -2.84 | -3.20 | -1.39 |
| | | Max | 0.01 | 2.42 | 0.58 |
| | | ROM | 2.85 | 5.62 | 1.97 |
| Trot | Collected | Min | -1.27 | -0.45 | -0.15 |
| | | Max | 0.23 | 0.24 | 0.10 |
| | | ROM | 1.50 | 0.69 | 0.25 |
| | Medium | Min | -0.19 | -0.81 | -1.29 |
| | | Max | 0.91 | 2.14 | 0.02 |
| | | ROM | 1.10 | 2.95 | 1.31 |
| | Extended | Min | -0.86 | -1.39 | -0.35 |
| | | Max | 0.27 | 0.43 | 0.31 |
| | | ROM | 1.13 | 1.82 | 0.66 |
| Left Canter | Collected | Min | -0.33 | -5.48 | -1.12 |
| | | Max | 0.31 | 2.46 | 0.14 |
| | | ROM | 0.64 | 7.94 | 1.26 |
| | Medium | Min | -0.58 | -7.52 | -0.54 |
| | | Max | 1.01 | 3.45 | 1.82 |
| | | ROM | 1.59 | 10.97 | 2.36 |
| | Extended | Min | -0.20 | -6.06 | -0.58 |
| | | Max | 0.74 | 3.56 | 0.52 |
| | | ROM | 0.94 | 9.62 | 1.10 |

Legend: ROM: range of motion.

The pitch ROM of the rider's pelvis, as reported in Chapter 5, ranges from about 9° to 11° (Table 5.3). Therefore, it is evident from these data that the pitch of the rider's pelvis is not primarily influenced by the pitch of the riding simulator, given the disparity between the pitch ROM of the simulator and the rider's pelvis. It is entirely possible, due to these very small angular displacement values, that the angular displacement of the riding simulator measured and reported in Table 4.4 is caused by measurement error or by the rider's influence on the simulator's movement. If this is the case, this factor would not be consistent between participants. As the rider does not seem to be coupling the pitch of their pelvis to the pitch of the riding simulator, specifically indicated by the differences in ROM, an alternative signal was sought for the coordination analysis.

The riding simulator's mechanically driven anterior-posterior, lateral and vertical displacements are described in Section 3.2.1 (specifically, Figure 3.5). The riding simulator's trot is characterised by anterior-posterior and vertical displacement, with relatively little lateral displacement (Table 3.6). Therefore, the simulator-rider coordination was analysed as the relative phase between the vertical displacement of the riding simulator and the pitch of the rider's segments in the sagittal plane.

4.3.1.1 Discrete relative phase

A peaking function in MATLAB (*findpeaks*) was used to determine the location (time in samples) of the local maxima of each cycle for 10 consecutive cycles of the pelvis and trunk pitch, and the vertical displacement of the riding simulator. The discrete relative phase between the vertical displacement of the riding simulator and the pelvis or trunk pitch was then calculated as:

$$DRP = \left(\frac{\Delta t}{T} \right) \times 360^\circ \quad (5.1)$$

where Δt represents the difference between the timing of the peak of the vertical displacement of the riding simulator and the pelvis or trunk pitch, respectively, and T the overall duration of the cycle (101 samples) (Van Emmerik, Miller and Hamill, 2014). As positive pitch values indicated posterior pitch, the

DRP compared the relative timing in degrees of the peak vertical displacement of the riding simulator and the peak posterior pitch of the pelvis or trunk, respectively. Ten DRP values were calculated for the two couplings (simulator-pelvis, simulator-trunk) for each participant. Coordination variability of the DRP values between the 10 cycles was calculated as the circular standard deviation in MATLAB (CircStat, Berens (2009)).

4.3.1.2 Continuous Relative Phase

The steps to calculate the continuous relative phase (CRP) involved: (1) inspection, (2) normalisation, and (3) CRP calculation using the Hilbert transform. The rationale for each step will be presented with the methods employed. Briefly, CRP is calculated from the phase-plane: a plot of the normalised angular velocity versus the normalised angular displacement. The phase angle is calculated as the polar coordinates of each data point on the phase plane, and the CRP is the difference in phase angles at each time point (Wheat and Glazier, 2006).

4.3.1.2.1 Inspection

The data were inspected to determine whether they were sinusoidal or non-sinusoidal (Figure 5.2). This is an important consideration for the calculation of the CRP, as it is based on the assumption that the waveforms are sinusoidal with a one-to-one frequency ratio (Hamill, Haddad and McDermott, 2000). In many human movement applications, including the present study, the sinusoidal assumption is violated. This influences the shape of the phase-plane; whereas a sinusoidal oscillation would result in a circular phase-plane, non-sinusoidal trajectories do not (Figure 5.3). As the CRP is calculated from the phase-plane, the deviation from the circular assumption results in error propagation.

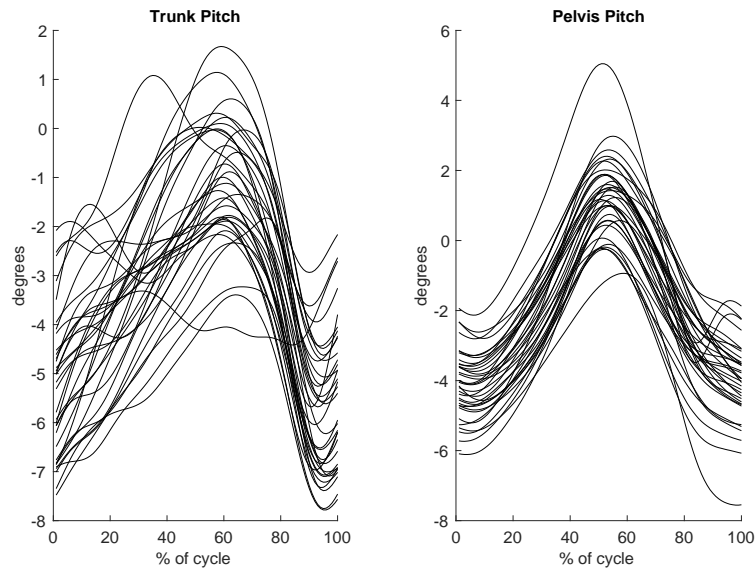


Figure 4.2. Time-normalised and filtered trunk (left) and pelvis (right) pitch waveforms for one subject over 34 cycles of the vertical displacement of the riding simulator in medium trot, sitting.

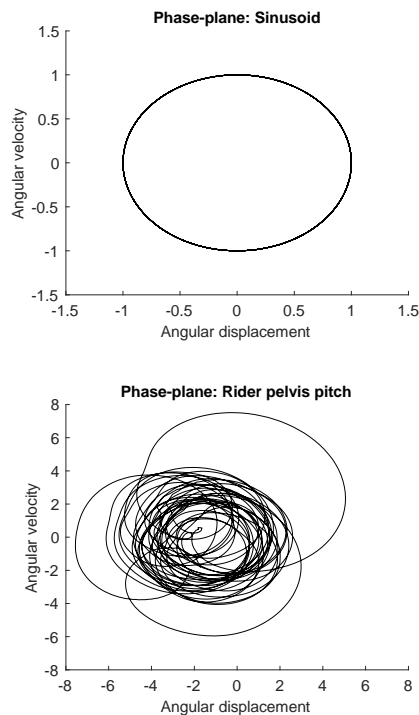


Figure 4.3. An example of phase-planes for a sinusoidal signal (top) and the filtered, but not normalised trajectory of an example rider's pelvis pitch in medium trot.

4.3.1.2.2 Normalisation

The normalisation of the signals centres the trajectories around the origin of the phase space (Lamb and Stöckl, 2014), but also accounts for differences in the frequency and amplitude of the two signals. This is particularly relevant in the present study, as the pitch of the rider's segments was measured in degrees, while the vertical displacement of the riding simulator was measured in millimetres with large differences in amplitudes. If not normalised, the resulting CRP would contain artefacts, that would then result in a spurious increase in measures of variability (Peters *et al.*, 2003). Several approaches have been presented for normalisation (Lamb and Stöckl, 2014; Hamill, Haddad and McDermott, 2000). In the present study, data were normalised as per equation 5.1, where θ' is the normalised angular position at point i of the j^{th} cycle. Data were then reshaped to the range between -1 and 1 (as recommended by Lamb and Stöckl, (2014)). This was accomplished using the *reshape* function in MATLAB.

$$\theta'_{i,j} = 2 \left(\frac{\theta_{i,j} - \min(\theta_{i,j})}{\max(\theta_{i,j}) - \min(\theta_{i,j})} \right) - 1 \quad (4.2)$$

Normalisation based on the cycle minimum and the maximum was chosen rather than normalisation by trial minimum and maximum to account for outliers. If the trial contains outliers and normalisation based on the trial minimum/maximum is performed, the outliers would become the reference cycle, and distortion of the entire cycle would occur (Hamill, Haddad and McDermott, 2000). Finally, normalisation to the range between -1 and 1 allowed the true spatial and temporal properties of the cycle to be retained, where the 0 value of the displacement referred to the point at which the rider's segment pitch crossed from anterior to posterior or vice versa. Furthermore, when performing the calculation of the CRP based on the Hilbert Transform, Lamb and Stöckl (2014) suggest that centring the range of the signal's amplitude around zero ensures that the analytic signal will have the same imaginary component as the raw data, which allows the resulting phase angles to have values in the range of -180° to 180°.

4.3.1.2.3 Calculation of CRP using the Hilbert Transform

The time series violated the sinusoidal assumption of the phase-plane calculation of CRP. If the CRP is calculated based on the phase-plane of these data, it results in frequency and amplitude artefacts in the CRP values. To circumvent this issue and calculate the CRP of non-sinusoidal kinematic data, Lamb and Stöckl (2014) suggest calculating the CRP with centred, normalised data using the Hilbert transform. The Hilbert transform creates an analytic signal from the raw data, which shifts the phases of all the frequency components by $-\pi/2$ radians (-90°). Therefore, the imaginary portion of the Hilbert transform is analogous to the first derivative of the raw signal. The Hilbert transform was applied to the i^{th} sample of the j^{th} cycle of the normalised vertical displacement of the riding simulator, and the normalised angular displacement of the rider's pelvis and trunk, respectively, using the *Hilbert* function in MATLAB, then the phase angle was calculated as:

$$\varphi_{i,j} = \tan^{-1} \frac{H_{i,j}}{x_{i,j}} \quad (4.3)$$

where φ is the phase angle at the i^{th} sample of the j^{th} cycle, H is the value of the imaginary portion of the Hilbert transform and x is the real portion of the Hilbert transform (the original signal).

Then, the continuous relative phase (CRP_φ) between the vertical displacement of the riding simulator and pitch of the rider's pelvis and trunk, respectively, were calculated as follows:

$$\begin{aligned} CRP_{i,j} &= \varphi_{1i,j} - \varphi_{2i,j} \\ &= \tan^{-1} \left(\frac{H_{1i,j}x_{2i,j} - H_{2i,j}x_{1i,j}}{x_{2i,j}x_{1i,j} + H_{1i,j}H_{2i,j}} \right) \end{aligned} \quad (4.4)$$

Where H_1 and H_2 refer to the imaginary portion of the Hilbert transform of the vertical displacement of the riding simulator and the angular displacement of the rider's pelvis or trunk, respectively, x_1 and x_2 refer to the normalised vertical displacement of the riding simulator and angular displacement of the rider's pelvis or trunk, respectively, at the i_{th} time point of the j_{th} cycle, respectively (Lamb and Stöckl, 2014).

This study aimed to obtain a measure of coordination variability from the CRP. Accuracy of the coordination variability is achieved when the CRP time-series does not contain spurious variability due to error or discontinuities (Preatoni *et al.*, 2013). Spurious variability within the CRP was detected at the beginning and end of the stride when the CRP was calculated on signals interpolated to 101 points per cycle. This is a result of the Gibbs phenomenon, which causes 'ringing' (pictured in Figure 5.4) at the extremities of the signal (Lamb and Pataky, 2018). This was eliminated by interpolating the cycle over 1001 samples.

CRP data were inspected for discontinuities, which were values that 'jumped' between 180° and -180° at consecutive time points. The *unwrap* function in MATLAB was used to eliminate these discontinuities, by shifting the angles by adding multiples of $\pm 360^\circ$ until the jump is less than 180° . Finally, coordination variability was calculated as the point-to-point circular standard deviation of the CRP between the vertical displacement of the riding simulator and the pitch of the rider's pelvis and trunk. For further comparison of the DRP and CRP, the mean CRP variability was calculated as the circular mean of the standard deviation of the simulator-pelvis and simulator-trunk CRP, respectively.

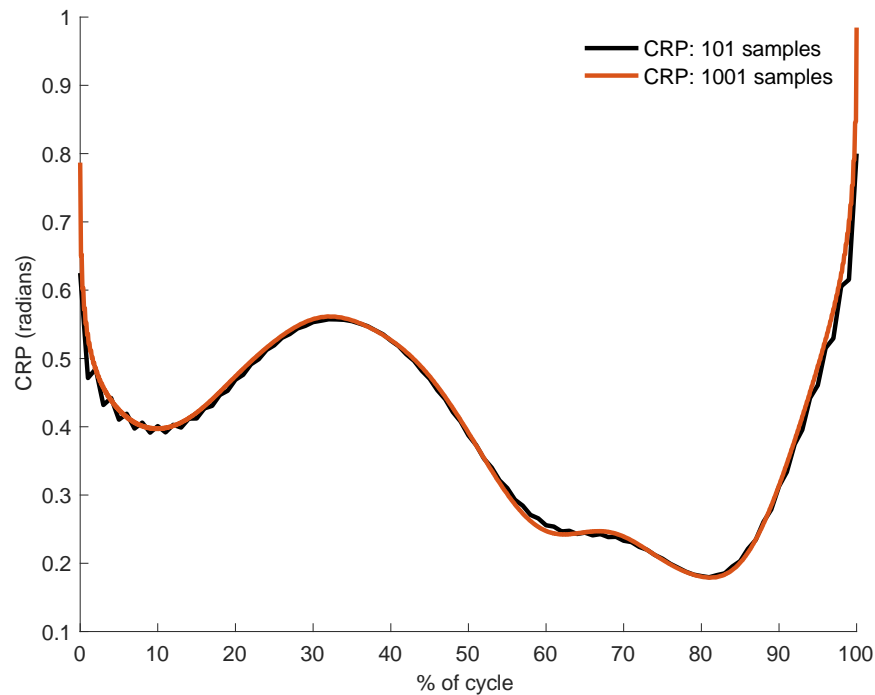


Figure 4.4. Illustration of the Gibbs phenomenon in an example cycle for the simulator-pelvis CRP. The CRP was calculated from raw signals interpolated over 101 points (black) or 1001 points (red).

4.3.1.3 Statistical Analysis

Correlation between the stride-to-stride circular standard deviation of the DRP and CRP (DRP or CRP variability, respectively) were assessed as Pearson's correlation coefficient in SPSS (version 26, IBM Corp., Armonk, N.Y., USA). Separate paired-samples t-tests were used to compare differences between the CRP and DRP variability for the trunk and pelvis. Significance was set at $p = 0.05$ for all tests.

4.3.2 Results

The mean and standard deviation of CRP and DRP variability are presented in Table 4.6. Full statistical outputs are available in Appendix C. CRP or DRP variability were not significantly correlated for the simulator-pelvis coupling ($r(26) = 0.19$, $p = 0.322$), but were moderately significantly correlated for the simulator-trunk coupling ($r(26) = 0.61$, $p = 0.001$). A paired samples t-test indicated that, for the simulator-pelvis coupling, coordination variability was significantly greater by $5.24 \pm 4.66^\circ$ when calculated by CRP

than DRP ($t(26) = 5.95$, $p < 0.001$). No significant difference was found between simulator-trunk CRP and DRP variability ($p = 0.740$).

Table 4.6. Means \pm standard deviation of the circular standard deviation of the discrete relative phase and continuous relative phase for the simulator-pelvis and simulator-trunk couplings, reported in degrees, in simulated medium trot. Grey shading indicates means that were significantly different ($p < 0.05$).

| | Discrete Relative Phase (°) | Continuous Relative Phase (°) |
|------------------|-----------------------------|-------------------------------|
| Simulator-pelvis | 5.55 \pm 3.27 | 10.79 \pm 4.01 |
| Simulator-trunk | 20.68 \pm 23.91 | 21.89 \pm 11.51 |

4.3.3 Discussion

This study aimed to compare measures of coordination variability calculated as the discrete relative phase (DRP) or the mean of the circular standard deviation of the continuous relative phase (CRP) of the coupling between the vertical displacement of the riding simulator and the pitch rotation of the rider's trunk and pelvis, separately. The results suggest that the DRP significantly underestimates the coordination variability of the coupling between the vertical displacement of the riding simulator and the rider's pelvis ($p < 0.001$), but not the rider's trunk ($p = 0.322$). This is most likely due to the high variability of the trunk segment and the multiple peaks of trunk pitch that may occur in a single movement cycle. As shown in Figure 4.2, the location of the maximal peak posterior pitch of the trunk can be variable from cycle to cycle and multiple peaks may be present. The DRP as calculated by Equation 5.1 only considers the relative timing of the single greatest peak of the pitch trajectory to the peak vertical displacement of the riding simulator. Therefore, increased variability of the DRP may be influenced by variability in the peak selection in this case. In the case of the rider, it is impossible to pick the most relevant peak for analysis, as previous studies have not determined the functional relevance of each peak in the rider's trunk pitch. This is overcome with CRP analysis, which is robust to multiple peaks per cycle, provided careful calculation including normalisation and calculation of the complex plane using the Hilbert transform are performed.

Several studies have analysed the coordination between riders' segments and a horse or riding simulator using the discrete relative phase (DRP) (Baillet *et al.*, 2017; Olivier *et al.*, 2017; Engell *et al.*, 2016; Viry *et al.*, 2013, 2015; Lagarde *et al.*, 2005). This method offers a relatively straightforward approach to quantitatively describe the coordination between horse and rider by comparing the temporal alignment of an event in the rider's technique with a key event in the horse's gait cycle. However, the key events must have functional relevance and relate to the objectives of the research questions. To work an example: the peak vertical displacement of the horse's sacrum in trot corresponds to the suspension phase of trot (Clayton and Hobbs, 2019a). As defined in this study, peak pitch may correspond to the peak posterior pitch of a rider segment. Therefore, the DRP would describe the temporal relationship between the peak posterior pitch of the rider's pelvis and the suspension phase in the trot. It would not describe the temporal relationship between horse and rider movements during other phases of the gait cycle, such as stance and the conclusions must reflect that. Further, as coordination strategies emerge from the complex interplay of constraints (environment, participant and task), the use of the DRP to analyse the coordination relationship between horse and rider during a continuous task such as gait is an erroneous proposition. If no *a priori* hypothesis is established regarding the point at which the rider's coordination with the horse should be the most stable, the CRP is more suitable than the DRP for measuring coordination variability throughout the gait cycle.

The continuous relative phase (CRP) quantifies the relationship between two segments at each time point of the cycle. It has been used in sports biomechanics to quantify the coordination between trunk and pelvis in the golf swing (Lamb and Pataky, 2018), pelvis-limb coupling in race walkers (Cazzola, Pavei and Preatoni, 2016), postural coordination in gymnastics (Marin, Bardy and Bootsma, 1999), and inter-limb coordination during hockey skating (Mazurek *et al.*, 2020), among others. One study (Lagarde *et al.*, 2005) calculated the instantaneous phases of the vertical displacement of horses and riders using the Hilbert transform but concluded that, for vertical motion of horse and rider, the DRP yielded similar results. Only

Wolframm, Bosga and Meulenbroek (2013) reported circular mean and standard deviation of the continuous relative phase between the horizontal acceleration of the rider's trunk compared to the horse's trunk.

Although the mean of the circular standard deviation of the CRP has been used in the present study and others (Wolframm, Bosga and Meulenbroek, 2013), summarising a continuous measure like the CRP may be problematic for several reasons. First, information regarding the points in the cycle where the greatest coordination variability occurs is lost. Coordination variability increases before a transition to a more stable state (Scott Kelso, 2009b), therefore, this information may have functional relevance. Second, this measure may be skewed if extreme values in the coordination variability are present at any point in the cycle. To overcome this the CRP can be analysed with statistical methods that retain the temporal scale of the data to identify areas where peaks in the coordination variability may have functional relevance. Statistical parametric mapping (SPM1D) has been used with CRP trajectories for hypothesis testing (Lamb and Pataky, 2018), and principal component analysis (PCA) has been used to distinguish patterns in the CRP trajectories (Mazurek *et al.*, 2020). While these studies looked at the coordination, rather than the coordination variability, similar approaches could be employed on the CRP variability to answer questions regarding the points in the gait cycle where the coordination between horse and rider is most variable. Due to the circular nature of the CRP values, care should be taken to ensure that the trajectories are within the range of 0-180° before statistical analysis with SPM1D or PCA. Further details on these approaches are covered in Chapter 6 and Chapter 7.

4.3.4 Conclusion

In conclusion, discrete and continuous methods exist to analyse the coordination and coordination variability between horse and rider. The discrete relative phase (DRP) is appropriate when the hypothesis pertains to a single gait event or the relative timing of an occurrence of an event, such as two maximums. The continuous relative phase (CRP) is more appropriate when the study aims to characterise the

coordination or coordination variability over the entire stride or when there is no *a priori* hypothesis relating the latency between single events in a cycle. The rider's trunk pitch shows multiple peaks of varying sizes in a single movement cycle. This suggests that the CRP is more appropriate to measure the coupling between the rider's trunk pitch and the vertical displacement of the riding simulator. The results of the statistical tests on the simulator-pelvis coupling show that when a single well-defined peak occurs within each trajectory of interest per cycle, the DRP may underestimate the coordination variability compared to the CRP. This occurs as the CRP considers both the timing of the peak and the similarity between the slopes of the two signals. Care must be taken in the calculation of the CRP; however, methods are well-described to use this measure within biological signals that are non-sinusoidal. The CRP, therefore, is a suitable and sensitive method to assess the simulator-rider coordination and coordination variability and will be used to meet the aims of the studies within this thesis.

5. Static pelvic posture is not related to dynamic pelvic tilt or competition level in dressage riders

5.1 Introduction

The dressage rider's ability to achieve dynamic postural stability is integral to their performance and safety. Previous research and lay coaching texts propose several factors that may influence the horse-rider interaction, including rider competition level and experience (Baillet *et al.*, 2017; Olivier *et al.*, 2017; Münz, Eckardt and Witte, 2014; Schöllhorn *et al.*, 2006; German National Equestrian Federation, 2005; Lagarde *et al.*, 2005; Peham *et al.*, 2001). Studies have analysed the relevance of the rider's pelvic technique to the quality of the horse-rider interaction, with significant interactions between rider experience level and the kinematics of the pelvis found in some (Münz, Eckardt and Witte, 2014) but not all (Eckardt and Witte, 2017) studies. Indeed, biomechanical models proposed by de Cocq, Muller, Clayton, and van Leeuwen (2013) suggest that several combinations of trunk stiffness and damping result in in-phase coordination with the horse. A variety of pelvic and trunk postures have been observed in experienced, competitive dressage riders at the halt and during sitting trot (Alexander *et al.*, 2015) and standing (Hobbs *et al.*, 2014). The largest of these studies used 3D motion capture to measure posture and flexibility in 134 competitive dressage riders standing and seated in a static saddle (Hobbs *et al.*, 2014). Their findings indicated that postural deviations from a neutral spine during standing, including lordosis, kyphosis, swayback and flatback, are common in riders, regardless of competition level or years of experience. As static postural assessment may reflect the individual's musculoskeletal balance and stability (Norris, 1995), it may provide a convenient tool to assess the rider. However, the relationship between static and dynamic postures in the rider is unclear. One known study to date has investigated this, observing strong significant correlations ($r = 0.83$, $p < 0.05$ for left rein; $r = 0.88$, $p < 0.05$ for right rein) between anterior-posterior pelvic tilt in halt and during the sit phase of rising trot in both directions for 16 experienced riders (Gandy *et al.*, 2018). However, in rising trot, the rider actively rises out of the saddle

on alternate diagonal stance phases, which places a greater demand on the legs, rather than the rider's lumbopelvic region, to determine the mechanical properties of the rider (de Cocq *et al.*, 2013). Therefore, analysis of the relationship between seated postures at halt and seated postures in walk, trot and canter is justified.

The influence of the rider's pelvic tilt on their functional range of pelvic motion in seated walk, trot and canter is unknown. Furthermore, the evidence suggesting the effect of rider skill or competition level is equivocal. At the individual level, the rider's functional range of motion may factor into their incidence of back pain. If the rider adopts a large, uncontrolled anterior pelvic tilt throughout the stride, they risk increased shearing forces on the lumbopelvic region due to reliance on the passive stability afforded by elastic recoil of non-contractile tissues of the spine and facet joint approximation, rather than active stability by muscular contraction (Norris, 2008). Similarly, restrictions due to pain or abnormal myofascial length and recruitment limit the available range of pelvic motion (Comerford and Mottram, 2012). Hobbs *et al.* (2014) reported back pain in individuals with and without a neutral standing posture, which suggests the development of back pain in the rider is unrelated to their static posture and may relate to the demands of the sport. Indeed, the majority of individuals can intentionally adopt anterior, posterior or neutral pelvic positions when seated (Hayden *et al.*, 2018), however, their ability to maintain these postures during dynamic movements is unclear. Therefore, investigation of the relationship between the rider's static pelvic posture in the saddle and dynamic technique is warranted to inform specific interventions to enhance rider health and performance and performance.

As the relationship between the rider's halt posture, competition level and gait are unknown, this study aimed to use a riding simulator to; (1) explore whether patterns of pelvic tilt are related to rider competition level; (2) to examine whether there is an association between rider pelvic tilt in their static, seated position and during riding; (3) to describe the characteristics of the rider's range of pelvic pitching motion (ROM), including total mean ROM, minimum and maximum; (4) to compare mean pelvic tilt

assessed in the walk, sitting trot, left canter and right canter to determine whether riders follow a common pelvic technique. We hypothesise that riders will show common patterns of pelvic tilt, related to competition level.

5.2 Methods

5.2.1 Participants

Thirty-five adult female dressage from the overall dataset were included in this study. The full inclusion criteria are described in Table 3.3. Riders were classed by their competition level based on the level of their three highest results in the last six months preceding the data collection. Advanced level riders were those competing in FEI classes. Intermediate level riders were competing at the upper levels of national competition, and novice level riders were competing at the introductory levels of national competition (BD Novice, Preliminary and Elementary). Full participant characteristics for each competition level category are detailed in Table 3.4. All participants were riding regularly at the time of the study, with no reported injury or pathology that stopped them from taking part in riding activities or competition.

5.2.2 Data acquisition

Kinematic data were captured with motion capture (Miquis M3, Qualisys AB, Gothenburg, Sweden) on the riding simulator (Eventing Simulator, Racewood Ltd., Tarporley, UK), as described in Section 3.2. As described in Section 3.2.5, riders were initially captured for two seconds in a static position (“halt”), and then for 10 seconds of a medium walk, medium trot, medium left canter and medium right canter. As described in Section 3.3, the data were processed to extract the angular displacement of the rigid body of the pelvis. Data were then filtered (Section 3.3.2), split into movement cycles, and time-normalised (Section 3.3.3).

5.2.3 Data processing

The mean, minimum and maximum pelvic pitch values were computed for six strides and averaged for the trial. Given the orientation of the local coordinate system, pitch values of -0.99° – 0.99° were

designated as neutral pelvic tilt, anterior as values $\leq -1.0^\circ$ and posterior as values $\geq 1.0^\circ$. The pitch range of motion was calculated as the difference between the average minimum and maximum pelvic pitch values.

5.2.4 Statistical analysis

The influence of gait and competition level on mean pelvic tilt, range of motion, and minimum and maximum values were investigated using SPSS (version 26, IBM Corp., Armonk, N.Y., USA). The hypothesis of normality and homogeneity of variance were analysed for each variable using the Shapiro Wilk test and Levene's test. A one-way ANOVA was conducted on the influence of the independent variable, competition level (novice, intermediate, advanced), on the mean pelvic tilt in halt and each gait (walk, trot, left canter and right canter). Values were corrected for sphericity using the Huynh-Feldt correction. If a significant *p*-value was obtained for the main or interaction effect of the ANOVA, a *post-hoc* was conducted using a Bonferroni corrected *t*-test for multiple comparisons. The correlation between mean pelvic tilt in halt, walk, trot, left canter and right canter were calculated using a Pearson's Product Moment test.

Range of pelvic pitching motion (ROM), and minimum and maximum pelvic tilt values were not normally distributed, therefore, differences between these variables across the competition level categories were analysed by separate Independent Samples Kruskal-Wallis Tests. The relationship between halt pelvic tilt values, total range of pelvic pitching motion (ROM), and minimum and maximum pelvic tilt values were analysed by separate Spearman's Rank-Order Correlation tests. The significance level for all tests was set to $p < 0.05$. Full details of statistical outputs are given in Appendix C.

5.3 Results

5.3.1 Mean pelvic tilt

Table 5.1 shows the mean (\pm SD) pelvic tilt overall, by competition level at the halt, and in each gait. Based on the results of the one-way ANOVA, there were no interaction effects of gait and competition level on mean pelvic tilt ($F(3.78, 68.18) = 1.35$; $p = 0.233$, $\eta^2 = 0.083$). The significant main effect of condition (halt,

walk, trot, left canter or right canter) ($F(2.13,68.18) = 4.48$; $p = 0.017$, $\eta^2 = 0.12$) on mean pelvic tilt was investigated post-hoc using a Bonferroni corrected t -test.

All riders tended to adopt a posterior pelvic tilt as the gait increased. The Bonferroni post hoc test indicated that mean pelvic tilt in the walk was significantly more anterior than trot ($p = 0.039$), left canter ($p = 0.015$) and right canter ($p = 0.001$), respectively.

Table 5.1. Mean pelvic tilt values \pm standard deviations in halt, walk, left canter and right canter by competition level.

| | Overall Mean | Novice | Intermediate | Advanced |
|---------------------|----------------------|---------------------|----------------------|----------------------|
| Halt | $-0.1 \pm 4.9^\circ$ | $1.9 \pm 4.3^\circ$ | $-0.4 \pm 5.7^\circ$ | $-2.3 \pm 3.6^\circ$ |
| Walk | $-0.01 \pm 3.3^{**}$ | $0.4 \pm 2.9^\circ$ | $-1.0 \pm 3.4^\circ$ | $1.1 \pm 3.3^\circ$ |
| Trot | $1.5 \pm 3.3^\circ$ | $1.8 \pm 2.6^\circ$ | $0.6 \pm 3.5^\circ$ | $2.5 \pm 3.7^\circ$ |
| Left Canter | $1.8 \pm 3.8^\circ$ | $1.9 \pm 5.0^\circ$ | $1.5 \pm 2.7^\circ$ | $2.2 \pm 4.1^\circ$ |
| Right Canter | $2.2 \pm 3.6^\circ$ | $2.7 \pm 4.5^\circ$ | $2.0 \pm 2.6^\circ$ | $1.9 \pm 4.2^\circ$ |

* Mean significantly ($p < 0.05$) different to all other means.

At the halt, novice riders tended to adopt a posterior pelvic tilt ($1.9 \pm 4.3^\circ$), intermediate riders adopted a neutral pelvic tilt ($-0.4 \pm 5.7^\circ$) and advanced riders adopted an anterior pelvic tilt ($-2.3 \pm 3.6^\circ$), however, there were no significant interactions ($p = 0.233$) between competition level and pelvic tilt. Furthermore, large standard deviation values (listed in Table 5.1) demonstrate the spread of individual strategies about the central tendency. Correlation coefficients indicated that halt posture did not correlate with pelvic tilt in any gait (halt-walk $r = 0.25$, $p = 0.143$; halt-trot $r = 0.07$, $p = 0.707$; halt-left canter $r = -0.04$, $p = 0.812$, halt-right canter $r = 0.13$, $p = 0.453$). Moderate significant correlations were observed between pelvic tilt in trot and right canter (trot-right canter $r = 0.49$, $p = 0.003$) and large between walk, trot and canter (walk-trot $r = 0.68$, $p = 0.001$; walk-left canter $r = 0.70$, $p = 0.001$; walk-right

canter $r = 0.68$, $p = 0.001$; trot-left canter $r = 0.62$, $p = 0.001$; left canter-right canter $r = 0.89$, $p = 0.001$).

5.3.2 Pelvis range of motion

Riders increased their pelvic range of motion (ROM) as they progressed from walk to trot and both leads of canter. No significant correlations were found between halt pelvic tilt values and ROM in any gait (walk $r = -0.30$, $p = 0.085$; trot $r = 0.10$, $p = 0.572$; left canter $r = -0.15$, $p = 0.397$; right canter $r = -0.10$, $p = 0.557$). The mean range of motion (\pm standard deviation) by competition level category is listed in Table 5.2. An Independent Samples Kruskal-Wallis test found no significant differences between competition levels and range of motion in any gait. Greater standard deviation of the mean was observed for novice riders in left canter, while mean range of motion was greater and more variable in right canter for intermediate and advanced riders, although this did not reach statistical significance.

Table 5.2. Mean range of motion \pm standard deviation by competition level category.

| | Novice | Intermediate | Advanced |
|--------------|-----------------|-----------------|-----------------|
| Walk | 7.4 \pm 3.4° | 6.6 \pm 2.7° | 6.7 \pm 2.7° |
| Trot | 11.2 \pm 4.0° | 9.4 \pm 2.2° | 9.9 \pm 2.8° |
| Left Canter | 14.1 \pm 4.1° | 12.9 \pm 3.9° | 13.2 \pm 4.5° |
| Right Canter | 14.0 \pm 3.1° | 13.6 \pm 4.2° | 14.6 \pm 5.2° |

5.3.3 Minimum and maximum tilt values

Minimum and maximum values grouped by riders' halt pelvic tilt are displayed in Figure 5.1 and data to describe each rider's pelvic strategy are displayed in Table 5.3. Minimum and maximum values were the same across all categories of level, except in right canter, where the maximum value was significantly different between competition level categories ($H(2) = 8.1$, $p = 0.017$). Pairwise comparisons with adjusted p values showed that novice riders' maximum pelvic tilt values were significantly more posterior than advanced riders ($p = 0.016$, $r = 0.33$) and intermediate riders ($p = 0.011$, $r = 0.49$).

Table 5.3. As riders progressed through the gaits, individuals exhibited unique pelvic tilt strategies. The rider's dynamic pelvic strategy was determined by their minimum and maximum pelvic tilt values. Riders were anterior if their minimum and maximum pelvic tilt values were less than 0°, anterior/posterior if their minimum was less than 0° and maximum greater than 0°, and posterior if their minimum and maximum values were both greater than 0°.

| Pelvic tilt strategy determined by minimum and maximum values | | | | | |
|---|-----------|--------------------|--------------------|--------------------|--------------------|
| Competition Level | Halt | Walk | Trot | Left Canter | Right Canter |
| Novice | anterior | anterior/posterior | anterior/posterior | anterior/posterior | anterior/posterior |
| | anterior | anterior/posterior | posterior | anterior/posterior | anterior/posterior |
| | anterior | anterior/posterior | anterior/posterior | anterior/posterior | anterior/posterior |
| | neutral | anterior/posterior | anterior/posterior | anterior/posterior | posterior |
| | neutral | anterior/posterior | anterior/posterior | anterior/posterior | posterior |
| | posterior | anterior/posterior | anterior | anterior/posterior | anterior/posterior |
| | posterior | anterior/posterior | posterior | anterior/posterior | anterior/posterior |
| | posterior | anterior/posterior | anterior/posterior | anterior/posterior | anterior/posterior |
| | posterior | anterior/posterior | anterior/posterior | anterior/posterior | anterior/posterior |
| | posterior | posterior | posterior | anterior/posterior | anterior/posterior |
| | posterior | anterior/posterior | anterior/posterior | anterior/posterior | anterior/posterior |
| Intermediate | anterior | anterior/posterior | anterior/posterior | posterior | anterior/posterior |
| | anterior | anterior | posterior | anterior/posterior | anterior/posterior |
| | anterior | anterior | anterior/posterior | anterior/posterior | anterior/posterior |
| | anterior | anterior/posterior | anterior/posterior | posterior | anterior/posterior |
| | anterior | anterior | anterior/posterior | anterior | anterior/posterior |
| | neutral | anterior/posterior | anterior/posterior | anterior/posterior | anterior/posterior |
| | neutral | anterior/posterior | posterior | anterior/posterior | anterior/posterior |
| | neutral | anterior | anterior/posterior | anterior | anterior |
| | neutral | anterior | posterior | anterior/posterior | anterior/posterior |
| | neutral | anterior | anterior/posterior | anterior/posterior | anterior/posterior |
| | posterior | posterior | posterior | anterior/posterior | anterior/posterior |
| | posterior | anterior/posterior | anterior/posterior | anterior/posterior | anterior/posterior |
| | posterior | anterior/posterior | anterior/posterior | anterior/posterior | anterior/posterior |
| | posterior | anterior/posterior | anterior/posterior | anterior/posterior | anterior/posterior |
| Advanced | anterior | anterior/posterior | posterior | anterior/posterior | posterior |
| | anterior | anterior/posterior | anterior/posterior | anterior/posterior | anterior/posterior |
| | anterior | anterior/posterior | anterior | anterior/posterior | anterior/posterior |
| | anterior | anterior/posterior | posterior | anterior/posterior | posterior |
| | anterior | anterior/posterior | anterior/posterior | anterior/posterior | anterior/posterior |
| | neutral | anterior/posterior | anterior/posterior | anterior/posterior | anterior/posterior |
| | neutral | anterior/posterior | anterior/posterior | anterior/posterior | anterior/posterior |
| | posterior | anterior | anterior/posterior | anterior | anterior/posterior |
| | posterior | anterior/posterior | posterior | anterior/posterior | anterior/posterior |

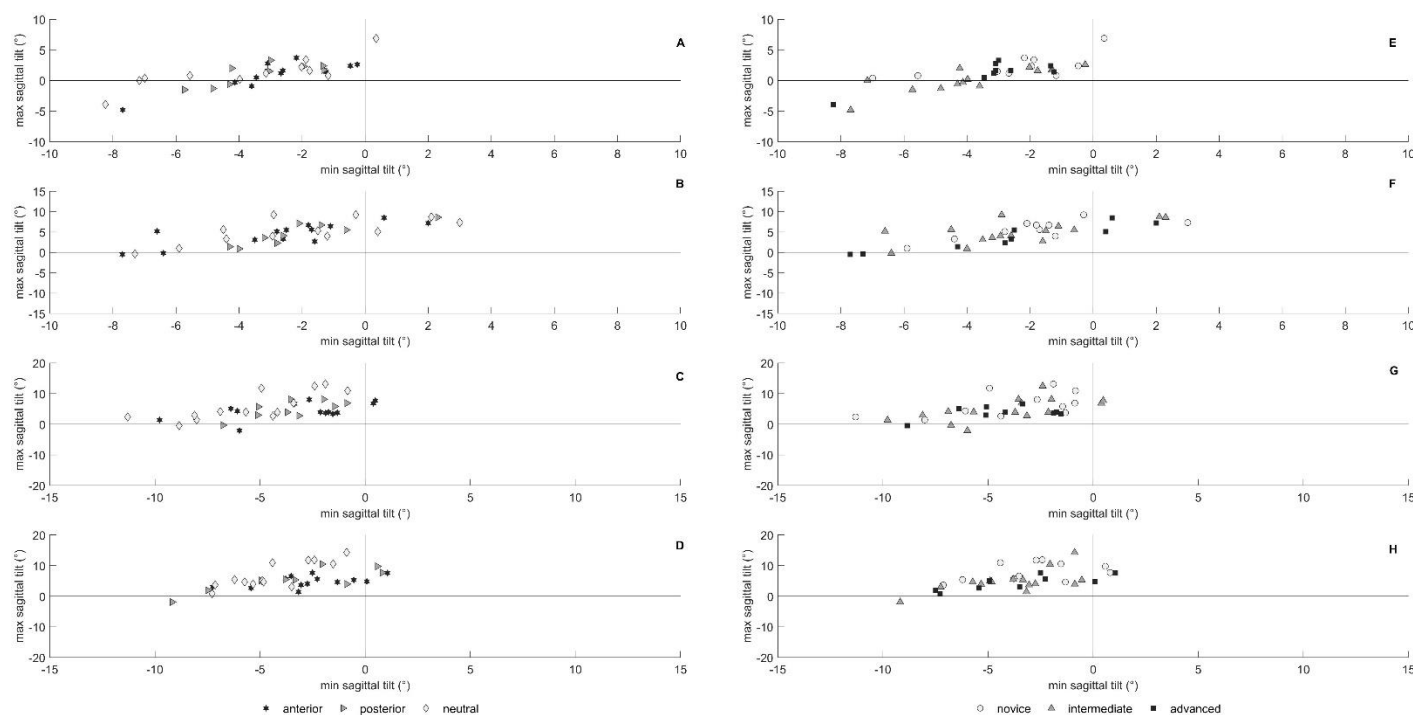


Figure 5.1. Riders' minimum and maximum pelvic tilt by halt pelvic posture category in (A) walk, (B) trot, (C) left canter, and (D) right canter, and by competition level category in (E) walk, (F) trot, (G) left canter, and (H) right canter. Posture categories were defined by the rider's pelvic tilt value at halt. Anterior was defined as values of -10° or less, neutral as between 0.99° and -0.99° and posterior as 1° or greater. Competition level categories were defined by the level of their last three results in competition as novice (British Dressage Novice, Preliminary or Elementary), intermediate (British Dressage Medium, Advanced Medium or Advanced) and advanced (FEI Prix St Georges, Inter I or II or Grand Prix).

No significant correlations were found between pelvic tilt at halt and any minimum or maximum value (walk min-halt $r = -0.004$, $p = 0.983$; walk max-halt $r = -0.10$, $p = 0.582$; trot min-halt $r = -0.06$, $p = 0.745$; trot max-halt $r = -0.05$, $p = 0.778$; left canter min-halt $r = -0.004$, $p = 0.984$; left canter max-halt $r = -0.08$, $p = 0.651$; right canter min-halt $r = -0.27$, $p = 0.125$; right canter max-halt $r = -0.27$, $p = 0.117$).

The dynamic pelvic strategy (Figure 5.1) was determined from the minimum and maximum pelvic tilt values and described as anterior if their minimum and maximum pelvic tilt values were less than 0° , anterior/posterior if their minimum was less than 0° and maximum greater than 0° , and posterior if their minimum and maximum values were greater than 0° . As a whole, most riders exhibited an

anterior/posterior strategy. Outliers indicate that individual strategies in each gait exist. In walk, seven riders remained anterior throughout. Six of these riders were classed as intermediate, three were anterior at halt and three were neutral. One advanced rider was posterior at halt, yet anterior throughout in walk (min: -8.2° , max: -3.9°). In trot, two riders that were classed at halt as posterior and two neutral maintained anterior pelvic tilt throughout the stride. One novice rider, posterior at halt, displayed a large anterior minimum (-13.9°) and near-neutral maximum (-0.9°). One rider with an anterior tilt at halt and one neutral remained posterior throughout. Two intermediate riders, anterior and neutral at halt, respectively, remained anterior throughout.

5.4 Discussion and Implications

The lumbopelvic region is the main interface between horse and rider movement. This is the first known study to compare static pelvic posture to pelvic pitching motion in simulated walk, trot and canter across levels of dressage rider. This study aimed to analyse the relationships between gait and competition level on static and dynamic mean pelvic tilt, range of pitching motion, minimum and maximum. It was hypothesised that riders would show common patterns of pelvic tilt, related to competition level. This hypothesis was partially accepted as significant differences between competition levels were observed for maximum pelvic tilt in right canter, however, no other significant differences related to competition level were found.

5.4.1 Comparison between halt pelvic posture and mean pelvic posture in motion

Static assessment of the rider's posture is common in equestrian coaching practice and published research (Guire *et al.*, 2017; Hobbs *et al.*, 2014). Assessing the rider in a static position allows the coach to observe the rider's posture closely from all angles, which can be difficult to achieve during riding. Accordingly, as riding is considered a postural sport, it is expected that the rider's seated, static posture will reflect their dynamic patterns (Schiavone and Tulli, 1994). It is assumed that a neutral pelvis and spinal posture are

optimal for the rider to absorb the forces generated by the horse without incurring back pain (Wanless, 2017). Previous evidence found significant correlations between pelvic asymmetry in the sagittal plane observed in static seated posture and end of range clinical tests (Al-Eisa *et al.*, 2006), and between pelvic tilt at halt and in the sit phase of rising trot in riders (Gandy *et al.*, 2018). However, in the present study, no dynamic postures were correlated to the rider's halt posture, suggesting that the rider's pelvic tilt in motion is not related to their position at halt. The present results contrast with Gandy *et al.* (2018), who observed good correlation between anterior-posterior pelvic rotation in rising trot and halt posture. This illustrates differences in the biomechanical demands of rising trot to sitting trot, whereby the rider uses their legs to rise out of the saddle, rather than the lumbopelvic-hip complex to absorb the motion.

Few studies have characterised the pelvic technique of the rider, therefore, anatomical and functional factors relating to the rider's technique are relatively unknown. In the current study, moderate and large significant correlations were observed between mean pelvic tilt in walk, trot, left canter and right canter. This suggests that riders oscillate around a similar mean value in all gaits. As speed increased from walk to trot and canter, a significant increase in posterior pelvic tilt was observed (trot $p = 0.039$; left canter $p = 0.015$; right canter $p = 0.001$). Byström *et al.* (2015), and Engell *et al.* (2016) also observed greater posterior pelvic tilt when riders were actively influencing their horse's stride in collected trot or passage, accompanied by greater coupling between horse and rider. Whilst the riders in the present study did not have to initiate upward transitions, as an attendant changed the gaits, the increase in posterior tilt may be a response to the increase in displacement of the simulator, allowing greater coincident movement between horse and rider. Large between-rider variation of the mean tilt indicates that riders possess individual strategies, which are underpinned by variability in the rider's minimum and maximum tilt values in walk, sitting trot and both directions of canter. Further work should aim to investigate the kinematics of the pelvis related to the rider's riding technique and the coincident movement of horse and rider.

5.4.2 Competition level

Previous research has suggested skill-related differences in rider technique (Baillet *et al.*, 2017; Eckardt and Witte, 2017; Olivier *et al.*, 2017; Münz, Eckardt and Witte, 2014; Biau *et al.*, 2013; Kang *et al.*, 2010; Schils *et al.*, 1993). A diverse range of criteria has been used to classify rider skill, including years of experience, competition level and professional status. Statistically significant differences have been found in riders' postural strategy between skill level groups in studies that assessed the coordination between the rider's trunk and the movement of the horse (Baillet *et al.*, 2017; Biau *et al.*, 2013; Lagarde *et al.*, 2005; Münz *et al.*, 2014; Olivier *et al.*, 2017; Peham *et al.*, 2001), but not by Eckardt and Witte (2017). Current research suggests that advanced riders display less variability in their postural strategy (Lagarde *et al.*, 2005), ride the horse closer to their natural, preferred speed (Peham *et al.*, 2001), rely less on visual cues to synchronise their movements with the horse (Olivier *et al.*, 2017), tend to match the oscillation of the horse's trunk with coordinated oscillations of their pelvis (Eckardt and Witte, 2017), and reach maximal dorsal tilt later in the stride in canter than beginner riders (Münz, Eckardt and Witte, 2014). However, these studies have relied on small sample sizes and, in some cases, different horses for beginner and advanced riders, which influence the demands imposed on each skill group.

In the current study, all riders were exposed to the same oscillation, by using a riding simulator. Contrary to our hypothesis, competition level was not significantly related to halt pelvic posture, dynamic mean pelvic tilt or range of motion (ROM). Competition level influenced maximum pelvic tilt values in right canter only. Novice riders had a significantly ($p = 0.017$) greater posterior maximum pelvic tilt ($8.1^\circ \pm 3.0$) than intermediate ($4.9^\circ \pm 3.6$) or advanced ($4.4^\circ \pm 2.4$) riders in right canter. As previously stated, the difference between left and right canter on the riding simulator is marginal (41 mm greater mediolateral displacement to the opposite side). Therefore, differences in the rider's posture between the two leads of canter were surprising. Right-sided asymmetries are common findings in equestrian research. Symes and Ellis (2009) observed greater chaos of experienced riders' left and right shoulder displacement in right

canter on live horses. Münz et al. (2014) also observed significantly greater posterior pelvic tilt in right canter in beginner riders compared to professionals, although their study did not compare right and left canter, therefore it is unclear whether novice riders' posterior pelvic tilt is related to the direction of canter or the asymmetrical movement of canter itself. Interestingly, riders competing at an advanced competition level and those with over 40 years of experience exhibited greater right ROM in a seated lateral flexion test (Hobbs *et al.*, 2014). It is unclear whether directional bias in novice riders results from their strategies, amplified by the small number of riders in the novice group ($n = 11$), thus further investigation is needed.

The present results suggest that once riders achieve the motor control necessary to maintain stability on the horse, that other factors, such as the morphological constraints imposed by mobility, flexibility and patterns of muscle activation, have a greater influence on motion in the sagittal plane than competition level. Intra-subject variation within each competition level, particularly in the minimum and maximum values between each gait, indicates that riders possess individual neuromuscular strategies to achieve and maintain dynamic postural stability on the horse. Many factors may influence the rider's ability to participate in competitions, therefore, individual assessment of biomechanical indicators of rider skill, rather than the use of competition level as a classification factor, may provide greater objectivity in rider assessment and research. Competitive riders may adopt multiple pelvic strategies, however, the classification of rider skill based solely on the pelvis may be reductive. Further studies integrating measures of pelvic tilt into whole-body kinematics of the rider may provide greater evidence towards quantitative assessment of rider skill that is independent of competition level.

5.4.3 Range of motion

Many factors may influence the lumbopelvic-hip range of motion (ROM) in riders, including subject-specific characteristics such as age, flexibility, pain, disease and hip morphology (Comerford and Mottram, 2012). The overall mean ROM values found in the present study (walk: $6.9^\circ \pm 2.9$; trot: $10.1^\circ \pm 3.0$; left

canter: $9.1^{\circ} \pm 3.1$; right canter: $9.2^{\circ} \pm 2.9$) were smaller than those found in high-level horse and rider pairs in walk ($9.7^{\circ} \pm 2.0$) and trot ($13.9^{\circ} \pm 2.2$) by Byström, Rhodin, von Peinen, Weishaupt & Roepstorff (2009, 2010). Similarly, these values were smaller than those found by Münz et al., (2014) in walk (beginner: $8.1^{\circ} \pm 4.1$, pro: $11.1^{\circ} \pm 3.6$), trot (beginner: $13.5^{\circ} \pm 4.1$, pro: $14.8^{\circ} \pm 7.5$), and canter (beginner: $22.2^{\circ} \pm 7.8$, pro: $18^{\circ} \pm 5$). The rider's pelvic range of motion may be most influenced by the horse; therefore, smaller ranges seen in the present study may be due to the use of the riding simulator. No significant differences were found in the present study between ROM and competition level. As the horse dictates the frequency and amplitude of movement, differences between horses may result in varying ranges of rider pelvic rotation.

Riders increased their pelvic ROM as the gait increased. However, no significant correlations were found between halt pelvic tilt values and ROM in any gait. Some evidence suggests that the functional characteristics of the rider's posture may influence available ROM during riding. Alexander et al., (2015) investigated the effects of a taping intervention applied to the rider's thoracic spinal region on their kinematics in sitting trot. Riders exhibited a significantly greater lumbar range of motion following the intervention. This evidence suggests that restriction of the thoracic region results in a compensatory increase in lumbar ROM. Sagittal analysis of the rider's pelvis may be insufficient to fully elucidate the patterns of asymmetrical movement in the rider's pelvis and their causes. Further studies should investigate the functional range of motion utilised during riding, within the context of the individual's available range, assessed during a dynamic ROM test and riding.

5.4.4 Minimum and maximum pelvic tilt values

Analysis of the minimum and maximum pelvic tilt values in walk, trot and canter reveal interesting insights into riders' postural strategies. There was no relationship between the rider's halt posture and their minimum and maximum pelvic tilt values, which suggests that halt values, do not reflect end ranges of anterior or posterior pelvic tilt during riding in the current study.

Changes in the position of the riders' minimum and maximum pelvic tilt values relative to the neutral origin underline the importance of single-subject analysis. Most riders tended to adopt an anterior/posterior strategy, with a minimum tilt in the anterior range and maximum tilt in the posterior range in each gait. Some riders, however, stayed anterior or posterior throughout the stride. The fluctuation of some riders from posterior pelvic tilt at halt to anterior throughout the stride in walk, to posterior throughout in trot and anterior/posterior in canter reflect individual strategies to remain stable and upright as the horse moves. Maintaining an anterior or posterior pelvic tilt throughout the stride increases the potential for back pain due to compressive and shear forces on the lumbar spine (Norris, 2008). These postural strategies may relate to the individual's learned motor control strategies and segmental control. The position of the pelvis and the phase of the horse's stride influences muscular activation patterns in the trunk and movement of the limbs (Comerford and Mottram, 2012), therefore, the variety of strategies observed in this study warrant further investigation of their influence on the whole body kinematics of the rider. Moreover, variability in the rider's patterns results from the interactions of the rider's structural and functional characteristics, which, as this study shows, are not evident from static assessment or examination of group means. Further research should aim to understand the factors that influence the rider's strategies and aim to assess whether individuals aggregate around certain factors, which favour group analysis, or whether individual rider strategies are diverse and require single-subject analysis.

5.4.5 Study limitations

Several studies to date have used riding simulators to analyse rider kinematics (Baillet *et al.*, 2017; Olivier *et al.*, 2017; Cha, Lee and Lee, 2016; Yoo *et al.*, 2014; Biau *et al.*, 2013). However, the differences between rider biomechanics observed on the riding simulator and in field conditions are unknown. Riders in the present study used a generic saddle that was not fitted to the individual rider, although they adjusted the

stirrups to their preferred length. The characteristics of the saddle, including seat slope and stirrup length, may influence the rider's hip angle and spinal curves (Greve and Dyson, 2013).

6.0 Conclusions

Riders adopt a dynamic technique on a riding simulator that cannot be predicted from their static riding position. Minimum and maximum values can indicate the characteristics of the rider's strategy; whether they maintain an anterior or posterior pelvic tilt throughout, or oscillate between anterior and posterior ranges. However, minimum and maximum values in walk, trot and canter are not associated with halt posture. Assessment of pelvic tilt at halt is insufficient to differentiate between elite and sub-elite riders, and competent riders possess individual strategies that may be obscured by group means. Therefore, the subsequent studies of this thesis will use dynamic measures, and continuous, rather than discrete measures where possible, to characterise the rider's technique. The data regarding the rider's competition level suggest that riders should not be grouped by competition level when assessing their pelvic posture. The subsequent chapters of this thesis will assess whether other variables may discriminate between competitive levels in dressage riders.

6. Coordination variability in skilled riders on the riding simulator in medium and extended trot

6.1 Introduction

Dressage riders aim to give subtle cues so that '*the horse... gives the impression of doing, of its own accord, what is required*' (p. 9 Fédération Internationale Équestre (2020)). To achieve this, the rider aims to increase the horse's sensitivity to their cues as it progresses in training. The rider applies pressure with their hands on the reins and their legs on the horse's side to cue the horse to change speed or direction. As the horse becomes more sensitive to the rider's cues, the rider can also give subtle cues with their seat by varying the pressure and timing of their weight distribution in the saddle. For example, the rider can cue the horse to take shorter steps within a gait by following the horse's movement closely with their pelvis (Engell *et al.*, 2016). The subtlety of the cues from their seat is contingent on the rider's ability to isolate the movement to their lumbopelvic-hip region. The rider should sit in balance without relying on the reins for stability (Zettl, 1998). The movement of the horse should not influence the stability of the rider's hands, legs, or head. This technique, known as the 'independent seat' (Kottas-Heldenburg and Fitzpatrick, 2014), is important to the dressage rider's ability to give subtle cues, stay in balance, and give the impression of a harmonious horse-rider interaction.

To achieve the independent seat, the rider must be able to self-organise to allow the pelvis to move independently. This can be a challenge as the pelvis may be strongly influenced by the movement of the horse when the rider is sitting in the saddle. Coordination variability can be interpreted as a measure of the stability between two oscillators, such as horse and rider (Oullier *et al.*, 2006). Only Lagarde *et al.* (2005) has reported the coordination variability between a horse and multiple rider segments, including the head, arm, hip, and leg, during sitting trot. Their comparison of a novice and professional rider illustrated the independent seat. The professional was able to follow the horse's movement consistently

with their trunk, while keeping a stable coupling between their hands and the horse from stride to stride. The novice had significantly greater coordination variability of the head and arm markers and lacked resonance to the horse with their trunk. This suggests that the movement of the professional rider's seat and trunk did not influence the stability of the rider's hands, which is the basis for the independent seat. As subsequent studies focussed on the coordination between a single rider segment such as trunk or pelvis and a horse (e.g. Eckardt and Witte (2017) and Münz, Eckardt and Witte (2014)), there is limited knowledge of how riders achieve balance in the saddle or further descriptions of the independent seat. To date, Lagarde *et al.* (2005) remain the most comprehensive analysis of coordination variability of the rider.

In studies of human balance on a moving platform, the segments closest to the platform are the first to react to perturbations (Chen *et al.*, 2014). It follows that to achieve an independent seat the rider must anticipate the horse's movement with their pelvic region. This is likely a skill developed with practice. For example, experienced riders may exhibit greater coupling between their pelvis and the horse than novice counterparts (Eckardt and Witte, 2017; Münz, Eckardt and Witte, 2014) and less variability of the angle between their trunk and the horse's head (Peham *et al.*, 2001). However, the existing evidence does not explain how experienced riders self-organise to respond to perturbations caused by the horse.

Ko and Newell (2001) illustrated the specificity of an individual's balance strategy to the characteristics of the perturbation. When the frequency and amplitude of anterior-posterior translation of a moving platform were varied, different hip, knee and ankle coordination strategies emerged to reflect the significance of the challenge to the individual's balance. In dressage riding, riders cue the horse to vary their speed and tempo within a gait and perform transitions between gaits. Therefore, like the findings of Ko and Newell (2001), it is expected that dressage riders alter their technique according to the characteristics of the perturbations produced during locomotion. Byström *et al.* (2015) and Engell *et al.* (2016) examined high-level riders' kinematics in several speeds of sitting trot on an equine treadmill.

While neither assessed the coordination variability between the rider's segments and the horse directly, they did find significant differences between the speeds of trot that would indicate that riders position themselves differently in the saddle to cue the horse to perform slower or faster trot speeds. It is unclear whether this was precipitated by changes in the perturbations associated with slower or faster trot speed, or whether they related to the rider's cues to the horse to speed up or slow down. Therefore, a standardised oscillation, similar to the moving platform used by Ko, Challis and Newell (2003, 2001), Ko and Newell (2001) and Goldsztein (2016) may help to provide insight into the rider's balance strategies and help to define the independent seat. The riding simulator is akin to a moving platform that produces similar oscillations to a horse's trunk during locomotion. Comparisons of novice and expert riders on the riding simulator (Baillet *et al.*, 2017; Olivier *et al.*, 2017) suggest that simulators may be specific enough to discriminate between experience levels. However, it is unclear whether this is still the case between different levels of competitive dressage riders.

This study aims to investigate the influence of segment, competition level and gait (medium or extended trot) on the coordination variability of the rider's segments to the riding simulator. As previous research has identified the rider's pelvis as the main coupling interface between horse and rider (Eckardt and Witte, 2017; Münz, Eckardt and Witte, 2014), it is hypothesised that all riders will show the least continuous relative phase variability of the simulator-pelvis relationship, indicating strong coupling. It was hypothesised that there would be differences due to international or national competition level on the coordination variability between the rider's head, trunk, pelvis or foot in pitch, relative to the vertical displacement of the riding simulator in simulated medium and extended trot.

6.2 Methods

6.2.1 Study design

This cross-sectional study analysed the effect of gait (medium or extended trot), segment pitch (pelvis, trunk, head, left foot), and competition level (International or National) as independent factors on the riding simulator-segment coordination and coordination variability (dependent factors).

6.2.2 Participant characteristics

Kinematic data from twenty-eight female riders from the overall dataset were used in this study. Inclusion was determined by the inclusion criteria, outlined in Section 3.2.1 and Table 3.3. Briefly, riders were included if they had results in competitions sanctioned by the national equestrian federation, British Dressage (BD), at the levels Medium to Advanced, or in competitions sanctioned by the Fédération International Équestre (FEI), which includes the levels Prix St. Georges to Grand Prix (Olympic level) in the 12 months preceding the data collection. Riders were assigned to one of two groups according to the affiliation of their highest competition level: international (n=14) if their highest level was FEI-affiliated, and national (n=14) if their highest level was BD-affiliated. Full participant characteristics are detailed in Table 3.4.

6.2.3 Data collection

The riders' trials in medium and extended trot, collected as per the protocol described in Section 3.2 using motion capture (Miquis M3, Qualisys AB, Gothenburg, Sweden), were used in this study. The riding simulator (Eventing Simulator, Racewood Ltd, Tarporley, UK) produces greater anterior-posterior displacement in extended trot than medium trot (Figure 6.1), while vertical displacement and frequency of oscillations remain approximately the same (further details on the simulator are given in Section 3.2.4).

6.2.4 Data Analysis

The data analysis utilised in this study combined the standard protocol for processing described in Section 3.3 and the protocol for the calculation of the continuous relative phase (CRP) detailed in Section 4.3.

Rigid bodies were formed for the rider's pelvis, trunk, head and foot, and the riding simulator (Section 3.3.1). Pitch rotation of the rider's head, trunk, pelvis and foot were calculated, corresponding to the second Euler rotation of the respective local coordinate system relative to the global coordinate system. Vertical displacement of the rigid body of the simulator was also calculated. These were then filtered (Section 3.3.2) and split into movement cycles (Section 3.3.3).

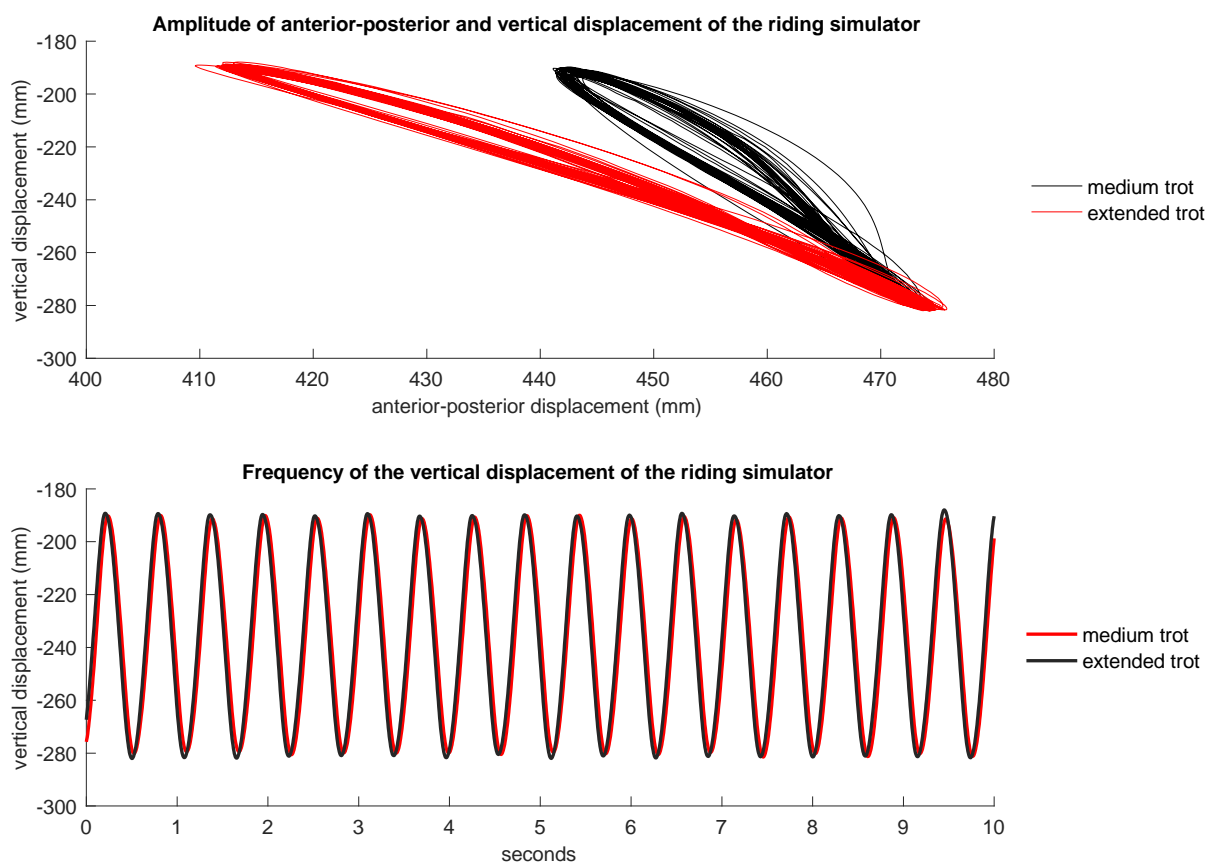


Figure 6.1. Characteristics of the riding simulator's displacement and displacement frequency in medium and extended trot. As evident in the plot of the anterior-posterior displacement relative to the vertical displacement (top), extended trot results in greater anterior-posterior but not vertical displacement or vertical displacement frequency than medium trot.

Ten consecutive cycles in medium and extended trot were analysed, starting from the third valid cycle for each rider. The protocol developed in Section 4.3.1 to calculate the CRP was then used to process the data for each rider. The data were scaled and normalised (see Section 4.3.1.2.2). It is important to note that the signals were time-normalised over 1001 points to account for aliasing errors and the Gibbs phenomenon, which is described in more detail in Section 4.3.1.2. The continuous relative phase between the vertical displacement of the riding simulator and the pitch of the rider's head, trunk, pelvis and foot, respectively, was calculated with the Hilbert transform (Section 4.3.1.2.3). The circular standard deviation of the continuous relative phase (CSD_{ϕ}) was calculated for each segment pair between each of the 1001 samples of the 10 cycles comprising the rider's trial using the CircStat (Berens, 2009) package in MATLAB (R2020a, The MathWorks Inc., Natick, Mass., USA). This resulted in 28 continuous CSD_{ϕ} time series of 1001 samples.

6.2.5 Statistical analysis

Analysing the CSD_{ϕ} as a continuous time-series allowed retention of the functional relevance of changes in the level of variability within the cycle. The effect of competition level, segment, and gait on CSD_{ϕ} over the cycle was analysed using a one-dimensional statistical parametric mapping (SPM1D) three-way ANOVA (spm1d.org) in MATLAB. This was particularly relevant in the present study as the riding simulator does not produce identifiable stance or swing phases, thus analyses based on discrete events within the cycle are impossible. Briefly, SPM1D uses Random Field Theory (RFT) to calculate the critical threshold at which α % (in this case, 5%) of smooth random curves would be expected to cross (Friston, 2003). If the scalar output statistic calculated separately at each time node exceeds the critical threshold, the null hypothesis is rejected. P-values for each cluster of threshold crosses indicate the probability that supra-threshold clusters could have been produced by a random field process with the same temporal smoothness (Adler and Taylor, 2007).

As there was a significant main effect of segment and interaction between segment and gait, *post hoc* SPM1D paired *t*-tests were conducted between segments within the gaits, and within the segment between the gaits. A type I family-wise error rate of $\alpha = 0.05$ was retained by calculating a Bonferroni correction.

6.4 Results

The three-way repeated-measures SPM1D ANOVA (Figure 6.2) showed a significant main effect for segment ($p < 0.001$, 1-100% of cycle) and gait ($p < 0.001$, 0-30% of cycle; $p = 0.002$, 92-100% of cycle) but not competition level. No interactions between gait, segment or competition level were found. Post-hoc SPM1D *t*-tests (Figure 6.3) reveal intersegmental differences in medium and extended trot, respectively. In medium trot, simulator-pelvis CSD_{ϕ} was significantly ($p < 0.001$) less than simulator-trunk CSD_{ϕ} from 0-60% of the cycle, which coincides with the ascent phase of the riding simulator's cycle. Simulator-pelvis CSD_{ϕ} was significantly ($p < 0.001$) less than simulator-head and simulator-foot CSD_{ϕ} for the entire cycle. Simulator-trunk CSD_{ϕ} was significantly ($p < 0.001$) less than simulator-head CSD_{ϕ} , but only from 0-18% and 60-100% of the cycle. Simulator-trunk CSD_{ϕ} was significantly ($p < 0.001$) less than simulator-foot CSD_{ϕ} from 60-100% of the cycle, which corresponds to the downward portion of the riding simulator's cycle. There were no significant differences between simulator-foot or simulator-head CSD_{ϕ} .

In extended trot, simulator-pelvis CSD_{ϕ} was less than simulator-trunk CSD_{ϕ} from 0-70%, however, this did not reach statistical significance. Figure 6.3 suggests that the lack of significant supra-threshold clusters between pelvis and trunk in extended trot, compared to medium trot, is due to decreased simulator-trunk CSD_{ϕ} in extended trot. Simulator-pelvis CSD_{ϕ} was significantly ($p < 0.001$) less than simulator-head CSD_{ϕ} from 0-37% of the cycle. Simulator-pelvis CSD_{ϕ} was significantly ($p < 0.001$) less than simulator-foot CSD_{ϕ} from 6-84% of the cycle. Simulator-trunk CSD_{ϕ} was significantly ($p < 0.001$) less than simulator-head CSD_{ϕ} from 0-29%, 42-56% and 61-100% of the cycle. Simulator-trunk CSD_{ϕ} was significantly ($p < 0.001$) less than simulator-foot CSD_{ϕ} from 13-96% of the cycle. Significant differences were found between simulator-head

CSD_{ϕ} and simulator-foot CSD_{ϕ} in medium trot, from 50-75% of the cycle ($p < 0.001$), but none were found in extended trot.

Planned *post hoc* comparisons of segments between medium and extended trot are illustrated in Figure 6.4. Only simulator-trunk CSD_{ϕ} displayed significant differences between medium and extended trot; CSD_{ϕ} was significantly ($p < 0.001$) greater in medium than extended trot from 50-100% of the cycle.

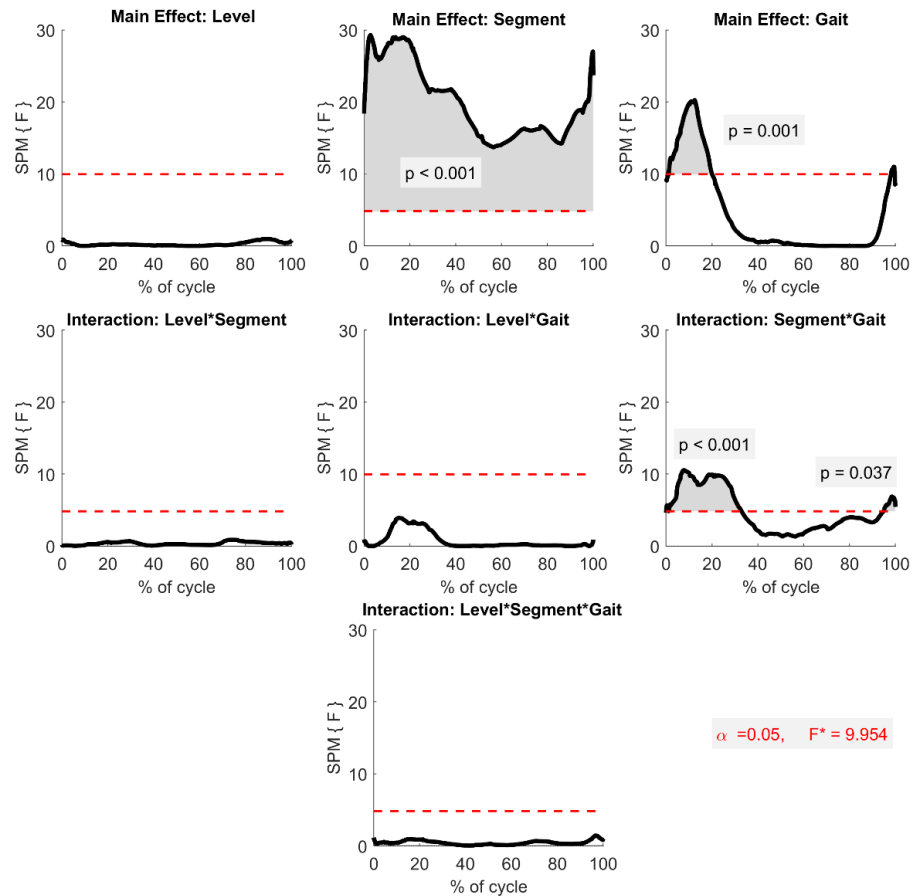


Figure 6.2. Results of three-way repeated-measures SPM1D ANOVA on simulator-segment CSD_{ϕ} by segment (pelvis, trunk, head and foot), by level (national, international) and gait (medium and extended trot). $F(t)$ trajectory (black) and corresponding critical thresholds calculated using random field theory (horizontal red dashed lines) for the main effect of level, the main effect of segment and interactions. NB: critical threshold values vary as they represent the critical threshold at which α % (in this case, 5%) of smooth random curves would be expected to cross.

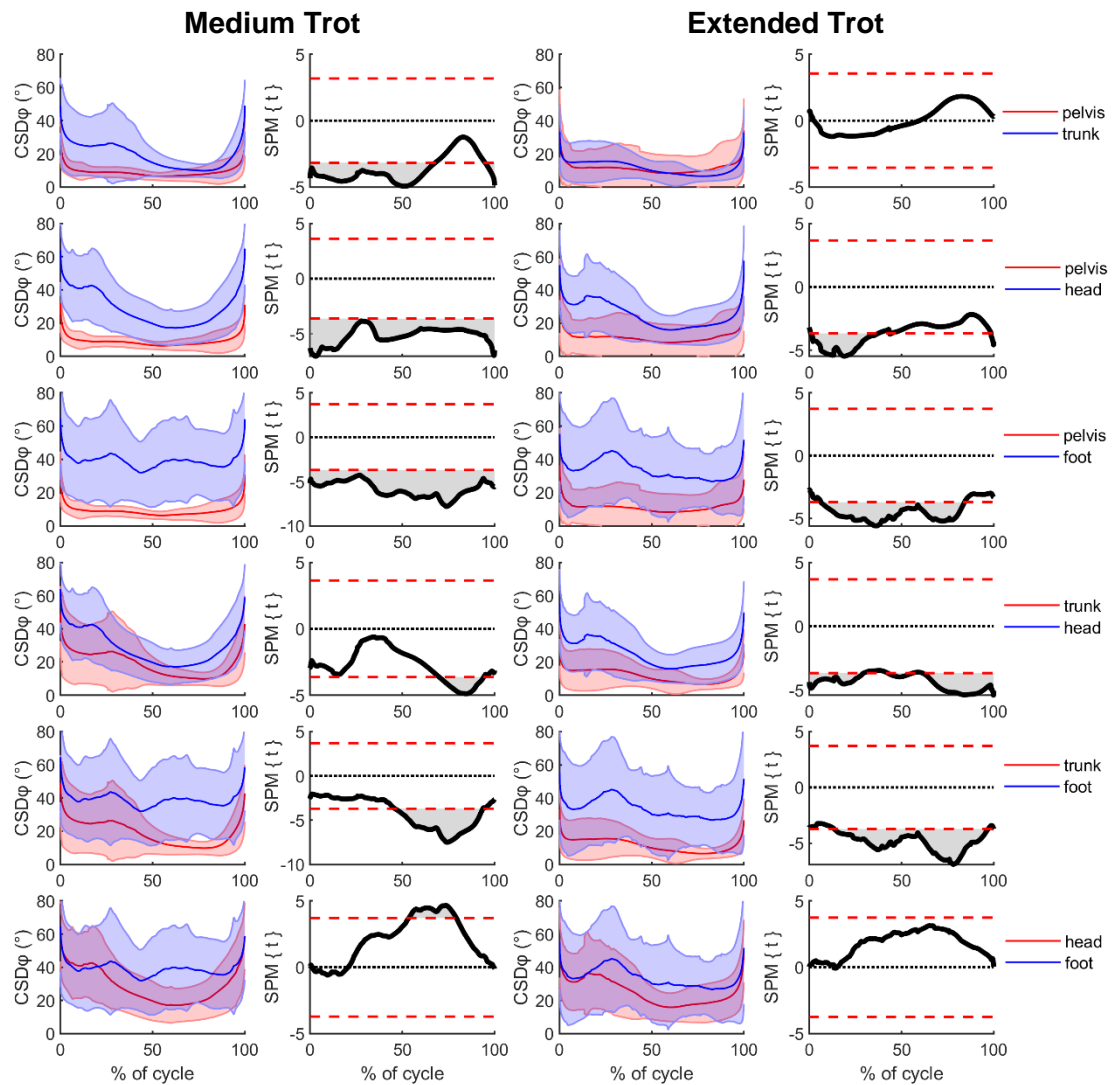


Figure 6.3. Results of the post-hoc Bonferroni-corrected SPM1D paired t-tests in medium (left) and extended (right) trot. Group mean and error cloud CSD_{ϕ} trajectories for the paired segments (legend to far right) to the left of corresponding SPM1D $T(t)$ trajectories. Red dotted lines indicate corresponding critical thresholds on SPM1D plots, while shaded areas indicate supra-threshold clusters with significance at the level of $p < 0.001$.

Medium vs Extended

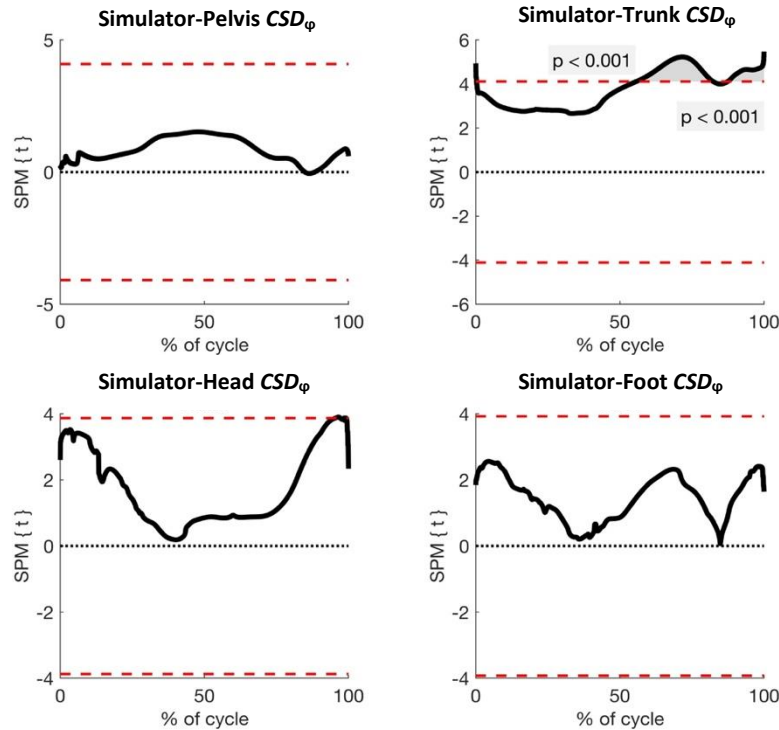


Figure 6.4. Multiple SPM1D paired t-tests to analyse the difference between simulator-segment CSD_{ϕ} values within a segment between medium and extended trot. Red dotted lines indicate corresponding critical thresholds.

6.5 Discussion

This study investigated the influence of the riding simulator's gait (medium or extended trot), dressage competition level (national or international), and the segment on the circular standard deviation of the continuous relative phase (CSD_{ϕ}) between the vertical displacement of a riding simulator and the pitch rotation of the rider's head, trunk, pelvis, and left foot. It was hypothesised that there would be differences due to international or national competition level on the coordination variability between the rider's head, trunk, pelvis or foot in pitch, relative to the vertical displacement of the riding simulator in simulated medium and extended trot. The hypothesis was partially rejected as there was no significant interaction between competition level and CSD_{ϕ} in medium or extended trot. The pelvis exhibited the lowest CSD_{ϕ} in medium trot, however, in extended trot CSD_{ϕ} of the trunk and pelvis were not significantly

different, likely due in part to significantly ($p < 0.001$) lower simulator-trunk CSD_ϕ and a non-significant increase in the simulator-pelvis CSD_ϕ .

Only two studies have analysed the coordination variability between horse and rider (Lagarde *et al.*, 2005; Peham *et al.*, 2001). As both studies only assessed two riders, this study is the largest known study of coordination variability in competitive dressage riders. Low coordination variability of the simulator-pelvis coupling observed in this study attests to its importance to the rider's dressage technique. The role of the pelvis in sitting trot is twofold: (1) its coincident movement controls displacements of the rider's centre of mass in response to perturbations caused by movements of the horse's trunk (de Cocq *et al.*, 2013); and (2) the rider can actively use their seat to influence the horse's gait by altering their weight distribution in the saddle and the timing of their pelvic pitch (Engell *et al.*, 2016; Byström *et al.*, 2015). The present results support the first, as the low CSD_ϕ (Figure 6.3) of the pelvis in medium and extended trot suggests that riders strongly couple the pitch rotation of their pelvis to the vertical displacement of the riding simulator. A riding simulator was used to test riders; therefore, these results represent the rider's passive technique, and further studies should investigate the coordination variability of the rider's technique when they are tasked with actively influencing the horse's gait.

The importance of the pelvis is supported by equestrian coaching (Wanless, 2017) and research that has sought to understand its functional characteristics during riding (Eckardt and Witte, 2017; Engell *et al.*, 2016; Byström *et al.*, 2015; Münz, Eckardt and Witte, 2014). This study underlines its importance, but also expands on the role of the pelvis to the rider's self-organisation as they perform simulated sitting trot and offers a new variable: the circular standard deviation of the continuous relative phase (CSD_ϕ). The CSD_ϕ measures the stability of the coordination between the rider's segments and the simulator during the movement cycle. The rhythm and regularity of the horse's gait have a substantial bearing on the performance outcomes in dressage (Fédération Internationale Équestre, 2020). The rider can influence the horse's gait with their pelvis (Engell *et al.*, 2016; Byström *et al.*, 2015) and regulate the horse's gait

variability with their overall technique (Peham *et al.*, 2004). Therefore, the simulator-pelvis CSD_{ϕ} describes the quality of the rider's pelvis technique and is a relevant parameter to analyse horse-rider interaction. It is important to note that this variable is derived from circular standard deviation of the continuous relative phase, which is a higher-order variable that compresses the angular displacement and velocity of each coupling pair into a single continuous time series. Therefore, the CSD_{ϕ} indicates the stability of the coordination but does not provide any information to describe the orientation of the pelvis. Different pelvis orientations may give rise to similarly stable coupling patterns (e.g. motor equivalence), although they may not be viewed as optimal from an aesthetic or injury prevention perspective (Glazier and Davids, 2009). Further investigation of the influence of the pelvis orientation on measures of the coordination variability is certainly warranted.

The significant decrease in the variability of the simulator-trunk CSD_{ϕ} from medium to extended trot is also quite remarkable. In medium trot, there was significantly ($p < 0.001$) more variability of the simulator-trunk CSD_{ϕ} than the simulator-pelvis CSD_{ϕ} for 0-70% of the cycle (Figure 6.3). In extended trot, no significant differences between the two couplings were apparent. A corresponding significant decrease in the variability of simulator-trunk CSD_{ϕ} between medium and extended trot was also found (Figure 6.4). Greater anterior-posterior displacement of the riding simulator in extended trot (Figure 6.1) provoked a decrease in the simulator-trunk CSD_{ϕ} . This suggests that increasing the anterior-posterior displacement of the riding simulator induces greater stability of the simulator-trunk coupling. Similar findings are reported by Ko and Newell (2001) during standing on a platform with varying frequencies and amplitudes of anterior-posterior displacement. As the frequency of the oscillations increased, the platform-ankle and platform-hip coupling variability decreased to stabilise the legs. Ko and Newell explained that as the oscillation frequency of the platform increased, the participants '*systematically exploited the available joint-space degrees of freedom to preserve postural stability in response to dynamic changes in the surface of support*'. For example, at lower oscillation frequencies, the participants invoked an ankle strategy,

whereby the other segments were held rigidly, and ankle flexion supported the maintenance of balance. However, as the platform oscillation frequency increased, the participants employed coordinated movements of the hips to keep the centre of mass within the base of support. As the rider is sitting in the saddle the pitch rotations of the trunk and pelvis are integral to control the position of the rider's centre of mass (de Cocq *et al.*, 2013). This is similar to how ankles, knees and hips coordinate when standing. Therefore, joint increases of stability of the coordination between the simulator and the rider's trunk and the amplitude of anterior-posterior displacement of the simulator fit within the context of previous studies. This makes intuitive sense to the rider; as the simulator's amplitude increased, there was a greater inertial effect on the rider's trunk and so they stabilised its coordination to the riding simulator to maintain balance in the saddle. By extension, this preserves the stability of the simulator-pelvis interaction, not only to stabilise the rider's centre of mass but also to maintain control of the seat. Therefore, the pitch rotations of both trunk and pelvis are necessary to maintain balance in the saddle, particularly as the amplitude of the anterior-posterior displacement increase.

Simulator-head and simulator-foot CSD_{ϕ} were significantly greater than simulator-pelvis and simulator-trunk CSD_{ϕ} in both gaits. Head and foot couplings also displayed observably larger inter-individual differences (Figure 6.3). This indicates that the coupling between the vertical displacement of the riding simulator and the foot or head is less stable than the pelvis and trunk. Indeed, de-coupling of the head and the foot to the vertical displacement of the simulator could be a functional asset that allows the rider to use their legs and feet to cue the horse's gait and direction, and allows their head to remain stable to facilitate visual perception during riding. No previous studies have analysed the pitch of the rider's foot during sitting trot. However, Lagarde *et al.* (2005) indicated that professional riders may use rhythmical dorsiflexion and plantarflexion of the foot to dampen the movement of the horse during the sitting trot. If that were the case for the present population of riders, lower coordination variability of the foot segment would be expected to indicate simulator-foot coordination. This was not the case in the present

study. Additionally, the riders' foot CSD_{φ} did not significantly increase between medium and extended trot, although the extent of the significant differences within the movement cycle between the simulator-trunk CSD_{φ} and simulator-foot CSD_{φ} increased with the gait, likely explained by the decrease in simulator-trunk CSD_{φ} .

As for simulator-head CSD_{φ} , only Olivier *et al.* (2017) have investigated head stability in a variety of visual conditions in a simulated gallop. These authors tested the postural stability of Club and professional riders exposed to different visual scenes on a riding simulator in gallop. They found that the position of the rider's head was significantly more variable than their lumbar spine in the frontal and transverse planes, but not the sagittal plane. In the present study, the pitch of the rider's head in sitting trot was analysed which could explain the contrast between these results and those of Olivier *et al.* Significantly less stability of the couplings between the simulator-head and foot relative to simulator-pelvis (Figure 6.3) may indicate that these segments do not couple to the vertical displacement of the riding simulator, rather they may be influenced by other planes of simulator movement. It is also possible that the cyclical movement of the simulator, rather than the forward travel and ground reaction forces produced by the live horse during locomotion resulted in less coupling between simulator-foot and simulator-head. Similarly, the riders were not required to actively cue the simulator to maintain its speed with their legs or maintain visual perception during the task. As coordination patterns can be task-specific (Renshaw, Davids and Savelsbergh, 2010), increased variability of the head and foot may be related to the task of riding the simulator, and further work is needed to replicate these results in riders on live horses.

To date, variability in equestrian rider technique has been perceived as detrimental to performance and attributed to lack of rider skill (Lagarde *et al.*, 2005; Peham *et al.*, 2004). As horses and riders are biological systems, some inherent variability is expected between movement cycles. Previous studies analysing horse-rider coordination have typically adopted the novice-expert paradigm (Eckardt and Witte, 2017; Münz, Eckardt and Witte, 2014; Lagarde *et al.*, 2005; Peham *et al.*, 2001), which infers that the

coordination between horse and rider is determined by the single constraint of rider experience. However, the perception of the task of riding may be drastically different between novice and professional riders. While there may be large disparities between the capabilities of novice and advanced dressage riders, there is an emphasis on training an independent seat from the lowest levels of competition (Zettl, 1998). In this study, the task was standardised between participants by using a riding simulator. The lack of significant differences between competition level categories for any simulator-segment CSD_{ϕ} was not surprising between national and international dressage riders in the controlled environment of the riding simulator. Still, Olivier *et al.* (2017) did find significant differences between riders' postural stability when testing comparable levels (Club riders and professional) to the present study on a riding simulator in gallop. As Olivier *et al.* (2017) tested postural stability in different visual conditions, these differences related to the visual conditions and their results should likely be compared to the present study with caution.

It is interesting to observe high inter-individual differences in the CSD_{ϕ} of the simulator-head and simulator-foot couplings (Figure 6.3). These observed differences are likely indicative of individual coordination strategies at the extremities. In contrast, relatively lower inter-individual variability was observed for the simulator-pelvis and simulator-trunk CSD_{ϕ} in both gaits. As competition level category was not significant, and as the task and environment were standardised for each rider using the riding simulator, this suggests that the inter-rider variability in these segments' CSD_{ϕ} is influenced by other participant constraints. Therefore, these results suggest that there are unknown individual factors that influence the stability of the coordination between the vertical displacement of the riding simulator and the pitch of the rider's segments, particularly when the rider has amassed sufficient experience to compete at national and international level dressage competitions. As the simulator is oscillating with a consistent frequency and amplitude, the variability of the coordination between the rider and the riding simulator may be viewed as the baseline variability of the rider in the horse-rider dyad. In experienced

riders, inter-segmental variability may serve as a functional asset that allows the rider to achieve the independent seat and maintain balance in the saddle.

6.5 Conclusions

In conclusion, these results capture the underlying variability of multiple simulator-rider couplings and provide an insight as to how competitive dressage riders achieve an independent seat. The rider's pelvis displayed the strongest coupling to the riding simulator that was resilient to changes in the amplitude of anterior-posterior displacement from medium to extended trot. These results suggest that the significantly stronger coupling of the pelvis than the trunk, head and feet in medium trot define the equestrian concept of the independent seat. Weaker coupling of the head and feet to the vertical displacement of the riding simulator indicates that the rider achieves enough stability by initiating coincident movement of the pelvis and trunk, so that variability at the extremities does not diminish the rider's stability in the saddle. Significantly decreased simulator-trunk CSD_ϕ in extended trot suggests that the rider maintains the stability of their seat by initiating stronger coupling between their trunk and the vertical displacement of the simulator as the amplitude of anterior-posterior displacement increases. Therefore, the independence of the seat may decrease as the perturbation to the rider's seated position in the saddle increases to allow the rider to remain in balance. Variability between riders observed suggests that riders may have individual coordination strategies that can be assessed using the continuous relative phase. Therefore, the next study of this thesis will examine the features of simulator-rider coordination.

7. Principal component analysis of the coordination between rider and riding simulator in medium and extended trot

7.1 Introduction

The quality of the rider's seat is important for the rider's performance and stability in the saddle. The previous chapter confirmed that the coordination variability of the rider's pelvis is low compared to the other segments in simulated medium and extended trot. While the variability was described, other characteristics of the coordination between the vertical displacement of the riding simulator and the rider's pelvis are not known. Riders are judged on their ability to '*...smoothly absorb the movements of the horse*' during the dressage test (Fédération Internationale Équestre, 2020). Equestrian coaches are adept at scrutinising the technique of the rider's seat (Blokhuys *et al.*, 2008) and judges award better marks to riders that can achieve and maintain consistently high levels of coordination with a horse, known as 'harmony' (Peham *et al.*, 2001). As harmony is important for the rider's stability in the saddle and performance, it is instilled in the rider from the beginning of their progression in dressage. The complex coordination of many degrees of freedom (DoF) inherent to both rider and horse is no trivial task, therefore, it is expected that the rider develops their ability to achieve consistent harmony on different horses with practice (German National Equestrian Federation, 2005). The ability to achieve harmony with different horses is also important for the rider's progression within the sport; professional riders may ride a variety of horses in training and competition, therefore must be able to adapt to each one.

Several studies have assessed horse- or simulator-rider harmony (Baillet *et al.*, 2017; Eckardt and Witte, 2017; Münz, Eckardt and Witte, 2014; Lagarde *et al.*, 2005; Peham *et al.*, 2001). These are explored in-depth in Section 2.2. The results of these studies show the influence of various aspects of rider experience on harmony that are consistent with established concepts in dynamical systems theory (Davids *et al.*, 2003). They can adapt to the changing conditions imposed by horses with different gaits and behaviours

(Peham *et al.*, 2001). They display less movement variability in segments that influence the interaction with the horse (Eckardt and Witte, 2017; Münz, Eckardt and Witte, 2014; Lagarde *et al.*, 2005; Peham *et al.*, 2001). For example, to keep their hands steady on the reins, they keep their arm from shoulder to wrist significantly more in-phase with the horse's movement than a novice rider (Lagarde *et al.*, 2005). Additionally, they reciprocate the horse's trunk movements with roll, pitch and yaw movements of their pelvis that coincide in timing with the rotations of the horse's trunk and the saddle (Eckardt and Witte, 2017; Münz, Eckardt and Witte, 2014; Byström *et al.*, 2009, 2010). Finally, they can maintain an upright trunk and stable trunk coordination pattern that is resilient to changes in oscillation frequency better than non-riders during a simulated riding task (Baillet *et al.*, 2017).

Despite the importance of the rider's seat to their performance (Engell *et al.*, 2015; Nevison and Timmis, 2013), a limited number of studies have assessed its movement during riding (Engell *et al.*, 2016; Byström *et al.*, 2009, 2010, 2015), and even fewer have assessed its role in producing harmony (Eckardt and Witte, 2017; Münz, Eckardt and Witte, 2014). Given that coordination arises from the complex interaction between participant, environmental and task constraints (Newell, 1986), it is unlikely that all riders faced with a similar task and environment will produce the same coordination pattern to achieve harmony. When considering competitive riders, studies have observed increases in asymmetry (Hobbs *et al.*, 2014) and decreased spinal motor control (Deckers *et al.*, 2020) associated with higher competition levels.

The combination of increased potential physical limitations but high competitive performance in riders, seen by these studies (Deckers *et al.*, 2020; Hobbs *et al.*, 2014) is paradoxical. No currently published study has linked the aetiology of rider back pain or injury to sport-specific movements. Therefore, it is unclear how riding or competition level specifically influences spinal motor control or back pain. These studies (Deckers *et al.*, 2020; Hobbs *et al.*, 2014), however, do suggest that asymmetry and motor control is independent of competition level. The evidence presented in Chapter 5 and 6 suggest that the rider's pelvic posture and segmental coordination variability to the riding simulator are also independent of

competition level. Therefore, similar to other high-level athletes, such as pistol shooters (Scholz, Schoner and Latash, 2000) and javelin throwing (Morriss, Bartlett and Fowler, 1997), equestrian riders may be able to adapt their technique to meet the performance goals required during competition. As gait kinematics (Holmstrom *et al.*, 1994) and behaviour (Sackman and Houpt, 2019) can vary between horses, the rider must be able to adapt their coordination strategy to suit their horse. However, as evidenced by Hobbs *et al.* (2014) and Deckers *et al.* (2020), riders may also need to adapt their coordination strategies to manage the effects of their own postural asymmetries or poor motor control. Therefore, horse-rider coordination is highly complex and likely depends on individual factors that relate to both horse and rider, however, the contribution of these factors is ill-defined.

As previous studies examining groups of riders have presented group means to describe coordination patterns (Eckardt and Witte, 2017; Münz, Eckardt and Witte, 2014), individual variation in horse-rider coordination is unknown. Moreover, the use of discrete measures such as cross-correlation (Eckardt and Witte, 2017; Münz, Eckardt and Witte, 2014) or discrete relative phase (Baillet *et al.*, 2017; Lagarde *et al.*, 2005) reduces the study of the dynamic movement to a single point in the cycle, which may disregard important information about the coordination strategy over the entire stride. Therefore, it is jointly unclear whether competition level or other participant constraints, influence the features of the coordination patterns initiated by the pelvis.

Additionally, manipulation of the task and environmental constraints during riding may influence the impact of competition level on the outcome of harmony. Although previous studies have found significant differences between harmony due to competition level (Baillet *et al.*, 2017; Lagarde *et al.*, 2005; Peham *et al.*, 2001), Eckardt and Witte (2017) did not find significant differences between 10 experienced and 10 novice riders in the cross-correlation between the pitch rotation of the rider's pelvis and the trunk of a horse. In contrast to other studies (Lagarde *et al.*, 2005; Peham *et al.*, 2001), these riders rode their own horses or familiar riding school horses, thereby reducing the unfamiliarity of the horse, decreasing task

and environmental variability. Under the controlled experimental conditions of a riding simulator, experienced and naïve riders studied by Baillet *et al.* (2017) showed significantly different trunk coordination patterns. Taken together, even a few years of riding experience may minimise the influence of experience or competition level when environmental and task constraints are similar between participants.

As the pelvis region forms the interface between horse and rider movement during seated riding, the purpose of this study was to use principal component analysis (PCA) to investigate the features of the continuous coordination, quantified using the continuous relative phase (CRP) between the vertical displacement of a riding simulator and the pitch of the rider's pelvis during the simulated medium and extended trot. This study aimed to: (1) quantify and explain the functional significance of the features of coordination in medium and extended trot; (2) assess whether differences in the features of coordination occurred due to competition level; and (3) investigate whether the rider's coordination patterns significantly changed between simulated medium and extended trot.

7.2 Methods

7.2.1 Participants

The kinematic data for forty female competitive dressage riders, collected using motion capture (Miquis M3, Qualisys AB, Gothenburg, Sweden) on the riding simulator (Eventing Simulator, Racewood Ltd., Tarporley, UK) in simulated medium and extended trot was extracted from the overall dataset based on the inclusion criteria outlined in Section 3.2.1 and Table 3.3 and the availability of the rider's data at the time of data analysis. Riders were categorised as intermediate or advanced based on their self-reported highest level competed within 12 months preceding the data collection. Intermediate riders ($n = 15$) were those who reported a competition level at the nationally affiliated British Dressage (BD) levels BD Preliminary to Elementary. Advanced riders ($n = 25$) were those who were competing at BD levels Medium

to Advanced or internationally affiliated FEI competitions (FEI Prix St Georges up to FEI Grand Prix). Full participant characteristics are detailed in Table 3.4.

7.2.2 Data processing

Ten seconds of medium and extended sitting trot were analysed from the riders' trials. Similar to Chapter 6, the data were analysed using a combination of the protocol described in Section 3.3, including extraction of the pitch of the rigid body of the rider's pelvis (Section 3.3.2), filtering (Section 3.3.3) and time-normalisation (3.3.4), and the method described in Section 4.3.2.1 for calculation of the continuous relative phase (CRP). Data from the third valid cycle onward were analysed for each rider, to avoid aliasing effects, for a total of ten cycles per rider. However, cycles were discarded if there were continuous gaps of 0.4s or more (further details in Section 3.3), which resulted in three riders who had seven valid cycles and one rider with eight valid cycles, for 389 total cycles.

7.2.3 Continuous relative phase

The continuous relative phase (CRP) was calculated by determining the phase difference between the Hilbert transform of the vertical displacement of the riding simulator and the pitch rotation of the riders' pelvis as described in Section 4.3.1.2. A value near 0° or 360° indicates that the segments are moving together, in-phase, a value near 180° indicates that the segments are moving opposite (anti-phase) and values in between are out-of-phase. The sign of the CRP waveform describes whether the segment is leading or lagging (Van Emmerik, Miller and Hamill, 2014). Positive values indicate that the simulator is leading the pelvis, while negative values indicate that the simulator is lagging the pelvis. To illustrate the differences between the competition level categories, the continuous circular mean and standard deviation were calculated with the CircStat toolbox (Berens, 2009) in MATLAB (R2020b, The MathWorks, Natick, Mass., USA) and the mean with error clouds were plotted.

7.2.4 Principal component analysis

Separate principal component analyses (PCA) was conducted on the simulator-pelvis CRP time-series in medium and extended trot, respectively. PCA extracts information about the features of the time series that explain the greatest amount of variation (Deluzio and Astephen, 2007). It is accomplished by a linear transformation of the data to a new, orthonormal coordinate system, defined by a set of new uncorrelated variables called principal components (PCs) (Cushion *et al.*, 2019; Witte *et al.*, 2010). Using PCA has the advantage of retaining the spatiotemporal characteristics of the time-series, so that the data, reduced to a small number of PCs that explain the maximal amount of variation, can be reconstructed and qualitatively analysed.

Two separate PCA analyses were performed: one in each gait. Cycles for all riders in each gait were concatenated into a matrix to yield two 389 x 1001 matrices. The PCA was performed with the individual time-points as variables and waveforms as cases (as per Deluzio and Astephen (2007) and Robertson *et al.* (2014)). Principal component scores (PC scores) refer to the transformation of the raw data into the variable space explained by the PCs (Cushion *et al.*, 2019; Deluzio *et al.*, 2014). PC scores, loading vectors and variation explained were obtained for each analysis. PC loading vectors are time series of the same length as the original data that express the specific pattern of variance in the data (Brandon *et al.*, 2013). The amount of variation explained by each PC was contained within a separate matrix. The cut-off for the number of PCs retained was set at the number needed to explain 90% of the variation (Deluzio *et al.*, 2014). This resulted in three PCs retained for further qualitative and statistical analysis in medium and extended trot.

To qualitatively describe the distinctive features of each PC, waveforms corresponding to the 5th (low) and 95th (high) percentile of each PC score were plotted (Brandon *et al.*, 2013). As observed differences between the raw waveforms occur due to the contribution of multiple PCs, single component reconstructions for high, low and mean values of each PC score were also plotted. Single component

reconstructions were calculated as per Brandon *et al.* (2013) by adding the product of the PC coefficients and the score representing the 5th or 95th percentile to the mean waveform.

7.2.5 Statistical analysis

The PC scores within each competition level group were tested for normality using a Kolmogorov-Smirnov test in a MATLAB toolbox (normalitytest, Ipek (2020)). They were normally distributed. To investigate the relationship between competition level category and PC scores, linear mixed models were used in SPSS (version 26, IBM Corp., Armonk, N.Y., USA). The dependent variable for each linear mixed model was the PC score. Competition level category was entered as a fixed effect (0 = advanced, 1 = intermediate), and the cycle number (maximum of 10 per rider) was entered as a random effect. The model was built with an interaction term for fixed and random effects. The random-effects had intercepts for the subjects and trials. An unstructured covariance structure was used. Visual inspection of the residual plots did not reveal any obvious deviations from homoscedasticity or normality. P-values were obtained by likelihood ratio tests of the full model with the effect against the model without the effect.

7.3 Results

7.3.1 Qualitative analysis of group principal component scores

The rider's pelvis pitch was in-phase with the vertical displacement of the riding simulator (as indicated by Figure 7.3), and the sign of the CRP indicated that the simulator led the pelvis from 0 to around 60% of the cycle (indicated by positive values) and switched to pelvis leading the simulator from 60-100% of the cycle (negative values). The mean \pm standard deviation CRP values were $5.2 \pm 18^\circ$ in medium trot and $4.2 \pm 16^\circ$ in extended trot.

Three PCs were required to account for >90% of the variance in the data in both medium and extended trot. Inspection of the plots of the reconstructed PCs based on the mean waveform and the 5th and 95th percentile PC scores indicate that the features of the time series are similar in medium (Figure 7.1) and extended (Figure 7.2) trot. The features of the PCs were interpreted as per the definitions proposed by

Brandon et al. (2013), as relating to differences in magnitude, shape, or a time shift. PC1, which accounted for 75% of the variance in medium trot and 69% in extended trot, related to differences in the magnitude of CRP throughout the cycle. The extreme raw waveforms (Figure 7.1D and 7.2D) suggest that a high PC score corresponded to the simulator leading the pelvis throughout the stride, while the pelvis led the simulator for low PC1 scores. Single component reconstruction (Figure 7.1G and Figure 7.2G) show the magnitude difference between low and high scores, while the loading vector (Figure 7.1A and Figure 7.2A) confirms the magnitude shift as the highest values of the loading vector occurs at the beginning and the end of the cycle with no zero-cross (Brandon *et al.*, 2013).

The second principal component accounted for greater variation in extended trot (17%) than medium trot (11%). This PC could be described as having shape difference and phase shift features. Although the shape of the loading vectors (Figure 7.1B and Figure 7.2B) and single component reconstruction (Figure 7.1H and Figure 7.2H) are similar for both medium and extended trot, the raw waveforms corresponding to the 5th and 75th percentiles (Figure 7.1E and Figure 7.2E) show functional differences between medium and extended trot. In medium trot, there is a shape difference between waveforms corresponding to low and high PC2 scores. The most marked differences occur at 70% of the cycle: the high value increasing in the positive direction, while the low value crosses the zero line. In extended trot, the waveform corresponding to a high PC2 score is a relatively consistent trajectory with negative values, while the low PC2 score has a similar shape to the high value in medium trot, crossing zero at around 60%. The zero-crossing of the loading vector confirms that the phase-shift observed in the single-component reconstruction relates to this PC.

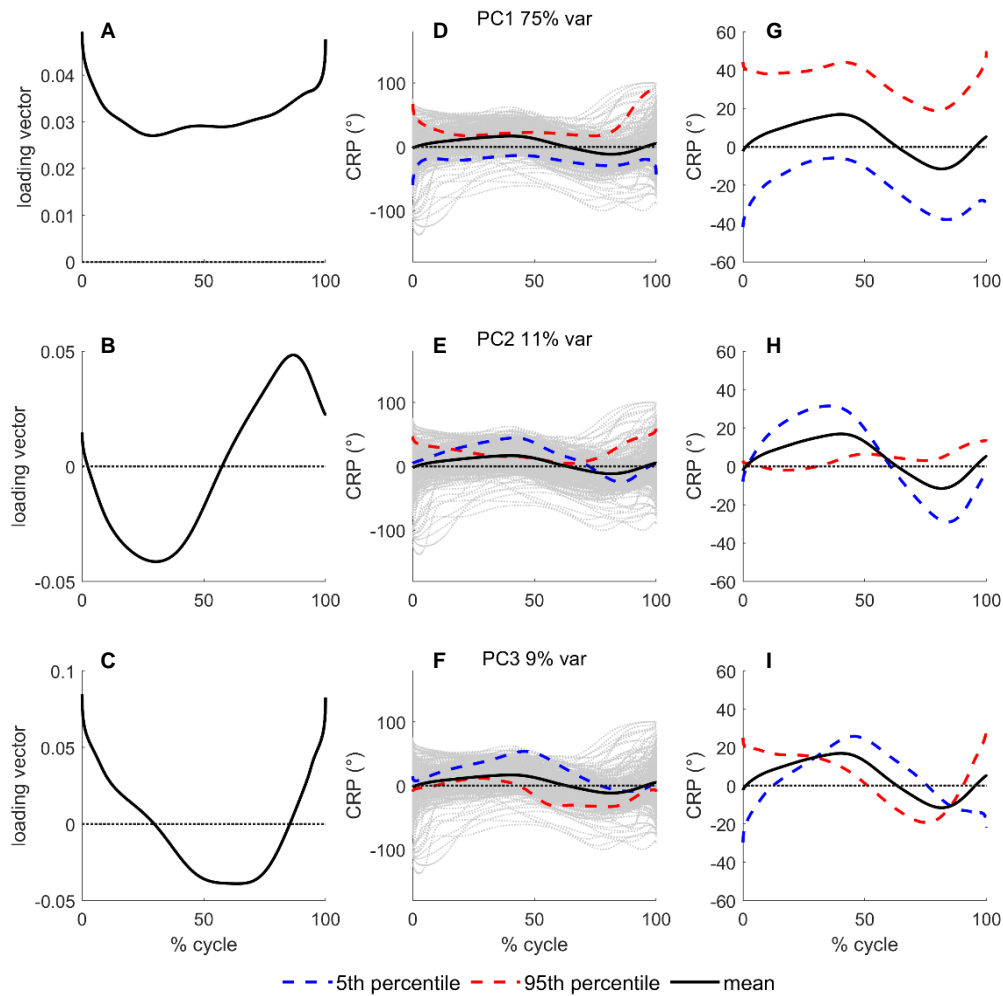


Figure 7.1. Plots to describe the principal components of the continuous relative phase between the riding simulator and the rider's pelvis in medium trot that explained at least 90% of the variance. **A-C:** Loading vectors for each PC score. **D-F:** Trajectories corresponding to the 5th and 95th percentile of the PC score plotted (red and blue dotted lines) with all trials (grey) and mean (bold black line). **G-I:** Single component reconstruction of the PC score for the 5th and 95th percentile scores and the mean time series.

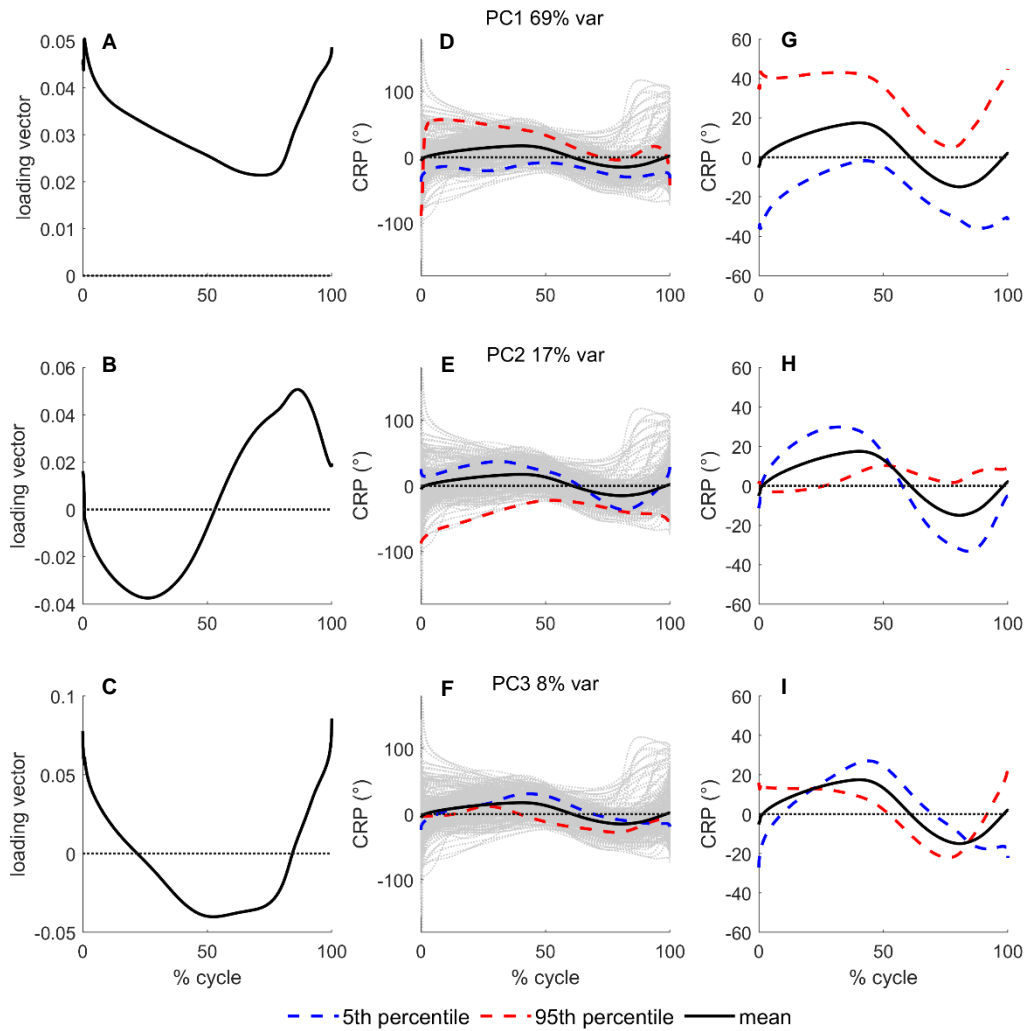


Figure 7.2. Plots to describe the principal components of the continuous relative phase between the riding simulator and the rider's pelvis in extended trot that explained at least 90% of the variability. **A-C:** Loading vectors for each PC score. **D-F:** Trajectories corresponding to the 5th and 95th percentile of the PC score plotted (red and blue dotted lines) with all trials (grey) and mean (bold black line). **G-I:** Single component reconstruction of the PC score for the 5th and 95th percentile scores and the mean time series.

PC3 accounted for similar variation in medium (8%) and extended (9%) trot. The loading vectors (Figure 7.1C and Figure 7.2C) and single component reconstruction trajectories for low and high values of PC3 were similar between medium and extended trot (Figure 7.1I and Figure 7.2I). PC3 corresponds to a time-shift difference, reflected by the zero-cross of the loading vector at 30% and 90% of the cycle. Differences in the CRP waveforms corresponding to low and high values of PC3 show observable differences between the gaits. While the shape of the CRP waveforms corresponding to high and low PC3 values is similar between medium and extended trot, the range of CRP values is smaller in extended trot, evidenced by lower local minimum and maximum CRP values observed in Figure 7.2F.

7.3.2 Effect of competition level on PC scores

The continuous circular mean \pm SD of the CRP within each competition level category in medium and extended trot is plotted in Figure 7.3. Box plots of the PC scores by cycle, grouped by competition level category are presented in Figure 7.4. Both figures and the statistical tests confirm no significant differences between the features of the CRP trajectories between the competition level categories.

The results of the mixed-effects models for each PC score are presented in Table 7.1, with further statistical outputs available in Appendix C. There were no significant main effects or interactions between competition level or cycle. There were significant random effects for the intercept + cycle by subject in each model (medium trot: PC1: Wald $Z = 3.15$, $p = 0.002$; PC2: Wald $Z = 3.40$, $p = 0.001$; PC3: Wald $Z = 3.58$, $p < 0.001$; extended trot: PC1: Wald $Z = 3.24$, $p = 0.001$, PC2: Wald $Z = 3.58$, $p < 0.001$; PC3: Wald $Z = 3.07$, $p = 0.002$). This suggests that there is a significant variation in the PC score between riders and between cycles that is not captured by the current parameters measured by the model.

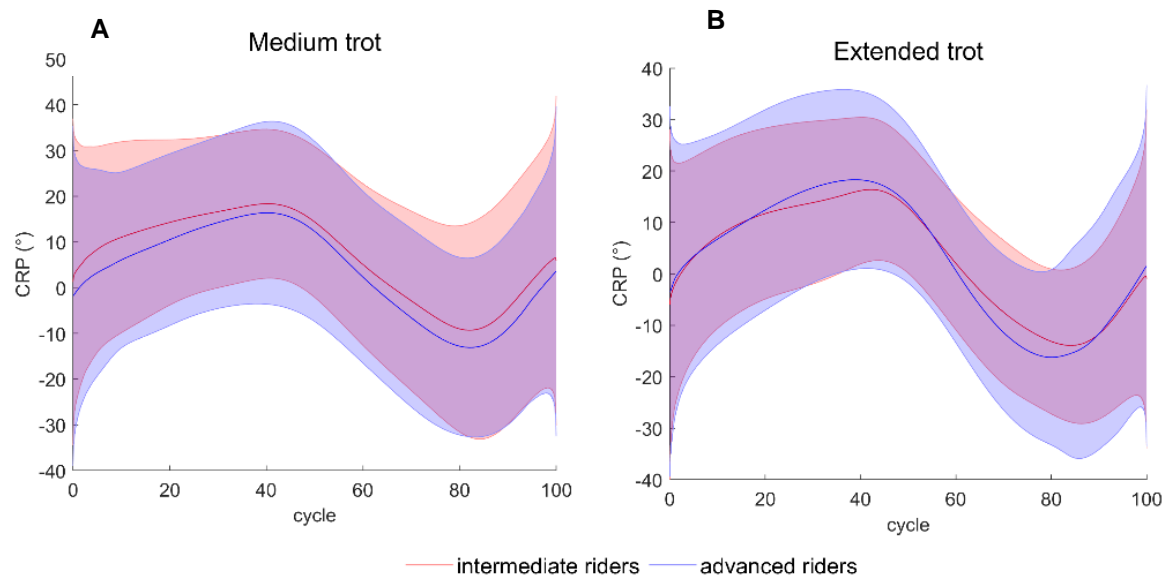


Figure 7.3. Group means \pm standard deviation for **(A)** simulator-pelvis CRP in medium trot and **(B)** simulator-pelvis CRP in extended trot.

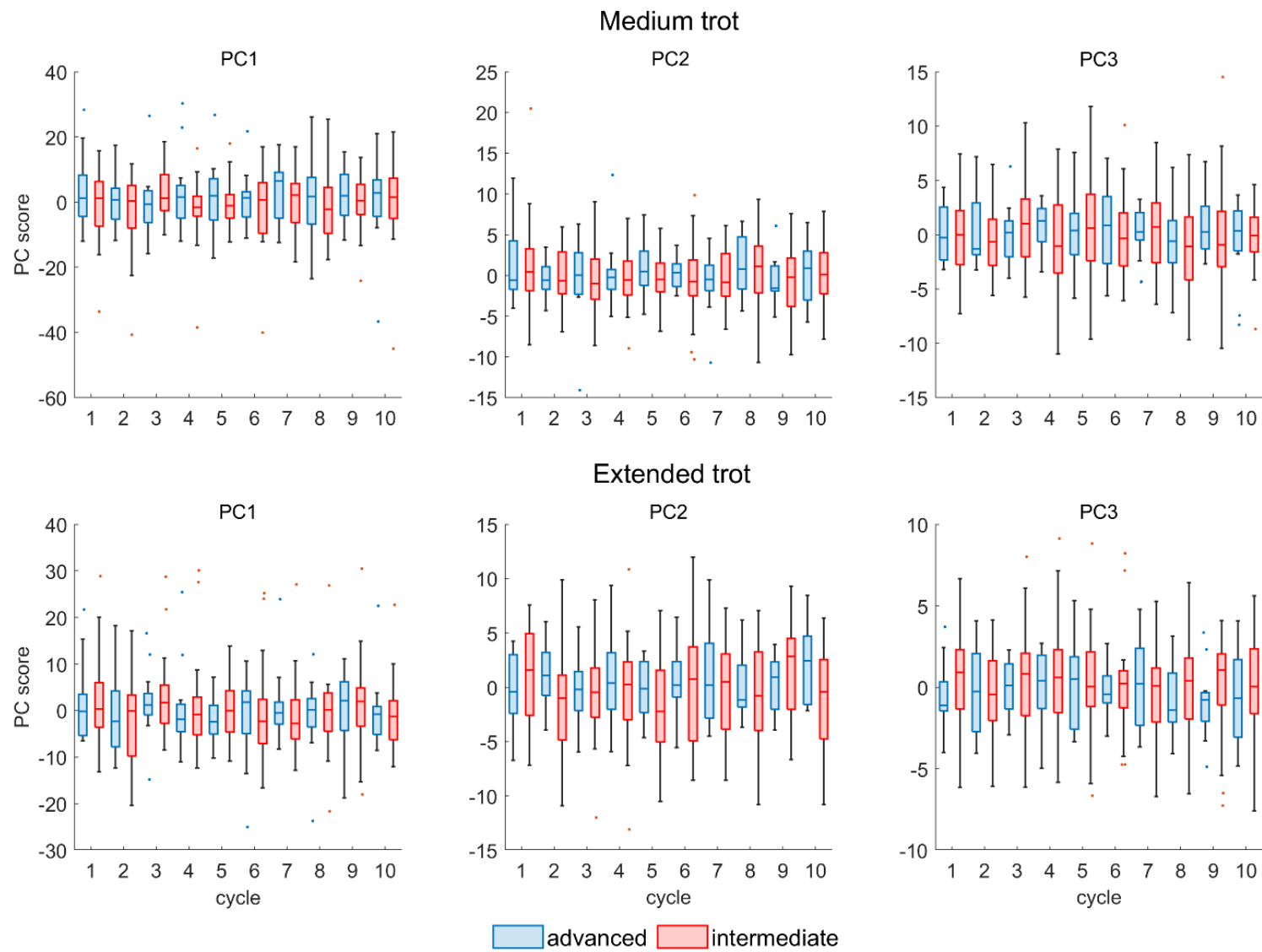


Figure 7.4. Box plots of the three PC scores needed to account for at least 90% of the variation in medium (top) and extended (bottom) trot by cycle, grouped by competition level category.

Table 7.1. Estimates of fixed effects for each mixed-effects models conducted to examine the influence of competition level on the PC scores in each gait.

| | | Coefficient | SE | df | t | p | |
|---------------|-----|---------------------|-------|------|--------|-------|-------|
| Medium trot | PC1 | Advanced | 1.64 | 1.63 | 367.99 | 1.01 | 0.314 |
| | | Intermediate | -3.26 | 2.03 | 364.01 | -1.61 | 0.109 |
| | | Cycle: Advanced | -0.18 | 0.36 | 123.17 | -0.51 | 0.613 |
| | | Cycle: Intermediate | 0.40 | 0.44 | 117.27 | 0.90 | 0.368 |
| | PC2 | Advanced | 0.42 | 0.61 | 368.93 | 0.70 | 0.486 |
| | | Intermediate | -0.34 | 0.76 | 367.04 | -0.45 | 0.656 |
| | | Cycle: Advanced | -0.43 | 0.13 | 100.81 | -0.30 | 0.762 |
| | | Cycle: Intermediate | 0.01 | 0.18 | 95.32 | 0.05 | 0.962 |
| | PC3 | Advanced | 0.46 | 0.49 | 375.91 | 0.09 | 0.926 |
| | | Intermediate | -0.13 | 0.61 | 375.29 | -0.21 | 0.834 |
| | | Cycle: Advanced | 0.05 | 0.14 | 65.04 | -0.32 | 0.703 |
| | | Cycle: Intermediate | -0.05 | 0.17 | 61.60 | -0.32 | 0.753 |
| Extended trot | PC1 | Advanced | 0.63 | 1.14 | 378.11 | 0.55 | 0.580 |
| | | Intermediate | 0.34 | 1.42 | 377.80 | 0.24 | 0.811 |
| | | Cycle: Advanced | -0.21 | 0.34 | 46.36 | -0.60 | 0.550 |
| | | Cycle: Intermediate | 0.04 | 0.43 | 44.03 | 0.10 | 0.917 |
| | PC2 | Advanced | 0.11 | 0.57 | 377.12 | 0.19 | 0.846 |
| | | Intermediate | -0.45 | 0.72 | 376.64 | -0.63 | 0.532 |
| | | Cycle: Advanced | 0.07 | 0.16 | 61.67 | 0.40 | 0.692 |
| | | Cycle: Intermediate | -0.05 | 0.21 | 58.49 | -0.26 | 0.793 |
| | PC3 | Advanced | -0.34 | 0.37 | 383.93 | -0.94 | 0.346 |
| | | Intermediate | 0.73 | 0.46 | 384.00 | 1.60 | 0.111 |
| | | Cycle: Advanced | 0.05 | 0.12 | 34.33 | 0.68 | 0.684 |
| | | Cycle: Intermediate | -0.09 | 0.15 | 32.88 | 0.55 | 0.553 |

Legend: PC: Principal component, SE: Standard error, df: Degrees of freedom, t: *t* statistic, *p*: statistical significance

7.4 Discussion

This study aimed to examine whether the features of harmony were determined by the rider's competition level in simulated medium and extended trot, quantified by the principal component scores (PC scores) of the continuous relative phase (CRP) between the vertical displacement of the riding simulator and the pitch rotation of the rider's pelvis. There were no significant differences in the PC scores relating to competition level. Previous studies have found significant differences in the coordination

between the skill level of riders riding live horses (Lagarde *et al.*, 2005; Peham *et al.*, 2001), but no previous study has examined the characteristics of the coordination that the rider initiates with their pelvis in a controlled setting. The present results suggest that, as coordination arises from the complex interplay of participant, environment and task constraints (Newell, 1986), the hallmark of equestrian skill may be the ability to adapt to the horse in complex environmental and task conditions. Between-rider variation in the features of the simulator-pelvis CRP suggests that other participant factors more strongly influence the characteristics of harmony, and these can be qualitatively described with principal component analysis (PCA).

The riders in this study pitched their pelvis in-phase to the vertical displacement of the riding simulator, which agrees with previous results that reported high levels of coordination between experienced riders' pelvis and a horse (Eckardt and Witte, 2017; Münz, Eckardt and Witte, 2014; Lagarde *et al.*, 2005). These previous studies presented the coordination between horse and rider at a discrete point in the stride, whereas this is the first known study to expand upon these results and offer a continuous, rather than a discrete, perspective on harmony. PCA identified several features of the simulator-pelvis coordination that occurred before or after the maximal vertical displacement of the riding simulator, which suggests that they would be overlooked in a discrete analysis of the relative timing of the peak of the vertical displacement of the riding simulator to the peak of the rider's pelvis pitch.

In medium and extended trot, PC1 (medium: 75% variation, extended: 69% variation) results in a difference in magnitude, PC2 results in differences in shape and phase shift (medium: 11%; extended: 17%) and PC3 results in a phase shift (medium: 9%; extended: 8%). This suggests that much of the difference between riders and cycles are related to differences in the sign of the CRP, reflected by PC1, but that other PCs that relate to shape and phase shift features can contribute greatly to the overall CRP trajectory. The CRP measures the continuous similarity of the time series of the vertical displacement of the riding simulator and the pitch of the rider's pelvis. As the rider's pelvis pitch was in-phase with the

vertical displacement of the riding simulator, which indicates the high temporal similarity of the signals' peaks, magnitude, shape and phase shift differences reflect differences in the slope of the rider's pelvis pitch trajectory as it adapts to the vertical displacement of the simulator. Lead and lag, indicated by the sign of the CRP value, reflect instances where the pelvis is moving faster (negative CRP values) or slower (positive CRP values) in pitch than the simulator. A zero cross of the CRP values, apparent in the features of PC2 and PC3, reflects a change in the coordination dynamics from lag to lead, and vice versa. PC2 has a zero cross just after 50% of the cycle that coincides with the peak vertical displacement of the simulator and posterior pitch of the pelvis. This pattern is illustrated by the low PC2 score in extended trot (Figure 7.2E) and the overall mean pattern (Figure 7.3). Conversely, PC3 has a zero crossing at about 30% and 90% of the cycle.

Differences in the sign of the CRP values and the location of the zero-cross likely relates to inherent rider characteristics. Walker *et al.* (2020) found that riders who could not perform posterior pelvic tilt on a Swiss ball without major compensations (assessed by a physiotherapist) had a greater phase shift between the maximal vertical displacement of a marker on the rider's hip and the horse's hip. It is certainly possible that the differences in the observed features of the CRP relate to riders' motor control, strength and mobility, however, the relationship between the rider's characteristics and their coordination strategies needs further investigation.

Observable and quantifiable differences between an individual's pelvis pitch to coordinate with the vertical displacement of the riding simulator in medium and extended trot are consistent with the concept of degeneracy, which states that there are multiple dynamically equivalent solutions to the same task goal (Williams *et al.*, 2016). Even among high-level competitors and between movement cycles, differences in the shape and timing of the coordination patterns exist that are not predicted by the individual's competition level. In this highly-controlled environment, it is hypothesised that the degeneracy observed is due to varying participant constraints, such as anthropometry, strength, flexibility and previous injury,

the influence of other segments (limbs and trunk) on the pelvis, and differences in the individual's own style of riding. This hypothesis is further underpinned by the significant ($p < 0.05$) random effects of cycle and individual, which suggest that unexplained variables account for variance between cycles and riders. These results have shown that differences may exist between riders' simulator-pelvis coordination patterns, however, they do not result in departures from predominately in-phase coordination, nor can they be predicted by competition level. Therefore, if the aim is to 'smoothly absorb the movement of the horse', riders may achieve this in multiple ways that consider their specific constraints. This finding agrees with de Cocq *et al.* (2013), who modelled several combinations of trunk stiffness and damping coefficient that could achieve harmony during the sitting trot.

On this basis, it could be suggested that equestrian coaching should encourage riders to explore coordination patterns that result in in-phase coordination between horse and pelvis, rather than modelling the aesthetics of an expert rider. However, dressage is a judged sport where the judge's perception of the horse-rider combination determines the outcome. Judges score the combination based on the impression of harmony and the rider's position in the saddle. The international rules of dressage (Fédération Internationale Équestre, 2020) set out that the rider's upper body should be '*tall and supple*' and their seat should be '*deep in the centre of the saddle, smoothly absorbing the movement of the Horse*'. Therefore, the rider's technique must be functional and adhere to the desired aesthetic of a dressage rider. Certainly, dressage coaches consider not only the rider's ability to absorb the movement of the horse but whether the pelvis is tilted forward or back, the position of their thighs and the impression of the rider as either tense or loose (Blokhuis *et al.*, 2008). It is unclear from this study whether any features would increase the perception of harmony as observed by a judge or coach. Therefore, before this information can be used to influence equestrian coaching and skill acquisition, further studies should determine the influence of horse-rider coordination features on the aesthetic perception and judged scores in dressage.

Comparison of intermediate and advanced riders gives a perspective of how experienced riders adapt to the constraints of environment and task. In this case, no significant main effects or interactions were found between any of the PC scores for cycle and competition level ($p > 0.05$). Performing sitting trot in equestrian dressage is an open skill and is typically performed with additional demands, such as directing the horse on a circle or initiating a lateral (side-stepping) movement. Therefore, dressage test riding features constantly changing environmental and task constraints. In contrast, the riding simulator performs a largely invariant, mechanically driven oscillation that simulates the trunk movement of the horse during trot. In conclusion, once riders begin competing at the national level, they have gained the self-organisation to successfully coordinate the movements of their seat with a trot-like rhythm of a riding simulator. However, as observed by Peham *et al.* (2001), the differences between riders may become evident when they are faced with achieving harmony on a variety of different horses.

The similar amount of variation explained by the first three PCs suggests that riders have comparable strategies in medium and extended trot on the simulator. However, in this case, the rider did not have to cue the simulator to perform extended trot. Studies by Byström *et al.* (2015) and Engell *et al.* (2016) suggest that riders adopt different techniques with their pelvis when cueing the horse to increase or decrease the stride length and frequency within a gait. Therefore, the present results do not truly reflect the strategy the rider would employ in extended trot, rather, they reflect the resilience of the rider's coordination strategy to changes in the amplitude of movement. When taken together, the in-phase coordination and the similarity of the coordination pattern between medium and extended trot suggest that competent riders initiate a highly stable coordination relationship between their seat and the riding simulator. Competitive riders from the lowest levels of national competition to the Olympic level of Grand Prix can achieve harmony with a riding simulator during medium and extended trot, although the exact pattern of coordination varies significantly between riders and even between cycles.

7.5 Conclusions

This study quantitatively and qualitatively analysed the coordination between the vertical displacement of a riding simulator and the pitch rotation of the rider's pelvis in simulated medium and extended trot. Three principal components were needed to account for >90% of the variation in both gaits and these were not related to competition level. Similar strategies were observed in medium and extended trot, characterised by in-phase coordination with the simulator. Significant variation between individuals and movement cycles suggests that there are variables other than competition level that may more accurately predict the coordination between a simulator or horse and the rider's pelvis and should be further investigated. As none of the variables tested in the preceding chapters has shown significance for the factor of competition level, its usefulness as a grouping factor is questioned and alternative methods to group riders by their kinematics should be sought.

8. Defining functional groups of rider trunk-pelvis technique in simulated medium trot using self-organising maps and *k*-means clustering

8.1 Introduction

Studies of the equestrian rider have sought to define optimal technique by analysing experts (Engell *et al.*, 2016; Byström *et al.*, 2009, 2010) and comparing expert and novice riders (Baillet *et al.*, 2017; Eckardt and Witte, 2017; Münz, Eckardt and Witte, 2014; Lagarde *et al.*, 2005; Peham *et al.*, 2001; Schils *et al.*, 1993), although this assumes that all experts or novices perform the task similarly. Underpinning the task of riding the horse is the demand for coordinating multiple degrees of freedom (DoF) in both horse and rider. Put simply, there is a limitless number of coordination possibilities in the rider alone, yet they must also coordinate with another living being, the horse. Dynamical systems theory states that coordination arises from the highly individual and complex interaction between the participant (horse and rider), task and environmental constraints (Newell, 1986). Therefore, it is unlikely that all riders within a given group, such as experience or competition level, have an identical technique. By grouping individuals by singular factors, the true nature of the intra-individual variability is obscured (Glazier and Mehdizadeh, 2019). Indeed, the results of Chapter 7 indicate that there is significant inter-individual variability of the simulator-pelvis coordination pattern that is not attributable to competition level. Individual riders may have novel movement solutions for the execution of sitting trot that is obscured by group means or summary statistics. As outlined in Section 4.2, the features that define techniques should be explored using continuous, rather than discrete, kinematic data (Schöllhorn *et al.*, 2002).

The concept of functional groups was proposed by Nigg (2010) and relates to groups of individuals whose response to a given stimulus are similar. To define a functional group, the movement patterns are grouped based on their distinctive features. One approach to generate novel groups based on the features of a time-series, rather than *a priori* categories, is the self-organising map (SOM). SOMs are a form of

unsupervised learning, that can take high-dimensional input data, for example, x, y and z coordinates for multiple motion capture markers, and project them onto a low-dimensional (typically two-dimensional) map. Through an iterative process, input data are mapped to neurons on the SOM, whereby similar patterns are mapped in proximity. Hoerzer *et al* (2015) described functional groups of runners' kinematics using a self-organising map (SOM) and *k*-means clustering. Similarly, SOMs have been used to analyse movement variability (Lamb *et al.*, 2007), sex- and speed-dependent changes in running biomechanics (Aljohani and Kipp, 2020), walking patterns (Schöllhorn *et al.*, 2002) and the effect of a rider on horse movement patterns (Schöllhorn *et al.*, 2006).

The movement of the rider's trunk and pelvis in the sagittal plane affects their balance in the saddle and can influence the horse's movement (Engell *et al.*, 2016; Byström *et al.*, 2015). Riders can control the horse's movements by varying the pressure exerted by their seat (Engell *et al.*, 2016; Byström *et al.*, 2015), but must also control movements of their trunk to maintain steady hands and stabilise their head position (Terada, Clayton and Kato, 2006). The suggestion of different patterns of rider trunk movement was first made by Terada, Clayton and Kato (2006), who quantified the kinematics of six high-level riders riding the same horse in sitting trot. The common strategy in five of six riders was a larger horizontal displacement of the hip marker than the shoulder, with the sixth rider displaying a larger shoulder than hip movement. Engell *et al.* (2016) succinctly described these strategies as 'moving the pelvis while stabilising the trunk' or 'rocking the pelvis around the hip joint'. Their observations suggest that researchers, and likely coaches and riders, can identify different strategies in the rider's trunk and pelvis movement in the sagittal plane. However, no study has elucidated whether groups of riders have similar techniques during sitting trot using continuous data.

The main objective of this study was to use SOMs and *k*-means clustering to separate riders' trunk and pelvis angular displacement in the sagittal plane into functional groups during simulated medium trot,

sitting. A riding simulator was used to standardise the oscillations for each participant. It was hypothesised that several groups would exist with characteristic kinematic profiles that could be described qualitatively.

8.2 Methods

8.2.1 Participants

The kinematic data for forty female competitive dressage riders, collected using motion capture (Miquis M3, Qualisys AB, Gothenburg, Sweden) on the riding simulator (Eventing Simulator, Racewood Ltd., Tarporley, UK) in simulated medium was extracted from the overall dataset based on the inclusion criteria outlined in Section 3.2.1 and Table 3.3, and the availability of the rider's data at the time of data analysis.

8.2.2 Data processing

The pitch of the rider's pelvis and trunk were extracted and processed, including the creation of rigid bodies, filtering, and time-normalisation to 101 points (Section 3.3). Ten cycles were included for all riders except rider 8, 10, 11 ($n = 7$) and 40 ($n = 8$) to eliminate cycles where significant gaps in the trajectories occurred (further details on gaps provided in Section 3.3). Cycles were then scaled to zero mean and to the range between -1 and 1 to enable an analysis of the features of the time-series. Finally, an input data matrix was created for the SOM: the normalised and scaled pelvis and trunk time-series were horizontally concatenated so that the data matrix comprised 389 rows (one row per cycle) and 202 columns (one column per data point).

This study aimed to group riders based on the pattern of their trunk and pelvis pitch during cycles of medium trot on the riding simulator. As the characteristics of these functional groups were unknown, unsupervised machine learning methods were chosen. A two-stage process was employed: first, a self-organising map (SOM) was trained with the parameters described in Table 8.1. A MATLAB toolbox (SOM Toolbox, Vesanto et al., 2000) was used for this analysis with the default options selected. Briefly, the SOM is an artificial neural network that is used for dimension reduction and pattern recognition (Lamb *et al.*, 2007). Through an iterative, competitive process, the SOM is trained to group similar vectors on the

map based on the Euclidean distance between the input vector and the output node (Aljohani and Kipp, 2020). Nodes are grouped based on a neighbourhood function, resulting in a map where all similar input vectors are grouped. The node associated with each input vector is known as the ‘best-matching unit’ (BMU), which is selected according to the similarity between the input values and the nodes in the grid. *K*-means clustering was applied to the SOM with a maximum of 10 clusters. The optimal cluster number was calculated as the Davies-Bouldin index (Davies and Bouldin, 1979), which calculates the lowest ratio of the average within-cluster centre distance to the average between cluster centre distance.

Table 8.1. Parameter selection for the self-organising map.

| SOM parameter option | Selected SOM parameter |
|------------------------|-----------------------------|
| Normalisation | Zero mean, range of -1 to 1 |
| Initialisation | Linear (PCA) |
| Lattice | Hexagonal |
| Neighbourhood function | Gaussian |
| Training algorithm | Batch |
| Map size | 13 x 8 |
| Quantisation error | 2.331 |
| Topological error | 0.033 |

The lowest Davies-Bouldin Index was assigned to the three-cluster solution (Figure 8.1). The assessment rate (Schöllhorn *et al.*, 2002) which is defined as the average ratio of the number of trials for a single subject separated in one cluster and the whole number of trials for the same subject was calculated for each individual. This gives information as to the proportion of the rider’s trials in a single cluster. Assessment rates for all riders individually are reported in Appendix E. The mean assessment rate \pm SD for the 40 riders was calculated. The three clusters gave an assessment rate of $87 \pm 17\%$, which was accepted as a definition of the functional groups as per Hoerzer *et al.* (2015). Visual inspection of the scaled and normalised data within the functional groups (Figure 8.2) suggested that the definition of the functional

groups was dependent on the relative timing of the peak posterior pitch of the trunk are reported in Appendix E.

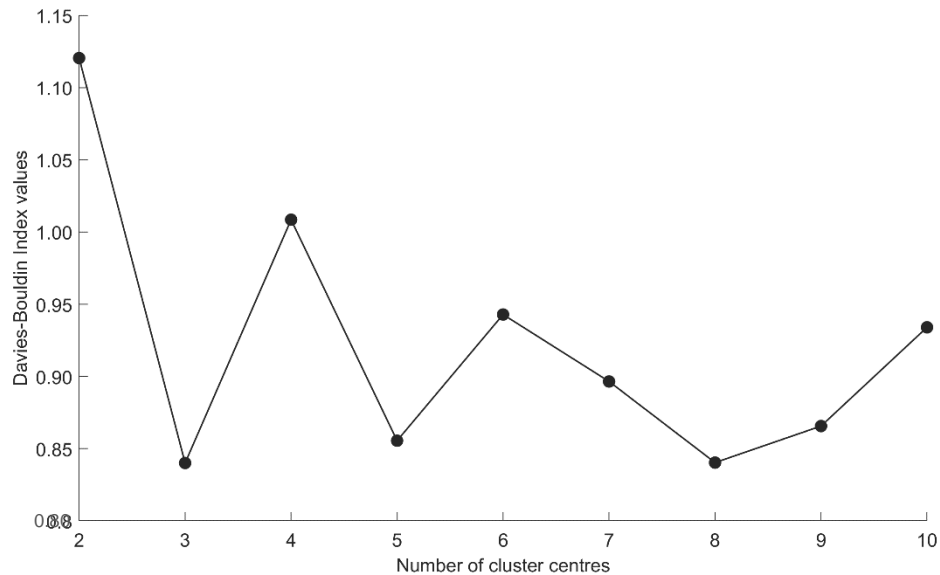


Figure 8.1. Davies-Bouldin Index calculated for clusters 1-10. The score for cluster 3 is 0.8401 and cluster 8 is 0.8420.

The percentages of the eight clusters within the three functional groups were calculated and reported in Table 8.2. Descriptive data were calculated for each of the eight clusters and reported in Table 8.3. The mean range of motion of the pelvis and trunk were calculated for each cycle and averaged within the cluster. The variability of the cycles within the cluster was calculated as the mean of the point-by-point standard deviation between cycles assigned to the cluster. Finally, the timing of the peak posterior pitch of the pelvis and trunk were calculated within each cluster as the mean index of the maximum value as a percentage of the overall cycle.

8.3 Results

The self-organising map (SOM) and subsequent *k*-means clustering identified three clusters as the solution with the lowest Davies-Bouldin Index value (Figure 8.1). Visual inspection of the three clusters (Figure 8.2) indicated that the most significant feature of the time series was the relative timing of the peak posterior trunk and pelvis pitch. The mean assessment rate for the three-cluster solution was $87 \pm 17\%$. As the majority of the riders' cycles are assigned to the same cluster this was accepted as the definition of the functional groups (Hoerzer *et al.*, 2015). In the present cohort of competitive female dressage riders, these groups can be described as functional group 1: where the peak posterior pitch of the trunk occurs after the peak posterior pitch of the pelvis within the cycle; functional group 2: where the peak posterior trunk and pelvis pitch are temporally aligned; and functional group 3: where trunk and pelvis pitch in opposite directions with the peak posterior pitch of the pelvis coinciding with the peak anterior pitch of the trunk, and vice versa.

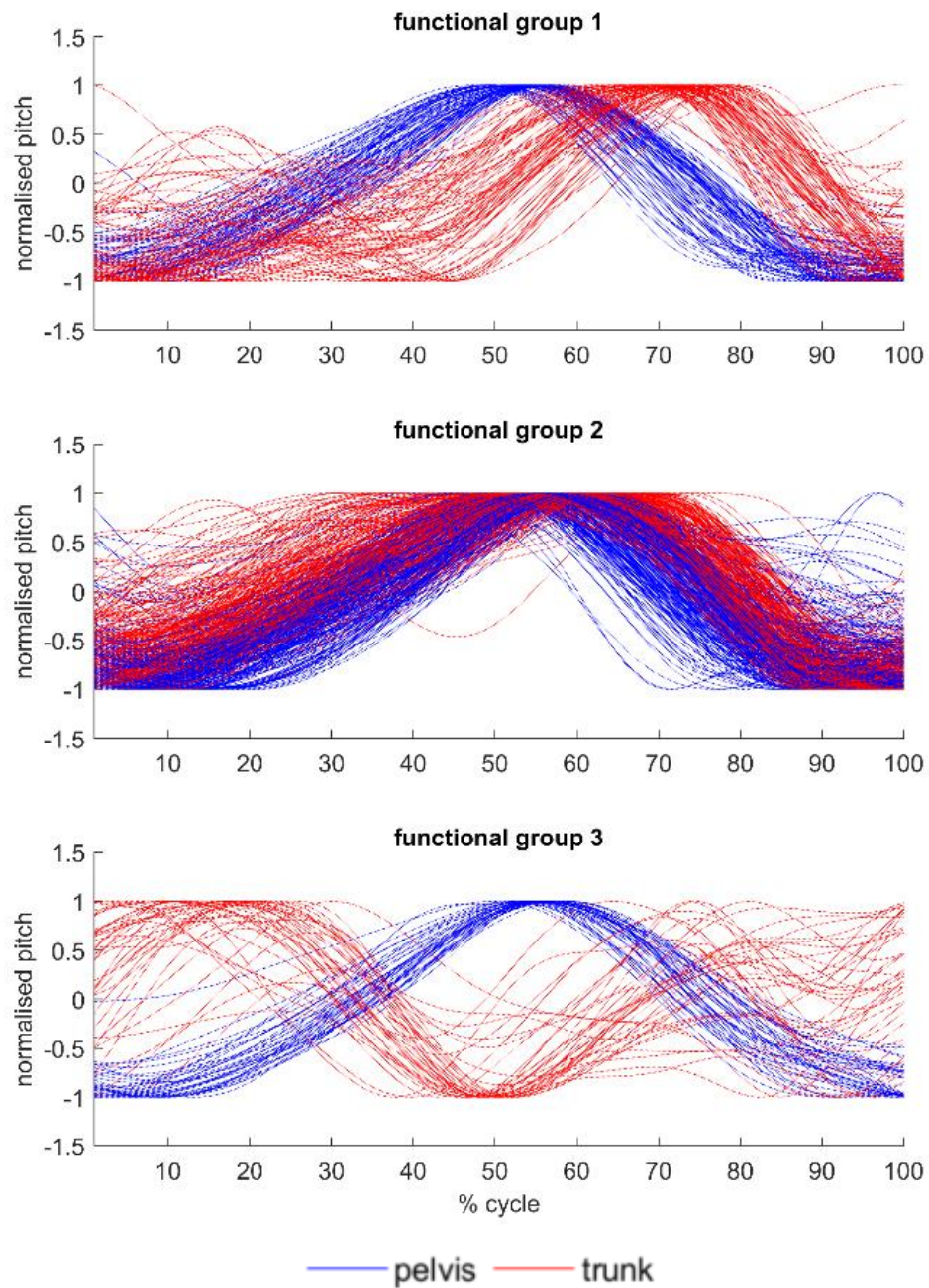


Figure 8.2 Time-normalised and scaled trajectories for the trunk (red) and pelvis (blue) pitch for the three functional groups for all ($n = 389$) cycles.

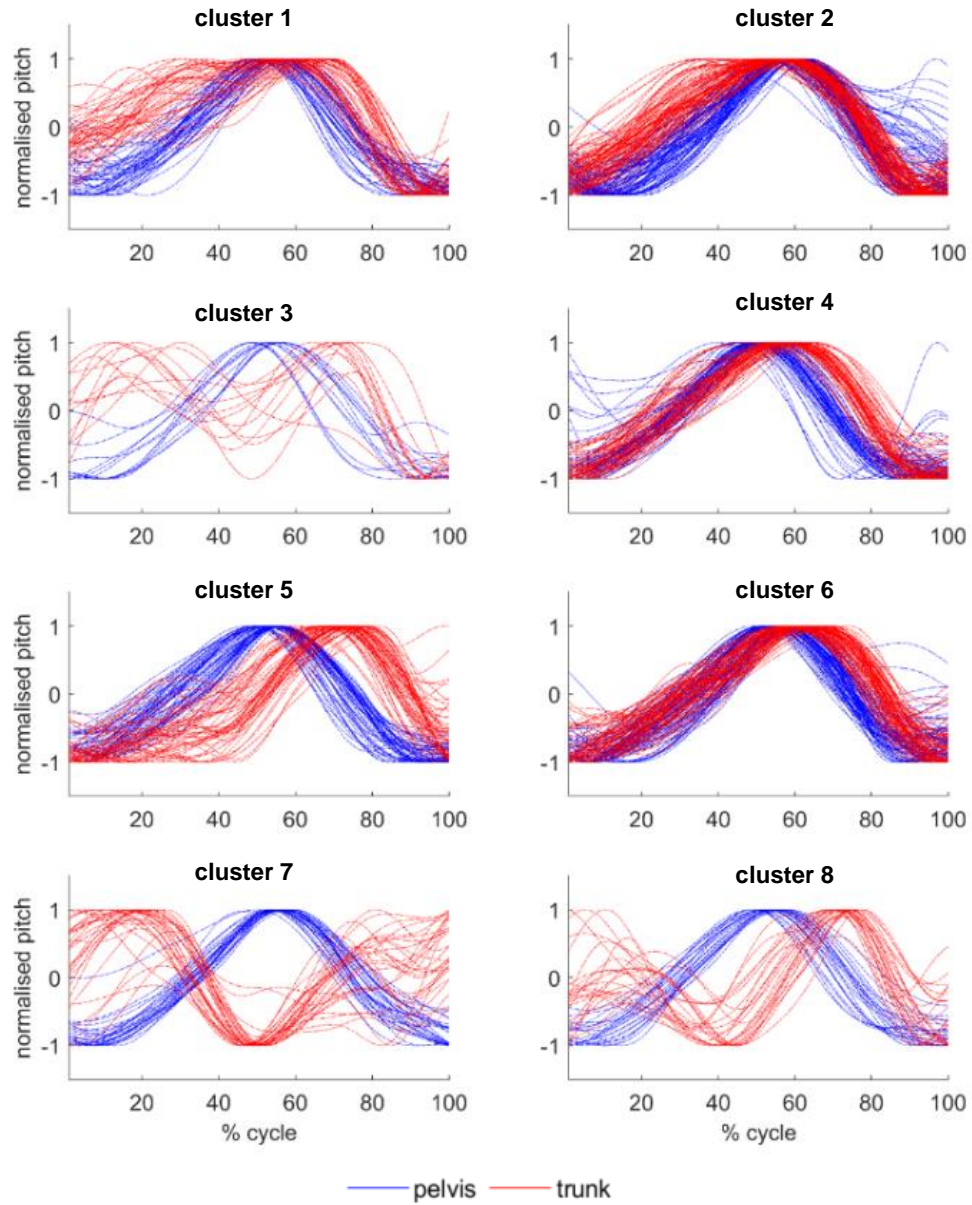


Figure 8.3 Time-normalised and scaled trajectories for the trunk (red) and pelvis (blue) pitch for the eight clusters for all ($n = 389$) cycles.

Table 8.2. Percentage (%) of each of the eight clusters within each functional group and of the total number of cycles. *N* is the percentage of the functional group of the overall number of cycles (*n* = 389).

| Functional Group | % | Cluster | | | | | | | |
|------------------|-----|---------|----|---|----|----|----|----|----|
| | | 1 | 2 | 3 | 4 | 5 | 6 | 7 | 8 |
| 1 | 20 | 0 | 0 | 4 | 0 | 65 | 7 | 0 | 23 |
| 2 | 71 | 16 | 33 | 1 | 22 | 0 | 28 | 0 | 0 |
| 3 | 10 | 0 | 0 | 6 | 0 | 0 | 0 | 76 | 8 |
| Total (%) | 100 | 11 | 23 | 3 | 15 | 14 | 21 | 7 | 5 |

While the maximal posterior pitch of the pelvis defined the functional groups, the plots indicated that clusters might exist to group riders by other features of the time series. Eight was the next lowest Davies-Bouldin Index value (0.8420). The mean assessment rate for eight clusters was $63 \pm 24\%$. The proportion of the clusters within each functional group (Table 8.2) suggests that some of the eight clusters grouped edge cases where features of the waveform were not strictly confined to one functional group. For example, clusters 3, 6, and 8 contained small percentages of more than one functional group. As visualised in Figure 8.4, cluster 8 can be described as a time-shifted analogue of functional group 1, to the point that the peak anterior trunk pitch (minimum) nearly coincides with the peak posterior pelvis pitch. Other clusters were associated with only one functional group, representing subsets of the functional group with slight variations in areas of the time series other than the relative timing of the posterior pitch of the pelvis and trunk.

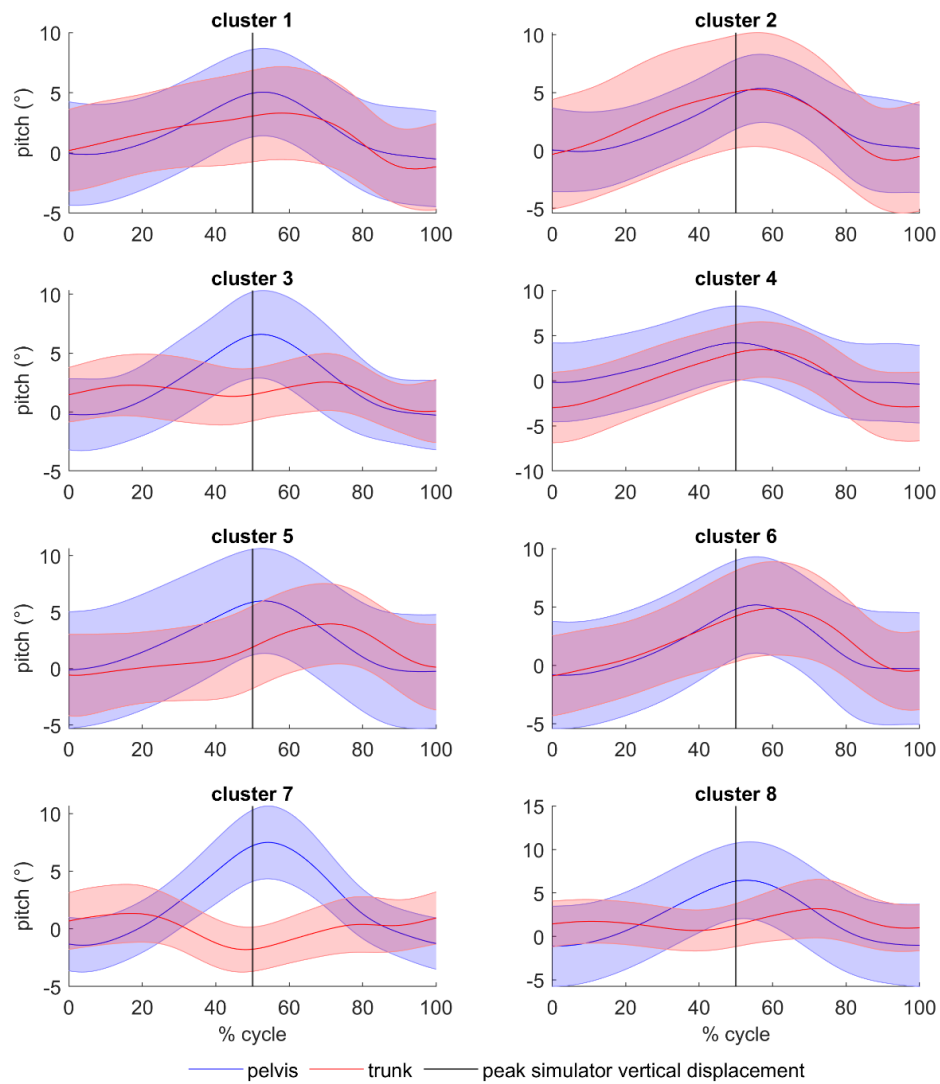


Figure 8.4. Mean (bold red or blue lines) and error clouds of unscaled, normalised pelvis (blue) and trunk (red) pitch trajectories within each cluster. The black line indicates the timing of the maximal vertical displacement of the riding simulator.

Table 8.3. Characteristics and qualitative interpretation of clusters representing sub-groups of the functional groups of rider trunk-pelvis movement in sitting trot. Mean peak timing given as a percentage of the period of the movement cycle of the riding simulator.

| Cluster | Mean range of motion (°) | | Mean standard deviation (°) | | Mean peak timing (% of cycle) | | Qualitative interpretation |
|----------|--------------------------|-------------|-----------------------------|-------------|-------------------------------|---------------|--|
| | Pelvis | Trunk | Pelvis | Trunk | Pelvis | Trunk | |
| 1 | 5.99 ± 1.85 | 5.03± 2.94 | 3.81± 0.18 | 3.51 ± 0.21 | 52.90 ± 2.98 | 56.77 ± 9.92 | Peak posterior pitch of pelvis coincides with peak vertical displacement of riding simulator. Trunk peak follows pelvis. Smaller trunk ROM than pelvis, flatter slope than pelvis during ascent and early descent stage of cycle. |
| 2 | 6.07± 2.02 | 6.53 ± 2.15 | 3.30 ± 0.36 | 4.78 ± 0.23 | 56.78 ± 3.40 | 54.10 ± 5.62 | Similar strategy to cluster 1, with greater trunk ROM, mean trunk posterior pitch and trunk coefficient of variation. |
| 3 | 7.57 ± 2.13 | 3.09 ± 1.34 | 3.29 ± 0.38 | 2.41 ± 0.20 | 52.39 ± 3.21 | 67.02 ± 12.16 | Two peaks of posterior trunk pitch per cycle. Trunk pitches anteriorly as pelvis reaches peak posterior pitch. Peak posterior pelvis pitch at around peak vertical displacement of riding simulator. Small trunk range of motion compared to pelvis. |
| 4 | 4.96 ± 1.74 | 6.98 ± 2.48 | 4.22 ± 0.08 | 3.43 ± 0.27 | 52.25 ± 10.44 | 57.08 ± 3.47 | Peak posterior pitch of pelvis coincides with peak vertical displacement of riding simulator. Peak posterior trunk pitch after pelvis. Similar slope of trunk and pelvis on ascent of simulator, sharper peak of anterior trunk on descent. Smaller pelvis ROM than trunk. |
| 5 | 6.69 ± 2.23 | 4.97 ± 2.03 | 4.90 ± 0.19 | 3.43 ± 0.20 | 52.80 ± 2.48 | 71.79 ± 5.66 | Pelvis peak posterior pitch coincides with peak vertical displacement of riding simulator, trunk follows at ~70%. Trunk in anterior pitch from 0-40% of cycle. Trunk and pelvis similar slope from 75-100% of cycle. Smaller trunk ROM than pelvis. |
| 6 | 6.52 ± 1.58 | 6.20 ± 3.07 | 4.44 ± 0.22 | 3.50 ± 0.28 | 55.41 ± 2.97 | 61.31 ± 3.77 | Similar trunk-pelvis trajectories. Pelvis and trunk peak occurring at ~60%. Pelvis reaching maximal anterior pitch before trunk; trunk leading pelvis in descent phase of cycle. Greater pelvis ROM than trunk. |
| 7 | 9.59 ± 2.81 | 3.66 ± 1.57 | 2.48± 0.35 | 2.23 ± 0.20 | 54.63 ± 2.00 | 18.76 ± 13.69 | Similar strategy to cluster 3, with greater peak anterior trunk pitch. Trunk reaches peak anterior pitch before pelvis reaches peak posterior pitch. |
| 8 | 8.25± 2.28 | 2.93 ± 1.46 | 4.55 ± 0.14 | 2.72 ± 0.33 | 52.88 ± 2.71 | 66.39 ± 18.91 | Similar strategy to cluster 3 with greater trunk and pelvis ROM. Most prominent peak posterior pitch of trunk occurs at ~66% of cycle, however large standard deviation indicates that it may also occur before peak posterior pelvis pitch in the cycle. |

8.4 Discussion

This study's main objective was to explore whether functional groups of dressage rider trunk and pelvis pitch could be defined based on the features of the time series. The study applied a self-organising map (SOM) and *k*-means clustering to define functional groups of rider trunk and pelvis pitch in simulated medium trot, sitting, for 40 riders over 389 cycles of the vertical displacement of the riding simulator. This is the first known study to use SOM and *k*-means clustering to explore functional groups of movement in equestrian riders. Three was the number of groups with the lowest Davies-Bouldin Index value (Figure 8.1). The mean assessment rate (Schöllhorn *et al.*, 2002) for three groups was 87%, which indicated that most of the individual riders' trials were assigned to a single group. Therefore, these groups were deemed to constitute a functional group (Hoerzer *et al.*, 2015). Visual inspection of the time-series within the functional groups (Figure 8.2) indicates that functional groups were defined by the relative timing of the peak posterior pitch of the riders' trunk and pelvis. Inspection of the other areas of the trajectories within the functional groups suggested that perhaps a more sensitive segmentation of the riders' trajectories could elicit greater exploration of functional outcomes within and between functional groups. The data were split into eight clusters, based on the next lowest Davies-Bouldin Index value, and the data were plotted for qualitative analysis. Functional interpretation of these clusters revealed between-cluster differences that related to the relative timing of trunk-pelvis posterior pitch, the timing of the pelvis posterior pitch relative to the peak vertical displacement of the riding simulator and differences in the range of motion of the trunk relative to the pelvis. This study is an important first exploratory step to understanding the diversity of movement strategies that nationally competitive dressage riders employ to accomplish sitting trot in the sagittal plane.

8.4.1 Functional Groups and movement interpretation

The SOM and *k*-means clustering approach has been used by Hoerzer *et al.* (2015) and Eslami *et al.* (2017). Similar to Hoerzer *et al.* functional groups were considered to be one where the assessment rate indicated that most of the individual's cycles were assigned to the same group, as it is assumed

that inter-individual variability will be higher than intra-individual variability. Inspection of plots of the time-normalised, scaled trunk and pelvis pitch trajectories within the three functional groups (Figure 8.2) indicates that this clustering is based on the relative timing of the peak posterior pitch of the pelvis and trunk. This finding aligns with Terada, Clayton and Kato (2006) who observed two strategies in competent riders during sitting trot, interpreted by Engell *et al.* (2016) as: ‘moving the pelvis while stabilising the trunk’ or ‘rocking the pelvis around the hip joint’. The first strategy, ‘moving the pelvis while stabilising the trunk’, would imply that the pelvis is moving independently from the trunk, which is represented by functional group 3. This group (10% of all cycles) is described as opposite rotations of trunk and pelvis, where the peak posterior pitch of the pelvis coincides with the peak anterior pitch of the trunk and vice versa. Most of the cycles from functional group 3 were assigned to cluster 7 (86%), although small proportions of cycles were assigned to clusters 3 (6%) and 8 (8%). Visual inspection suggests that the key differences between clusters 3 and 7 are due to greater anterior trunk pitch in cluster 7. Cluster 8 is a similar pattern to cluster 3, but with greater pelvis ROM (Table 8.3). If the rider is moving the pelvis below a fixed trunk, one would expect that the pelvis range of motion (ROM) would be larger than the trunk ROM. This rings true for clusters 3,7 and 8; the pelvis ROM is substantially greater than trunk ROM. In the study conducted by Terada, Clayton and Kato (2006), five out of six riders displayed this pattern, while in the present study, this functional group represented the least cycles.

The second strategy observed by Terada, Clayton and Kato (2006), ‘rocking the pelvis around the hip joint’, would imply that the pelvis and trunk are moving together, and greater movement occurs at the hip joint to absorb the movement of the horse. This is represented by functional group 2, which is comprised of clusters 1, 2, 4 and 6. This is the most common strategy employed by riders; 71% of all trials were assigned to this functional group. The trunk and pelvis move coincidently anteriorly and posteriorly, with similar ROM. Variations of this technique are represented by the slight differences between clusters 1,2,4 and 6. These indicate that riders manage individual differences, likely in anthropometry and other participant-related factors to achieve the same outcome.

The first functional group, where the maximal posterior pitch of the trunk is time-shifted ~15-20% (Table 8.3) of the cycle compared to the pelvis, is in line with Engell *et al.* (2016) who observed a lag of 13% of the stride cycle between the pitch of the rider's trunk and pelvis when the rider was passively riding the horse in sitting trot, compared to 11% when actively influencing the movement with coordinated movements of their seat. Riding the simulator is a largely passive activity for the rider as they cannot influence its movement with their seat or legs during the trial. It is unclear whether increased dissociation observed in functional group 1 result from the rider's intent to passively ride the simulator, or whether other participant factors such as anthropometry, strength or saddle fit influenced the incidence of this functional group. Furthermore, the small difference between the time-shift of the maximal pitch rotations of the trunk and pelvis observed by Engell *et al.* (2016) may have resulted from the increases in horse speed observed between the active and passive sitting trot. In the same way, the contribution of the characteristics of the riding simulator's movement to the characteristics of the rider's trunk-pelvis coordination is unknown.

Assessment of the timing of the peak posterior pelvic pitch relative to the peak vertical displacement of the riding simulator yields substantial insights as to how riders move within the stride. Previous studies have reported that the rider's trunk inclines posteriorly during early stance and anteriorly during late stance of the diagonal pairs of the horse's limbs in trot, with the peak anterior pitch coinciding with the push-off into suspension (Engell *et al.*, 2016; Terada, Clayton and Kato, 2006). In a live horse, the vertical position of the trunk reaches its minimum during mid-stance and maximal during the push-off into suspension (Clayton and Hobbs, 2017). Therefore, in the cycle of the riding simulator, mid-stance corresponds to the minimum vertical displacement and the maximum vertical displacement corresponds to the peak of the suspension phase. In the present study, this pattern was seen in functional group 3: the pelvis reached maximal posterior pitch during the minimum vertical displacement of the simulator and peak anterior pitch around the time of the peak vertical displacement of the simulator, with the trunk moving opposite. However, for most of the riders, the convention described by Terada, Clayton and Kato (2006) is inversed: riders reached peak posterior

pitch in both trunk and pelvis around the maximal vertical displacement of the simulator (suspension) and peak anterior pitch around the minimal vertical displacement of the simulator (mid-stance). As previous studies have assessed small (<10) groups of riders, observations in previous studies may have been limited by the smaller groups of riders. It is also worth noting that the stride cycle used in this study would represent only half of the stride; the stride cycle of the live horse has two diagonal support phases, and therefore two cycles of maximal vertical displacement of the sacrum.

8.4.2 Limitations and future directions

The variety of techniques employed by equestrian riders has remained largely unexplored. That said, given the contribution of the horse to the movement pattern of the rider, the use of a riding simulator may not elicit all of the possible trunk-pelvis strategies that riders employ, due to the lack of forward travel and ground reaction forces. Furthermore, these strategies are only representative of the present cohort of female, competitive dressage riders, and therefore, are not exhaustive. Future studies should aim to include as many riders as possible to discover whether the patterns observed in this study are indicative of the wider equestrian population, or whether other classifications may exist.

While the riding simulator standardised the experimental conditions for all participants, it is possible that the functional groups described in this study relate to the specific task and environmental constraints of simulated riding, rather than those experienced with live horses. For example, the head position of the riding simulator remains mostly static throughout the trial, whereas a live horse's head moves with each stride, creating greater interaction between the rider's hands on the reins that connects to the bit in the horse's mouth. Terada, Clayton and Kato (2006) found that experienced riders moved their trunk and arm to accommodate the horse's movement but also maintained a consistent tension on the reins. Similarly, in their study of horse movement using a SOM and clustering approach, Schöllhorn *et al.* (2006) found that the trajectories of the horse's head are most influenced by the rider, which underscores the interaction between the rider's hands and the horse's mouth.

It is possible that the distribution of the functional groups may be influenced by the mechanical interaction with the horse, therefore, similar live horse studies are needed. Several studies have shown that the rider can influence the horse's gait kinematics; Peham *et al.* (2001) found significant differences in the horses' speed between a novice and professional rider and Lagarde *et al.* (2005) found significant differences in the interval between the successive extensions of the horses' limbs in trot. Licka, Kapaun and Peham (2010) found that the presence of a rider could increase the horse's asymmetries, and therefore the subjective evaluation of lameness. As many horse-related factors may influence the rider, such as the saddle (Clayton *et al.*, 2018) and the horse's behaviour (e.g. their 'rideability') (König von Borstel and Glißman, 2014), the influence of the horse on the rider is not as clearly defined. Interesting data was presented by Wolframm, Bosga and Meulenbroek, (2013), who looked at the predictability of horse and rider trunk acceleration patterns (entropy). No clear pattern between horse and rider entropy was found. Some riders' trunk accelerations were more predictable than their horse, and vice versa. The functional asymmetries (see Section 2.1.4 for review), injuries, disciplines and skill level (see Section 2.2 for review) of the horse-rider combination is likely to influence their kinematics. The strategies observed in this study may stem from a singular or mutual adaptation of rider and horse. However, much further research, employing pattern recognition analyses, such as the SOM, is certainly needed.

This study has grouped riders based on the features of their pelvis and trunk pitch time series. Chapters 6 and 7 did not find any association between the characteristics of the rider's coordination and competition level. No other valid grouping variable or factor was collected during data collection, however, future studies may gather data that could explain why riders were assigned to specific clusters using regression models or other means, such as those employed by Hoerzer *et al.* (2015). Nonetheless, the SOM and *k*-means clustering were able to successfully define functional groups in this homogenous population, therefore, further studies could employ unsupervised classification methods with interventions, such as different saddles, horses, or rider traits. Other studies have concatenated the three-dimensional coordinates of individual markers, rather than rigid bodies, for

analysis by SOM. While this could provide greater information about rider groups, the results of this study suggest that pitch trajectories may provide enough information to obtain functional groups of riders.

8.5 Conclusions

This study has shown that female competitive dressage riders can be grouped by the features of their trunk and pelvis pitch time-series during simulated sitting trot. A pattern recognition approach identified three functional groups, defined by the relative timing of the maximal posterior trunk and pelvis pitch. Maximal posterior trunk pitch occurred coincidentally or very slightly after the pelvis for most of the riders, although for a small proportion, trunk and pelvis pitched oppositely. Further segmentation of the functional groups into eight clusters revealed diverse strategies that likely relate to the rider's constraints. Future research should continue to investigate the existence and cause of diverse rider movement patterns and relate these to the horse.

9. Summary and implications

The ethical and welfare implications of riding an animal in sporting competition have rightly cemented the horse as the focus of research in equestrian sport. However, as highlighted by the literature presented in Section 2.2, the rider's role in the performance outcomes cannot be overlooked. Research presenting biomechanical analyses of the rider during simulated or live riding have emerged in the last two decades, in addition to significant interest in the practical applications of rider biomechanics to coaching and rider assessment. However, many questions remain regarding the rider's performance and the most accurate methods to capture and quantify the rider's biomechanics and the coordination between horse and rider. This section will present a summary to detail the rationale and link between the chapters of this thesis, followed by discrete summaries for each chapter.

Underpinning the rationale for rider biomechanical assessment is the high prevalence of rider back pain (Hobbs *et al.*, 2014; Pugh and Bolin, 2004), alongside the proliferation of technologies that allow increasing levels of precision in field-testing, including inertial measurement units (Eckardt and Witte, 2017; Gandy *et al.*, 2014; Münz *et al.*, 2013). As outlined in Section 2.1, several studies (Eckardt and Witte, 2017; Engell *et al.*, 2016; Alexander *et al.*, 2015; Byström *et al.*, 2009, 2010, 2015; Gandy *et al.*, 2014; Münz, Eckardt and Witte, 2014) have analysed the rider's kinematics on live horses and using riding simulators, with particular focus on the rider's pelvis. However, no studies have considered the accuracy of the common practice of affixing motion capture markers to tight clothing overlying the rider's pelvic landmarks, rather than directly to the skin.

Many of these studies grouped riders by their competition level (Baillet *et al.*, 2017; Eckardt and Witte, 2017; Olivier *et al.*, 2017; Münz, Eckardt and Witte, 2014) and use discrete methods (Kang *et al.*, 2010; Terada, Clayton and Kato, 2006; Lovett, Hodson-Tole and Nankervis, 2005; Schils *et al.*, 1993), such as the mean of a variable within the movement cycle, to analyse the dynamic interaction between horse and rider. Whereas continuous data presented in figures (Engell *et al.*, 2016; Byström *et al.*, 2009,

2010) offer insight into the effect of the phases of the horse's stride on the rider's kinematics. With regards to the interaction between horse and rider, several studies (Wolframm, Bosga and Meulenbroek, 2013; Lagarde *et al.*, 2005; Peham *et al.*, 2001) presented interesting approaches to analysing the horse-rider coordination in live horses, using analytical tools from dynamical systems theory, such as the discrete or continuous relative phase. Therefore, based on the remaining questions derived from the previous literature, this thesis set out to investigate the dynamic technique of the female equestrian rider.

The questions answered in this thesis progressed from the validity of a static capture of the rider to predict their dynamic technique, to dynamic analyses of the rider's coordination strategy and trunk-pelvis technique. Each study was underpinned by gaps in the currently published literature. Chapter 5 compared the static pelvic posture of the rider in the sagittal plane to their dynamic pelvic posture during a simulated walk, trot, and canter. Several previous studies (Guire *et al.*, 2017; Hobbs *et al.*, 2014) had analysed the rider's static posture and it was questioned whether a static capture could predict the rider's dynamic technique. The results indicated that there is no relationship between the rider's pelvic posture at the halt and mean pelvic pitch in any gait.

As mentioned earlier in this section and explored in Section 2.2, many studies have analysed the influence of rider experience or competition level on their kinematics. A key component of performance analysis is the ability to identify facets of technique that contribute to high performance (Lees, 2010). Some studies have found an interaction of skill level on the significant differences between variables measured in riders relating to their kinematics and horse-rider coordination (Baillet *et al.*, 2017; Olivier *et al.*, 2017; Lagarde *et al.*, 2005; Peham *et al.*, 2001). However, as the experience gap narrows between riders, the effect of skill on kinematic variables seems to be equivocal (Eckardt and Witte, 2017) (see Section 2.2 for full critical analysis). Only Olivier *et al.* (2017) have compared low-level competitive riders and high-level professionally competitive riders. Therefore, prior to this thesis, questions remained as to whether any characteristics relating to the rider's kinematics or

horse-rider coordination were more common within high-level than low-level competitive riders. If characteristics could be found to distinguish high-level from low-level riders, then these may form the basis for rider education.

Competitive female dressage riders were solicited for the overall dataset that supplied the data for analysis within each of the experimental chapters. The inclusion criteria for each study was defined in Section 3.2.1 and participant characteristics for each study are presented in Table 3.4 To standardise the 'horse' variable between riders, and to allow the greatest possible number of rider participants, a riding simulator (Eventing Simulator, Racewood, Tarporley, UK) was used. Riding simulators have been used to analyse the rider's kinematics and coordination strategy in previous studies (Baillet *et al.*, 2017; Clayton, Smith and Egenvall, 2017; Olivier *et al.*, 2017; Biau *et al.*, 2013). The experimental chapters analysed the influence of dressage competition level on the rider's pelvic posture and dynamic pelvic tilt (Chapter 5), coordination variability of their head, trunk, pelvis and foot to the riding simulator in medium and extended trot (Chapter 6), and features of the simulator-pelvis coordination strategy (Chapter 7). Competition level was not significantly related to any measured variable. This suggests that once riders reach the levels of nationally-affiliated dressage, analyses of the rider's kinematics on the riding simulator cannot distinguish between low-level and elite competitors.

Lack of factors relating to competition level suggests that inherent rider factors, and potentially those relating to the horse, influence the rider's kinematics and coordination. Based on the method proposed by Schöllhorn *et al.* (2006), self-organising maps and *k*-means clusters were used to identify 'functional groups' (Hoerzer *et al.*, 2015) of rider trunk-pelvis kinematics in sitting simulated medium trot. These functional groups may be influenced by the rider's anthropometry or the gait and behaviour characteristics of their own horse. However, it is outside of the scope of this thesis to investigate these factors, and evidently, this method offers interesting potential for future investigations.

The methods to inform these studies was developed based on previous investigations of the rider using motion capture (Engell *et al.*, 2016, 2018; Alexander *et al.*, 2015; Byström *et al.*, 2009, 2010). Chapter 3 presented an explanation and justification for the data capture protocol on the riding simulator using optical motion capture cameras (Miquis M3, Qualisys AB, Gothenburg, Sweden). Subsequent data processing routines that were used before specific analyses within the studies was presented and justified (Section 3.3).

Chapter 4 presented specific methodological considerations for two important aspects of this thesis: the effect of rider clothing on motion capture markers and the development of the calculation of the coordination variable used in Chapter 6 and 7. As evidenced by Camomilla and Bonci (2020) and Camomilla, Bonci and Cappozzo (2017) soft tissue artefact can contribute to error in the measurement of the pelvic bony landmarks and pelvic orientation. However, all known rider studies have affixed the motion capture markers to the rider's trousers due to the practicalities and safety of riding a horse or riding a simulator. Section 4.2 of Chapter 4 compared measures of measurement error on the skin-affixed and trouser-affixed motion capture markers. No significant differences in error were found.

Section 4.3 of Chapter 4 explored and justified the considerations for the calculation of the coordination measure used in Chapter 6 and 7: the continuous relative phase (CRP). As per the methods proposed by Lamb and Stöckl (2014), the considerations for time-normalisation, scaling, and calculation of the continuous relative phase using the Hilbert transform was explored, referenced and justified. Coordination variability was defined as the circular standard deviation between movement cycles (Olivier *et al.*, 2017). The measures of coordination variability between the CRP and discrete relative phase (DRP) were calculated and significant differences were tested. The CRP variability was significantly greater for the simulator-pelvis segment than DRP coordination variability. Therefore, the DRP may underestimate the coordination variability of the simulator-pelvis coupling. In addition, the CRP may provide valuable insights that pertain to the phase of the movement cycle itself (e.g. upward or downward phase). These are explored in Chapter 6 and 7.

9.1 Summary and implications of individual chapters

9.1.2 Chapter 4

Chapter 4 addressed issues related to the measurement of the rider's kinematics and the calculation of horse-rider harmony, respectively. As stated in Section 4.2, motion capture error can relate to the motion capture cameras themselves or to the displacement of the markers relative to the underlying bone, known as soft tissue artefact (STA), which may be influenced by body mass index (BMI) (Camomilla and Bonci, 2020). As STA has a frequency component similar to the underlying bone itself, it is not attenuated by filtering it can influence the subsequent calculations of rigid bodies. Therefore, the first part of this study aimed to assess whether: (1) there was a relationship between STA and BMI in riders when assessed with markers affixed to skin or trousers; and (2) whether STA increased when markers were affixed to clothing, rather than directly to the skin. Four competent female riders rode the riding simulator in medium walk, trot and left canter in shorts and a sports bra and they were matched by BMI to four female riders from the existing dataset who rode with tight-fitting riding trousers or tights. The STA was calculated for each marker as per Cereatti *et al.* (2017) and the effect on the resulting rigid body was calculated as the residual of the rigid body.

There were no significant differences between skin and trouser affixed markers for any STA parameter. Additionally, the BMI was not significantly correlated with any STA parameter. The direction of the STA related to the largest direction of motion of the riding simulator in each gait. Therefore, the error of the markers is most influenced by the movement of the simulator in each gait, rather than the BMI of the rider or the clothing. As the movement of the riding simulator is the same for every individual, the magnitude of the error is consistent across all participants. This study could not conclude whether affixing markers to skin or trousers significantly influenced the accuracy of the markers to track their underlying bony landmarks. Therefore, the amount of error on the resulting measures, such as the tilt range of motion, introduced by the STA during riding is still unknown. As the pelvic orientation may have clinical relevance for the rider, further work is needed to quantify the accuracy of pelvis markers during riding. In conclusion, these results suggest that affixing markers to

tight-fitting trousers do not introduce additional error detected with the STA protocol used, compared to affixing markers directly to the skin. Given the diverse range of markers used to form the rigid body of the pelvis, it is recommended that the standard pelvis coordinate system (Wu *et al.*, 2002) be used when studies wish to report the kinematics of the pelvis to allow direct comparison of results.

The second part of Chapter 4 aimed to analyse the differences in coordination variability measures obtained by discrete relative phase (DRP) or continuous relative phase (CRP). Considerations for processing the rider's kinematic data for subsequent CRP analysis were presented. The CRP and DRP between the vertical displacement of the riding simulator and the rider's trunk and pelvis pitch were calculated for 28 female riders in medium trot. The difference between coordination variability calculated with CRP or DRP was statistically assessed.

A key assumption of CRP and DRP calculations is that the signals maintain a consistent frequency (e.g. sinusoidal time-series) (Wheat and Glazier, 2006). Certainly, the repeatable movement of the vertical displacement of the riding simulator meets this assumption, however, the pitch rotations of the rider's pelvis and trunk did not. The rider signals did, however, contain a prominent peak, which corresponded to the peak posterior pitch. The DRP was calculated as the latency between the peak posterior pitch of the rider's trunk or pelvis, to the peak vertical displacement of the riding simulator in 28 female riders during simulated medium trot. For the CRP calculations, the signals were time-normalised 1001 points and scaled to the unit mean and the range between -1 and 1. The CRP was then calculated using the Hilbert transform, which is recommended if the signals are not sinusoidal (Lamb and Stöckl, 2014). The measure of coordination variability is only accurate if the CRP data do not contain spurious variability or discontinuities (Cazzola, Pavei and Preatoni, 2016). Based on the results of this study, it is recommended to time-normalise the data to 1001 points, rather than 101, which is the standard in biomechanics. This is due to the Gibbs phenomenon, which results in random variability at the ends of the cycles (Lamb and Pataky, 2018).

Coordination variability for each rider was calculated with circular statistics as the trial (10 cycles per rider) mean point-by-point standard deviation of the CRP and the trial mean standard deviation of the DRP. Paired sample t-tests indicated that simulator-pelvis coordination variability was significantly greater when calculated by CRP than DRP ($p < 0.001$), however simulator-trunk coordination variability was not significantly different. CRP and DRP were moderately significantly correlated for simulator-trunk ($r = 0.61$, $p = 0.001$), but not for simulator-pelvis. The implications of this study are threefold: (1) care should be taken in the calculation of the CRP and the Hilbert transform should be used; (2) the CRP, rather than DRP should be used to represent the coordination between horse and rider unless the hypothesis pertains specifically to the relative timing between the peak of a signal or gait event; and (3) for analyses of the horse-pelvis coupling, the DRP may significantly underestimate the actual coordination variability, and the standard deviation of the mean CRP should be used instead.

9.1.1 Chapter 5

This study aimed to explore the relationship between competition level and measures of sagittal pelvic posture ('pelvic tilt') in static and dynamic conditions during simulated medium walk, trot and left/right canter. Based on the preceding studies it was hypothesised that competition level would influence pelvic tilt and that static pelvic posture would relate to dynamic pelvic tilt. Riders were split into groups based on their self-reported competition level. Novice riders ($n = 9$) were those competing in British Dressage (BD) Preliminary, Novice and Elementary, intermediate ($n = 15$) were competing at BD Medium, Advanced Medium and Advanced, and international ($n = 9$) were competing at the international (FEI) levels.

The hypothesis was only partially accepted; no relationship was found between competition level and static pelvic posture and mean pelvic tilt, tilt ROM or minimum pelvic tilt in simulated walk, trot or canter. In right canter, novice riders had significantly ($p = 0.017$) greater maximum pelvic tilt than the other levels. As a group, riders' pelvic tilt was significantly more posterior in trot and both leads of canter than in walk, indicated that riders increase posterior pelvic tilt to cope with greater movement amplitudes and frequencies. However, Table 5.3 illustrates that riders had individual strategies

described as either anterior throughout, anterior-posterior or posterior throughout, depending on whether their minimum and maximum values described anterior or posterior orientations. Therefore, the findings of this study suggest that rider pelvic technique should be assessed dynamically, and static assessments may provide limited value to the coach or clinician. Furthermore, it is unlikely that riders need to maintain a neutral pelvis to achieve harmony with the horse, given that riders competing at the highest levels of dressage were not more likely than those at the lowest levels to have a neutral pelvis. Deviation from a neutral pelvis may be a functional adaptation that allows the rider to achieve harmony given their unique characteristics. Competitive riders may have a greater incidence of back pain (Deckers *et al.*, 2020; Lewis *et al.*, 2019; Hobbs *et al.*, 2014), which may be reflected by deviations from the neutral pelvic posture. However, the relationship between pelvic posture and technique in the saddle and rider back pain is not known. Besides, the relationship between back pain and pelvic tilt/lumbar lordosis is questioned, rather, low back pain is attributed to lack of muscle endurance, and weakness (Nourbakhsh and Arab, 2002). Therefore, the implications of this study are as follows: (1) riders should be assessed dynamically; (2) riders should be assessed independently of competition level; and (3) the relationship between rider back pain and pelvic technique or posture should be investigated further.

9.2.3 Chapter 6

This chapter presented the continuous coordination variability between the rider's head, trunk, pelvis and foot and the vertical displacement of the riding simulator during simulated medium and extended trot. This is the first known equestrian study to present the coordination variability as a continuous time series, rather than a scalar value. The influence of segment (head, trunk, pelvis, foot), competition level, and gait (medium or extended trot) on the coordination variability to the riding simulator was assessed for 40 nationally and internationally competitive dressage riders. Hypothesis testing was conducted using statistical parametric mapping (SPM1D) to compare the time series of the continuous relative phase variability. Several studies have used SPM1D to analyse equine

locomotion (Hobbs *et al.*, 2018; Hobbs, Robinson and Clayton, 2018) and now the results of Chapter 6 show that SPM1D can be used to test hypotheses relating to the rider.

Lack of significant differences between competition levels for the coordination variability of any simulator-segment pair suggests that participant factors other than competition level influence coordination variability when the task and environment are standardised using a riding simulator. The coordination variability observed during riding on the riding simulator represents the baseline coordination variability of the rider and illustrates the rider's strategy to achieve an independent seat. As such, the low coordination variability of the simulator-pelvis coupling, but significantly higher coordination variability of the simulator-head and simulator-foot illustrates how the rider can uncouple their head and foot from the vertical displacement of the riding simulator to achieve independence of the extremities. Significant differences in the riders' simulator-trunk, but not simulator-pelvis variability from medium to extended trot suggest that the rider stabilises their pelvis by stabilising the coordination between the simulator and their trunk pitch. As discussed by Terada, Clayton and Kato (2006), the rider's trunk and arm movements act to stabilise the rider's wrist position, which is important to maintain a stable contact on the reins. As the riding simulator does not provide the same feedback with its head and neck, it is unclear whether the increased coupling between simulator-trunk was a result of inertial effects of the increased anterior-posterior displacement or whether riders stabilised their trunk to stabilise their hand position on the reins.

The implications of this study are: (1) as the anterior-posterior displacement increases, the riders' trunk becomes more integral to maintaining balance and stability of the pelvis; (2) the extent of the proprioceptive feedback of the horse's head/neck on their coordination strategy is not known, therefore live horse studies are needed; (3) the coordination variability to a riding simulator provides a baseline assessment of the coordination variability; and (4) A continuous measure of the coordination variability can detect changes in the level of the coordination variability with relation to the movement cycle.

9.2.4 Chapter 7

The features of the continuous relative phase (CRP) between the vertical displacement of the riding simulator and the pitch of the rider's pelvis in medium and extended trot were analysed with principal component analysis (PCA). No previous study has quantified the features of the coordination between the rider's pelvis and a horse or simulator. Using PCA the features of the CRP for 10 cycles (with some exceptions due to gaps) of 40 riders' trials in medium and extended trot were quantified and described. Principal component (PC) scores that explained at least 90% of the variance were retained.

Overall, the rider's pelvis pitch was in-phase with the vertical displacement of the riding simulator. Three PC scores were required to describe at least 90% of the variance in both medium and extended trot. These features were qualitatively described as per Brandon *et al.* (2013). The first PC described 75% and 69% of the variance in medium and extended trot, respectively. This PC score described whether the rider's pelvis pitch led or lagged the simulator. The mean CRP trajectories (Figure 7.3) showed that typically riders' pelvis pitch lagged the simulator on its ascent (positive CRP values) and moved ahead of the simulator (negative CRP values) on its descent. High and low values of PC1 in medium and extended trot indicated that some riders maintained a lead or lag throughout the cycle. As the rider was in-phase with the simulator, the lead or lag described whether the pelvis was moving faster or slower in pitch than the vertical displacement of the simulator. The other two PC scores related to different shapes of the CRP trajectory and shifts in the timing of the change between simulator lead or lag.

The mixed linear models confirmed that the PC scores were not significantly related to competition level. The implication of this is comparable to the preceding chapters: competition level may not significantly influence the coordination between a riding simulator and rider when the riders are at the national level. However, the model suggested that other factors influenced the variance within the rider's trial and between riders that were not captured by the model. The conclusions of this study stated that competitive riders display the principle of motor equivalence: they can achieve the same goal of harmony with potentially vastly different participant characteristics, such as anthropometry,

strength and flexibility. It was unclear from this study whether the features of the CRP would be discernible by judges or coaches. Therefore, while riders should be encouraged to find individual solutions to accomplish harmony, their implication on the impression of harmony perceived by judges needs further research. In addition, the adaptation of the rider to the unique biomechanics of the horse should be considered in future live horse studies.

The implications of this study are: (1) riders can achieve harmony in myriad ways that can be quantified by the CRP; (2) factors that influence harmony are yet unknown but do not relate to competition level in competitive dressage riders; (3) further work is needed to identify whether any of these features result in better scores from dressage judges.

9.2.5 Chapter 8

Chapter 8 forms the start of a potentially significant line of inquiry for the rider: the use of unsupervised machine learning tools for pattern recognition of rider kinematic data. The previous chapters have established that grouping riders by their competition level may conceal their functionally relevant information regarding their movement patterns. This study aimed to explore the strategies of riders' trunk and pelvis pitch and group 40 competitive dressage riders into functional groups in medium trot. Self-organising maps (SOM) and *k*-means clustering were used to cluster riders into functional groups, defined as per Hoerzer *et al.* (2015) as clusters that contained most of the rider's trials. The SOM was trained on a matrix containing 389 cycles from 40 riders' trunk and pelvis pitch in medium trot. The results of the SOM were clustered by *k*-means clustering; three clusters achieved the best quality score (Davies-Bouldin Index). A mean of 87% of the riders' cycles from their trial was assigned to the same cluster, therefore these were considered as the functional groups. Visual inspection of the functional groups indicated that the cycles were clustered based on the relative timing of the posterior pelvis and trunk pitch. Seventy-one per cent of the cycles were assigned to the functional group where trunk and pelvis peaks coincided. Twenty per cent of the cycles were assigned to a functional group where the peak posterior trunk pitch occurred after the pelvis peak, and 10% were assigned to a group where trunk and pelvis pitch occurred oppositely.

The plots of the functional groups indicated that this grouping was not sensitive to the areas of the time series apart from the peaks. Therefore, the cycles were segmented into eight clusters, the clustering solution with the next lowest Davies-Bouldin Index. Inspection of these clusters showed differences in the ranges of motion and latency between trunk and pelvis posterior pitch. This study attests to the diverse strategies that riders employ during sitting trot on a riding simulator. The implications of this study are that: (1) riders most frequently pitch their trunk and pelvis coincidentally during simulated sitting trot, however, some riders may dissociate trunk and pelvis pitch; (2) pattern recognition approaches can be used to develop novel groupings of riders that may not be detectable if riders are grouped conventionally; (3) further work is needed to expand the current findings beyond trunk and pelvis.

9.3 Limitations

There are three main limitations inherent to the studies contained within this thesis. First, this thesis did not test the validity of the results obtained on the riding simulator to the live horse setting. It is acknowledged that there is a potential limitation in the ecological validity of the results obtained during testing on a riding simulator. Several previous studies have used riding simulators to answer targeted research questions (Baillet *et al.*, 2017; Olivier *et al.*, 2017). The design of the studies contained in this thesis pertained to specific research questions regarding between-participant variation and the riding simulator made it possible to standardise the conditions across all participants. Therefore, the riding simulator is a useful tool to allow standardisation across participants, but the potentially low ecological validity to the live horse restricts the ability to compare these results with live riding, but could, nonetheless, form a baseline for further investigation.

The trunk-pelvis movement strategies reported in Chapter 8 and the simulator-rider coordination strategies reported in Chapter 6 and 7 represent the rider's coordination on the simulator. It is unknown whether the riders would produce similar strategies on the live horse, or how riders adapt

their own strategy to suit their horse. It is also questioned whether the strategies carry over from the live horse to the simulator. Certainly, further research is needed to answer these pertinent questions.

Another potential limitation relates to the saddle. The same 17.5-inch dressage saddle (Devoucoux, Biarritz, France) was used for all participants. Riders were able to adjust the stirrups to their preference; however, the other characteristics of the saddle were not adjustable. No study has directly assessed the influence of different saddle seat configurations on the rider's kinematics. However, the type of saddle can influence rider back pain (Quinn and Bird, 1996), and the unfamiliar saddle may have influenced the rider's movement during the trials. In addition to the seat itself, the movement of the saddle relative to the horse may influence the rider's kinematics (Mackechnie-Guire *et al.*, 2018). To minimise this limitation, the saddle was secured on the riding simulator with a rubberised non-slip pad and girth. It was also adjusted between riders to ensure it was centrally placed for each trial.

Finally, the participants who volunteered for the data collections were competitive female dressage riders without any condition that prevented them from competitive riding. The application of these results to male, non-competitive riders, or pathological individuals should be approached with caution.

10. Conclusion

In conclusion, the results of this programme of research have advanced the knowledge and understanding of the kinematics of competitive dressage riders within the context of the traditional performance indicators, including harmony. This thesis aimed to use continuous methods to analyse simulator-rider coordination and the influence of competition level. These aims were met by analysing angular displacements in pitch of multiple rider segments in a population of competitive dressage riders at the nationally and internationally affiliated levels of competition. The methods were developed to balance practical considerations and to meet the aims and objectives of the thesis.

Throughout the thesis, no measured variable was significantly related to competition level. Therefore, it is more likely that other factors have a greater influence on the rider's kinematics and the characteristics of simulator-rider coordination than the highest competition level that the rider could attain. Comparison of riders' pelvic posture at halt and in simulated medium walk, trot, and both leads of canter suggested that riders should be analysed dynamically as the static posture did not significantly correlate with any gait. Dynamic analyses of the rider provided new insight and approaches to assess how riders coordinate with the horse. Coordination variability of the rider's head, trunk, pelvis and left foot in medium and extended trot suggest that riders can achieve an independent seat at lower amplitudes of the simulator's anterior-posterior displacement, however, the trunk aids in maintaining balance as anterior-posterior displacement increases. Riders achieve coordination between the simulator and their pelvis with features that are influenced by individual rider characteristics and the movement of the simulator. Finally, riders were grouped by their trunk and pelvis kinematics in medium trot using self-organising maps. These results show that researchers should expand beyond competition level as a grouping factor for equestrian rider analyses as within groups of competitive riders of similar levels there may be drastic differences in technique. Analysing continuous data reveals patterns in kinematics and coordination that would be overlooked or underestimated with discrete analyses. These approaches have significant potential to understand the

relationship between horse and rider and further increase rider performance to ultimately benefit horse welfare.

References

- Abt, G. *et al.* (2020) 'Power, precision, and sample size estimation in sport and exercise science research', *Journal of Sports Sciences*. Routledge, pp. 1933–1935. doi: 10.1080/02640414.2020.1776002.
- Ahmad, N. *et al.* (2013) 'Reviews on various inertial measurement unit (IMU) sensor applications', *International Journal of Signal Processing Systems*, pp. 256–262. doi: 10.12720/ijsp.1.2.256-262.
- Al-Eisa, E. *et al.* (2006) 'Effects of pelvic asymmetry and low back pain on trunk kinematics during sitting: A comparison with standing', *Spine*, 31(5), pp. E135–E143.
- Alexander, J. *et al.* (2015) 'Postural characteristics of female dressage riders using 3D motion analysis and the effects of an athletic taping technique: A randomised control trial', *Physical Therapy in Sport*, 16(2), pp. 154–161. doi: 10.1016/j.ptsp.2014.09.005.
- Aljohani, M. and Kipp, K. (2020) 'Use of self-organizing maps to study sex- and speed-dependent changes in running biomechanics', *Human Movement Science*, 72, pp. 1–10. doi: 10.1016/j.humov.2020.102649.
- Arutyunyan, G., Gurfinkwl, V. and Mirskii, M. (1968) 'Investigation of aiming at a target', *Biophysics*, 14, pp. 1162–7.
- Austin, G. P. (2001) 'Motor control of human gait: A dynamic systems perspective', *Orthopaedic Physical Therapy Clinics of North America*, pp. 17–34.
- Back, W. *et al.* (1995) 'Kinematic response to a 70 day training period in trotting Dutch Warmbloods', *Equine Veterinary Journal*, 27(18 S), pp. 127–131. doi: 10.1111/j.2042-3306.1995.tb04904.x.
- Baillet, H. *et al.* (2017) 'Human energy expenditure and postural coordination on the mechanical horse', *Journal of Motor Behavior*, 49(4), pp. 441–457. doi: 10.1080/00222895.2016.1241743.
- Barrey, E. *et al.* (2002) 'Early evaluation of dressage ability in different breeds', *Equine Veterinary Journal Supplement*, 34, pp. 319–324. doi: 10.1111/j.2042-3306.2002.tb05440.x.
- Batschelet, E. (1981) *Circular statistics in biology*. London: Academic Press.
- Bauer, H. U. and Schöllhorn, W. (1997) 'Self-organizing maps for the analysis of complex movement patterns', *Neural Processing Letters*, 5(3), pp. 193–199. doi: 10.1023/A:1009646811510.
- Beale, L. *et al.* (2015) 'Oxygen cost of recreational horse-riding in females', *Journal of Physical Activity and Health*, 12(6), pp. 808–813. doi: 10.1123/jpah.2012-0428.
- Berens, P. (2009) *CircStat: A MATLAB toolbox for circular statistics*, *MATLAB Central File Exchange*. Available at: <https://www.mathworks.com/matlabcentral/fileexchange/10676-circular-statistics-toolbox-directional-statistics>.
- Bernstein, N. A. (1967) *The Coordination and Regulation of Movements*. Oxford: Pergamon Press Ltd.
- Biau, S. *et al.* (2013) 'Preliminary study of rider back biomechanics', *Computer Methods in Biomechanics and Biomedical Engineering*, 16(SUPPL 1), pp. 48–49. doi: 10.1080/10255842.2013.815845.
- Billat, V. L. *et al.* (2001) 'Effect of free versus constant pace on performance and oxygen kinetics in running', *Medicine and Science in Sports and Exercise*, 33(12), pp. 2082–2088. doi: 10.1097/00005768-200112000-00017.

- Bird, S. (1996) 'Influence of saddle type upon the incidence of lower back pain in equestrian riders', *British Journal of Sports Medicine*, 30(2), pp. 140–144.
- Blokhuis, M. Z. *et al.* (2008) 'Assessing the rider's seat and horse's behavior: Difficulties and perspectives', in *Journal of Applied Animal Welfare Science*, pp. 191–203. doi: 10.1080/10888700802100876.
- Boashash, B. (2016) 'Time-frequency and instantaneous frequency concepts', in *Time-Frequency Signal Analysis and Processing: A Comprehensive Reference*. Elsevier Inc., pp. 31–63. doi: 10.1016/B978-0-12-398499-9.00001-7.
- Bondi, A. *et al.* (2020) 'Evaluating the suitability of an English saddle for a horse and rider combination', *Equine Veterinary Education*, 32(S10), pp. 162–172. doi: 10.1111/eve.13158.
- Bosch, S. *et al.* (2018) 'Equimoves: A wireless networked inertial measurement system for objective examination of horse gait', *Sensors (Switzerland)*, 18(3), p. 850. doi: 10.3390/s18030850.
- Boulay, C. *et al.* (2006) 'Sagittal alignment of spine and pelvis regulated by pelvic incidence: Standard values and prediction of lordosis', *European Spine Journal*, pp. 415–422. doi: 10.1007/s00586-005-0984-5.
- Brandon, S. C. E. *et al.* (2013) 'Interpreting principal components in biomechanics: Representative extremes and single component reconstruction', *Journal of Electromyography and Kinesiology*, 23(6), pp. 1304–1310. doi: 10.1016/j.jelekin.2013.09.010.
- British Dressage (2021a) *Circles & Serpentine, All About Dressage/Paces and Movements/Circles & Serpentine*. Available at: <https://www.britishdressage.co.uk/our-sport/all-about-dressage/paces-and-movements/circles-serpentine/>.
- British Dressage (2021b) *Competition Results, Competition Results*. Available at: https://britishdressage.online/search_results.
- British Dressage (2021c) *Dressage Defined, Dressage defined | British Dressage*. Available at: <https://www.britishdressage.co.uk/our-sport/all-about-dressage/dressage-defined/>.
- British Dressage (2021d) 'Section 1: British Dressage Rules', in *Members' Handbook 2021*. Meriden, West Midlands: British Dressage, pp. 62–157.
- British Dressage (2021e) 'Section 4: Judges', in *Members' Handbook 2021*. Meriden, West Midlands: British Dressage, pp. 210–219.
- British Horse Society (2011) *BHS Complete Manual of Equitation: The Training of Horse and Rider*. Shrewsbury, Shropshire: Quiller.
- Broderick, M. P. and Newell, K. M. (1999) 'Coordination patterns in ball bouncing as a function of skill', *Journal of Motor Behavior*, 31(2), pp. 165–188. doi: 10.1080/00222899909600986.
- Buganè, F. *et al.* (2014) 'Estimation of pelvis kinematics in level walking based on a single inertial sensor positioned close to the sacrum: Validation on healthy subjects with stereophotogrammetric system', *BioMedical Engineering Online*, 13(1). doi: 10.1186/1475-925X-13-146.
- Burgess-Limerick, R., Abernethy, B. and Neal, R. J. (1993) 'Relative phase quantifies interjoint coordination', *Journal of Biomechanics*, 26(1), pp. 91–94. doi: 10.1016/0021-9290(93)90617-N.
- Busquets, A. *et al.* (2013) 'Coordination analysis reveals differences in motor strategies for the high bar longswing among novice adults', *PLoS ONE*, 8(6). doi: 10.1371/journal.pone.0067491.
- Button, C. *et al.* (2000) 'Mechanical perturbation of the wrist during one-handed catching', *Acta*

Psychologica, 105(1), pp. 9–30. doi: 10.1016/S0001-6918(00)00044-5.

Button, C. *et al.* (2003) 'Examining movement variability in the basketball free-throw action at different skill levels', *Research Quarterly for Exercise and Sport*, 74(3), pp. 257–269. doi: 10.1080/02701367.2003.10609090.

Button, C., Wheat, J. S. and Lamb, P. F. (2014) 'Why coordination dynamics is relevant for studying sport performance', in Davids, K. (ed.) *Complex systems in sport*. Routledge, pp. 44–61.

Bye, T. L. and Chadwick, G. (2018) 'Physical fitness habits and perceptions of equestrian riders', *Comparative Exercise Physiology*, 14(3), pp. 183–188. doi: 10.3920/CEP180012.

Byström, A. *et al.* (2009) 'Basic kinematics of the saddle and rider in high-level dressage horses trotting on a treadmill', *Equine Veterinary Journal*, 41(3), pp. 280–284. doi: 10.2746/042516409X394454.

Byström, A. *et al.* (2010) 'Kinematics of saddle and rider in high-level dressage horses performing collected walk on a treadmill', *Equine Veterinary Journal*, 42(4), pp. 340–345. doi: 10.1111/j.2042-3306.2010.00063.x.

Byström, A. *et al.* (2015) 'Differences in rider movement pattern between different degrees of collection at the trot in high-level dressage horses ridden on a treadmill', *Human Movement Science*, 41, pp. 1–8.

Camomilla, V. *et al.* (2018) 'Trends Supporting the In-Field Use of Wearable Inertial Sensors for Sport Performance Evaluation: A Systematic Review', *Sensors*, 18(3), p. 873. doi: 10.3390/s18030873.

Camomilla, V. and Bonci, T. (2020) 'A joint kinematics driven model of the pelvic soft tissue artefact', *Journal of Biomechanics*, 111. doi: 10.1016/j.jbiomech.2020.109998.

Camomilla, V., Bonci, T. and Cappozzo, A. (2017) 'Soft tissue displacement over pelvic anatomical landmarks during 3-D hip movements', *Journal of Biomechanics*, 62, pp. 14–20. doi: 10.1016/j.jbiomech.2017.01.013.

Cappozzo, A. *et al.* (2005) 'Human movement analysis using stereophotogrammetry. Part 1: Theoretical background', *Gait and Posture*. Elsevier Ireland Ltd, pp. 186–196. doi: 10.1016/j.gaitpost.2004.01.010.

Caron, J. P. (2005) 'Intra-articular injections for joint disease in horses', *Veterinary Clinics of North America - Equine Practice*. Elsevier, pp. 559–573. doi: 10.1016/j.cveq.2005.07.003.

Cazzola, D., Pavei, G. and Preatoni, E. (2016) 'Can coordination variability identify performance factors and skill level in competitive sport? The case of race walking', *Journal of Sport and Health Science*, 5(1), pp. 35–43. doi: 10.1016/j.jshs.2015.11.005.

Cereatti, A. *et al.* (2017) 'Standardization proposal of soft tissue artefact description for data sharing in human motion measurements', *Journal of Biomechanics*, 62, pp. 5–13. doi: 10.1016/j.jbiomech.2017.02.004.

Cha, H. G., Lee, B. J. and Lee, W. H. (2016) 'The effects of horse riding simulation exercise with blindfolding on healthy subjects' balance and gait.', *Journal of physical therapy science*, 28(11), pp. 3165–3167. doi: 10.1589/jpts.28.3165.

Chang, R., Van Emmerik, R. and Hamill, J. (2008) 'Quantifying rearfoot-forefoot coordination in human walking', *Journal of Biomechanics*, 41(14), pp. 3101–3105. doi: 10.1016/j.jbiomech.2008.07.024.

Chen, C.-L. *et al.* (2014) *Effects of the type and direction of support surface perturbation on postural responses*, *Journal of NeuroEngineering and Rehabilitation*. doi: 10.1186/1743-0003-11-50.

Chèze, L. (2014) *Kinematic Analysis of Human Movement, Kinematic Analysis of Human Movement*. doi: 10.1002/9781119058144.

Chiari, L. *et al.* (2005) 'Human movement analysis using stereophotogrammetry. Part 2: Instrumental errors', *Gait and Posture*. Elsevier Ireland Ltd, pp. 197–211. doi: 10.1016/j.gaitpost.2004.04.004.

Clayton, H. M. (1994) 'Comparison of the stride kinematics of the collected, working, medium and extended trot in horses', *Equine Veterinary Journal*, 26(3), pp. 230–234. doi: 10.1111/j.2042-3306.1994.tb04375.x.

Clayton, H. M. (1995) 'Comparison of the stride kinematics of the collected, medium, and extended walks in horses.', *American Journal of Veterinary Research*, 56(7), pp. 849–852.

Clayton, H. M. *et al.* (2018) 'Comparison of rider stability in a flapless saddle versus a conventional saddle', *PLoS ONE*, 13(6). doi: 10.1371/journal.pone.0196960.

Clayton, Hilary M and Hobbs, S. J. (2017) 'An exploration of strategies used by dressage horses to control moments around the center of mass when performing passage', *PeerJ*, 2017(9), p. e3866. doi: 10.7717/peerj.3866.

Clayton, Hilary M. and Hobbs, S. J. (2017) 'The role of biomechanical analysis of horse and rider in equitation science', *Applied Animal Behaviour Science*, 190, pp. 123–132. doi: 10.1016/j.applanim.2017.02.011.

Clayton, H. M. and Hobbs, S. J. (2019a) 'A review of biomechanical gait classification with reference to collected trot, passage and piaffe in dressage horses', *Animals*. MDPI AG. doi: 10.3390/ani9100763.

Clayton, H. M. and Hobbs, S. J. (2019b) 'Ground Reaction Forces: The Sine Qua Non of Legged Locomotion', *Journal of Equine Veterinary Science*. W.B. Saunders, pp. 25–35. doi: 10.1016/j.jevs.2019.02.022.

Clayton, H. M., Schamhardt, H. C. and Hobbs, S. J. (2017) 'Ground reaction forces of elite dressage horses in collected trot and passage', *Veterinary Journal*, 221(January), pp. 30–33. doi: 10.1016/j.tvjl.2017.01.016.

Clayton, H. M., Smith, B. and Egenvall, A. (2017) 'Rein tension in novice riders when riding a horse simulator', *Comparative Exercise Physiology*, 13(4), pp. 237–242. doi: 10.3920/CEP170010.

de Cocq, P. *et al.* (2013) 'Modelling biomechanical requirements of a rider for different horse-riding techniques', *The Journal of experimental biology*, 216(10), pp. 1850–1861. doi: 10.1242/jeb.070938.

Comerford, M. and Mottram, S. (2012) *Kinetic Control*. Edited by M. Comerford and S. Mottram. Sydney: Churchill Livingstone.

Contino, E. K. (2018) 'Management and Rehabilitation of Joint Disease in Sport Horses', *Veterinary Clinics of North America - Equine Practice*. W.B. Saunders, pp. 345–358. doi: 10.1016/j.cveq.2018.04.007.

Cresswell, J. W. and Cresswell, D. J. (2018) *Research design : qualitative, quantitative & mixed methods approaches*. 5th edn. Los Angeles, California: SAGE Publications.

Della Croce, U. *et al.* (2005) 'Human movement analysis using stereophotogrammetry Part 4: Assessment of anatomical landmark misplacement and its effects on joint kinematics', *Gait and Posture*. Elsevier Ireland Ltd, pp. 226–237. doi: 10.1016/j.gaitpost.2004.05.003.

Della Croce, U., Cappozzo, A. and Kerrigan, D. C. (1999) 'Pelvis and lower limb anatomical landmark calibration precision and its propagation to bone geometry and joint angles', *Medical and Biological Engineering and Computing*, 37(2), pp. 155–161. doi: 10.1007/BF02513282.

- Cushion, E. J. *et al.* (2019) 'Principal component analysis reveals the proximal to distal pattern in vertical jumping is governed by two functional degrees of freedom', *Frontiers in Bioengineering and Biotechnology*, 7(AUG), p. 193. doi: 10.3389/fbioe.2019.00193.
- Daffertshofer, A. *et al.* (2004) 'PCA in studying coordination and variability: A tutorial', *Clinical Biomechanics*, 19(4), pp. 415–428. doi: 10.1016/j.clinbiomech.2004.01.005.
- Davids, K. *et al.* (2003) 'Movement systems as dynamical systems', *Sports Medicine*, 33(4), pp. 245–260. doi: 10.2165/00007256-200333040-00001.
- Davids, K., Button, C. and Bennett, S. (2008) *Dynamics of Skill Acquisition*. Champaign, IL: Human Kinetics. doi: 10.1016/b0-12-370870-2/00169-4.
- Davies, D. L. and Bouldin, D. W. (1979) 'A cluster separation measure', *IEEE Transactions on Pattern Analysis and Machine Intelligence*, PAMI-1(2), pp. 224–227. doi: 10.1109/TPAMI.1979.4766909.
- Deckers, I. *et al.* (2020) 'Assessing the sport-specific and functional characteristics of back pain in horse riders', *Comparative Exercise Physiology*, pp. 1–10. doi: 10.3920/CEP190075.
- Deckers, I. *et al.* (2021) 'Assessing the Sport-Specific and Functional Characteristics of Back Pain in Horse Riders', *Comparative Exercise Physiology*, 17(1), pp. 7–15. doi: 10.3920/CEP190075.
- Deluzio, K. J. *et al.* (2014) 'Analysis of biomechanical waveform data', in Robertson, D. G. E. *et al.* (eds) *Research Methods in Biomechanics*. 2nd edn. Champaign, IL: Human Kinetics, pp. 317–338.
- Deluzio, K. J. and Astephen, J. L. (2007) 'Biomechanical features of gait waveform data associated with knee osteoarthritis. An application of principal component analysis', *Gait and Posture*, 25(1), pp. 86–93. doi: 10.1016/j.gaitpost.2006.01.007.
- Deuel, N. R. and Park, J.-J. (1990) 'The gait patterns of Olympic dressage horses', *International Journal of Sport Biomechanics*, 6(2), pp. 198–226. doi: 10.1123/ijbs.6.2.198.
- Dierks, T. A. and Davis, I. (2007) 'Discrete and continuous joint coupling relationships in uninjured recreational runners', *Clinical Biomechanics*, 22(5), pp. 581–591. doi: 10.1016/j.clinbiomech.2007.01.012.
- Douglas, J.-L., Price, M. and Peters, D. M. (2012) 'A systematic review of physical fitness, physiological demands and biomechanical performance in equestrian athletes', *Comparative Exercise Physiology*, 8(1), pp. 53–62. doi: 10.3920/CEP12003.
- Dyson, S. (2017) 'Equine performance and equitation science: Clinical issues', *Applied Animal Behaviour Science*, 190, pp. 5–17. doi: 10.1016/j.applanim.2017.03.001.
- Eckardt, F., Münz, A. and Witte, K. (2014) 'Application of a full body inertial measurement system in dressage riding', *Journal of Equine Veterinary Science*, 34(11–12), pp. 1294–1299. doi: 10.1016/j.jevs.2014.09.009.
- Eckardt, F. and Witte, K. (2016) 'Kinematic analysis of the rider according to different skill levels in sitting trot and canter', *Journal of Equine Veterinary Science*, 39, pp. 51–57. doi: 10.1016/J.JEVS.2015.07.022.
- Eckardt, F. and Witte, K. (2017) 'Horse–rider interaction: A new method based on inertial measurement units', *Journal of Equine Veterinary Science*, 55, pp. 1–8. doi: 10.1016/j.jevs.2017.02.016.
- Edelman, G. M. and Gally, J. A. (2001) 'Degeneracy and complexity in biological systems', *Proceedings of the National Academy of Sciences of the United States of America*, 98(24), pp. 13763–13768. doi: 10.1073/pnas.231499798.

- Egenvall, A. *et al.* (2015) 'Stride-related rein tension patterns in walk and trot in the ridden horse', *Acta Veterinaria Scandinavica*, 57, p. 89. doi: 10.1186/s13028-015-0182-3.
- Eisersiö, M. *et al.* (2013) 'Movements of the horse's mouth in relation to horse-rider kinematic variables', *Veterinary Journal*, 198(SUPPL1), pp. e33–e38. doi: 10.1016/j.tvjl.2013.09.030.
- Elmeua González, M. and Šarabon, N. (2020) 'Muscle modes of the equestrian rider at walk, rising trot and canter', *PloS one*, 15(8), p. e0237727. doi: 10.1371/journal.pone.0237727.
- Van Emmerik, R. E. A., Miller, R. and Hamill, J. (2014) 'Dynamical systems analysis of coordination', in Robertson, D. G. E. *et al.* (eds) *Research Methods in Biomechanics*. 2nd edn. Champaign, IL: Human Kinetics, pp. 291–315.
- Van Emmerik, R. E. A. and Wagenaar, R. C. (1996) 'Effects of walking velocity on relative phase dynamics in the trunk in human walking', *Journal of Biomechanics*, 29(9), pp. 1175–1184. doi: 10.1016/0021-9290(95)00128-X.
- Engeli, E., Haussler, K. K. and Erb, H. N. (2004) 'Development and validation of a periarticular injection technique of the sacroiliac joint in horses', *Equine Veterinary Journal*, 36(4), pp. 324–330. doi: 10.2746/0425164044890599.
- Engell, M. T. *et al.* (2015) 'Does foot pronation in unmounted horseback riders affect pelvic movement during walking?', *Comparative Exercise Physiology*, 11(4), pp. 231–237. doi: 10.3920/CEP150019.
- Engell, M. T. *et al.* (2016) 'Postural changes and their effects in elite riders when actively influencing the horse versus sitting passively at trot', *Comparative Exercise Physiology*, 12(1), pp. 27–33. doi: 10.3920/CEP150035.
- Engell, M. T. *et al.* (2018) 'Head, trunk and pelvic kinematics in the frontal plane in un-mounted horseback riders rocking a balance chair from side-to-side', *Comparative Exercise Physiology*, 14(4), pp. 249–259. doi: 10.3920/CEP170036.
- Eslami, M. *et al.* (2017) 'Determination of functional groups in different levels in running gait; Lower limb mechanical energy analysis', in *35th Conference of the International Society of Biomechanics in Sports, Cologne, Germany*, pp. 378–379.
- Fédération Internationale Équestre (2017) 'Guidelines for the Marking of Fundamental Mistakes in Dressage Movements (acc. to the FEI Dressage Handbook and following proposals of the 5 * Judges' Seminar 2017)', pp. 1–10.
- Fédération Internationale Équestre (2021a) *Dressage /FEI.org, Dressage & Para Dressage*. Available at: www.fei.org/dressage.
- Fédération Internationale Équestre (2021b) *Dressage Tests, Dressage Tests - Senior*. Available at: <https://inside.fei.org/fei/your-role/organisers/dressage/tests>.
- Fédération Internationale Équestre (2020) *Dressage Rules*. Lausanne: Fédération Internationale Équestre.
- Forner-Cordero, A. *et al.* (2005) 'Principal component analysis of complex multijoint coordinative movements', *Biological Cybernetics*, 93(1), pp. 63–78. doi: 10.1007/s00422-005-0582-y.
- Friston, K. J. (2003) 'Statistical Parametric Mapping', in *Neuroscience Databases*. London: Springer US, pp. 237–250. doi: 10.1007/978-1-4615-1079-6_16.
- Gandy, E. A. *et al.* (2014) 'A preliminary investigation of the use of inertial sensing technology for the measurement of hip rotation asymmetry in horse riders', *Sports Technology*, 7(1–2), pp. 79–88. doi: 10.1080/19346182.2014.905949.

- Gandy, E. A. *et al.* (2018) 'Investigation of the use of inertial sensing equipment for the measurement of hip flexion and pelvic rotation in horse riders', *Comparative Exercise Physiology*, 14(2), pp. 99–110. doi: 10.3920/CEP170023.
- Gates, J. K. and Lin, C. Y. (2020) 'Head and Spinal Injuries in Equestrian Sports', *Current Sports Medicine Reports*, 19(1), pp. 17–23. doi: 10.1249/JSR.0000000000000674.
- German National Equestrian Federation (2005) *The principles of riding*. Shrewesbury: Kenilworth Press.
- German National Equestrian Federation (2006) *Advanced Techniques of Dressage*. Shrewesbury, Shropshire: Quiller.
- Girodroux, M., Dyson, S. and Murray, R. (2009) 'Osteoarthritis of the thoracolumbar synovial intervertebral articulations: Clinical and radiographic features in 77 horses with poor performance and back pain', *Equine Veterinary Journal*, 41(2), pp. 130–138. doi: 10.2746/042516408X345099.
- Glazier, P. S. and Davids, K. (2009) 'Constraints on the complete optimization of human motion', *Sports Medicine*, 39(1), pp. 15–28. doi: 10.2165/00007256-200939010-00002.
- Glazier, P. S. and Mehdizadeh, S. (2019) 'In search of sports biomechanics' holy grail: Can athlete-specific optimum sports techniques be identified?', *Journal of Biomechanics*, 94, pp. 1–4. doi: 10.1016/j.jbiomech.2019.07.044.
- Goldsztein, G. H. (2016) 'Reactions of standing bipeds on moving platforms to keep their balance may increase the amplitude of oscillations of platforms satisfying Hooke's law', *PLoS ONE*, 11(6), p. e0157675. doi: 10.1371/journal.pone.0157675.
- Greve, L. and Dyson, S. (2013) 'The horse–saddle–rider interaction', *The Veterinary Journal*, 195(3), pp. 275–281. doi: 10.1016/j.tvjl.2012.10.020.
- Guire, Russell *et al.* (2017) 'Investigation Looking at the Repeatability of 20 Society of Master Saddlers Qualified Saddle Fitters' Observations During Static Saddle Fit', *Journal of Equine Veterinary Science*, 56, pp. 1–5. doi: 10.1016/j.jevs.2017.04.001.
- Guire, R *et al.* (2017) 'Riders' perception of symmetrical pressure on their ischial tuberosities and rein contact tension whilst sitting on a static object', *Comparative Exercise Physiology*, 13(1), pp. 7–12. doi: 10.3920/CEP160026.
- Gunst, S. *et al.* (2019) 'Influence of functional rider and horse asymmetries on saddle force distribution during stance and in sitting trot', *Journal of Equine Veterinary Science*, 78, pp. 20–28. doi: 10.1016/j.jevs.2019.03.215.
- Hamill, J. *et al.* (1999) 'A dynamical systems approach to lower extremity running injuries', *Clinical Biomechanics*, 14(5), pp. 297–308. doi: 10.1016/S0268-0033(98)90092-4.
- Hamill, J. *et al.* (2006) 'Clinical relevance of variability in coordination', in Davids, K., Bennett, S., and Newell, K. M. (eds) *Human Movement Variability*. Champaign, IL: Human Kinetics, pp. 153–165.
- Hamill, J., Bates, B. T. and Holt, K. G. (1992) 'Timing of lower extremity joint actions during treadmill running', *Medicine and Science in Sports and Exercise*, 24(7), pp. 807–813. doi: 10.1249/00005768-199207000-00011.
- Hamill, J., Haddad, J. M. and McDermott, W. J. (2000) 'Issues in quantifying variability from a dynamical systems perspective', in *Journal of Applied Biomechanics*, pp. 407–418. doi: 10.1123/jab.16.4.407.
- Hamill, J., Palmer, C. and Van Emmerik, R. E. A. (2012) 'Coordinative variability and overuse injury', *Sports Medicine, Arthroscopy, Rehabilitation, Therapy and Technology*. BioMed Central, p. 45. doi:

10.1186/1758-2555-4-45.

Hampson, A. and Randle, H. (2015) 'The influence of an 8-week rider core fitness program on the equine back at sitting trot', *International Journal of Performance Analysis in Sport*, 15(3), pp. 1145–1159. doi: 10.1080/24748668.2015.11868858.

Harman, J. (1999) 'Tack and saddle fit.', *The Veterinary clinics of North America. Equine practice*, 15(1), pp. 247–261. doi: 10.1016/S0749-0739(17)30175-X.

Hayden, A. M. *et al.* (2018) 'The effect of pelvic motion on spinopelvic parameters', *Spine Journal*, 18(1), pp. 173–178. doi: 10.1016/j.spinee.2017.08.234.

Hobbs, S. J. *et al.* (2014) 'Posture, flexibility and grip strength in horse riders', *Journal of Human Kinetics*, 42(1), pp. 113–125. doi: 10.2478/hukin-2014-0066.

Hobbs, S. J. *et al.* (2018) 'Sagittal plane fore hoof unevenness is associated with fore and hindlimb asymmetrical force vectors in the sagittal and frontal planes', *PLOS ONE*. Edited by J. J. Loor, 13(8), p. e0203134. doi: 10.1371/journal.pone.0203134.

Hobbs, S. J., Robinson, M. A. and Clayton, H. M. (2018) 'A simple method of equine limb force vector analysis and its potential applications', *PeerJ*, 2018(2), p. e4399. doi: 10.7717/peerj.4399.

Hoerzer, S. *et al.* (2015) 'Defining functional groups based on running kinematics using Self-Organizing Maps and Support Vector Machines', *Journal of Biomechanics*, 48(10), pp. 2072–2079. doi: 10.1016/j.jbiomech.2015.03.017.

Holmstrom, M. *et al.* (1994) 'Biokinematic differences between riding horses judged as good and poor at the trot', *Equine Veterinary Journal*, 26(17 S), pp. 51–56. doi: 10.1111/j.2042-3306.1994.tb04874.x.

Holmström, M. and Drevemo, S. (1997) 'Effects of trot quality and collection on the angular velocity in the hindlimbs of riding horses.', *Equine veterinary journal. Supplement*, (23), pp. 62–65.

Holmstrom, M., Fredericson, I. and Drevemo, S. (1994) 'Biokinematic differences between riding horses judged as good and poor at the trot', *Equine Veterinary Journal*, 26(S17), pp. 51–56. doi: 10.1111/j.2042-3306.1994.tb04874.x.

Holmström, M., Fredericson, I. and Drevemo, S. (1995) 'Biokinematic effects of collection on the trotting gaits in the elite dressage horse', *Equine Veterinary Journal*, 27(4), pp. 281–287. doi: 10.1111/j.2042-3306.1995.tb03078.x.

Ipek (2020) 'Normalitytest'.

Jones, K. S. (2003) 'What Is an Affordance?', *Ecological Psychology*. Lawrence Erlbaum Associates Inc., pp. 107–114. doi: 10.1207/S15326969ECO1502_1.

Kang, O. D. *et al.* (2010) 'Comparative analyses of rider position according to skill levels during walk and trot in Jeju horse', *Human Movement Science*, 29(6), pp. 956–963. doi: 10.1016/j.humov.2010.05.010.

Kay, B. A. (1988) 'The dimensionality of movement trajectories and the degrees of freedom problem: A tutorial', *Human Movement Science*, 7(2–4), pp. 343–364. doi: 10.1016/0167-9457(88)90016-4.

Kim, M. J. *et al.* (2018) 'Equine exercise in younger and older adults: Simulated versus real horseback riding', *Perceptual and Motor Skills*, 125(1), pp. 93–108. doi: 10.1177/0031512517736463.

Knudson, D. (2017) 'Sports Biomechanics Confidence crisis of results in biomechanics research Confidence crisis of results in biomechanics research', *SportS Biomechanics*, 16(4), pp. 425–433. doi: 10.1080/14763141.2016.1246603.

- Ko, J. H. and Newell, K. M. (2001) 'Organization of postural coordination patterns as a function of scaling the surface of support dynamics', *Journal of Motor Behavior*, 47(5), pp. 415–426. doi: 10.1080/00222895.2014.1003781.
- Ko, Y. G., Challis, J. H. and Newell, K. M. (2001) 'Postural coordination patterns as a function of dynamics of the support surface', *Human Movement Science*, 20(6), pp. 737–764. doi: 10.1016/S0167-9457(01)00052-5.
- Ko, Y. G., Challis, J. H. and Newell, K. M. (2003) 'Learning to coordinate redundant degrees of freedom in a dynamic balance task', *Human Movement Science*, 22(1), pp. 47–66. doi: 10.1016/S0167-9457(02)00177-X.
- König von Borstel, U. and Glißman, C. (2014) 'Alternatives to Conventional Evaluation of Rideability in Horse Performance Tests: Suitability of Rein Tension and Behavioural Parameters', *PLoS ONE*. Edited by M. Hausberger, 9(1), p. e87285. doi: 10.1371/journal.pone.0087285.
- Kottas-Heldenburg, A. and Fitzpatrick, A. (2014) *Dressage Solutions A Rider's Guide*. Kenilworth Press.
- Kraft, C. N. *et al.* (2009) 'Magnetic resonance imaging findings of the lumbar spine in elite horseback riders: Correlations with Back pain, body mass index, trunk/leg-length coefficient, and riding discipline', *American Journal of Sports Medicine*, 37(11), pp. 2205–2213. doi: 10.1177/0363546509336927.
- van der Kruk, E. and Reijne, M. M. (2018) 'Accuracy of human motion capture systems for sport applications; state-of-the-art review', *European Journal of Sport Science*, 18(6), pp. 806–819. doi: 10.1080/17461391.2018.1463397.
- Kurz, M. J. and Stergiou, N. (2004) 'Applied dynamic systems theory for the analysis of movement', in Stergiou, N. (ed.) *Innovative analyses of human movement. Analytical tools for human movement research*. Champaign, IL: Human Kinetics.
- Lagarde, J. *et al.* (2005) 'Coordination dynamics of the horse-rider system', *Journal of Motor Behavior*, 37(6), pp. 418–424. doi: 10.3200/JMBR.37.6.418-424.
- Lamb, P. F. *et al.* (2007) 'Self-organizing maps as a tool to analyze movement variability', in *6th International Symposium on Computer Science in Sport*, pp. 76–82.
- Lamb, P. F. and Pataky, T. C. (2018) 'The role of pelvis-thorax coupling in controlling within-golf club swing speed', *Journal of Sports Sciences*, 36(19), pp. 2164–2171. doi: 10.1080/02640414.2018.1442287.
- Lamb, P. F. and Stöckl, M. (2014) 'On the use of continuous relative phase: Review of current approaches and outline for a new standard', *Clinical Biomechanics*. Elsevier Ltd, pp. 484–493. doi: 10.1016/j.clinbiomech.2014.03.008.
- Lames, M. (2006) 'Modelling the interaction in game sports - Relative phase and moving correlations', in *Journal of Sports Science and Medicine*. Dept. of Sports Medicine, Medical Faculty of Uludag University, pp. 556–560.
- Lamoth, C. J. C. *et al.* (2009) 'Steady and transient coordination structures of walking and running', *Human Movement Science*, 28(3), pp. 371–386. doi: 10.1016/j.humov.2008.10.001.
- Leardini, A. *et al.* (2005) 'Human movement analysis using stereophotogrammetry Part 3. Soft tissue artifact assessment and compensation', *Gait and Posture*. Elsevier Ireland Ltd, pp. 212–225. doi: 10.1016/j.gaitpost.2004.05.002.
- Lee, J. T. *et al.* (2015) 'The feasibility of an 8-week, home-based isometric strength-training program for improving dressage test performance in equestrian athletes', *Comparative Exercise Physiology*,

11(4), pp. 223–230. doi: 10.3920/CEP150018.

Lee, S., Lee, D. and Park, J. (2014) 'Effects of the indoor horseback riding exercise on electromyographic activity and balance in one-leg standing', *Journal of Physical Therapy Science*, 26(9), pp. 1445–1447. doi: 10.1589/jpts.26.1445.

Lees, A. (2010) 'Technique analysis in sports: a critical review'. doi: 10.1080/026404102320675657.

Lewis, C. L. *et al.* (2017) 'The Human Pelvis: Variation in Structure and Function During Gait', *Anatomical Record*, 300(4), pp. 633–642. doi: 10.1002/ar.23552.

Lewis, V. *et al.* (2019) 'A preliminary study investigating functional movement screen test scores in female collegiate age horse-riders', *Comparative Exercise Physiology*, 15(2), pp. 105–112. doi: 10.3920/CEP180036.

Licka, T., Kapaun, M. and Peham, C. (2010) 'Influence of rider on lameness in trotting horses', *Equine Veterinary Journal*, 36(8), pp. 734–736. doi: 10.2746/0425164044848028.

Lovett, T., Hodson-Tole, E. and Nankervis, K. (2005) 'A preliminary investigation of rider position during walk, trot and canter', *Equine and Comparative Exercise Physiology*, 2(2), pp. 71–76. doi: 10.1079/ecp200444.

Mackechnie-Guire, R. *et al.* (2018) 'Relationship between saddle and rider kinematics, horse locomotion, and thoracolumbar pressures in sound horses', *Journal of Equine Veterinary Science*, 69, pp. 43–52. doi: 10.1016/j.jevs.2018.06.003.

Mackechnie-Guire, R. (2020) 'Studies show the importance of biomechanics for horse and rider', *Horse&Hound*, p. 8.

MacKechnie-Guire, R. and Pfau, T. (2021) 'Differential Rotational Movement of the Thoracolumbosacral Spine in High-Level Dressage Horses Ridden in a Straight Line, in Sitting Trot and Seated Canter Compared to In-Hand Trot', *Animals*, 11(3), p. 888. doi: 10.3390/ani11030888.

Marin, L., Bardy, B. G. and Bootsma, R. J. (1999) 'Level of gymnastic skill as an intrinsic constraint on postural coordination', *Journal of Sports Sciences*, 17(8), pp. 615–626. doi: 10.1080/026404199365641.

Massion, J. and Woollacott, M. H. (2004) 'Posture and equilibrium', in Bronstein, A. M. *et al.* (eds) *Clinical disorders of balance, posture and gait*. 2nd edn. London: Arnold, pp. 1–19.

Mazurek, C. M. *et al.* (2020) 'Differences in inter-joint coordination between high- and low-calibre ice hockey players during forward skating', *Sports Biomechanics*. doi: 10.1080/14763141.2020.1797151.

Mcgreevy, P. *et al.* (2011) 'How riding may affect welfare: What the equine veterinarian needs to know', *Equine Veterinary Education*, 23(10), pp. 531–539. doi: 10.1111/j.2042-3292.2010.00217.x.

Mears, A. C., Roberts, J. R. and Forrester, S. E. (2018) 'Matching golfers' movement patterns during a golf swing', *Applied Sciences (Switzerland)*, 8(12), pp. 1–15. doi: 10.3390/app8122452.

Mitani, Y. *et al.* (2008) 'Effect of Exercise Using a Horse-Riding Simulator on Physical Ability of Frail Seniors', *Journal of Physical Therapy Science*, 20(3), pp. 177–183. doi: 10.1589/jpts.20.177.

Mo, S. and Chow, D. H. K. (2019) 'Differences in lower-limb coordination and coordination variability between novice and experienced runners during a prolonged treadmill run at anaerobic threshold speed', *Journal of Sports Sciences*, 37(9), pp. 1021–1028. doi: 10.1080/02640414.2018.1539294.

Morales, J. L. *et al.* (1998) 'Temporal and linear kinematics in elite and riding horses at the trot', *Journal of Equine Veterinary Science*, 18(12), pp. 835–839. doi: 10.1016/S0737-0806(98)80334-1.

- Morriss, C., Bartlett, R. M. and Fowler, N. (1997) 'Biomechanical analysis of men's javelin throw at the 1995 World Championships in athletics', *New Studies in Athletics*, 12, pp. 31–41.
- Münz, A. *et al.* (2013) 'A preliminary study of an inertial sensor-based method for the assessment of human pelvis kinematics in dressage riding', *Journal of Equine Veterinary Science*, 33(11), pp. 950–955. doi: 10.1016/j.jevs.2013.02.002.
- Münz, A., Eckardt, F. and Witte, K. (2014) 'Horse-rider interaction in dressage riding', *Human Movement Science*, 33(1), pp. 227–237. doi: 10.1016/j.humov.2013.09.003.
- Murray, R. C. *et al.* (2006) 'Association of type of sport and performance level with anatomical site of orthopaedic injury diagnosis', *Equine Veterinary Journal*, 38(SUPPL.36), pp. 411–416. doi: 10.1111/j.2042-3306.2006.tb05578.x.
- Murray, R. C. *et al.* (2010) 'How do features of dressage arenas influence training surface properties which are potentially associated with lameness?', *Veterinary Journal*, 186(2), pp. 172–179. doi: 10.1016/j.tvjl.2010.04.026.
- Naouma, H. and Pataky, T. C. (2019) 'A comparison of random-field-theory and false-discovery-rate inference results in the analysis of registered one-dimensional biomechanical datasets', *PeerJ*, 2019(12), p. e8189. doi: 10.7717/peerj.8189.
- Nelson-Wong, E. A. *et al.* (2009) 'Application of autocorrelation and cross-correlation analyses in human movement and rehabilitation research', *Journal of Orthopaedic and Sports Physical Therapy*, 39(4), pp. 287–295. doi: 10.2519/jospt.2009.2969.
- Nevison, C. M. and Timmis, M. A. (2013) 'The effect of physiotherapy intervention to the pelvic region of experienced riders on seated postural stability and the symmetry of pressure distribution to the saddle: A preliminary study', *Journal of Veterinary Behavior: Clinical Applications and Research*, 8(4), pp. 261–264. doi: 10.1016/j.jveb.2013.01.005.
- Newell, K. M. (1986) 'Constraints on the development of coordination', in *Motor development in children: Aspects of coordination and control*. Dordrecht: Nijhoff, pp. 341–360.
- Newell, K. M. *et al.* (2006) 'Variability in motor output as noise: A default and erroneous proposition?', in Davids, K., Bennett, S., and Newell, K. M. (eds) *Human Movement Variability*. Champaign, IL: Human Kinetics, pp. 3–22.
- Nigg, B. M. (2010) *Biomechanics of Sport Shoes*. Calgary: Topline Printing.
- Norris, C. M. (1995) 'Spinal Stabilisation. 4. Muscle Imbalance and the Low Back', *Physiotherapy*, 81(3), pp. 127–138. doi: 10.1016/S0031-9406(05)67068-X.
- Norris, C. M. (2008) *Back Stability*. Second. Champaign, IL: Human Kinetics.
- Nourbakhsh, M. R. and Arab, A. M. (2002) 'Relationship between mechanical factors and incidence of low back pain', *Journal of Orthopaedic and Sports Physical Therapy*, 32(9), pp. 447–460. doi: 10.2519/jospt.2002.32.9.447.
- Nuttall, F. Q. (2015) 'Body mass index: Obesity, BMI, and health: A critical review', *Nutrition Today*. Lippincott Williams and Wilkins, pp. 117–128. doi: 10.1097/NT.0000000000000092.
- O'Sullivan, P. B. *et al.* (2006) 'Effect of different upright sitting postures on spinal-pelvic curvature and trunk muscle activation in a pain-free population', *Spine*, 31(19). doi: 10.1097/01.brs.0000234735.98075.50.
- Olivier, A. *et al.* (2017) 'Head stability and head-trunk coordination in horseback riders: The contribution of visual information according to expertise', *Frontiers in Human Neuroscience*, 11, p. 11.

doi: 10.3389/fnhum.2017.00011.

Oomen, A. M. *et al.* (2012) 'Use of a pressure plate to analyse the toe-heel load redistribution underneath a normal shoe and a shoe with a wide toe in sound warmblood horses at the walk and trot', *Research in Veterinary Science*, 93(2), pp. 1026–1031. doi: 10.1016/j.rvsc.2012.01.010.

Oosterlinck, M. *et al.* (2013) 'Pressure plate analysis of toe-heel and medio-lateral hoof balance at the walk and trot in sound sport horses', *Veterinary Journal*, 198(SUPPL1), pp. e9–e13. doi: 10.1016/j.tvjl.2013.09.026.

Orth, D., Davids, K. and Seifert, L. (2016) 'Coordination in climbing: Effect of skill, practice and constraints manipulation', *Sports Medicine*, 46(2), pp. 255–268. doi: 10.1007/s40279-015-0417-5.

Oullier, O. *et al.* (2006) 'Variability in postural coordination dynamics', in Davids, K., Bennett, S., and Newell, K. (eds) *Movement System Variability*. Champaign, IL: Human Kinetics, pp. 25–46.

Palut, Y. and Zanone, P.-G. G. (2005) 'A dynamical analysis of tennis: Concepts and data', *Journal of Sports Sciences*, 23(10), pp. 1021–1032. doi: 10.1080/02640410400021682.

Park, J., Lee, S. and Lee, D. (2015) 'The effects of horseback riding simulator exercises on the muscle activity of the lower extremities according to changes in arm posture', *Journal of Physical Therapy Science*, 27(9), pp. 2731–2732. doi: 10.1589/jpts.27.2731.

Passos, P., Araújo, D. and Davids, K. (2013) 'Self-organization processes in field-invasion team sports implications for leadership', *Sports Medicine*. Springer, pp. 1–7. doi: 10.1007/s40279-012-0001-1.

Pataky, T. C. *et al.* (2019) 'On the validity of statistical parametric mapping for nonuniformly and heterogeneously smooth one-dimensional biomechanical data', *Journal of Biomechanics*, 91, pp. 114–123. doi: 10.1016/j.jbiomech.2019.05.018.

Pataky, T. C., Robinson, M. A. and Vanrenterghem, J. (2013) 'Vector field statistical analysis of kinematic and force trajectories', *Journal of Biomechanics*, 46(14), pp. 2394–2401. doi: 10.1016/j.jbiomech.2013.07.031.

Pataky, T. C., Robinson, M. A. and Vanrenterghem, J. (2018) *SPM1D Workshop Answers*.

Peeters, M. *et al.* (2013) 'Rider and Horse Salivary Cortisol Levels During Competition and Impact on Performance', *Journal of Equine Veterinary Science*, 33(3), pp. 155–160. doi: 10.1016/J.JEVS.2012.05.073.

Peham, C. *et al.* (2001) 'A new method to quantify harmony of the horse-rider system in dressage', *Sports Engineering*, 4(2), pp. 95–101. doi: 10.1046/j.1460-2687.2001.00077.x.

Peham, C. *et al.* (2004) 'Influence of the rider on the variability of the equine gait', *Human Movement Science*, 23(5), pp. 663–671. doi: 10.1016/J.HUMOV.2004.10.006.

Peters, B. T. *et al.* (2003) 'Limitations in the use and interpretation of continuous relative phase', *Journal of Biomechanics*, 36(2), pp. 271–274. doi: 10.1016/S0021-9290(02)00341-X.

Pfau, T. and Reilly, P. (2020) 'How low can we go? Influence of sample rate on equine pelvic displacement calculated from inertial sensor data', *Equine Veterinary Journal*, p. evj.13371. doi: 10.1111/evj.13371.

Phinyomark, A. *et al.* (2015) 'Do intermediate- and higher-order principal components contain useful information to detect subtle changes in lower extremity biomechanics during running?', *Human Movement Science*, 44, pp. 91–101. doi: 10.1016/j.humov.2015.08.018.

Preatoni, E. *et al.* (2013) 'Movement variability and skills monitoring in sports', *Sports Biomechanics*,

pp. 69–92. doi: 10.1080/14763141.2012.738700.

Prin-Conti, D. *et al.* (2017) 'Analysis of a horse simulator's locomotion by inertial sensors', *Computer Methods in Biomechanics and Biomedical Engineering*, 20(sup1), pp. 165–166. doi: 10.1080/10255842.2017.1382914.

Pugh, T. J. and Bolin, D. (2004) 'Overuse injuries in equestrian athletes.', *Current sports medicine reports*, 3(6), pp. 297–303.

Qualisys AB (2020) *Qualisys Track Manager User Manual*. Version 20. Gothenburg.

Quinn, S. and Bird, S. (1996) 'Influence of saddle type upon the incidence of lower back pain in equestrian riders', *Br J Sports Med*, 30, pp. 140–144. doi: 10.1136/bjism.30.2.140.

Renshaw, I., Davids, K. and Savelsbergh, G. J. P. (2010) *Motor Learning in Practice, Motor Learning in Practice*. London: Routledge. doi: 10.4324/9780203888100.

Rhodin, M. *et al.* (2005) 'The influence of head and neck position on kinematics of the back in riding horses at the walk and trot', *Equine Veterinary Journal*, 37(1), pp. 7–11. doi: 10.2746/0425164054406928.

Robertson, D. G. E. *et al.* (2014) *Research Methods in Biomechanics*. 2nd edn. Champaign, IL: Human Kinetics.

Robertson, D. G. E. and Caldwell, G. E. (2014) 'Planar Kinematics', in Robertson, D. G. E. *et al.* (eds) *Research Methods in Biomechanics*. Second. Champaign, IL: Human Kinetics, pp. 9–33.

Robinson, M. A., Vanrenterghem, J. and Pataky, T. C. (2015) 'Statistical Parametric Mapping (SPM) for alpha-based statistical analyses of multi-muscle EMG time-series', *Journal of electromyography and kinesiology : official journal of the International Society of Electrophysiological Kinesiology*, 25(1), pp. 14–19. doi: 10.1016/j.jelekin.2014.10.018.

Roost, L. *et al.* (2020) 'The effects of rider size and saddle fit for horse and rider on forces and pressure distribution under saddles: A pilot study', *Equine Veterinary Education*, 32(S10), pp. 151–161. doi: 10.1111/eve.13102.

Sabatini, A. M. (2011) 'Estimating three-dimensional orientation of human body parts by inertial/magnetic sensing', *Sensors*, 11(2), pp. 1489–1525. doi: 10.3390/s110201489.

Sackman, J. E. and Houpt, K. A. (2019) 'Equine Personality: Association With Breed, Use, and Husbandry Factors'. doi: 10.1016/j.jevs.2018.10.018.

Sainas, G. *et al.* (2016) 'Cardio-metabolic responses during horse riding at three different speeds', *European Journal of Applied Physiology*, 116(10), pp. 1985–1992. doi: 10.1007/s00421-016-3450-7.

Schiavone, P. A. and Tulli, A. (1994) 'Analysis of the Movements Involved in Horse-Riding', *Journal of Sports Traumatology and Related Research*, 16(4), pp. 196–205.

Schils, S. J. *et al.* (1993) 'Kinematic analysis of the equestrian - Walk, posting trot and sitting trot', *Human Movement Science*, 12(6), pp. 693–712. doi: 10.1016/0167-9457(93)90011-D.

Schöllhorn, W. I. *et al.* (2002) 'Identification of individual walking patterns using time discrete and time continuous data sets', *Gait and Posture*, 15(2), pp. 180–186. doi: 10.1016/S0966-6362(01)00193-X.

Schöllhorn, W. I. *et al.* (2006) 'A pattern recognition approach for the quantification of horse and rider interactions', *Equine Veterinary Journal*, 38(Suppl), pp. 400–405. doi: 10.1111/j.2042-3306.2006.tb05576.x.

Scholz, J. P., Schoner, G. and Latash, M. L. (2000) 'Identifying the control structure of multijoint

coordination during pistol shooting', *Experimental Brain Research*, 135(3), pp. 382–404. doi: 10.1007/s002210000540.

Scott Kelso, J. A. *et al.* (1981) 'Patterns of human interlimb coordination emerge from the properties of non-linear, limit cycle oscillatory processes: Theory and data', *Journal of Motor Behavior*, 13(4), pp. 226–261. doi: 10.1080/00222895.1981.10735251.

Scott Kelso, J. A. (1995) *Dynamic Patterns: The Self-Organization of Brain and Behavior*. Cambridge, MA: MIT Press.

Scott Kelso, J. A. (2009a) 'Coordination Dynamics', in Meyers, R. . (ed.) *Encyclopedia of Complexity and Systems Science*. Heidelberg: Springer, pp. 1537–1564.

Scott Kelso, J. A. (2009b) *Dynamic Patterns: The self-organization of brain and behavior*. Cambridge, MA: MIT Press.

Seay, J. F., Van Emmerik, R. E. A. and Hamill, J. (2011) 'Low back pain status affects pelvis-trunk coordination and variability during walking and running', *Clinical Biomechanics*, 26(6), pp. 572–578. doi: 10.1016/j.clinbiomech.2010.11.012.

Serrien, B. *et al.* (2015) 'Differences in ball speed and three-dimensional kinematics between male and female handball players during a standing throw with run-up', *BMC Sports Science, Medicine and Rehabilitation*, 7(1), p. 27. doi: 10.1186/s13102-015-0021-x.

Söderkvist, I. and Wedin, P. Å. (1993) 'Determining the movements of the skeleton using well-configured markers', *Journal of Biomechanics*, 26(12), pp. 1473–1477. doi: 10.1016/0021-9290(93)90098-Y.

Solé, M. *et al.* (2013) 'Evaluation of conformation against traits associated with dressage ability in unriden Iberian horses at the trot', *Research in Veterinary Science*, 95(2), pp. 660–666. doi: 10.1016/j.rvsc.2013.06.017.

Spörri, J. *et al.* (2016) 'Collecting Kinematic Data on a Ski Track with Optoelectronic Stereophotogrammetry: A Methodological Study Assessing the Feasibility of Bringing the Biomechanics Lab to the Field'. doi: 10.1371/journal.pone.0161757.

Symes, D. and Ellis, R. (2009) 'A preliminary study into rider asymmetry within equitation', *Veterinary Journal*, 181(1), pp. 34–37. doi: 10.1016/j.tvjl.2009.03.016.

Temcharoensuk, P. *et al.* (2015) 'Effect of horseback riding versus a dynamic and static horse riding simulator on sitting ability of children with cerebral palsy: a randomized controlled trial', *Journal of Physical Therapy Science*, 27(1), pp. 273–277. doi: 10.1589/jpts.27.273.

Terada, K. (2000) 'Comparison of head movement and EMG activity of muscles between advanced and novice horseback riders at different gaits', *Journal of Equine Science*, 11(4), pp. 83–90. doi: 10.1294/jes.11.83.

Terada, K. *et al.* (2017) 'Electromyographic activity of the rider's muscles at trot', *Equine and Comparative Exercise Physiology*, 1(3), pp. 193–198. doi: 10.1079/ECEP200420.

Terada, K., Clayton, H. and Kato, K. (2006) 'Stabilization of wrist position during horseback riding at trot', *Equine and Comparative Exercise Physiology*, 3(4), pp. 179–184. doi: 10.1017/s1478061506337255.

Teufel, W. *et al.* (2019) 'Validity of inertial sensor based 3D joint kinematics of static and dynamic sport and physiotherapy specific movements', *PLOS ONE*. Edited by J. L. Williams, 14(2), p. e0213064. doi: 10.1371/journal.pone.0213064.

The MathWorks Inc. (2020) 'MATLAB'. Natick, Mass.: The MathWorks Inc.

Tomczak, M. and Tomczak, E. (2014) *The need to report effect size estimates revisited. An overview of some recommended measures of effect size*, *TRENDS in Sport Sciences*.

Topley, M. and Richards, J.G. (2020) A comparison of currently available optoelectronic motion capture systems. *Journal of Biomechanics*. 106, pp. 1-5.

Vagenas, G., Palaiothodorou, D. and Knudson, D. (2018) *Thirty-year Trends of Study Design and Statistics in Applied Sports and Exercise Biomechanics Research*, *International Journal of Exercise Science*.

Valle, E. *et al.* (2013) 'Estimation of the workload in horses during an eventing competition', *Comparative Exercise Physiology*, 9(2), pp. 93–101. doi: 10.3920/CEP12028.

Vesanto, J. *et al.* (2000) 'SOM Toolbox for MATLAB 5'. Helsinki, Finland: Helsinki University of Technology.

Vicon Ltd (2015) *Nexus 1.8.5 Product Guide*. Oxford.

Viry, S. *et al.* (2013) 'Patterns of Horse-Rider Coordination during Endurance Race: A Dynamical System Approach', *PLoS ONE*. Edited by F. Hug, 8(8), p. e71804. doi: 10.1371/journal.pone.0071804.

Viry, S. *et al.* (2015) 'Combined influence of expertise and fatigue on riding strategy and horse-rider coupling during the time course of endurance races', *Equine Veterinary Journal*, 47(1), pp. 78–82. doi: 10.1111/evj.12236.

Walker, A. M. *et al.* (2016) 'The kinematics and kinetics of riding a racehorse: A quantitative comparison of a training simulator and real horses', *Journal of Biomechanics*, 49(14), pp. 3368–3374. doi: 10.1016/J.JBIOMECH.2016.08.031.

Walker, V. A. *et al.* (2013) 'The effect of collection and extension on tarsal flexion and fetlock extension at trot', *Equine Veterinary Journal*, 45(2), pp. 245–248. doi: 10.1111/j.2042-3306.2012.00617.x.

Walker, V. A. *et al.* (2020) 'Relationship between pelvic tilt control, horse-rider synchronisation, and rider position in sitting trot', *Comparative Exercise Physiology*, pp. 1–10. doi: 10.3920/cep190071.

Wanless, M. (2017) *The New Anatomy of Rider Connection*. North Pomfret, Vermont: Trafalgar Square.

Westerling, D. (1983) 'A study of physical demands in riding', *European Journal of Applied Physiology and Occupational Physiology*, 50(3), pp. 373–382. doi: 10.1007/BF00423243.

Wheat, Jonathan S and Glazier, P. S. (2006) 'Measuring coordination and variability in coordination', in Davids, K., Bennett, S., and Newell, K. M. (eds) *Movement System Variability*. Champaign, IL: Human Kinetics, pp. 167–181.

Wheat, Jonathan S. and Glazier, P. S. (2006) 'Measuring coordination and variability in coordination', in Davids, K., Bennett, S., and Newell, K. (eds) *Movement System Variability*. Champaign, IL: Human Kinetics, pp. 167–181.

Williams, G. K. R. *et al.* (2016) 'Coordination as a function of skill level in the gymnastics longswing', *Journal of Sports Sciences*, 34(5), pp. 429–439. doi: 10.1080/02640414.2015.1057209.

Williams, J. and Tabor, G. (2017) 'Rider impacts on equitation', *Applied Animal Behaviour Science*, 190, pp. 28–42. doi: 10.1016/J.APPLANIM.2017.02.019.

Wilson, C. *et al.* (2008) 'Coordination variability and skill development in expert triple jumpers', *Sports Biomechanics*, 7(1), pp. 2–9. doi: 10.1080/14763140701682983.

- Winter, D. A. (2009) *Biomechanics and Motor Control of Human Movement: Fourth Edition*, *Biomechanics and Motor Control of Human Movement: Fourth Edition*. doi: 10.1002/9780470549148.
- Witte, K. *et al.* (2010) 'Applying a principal component analysis to movement coordination in sport', *Mathematical and Computer Modelling of Dynamical Systems*, 16(5), pp. 477–488. doi: 10.1080/13873954.2010.507079.
- Witte, K., Schobesberger, H. and Peham, C. (2009) 'Motion pattern analysis of gait in horseback riding by means of Principal Component Analysis', *Human Movement Science*, 28(3), pp. 394–405. doi: 10.1016/j.humov.2009.04.002.
- Wolframm, I. A., Bosga, J. and Meulenbroek, R. G. J. (2013) 'Coordination dynamics in horse-rider dyads', *Human Movement Science*, 32(1), pp. 157–170. doi: 10.1016/j.humov.2012.11.002.
- Wright, L. R. and Peters, M. D. (2008) 'A heart rate analysis of the cardiovascular demands of elite level competitive polo', *International Journal of Performance Analysis in Sport*, 8(2), pp. 76–81. doi: 10.1080/24748668.2008.11868437.
- Wu, G. *et al.* (2002) 'ISB recommendation on definitions of joint coordinate system of various joints for the reporting of human joint motion - Part I: Ankle, hip, and spine', *Journal of Biomechanics*, pp. 543–548. doi: 10.1016/S0021-9290(01)00222-6.
- Yoo, J. H. *et al.* (2014) 'The effect of horse simulator riding on visual analogue scale, body composition and trunk strength in the patients with chronic low back pain', *International Journal of Clinical Practice*, 68(8), pp. 941–949. doi: 10.1111/ijcp.12414.
- Zehr, J. D., Howarth, S. J. and Beach, T. A. C. (2018) 'Using relative phase analyses and vector coding to quantify Pelvis-Thorax coordination during lifting—A methodological investigation', *Journal of Electromyography and Kinesiology*, 39, pp. 104–113. doi: 10.1016/j.jelekin.2018.02.004.
- Zettl, W. (1998) *Dressage in Harmony: from Basic to Grand Prix*. Boonsboro, MD: Half Halt Press, Inc.
- Zsoldos, R. R. and Licka, T. F. (2015) 'The equine neck and its function during movement and locomotion', *Zoology*, pp. 364–376. doi: 10.1016/j.zool.2015.03.005.

Appendix A

Ethics application and approval

A1 Letter of approval from Hartpury University Ethics Committee

A2 Participant informed consent and rider questionnaire

A2.2 Participant informed consent form

A2.2 Rider questionnaire

A2 – Letter of Approval from Hartpury University Ethics Committee

Celeste.Wilkins

From: Ethics
Sent: 10 June 2021 04:26
To: Celeste.Wilkins
Subject: APPROVED – ETHICS2018-03 – Celeste Wilkins

APPROVED – ETHICS2018-03 – Celeste Wilkins

Dear Celeste,

I can confirm that the Ethics committee approved your ethical application '*The influence of pelvic posture on rider biomechanics and measures of horse-rider movement synchrony*' on the 7th of November 2018.

Kind regards,

Lucy

Lucy Grieve *MCLIP AFHEA MA BA(hons)*
Learning Resources Administrator: Research & Digital Resources | ULC & CLC
Hartpury University & Hartpury College | Gloucester | GL19 3BE
Email: lucy.grieve@hartpury.ac.uk
Website: www.hartpury.ac.uk
Find It: www.hartpury.ac.uk/findit
Twitter: [Hartpury Libraries \(@HartpuryLibrary\)](https://twitter.com/HartpuryLibrary)

A2.1 Participant informed consent form



PLEASE READ THE FOLLOWING CAREFULLY

Date: July 2019

Subject – Research Project on rider posture and biomechanics

Dear Participant,

Thank you for agreeing to take part in this research project. It aims to understand the influence of rider posture on biomechanics, which will help to inform equestrian coaching, strength and conditioning, injury risk and injury rehabilitation.

The project will comprise a short session on the Racewood Eventing Simulator, where you will be asked to ride as you normally would in walk, trot (sitting and rising) and both leads of canter. You will be asked to fill out a short questionnaire and your position will be tracked using sensors and motion capture cameras. You are asked to wear tight-fitting riding tights and a tight-fitting vest top with your regular riding boots, helmet and gloves. We will take a video recording of the trials and will be happy to provide this to you after the data collection has been completed.

If you are happy to be involved, we would ask you to complete the consent form and return it to us.

We would like to thank you for your time in considering this opportunity to take part in this research project.

Yours sincerely,

Celeste Wilkins

Celeste Wilkins – PhD student, Hartpury University

This research project has received ethical approval from the Hartpury University, Research Ethics Committee

A2.1 Rider questionnaire

Rider Performance Questionnaire

Rider Name _____ Date of Birth _____
Height _____ Weight _____
Occupation _____

How many hours (on average) do you ride per week? _____

How many horses do you own/ride? _____

Do you care for your horse(s) or are they on full livery? _____

What level do you currently compete at in British Dressage? _____

Please record your top four results in the last year.

Have you experienced a significant injury in the last year? (tick one) yes ☐ no ☐

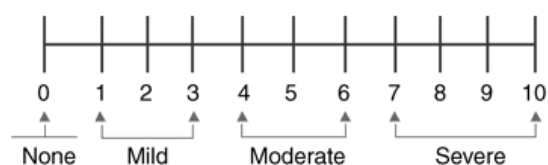
Was it horse-related? yes ☐ no ☐

Do you currently experience chronic pain? yes ☐ no ☐

If yes, please specify area(s) _____

Is this pain as a result of an injury? _____

Please rate the severity of your pain on the pain scale for each area



Are you left or right handed? _____

Do you currently partake in any off-horse fitness training or stretching regime? yes no

If yes, how often? _____

Is it led by: (circle one) a professional trainer or self-directed?

Please detail your typical routine:

Appendix B – Participant characteristics and inclusion in studies.

All riders who met the inclusion criteria for the study outlined in Table 3.3 were included if their data was available at the time of data analysis. Table IV outlines the participation status of riders within each of the experimental chapters in this thesis. As the chapter sequence does not represent a chronological order of data analysis, it is possible that some riders could be included in, for example, Chapter 6, but not Chapter 7.

All data were inspected prior to inclusion within studies. If key markers (any pelvis, trunk, head or foot marker and one or more of the markers on the riding simulator) were occluded during data capture, the individual's trial was discarded.

Table B1. Participant characteristics and inclusion in studies. Age is given in years, mass in kilograms, and height in metres. Dressage competition level refers to the highest level that the rider had ridden with three results in the last six months of competition for riders included in Chapter 5, and last 12 months for riders included in Chapter 6, 7, and 8. Trials with marker occlusion of any key marker were excluded; these individuals are highlighted in grey.

| Age | Mass | Height | Level | Chapter 4: Section 4.1 | Chapter 4: Section 4.2 | Chapter 5 | Chapter 6 | Chapter 7 | Chapter 8 |
|-----|------|--------|--------------------|---------------------------|---------------------------|-----------|-----------|-----------|-----------|
| 26 | 47 | 1.63 | BD Medium | | • | • | • | • | • |
| 49 | 52 | 1.57 | BD Medium | | • | • | • | • | • |
| 33 | 70 | 1.61 | BD Medium | | • | • | • | • | • |
| 23 | 60 | 1.68 | BD Advanced Medium | | • | • | • | • | • |
| 37 | 54 | 1.65 | BD Advanced Medium | | • | • | • | • | • |
| 29 | 80 | 1.77 | BD Advanced Medium | | • | • | • | • | • |
| 50 | 60 | 1.68 | BD Advanced Medium | | • | • | • | • | • |
| 57 | 70 | 1.78 | BD Advanced Medium | | • | • | • | • | • |
| 35 | 64 | 1.73 | BD Advanced Medium | | • | • | • | • | • |
| 24 | 63 | 1.77 | BD Advanced Medium | • | • | • | • | • | • |
| 62 | 60 | 1.68 | BD Advanced | | • | • | • | • | • |
| 29 | 60 | 1.68 | BD Advanced | | • | • | • | • | • |
| 28 | 70 | 1.83 | BD Advanced | | • | • | • | • | • |
| 18 | 62 | 1.67 | BD Advanced | | • | • | • | • | • |
| 27 | 59 | 1.65 | FEI I1 | • | • | • | • | • | • |
| 25 | 70 | 1.73 | FEI I1 | | • | • | • | • | • |
| 26 | 76 | 1.78 | FEI I1 | | • | • | • | • | • |
| 29 | 60 | 1.68 | FEI I2 | | • | | • | • | • |
| 34 | 72 | 1.67 | FEI I2 | • | • | • | • | • | • |
| 41 | 65 | 1.65 | FEI PSG | | • | • | • | • | • |
| 21 | 73 | 1.65 | FEI PSG | | • | • | • | • | • |
| 28 | 54 | 1.60 | FEI Grand Prix | | • | • | • | • | • |
| 24 | 55 | 1.55 | FEI Grand Prix | | • | • | • | • | • |
| 24 | 72 | 1.67 | FEI Grand Prix | • | • | | • | • | • |

| | | | | | | | | | |
|----|----|------|--------------------|---|---|---|---|---|---|
| 38 | 64 | 1.59 | FEI Grand Prix | | • | | • | • | • |
| 23 | 57 | 1.65 | BD Prelim | | | • | | • | • |
| 38 | 79 | 1.65 | BD Novice | | | • | | • | • |
| 23 | 56 | 1.66 | BD Novice | | | • | | • | • |
| 25 | 52 | 1.65 | BD Novice | | | • | | • | • |
| 25 | 70 | 1.62 | BD Novice | | | | | • | • |
| 52 | 62 | 1.50 | BD Novice | | | | | • | • |
| 52 | 64 | 1.54 | BD Novice | | | | | • | • |
| 20 | 60 | 1.63 | BD Novice | | | • | | • | • |
| 59 | 65 | 1.68 | BD Elementary | | | • | | • | • |
| 22 | 53 | 1.63 | BD Elementary | | | • | | • | • |
| 20 | 68 | 1.83 | BD Elementary | | | | | • | • |
| 26 | 65 | 1.67 | BD Elementary | | | • | | • | • |
| 22 | 51 | 1.70 | BD Elementary | | | • | | • | • |
| 36 | 57 | 1.75 | BD Elementary | | | • | | • | • |
| 21 | 53 | 1.55 | BD Elementary | | | • | | • | • |
| 56 | 60 | 1.60 | FEI I1 | | • | | • | | |
| 26 | 54 | 1.67 | FEI I2 | | • | • | • | | |
| 50 | 59 | 1.65 | FEI Grand Prix | | • | | • | | |
| 19 | 54 | 1.55 | BD Prelim | | | | | | |
| 43 | 50 | 1.62 | BD Medium | | | | | | |
| 24 | 57 | 1.57 | BD Advanced Medium | | | | • | | |
| 26 | 65 | 1.80 | BD Prelim | • | | | | | |
| 32 | 55 | 1.58 | BD Medium | • | | | | | |
| 41 | 62 | 1.62 | BD Advanced Medium | • | | | | | |
| 23 | 70 | 1.58 | BD Novice | • | | | | | |
| 24 | 62 | 1.50 | BD Novice | | | | | | |
| 19 | 53 | 1.51 | BD Prelim | | | | | | |

BD: British Dressage, **FEI:** Fédération Internationale Équestre, **PSG:** Prix St Georges, **I1:** Intermediare 1, **I2:** Intermediare 2.

Appendix C – Statistical Outputs

C1 – Chapter 4

C1.1 Section 4.2

C1.1.1 Descriptive statistics

C1.1.2 Normality tests

C1.1.3 Mann-Whitney U Test outputs

C1.1.4 Spearman's Correlation Test output

C1.2 Section 4.3

C1.2.1 Descriptive statistics

C1.2.2 Normality tests

C1.2.3 Pearson's correlation test outputs

C1.2.4 T-test outputs

C2 – Chapter 5

C2.1 Descriptive statistics

C2.2 Normality tests

C2.3 ANOVA output

C2.3.1 Post-hoc t-tests

C2.4 Kruskal-Wallis test outputs

C2.4.1 Range of motion

C2.4.2 Minimum pelvic tilt

C2.4.3 Maximum pelvic tilt

C2.5 Spearman correlation test outputs

C2.5.1 Halt posture – range of motion

C2.5.2 Halt posture – mean pelvic tilt

C2.5.3 Halt posture – minimum and maximum pelvic tilt

C3 – Chapter 7

C3.1 Descriptive statistics

C3.2 Normality tests

C3.3 Linear mixed model output

C1.1 Section 4.2

C1.1.1 Descriptive statistics

Table C1.1. Descriptive statistics for skin-affixed (n = 4 riders) and trouser-affixed (n = 4 riders) variables.

| | | Statistic | | | | | | | | | | | | | Std. Error | | |
|----------------------------|------------------------------------|-------------------------------------|----------------|----------------|--------------------|--------|----------|-------------------|---------|---------|-------|------------------------|----------|----------|------------|----------|----------|
| | | 95% Confidence Interval for Mean | | | 5% Trimmed Mean | | Variance | Std. Deviation | Minimum | Maximum | Range | Interquartile Range | Skewness | Kurtosis | | | |
| | | Mean | Lower Bound | Upper Bound | Mean | Median | | | | | | | | | Mean | Skewness | Kurtosis |
| Skin-affixed markers | Walk Left PSIS <i>rmsd</i> | 27.80 | 20.75 | 34.86 | 27.80 | 27.75 | 19.65 | 4.43 | 22.58 | 33.13 | 10.55 | 8.55 | 0.06 | -0.07 | 2.22 | 1.01 | 2.62 |
| | Walk Right PSIS <i>rmsd</i> | 26.74 | 17.95 | 35.53 | 26.95 | 28.64 | 30.53 | 5.53 | 18.67 | 31.02 | 12.35 | 9.61 | -1.69 | 3.04 | 2.76 | 1.01 | 2.62 |
| | Walk Left ASIS <i>rmsd</i> | 28.11 | 16.59 | 39.63 | 28.39 | 30.67 | 52.40 | 7.24 | 17.48 | 33.62 | 16.14 | 12.40 | -1.75 | 3.26 | 3.62 | 1.01 | 2.62 |
| | Walk Right ASIS <i>rmsd</i> | 28.62 | 21.89 | 35.34 | 28.82 | 30.46 | 17.88 | 4.23 | 22.31 | 31.24 | 8.93 | 6.86 | -1.93 | 3.77 | 2.11 | 1.01 | 2.62 |
| | Trot Left PSIS <i>rmsd</i> | 40.26 | 26.37 | 54.15 | 40.68 | 44.05 | 76.20 | 8.73 | 27.22 | 45.72 | 18.50 | 13.98 | -1.95 | 3.84 | 4.36 | 1.01 | 2.62 |
| | Trot Right PSIS <i>rmsd</i> | 35.37 | 21.99 | 48.75 | 35.38 | 35.49 | 70.71 | 8.41 | 26.84 | 43.67 | 16.83 | 15.59 | -0.03 | -5.15 | 4.20 | 1.01 | 2.62 |
| | Trot Left ASIS <i>rmsd</i> | 36.70 | 30.04 | 43.35 | 36.82 | 37.82 | 17.47 | 4.18 | 30.90 | 40.25 | 9.35 | 7.69 | -1.23 | 0.98 | 2.09 | 1.01 | 2.62 |
| | Trot Right ASIS <i>rmsd</i> | 41.30 | 32.85 | 49.74 | 41.38 | 42.05 | 28.14 | 5.31 | 35.07 | 46.01 | 10.94 | 9.87 | -0.38 | -3.73 | 2.65 | 1.01 | 2.62 |
| | Left canter Left PSIS <i>rmsd</i> | 46.12 | 22.48 | 69.76 | . | 48.26 | 90.57 | 9.52 | 35.72 | 54.39 | 18.67 | . | -0.96 | . | 5.49 | 1.23 | . |
| | Left canter Right PSIS <i>rmsd</i> | 40.79 | 15.42 | 66.16 | . | 44.63 | 104.30 | 10.21 | 29.21 | 48.52 | 19.31 | . | -1.45 | . | 5.90 | 1.23 | . |
| | Left canter Left ASIS <i>rmsd</i> | 43.98 | 32.23 | 55.74 | . | 43.47 | 22.38 | 4.73 | 39.53 | 48.95 | 9.42 | . | 0.48 | . | 2.73 | 1.23 | . |
| | Left canter Right ASIS <i>rmsd</i> | 43.48 | 11.84 | 75.11 | . | 48.96 | 162.14 | 12.73 | 28.92 | 52.55 | 23.63 | . | -1.58 | . | 7.35 | 1.23 | . |
| | Walk delta P | 86.46 | 66.29 | 106.63 | 86.81 | 89.60 | 160.63 | 12.67 | 68.45 | 98.20 | 29.75 | 22.38 | -1.36 | 2.57 | 6.34 | 1.01 | 2.62 |
| | Trot delta P | 124.60 | 97.80 | 151.39 | 124.64 | 124.96 | 283.56 | 16.84 | 105.71 | 142.75 | 37.04 | 32.31 | -0.08 | -3.16 | 8.42 | 1.01 | 2.62 |
| | Left canter delta P | 136.84 | 44.70 | 228.97 | . | 143.44 | 1375.56 | 37.09 | 96.89 | 170.18 | 73.29 | . | -0.78 | . | 21.41 | 1.23 | . |
| | Walk pitch ROM | 9.61 | 3.63 | 15.59 | 9.64 | 9.87 | 14.12 | 3.76 | 5.76 | 12.95 | 7.19 | 6.82 | -0.09 | -5.43 | 1.88 | 1.01 | 2.62 |
| | Trot pitch ROM | 10.72 | 2.24 | 19.20 | 10.52 | 8.96 | 28.40 | 5.33 | 6.65 | 18.30 | 11.65 | 9.53 | 1.46 | 1.80 | 2.66 | 1.01 | 2.62 |
| | Left canter pitch ROM | 19.12 | 5.67 | 32.58 | . | 18.96 | 29.34 | 5.42 | 13.79 | 24.62 | 10.83 | . | 0.14 | . | 3.13 | 1.23 | . |
| | Walk pelvis residual | 3.26 | 0.59 | 5.93 | 3.18 | 2.59 | 2.82 | 1.68 | 2.15 | 5.70 | 3.55 | 2.88 | 1.67 | 2.68 | 0.84 | 1.01 | 2.62 |
| | Trot pelvis residual | 2.59 | 1.73 | 3.44 | 2.59 | 2.64 | 0.29 | 0.54 | 1.97 | 3.09 | 1.12 | 1.01 | -0.28 | -4.04 | 0.27 | 1.01 | 2.62 |
| | Left canter pelvis residual | 3.69 | 0.91 | 6.48 | . | 3.17 | 1.26 | 1.12 | 2.93 | 4.98 | 2.05 | . | 1.64 | . | 0.65 | 1.23 | . |
| Trouser-affixed markers | Walk Left PSIS <i>rmsd</i> | 22.31 | 1.43 | 43.18 | 22.79 | 26.67 | 172.13 | 13.12 | 3.25 | 32.63 | 29.38 | 23.07 | -1.64 | 2.81 | 6.56 | 1.01 | 2.62 |
| | Walk Right PSIS <i>rmsd</i> | 30.82 | 21.13 | 40.51 | 30.74 | 30.12 | 37.10 | 6.09 | 24.30 | 38.75 | 14.45 | 11.62 | 0.62 | 0.51 | 3.05 | 1.01 | 2.62 |
| | Walk Left ASIS <i>rmsd</i> | 31.26 | 23.48 | 39.03 | 31.14 | 30.20 | 23.86 | 4.88 | 26.69 | 37.95 | 11.26 | 9.12 | 1.09 | 0.99 | 2.44 | 1.01 | 2.62 |
| | Walk Right ASIS <i>rmsd</i> | 31.35 | 23.54 | 39.15 | 31.24 | 30.39 | 24.04 | 4.90 | 26.51 | 38.09 | 11.58 | 9.10 | 1.06 | 1.66 | 2.45 | 1.01 | 2.62 |
| | Trot Left PSIS <i>rmsd</i> | 39.29 | 37.49 | 41.09 | 39.29 | 39.31 | 1.28 | 1.13 | 37.89 | 40.65 | 2.76 | 2.14 | -0.10 | 1.20 | 0.57 | 1.01 | 2.62 |
| | Trot Right PSIS <i>rmsd</i> | 38.19 | 35.44 | 40.94 | 38.24 | 38.64 | 2.99 | 1.73 | 35.93 | 39.56 | 3.63 | 3.17 | -0.87 | -1.23 | 0.86 | 1.01 | 2.62 |
| | Trot Left ASIS <i>rmsd</i> | 43.88 | 38.36 | 49.39 | 43.92 | 44.24 | 12.00 | 3.46 | 39.50 | 47.53 | 8.03 | 6.66 | -0.50 | -0.71 | 1.73 | 1.01 | 2.62 |
| | Trot Right ASIS <i>rmsd</i> | 40.81 | 33.97 | 47.64 | 40.88 | 41.47 | 18.47 | 4.30 | 35.35 | 44.93 | 9.58 | 8.17 | -0.64 | -1.52 | 2.15 | 1.01 | 2.62 |
| | Left canter Left PSIS <i>rmsd</i> | 45.53 | 34.84 | 56.23 | 45.56 | 45.80 | 45.19 | 6.72 | 37.91 | 52.62 | 14.71 | 12.87 | -0.14 | -3.25 | 3.36 | 1.01 | 2.62 |
| | Left canter Right PSIS <i>rmsd</i> | 45.20 | 34.30 | 56.09 | 45.18 | 45.09 | 46.86 | 6.85 | 37.92 | 52.69 | 14.77 | 13.06 | 0.05 | -3.70 | 3.42 | 1.01 | 2.62 |
| | Left canter Left ASIS <i>rmsd</i> | 42.34 | 35.01 | 49.66 | 42.27 | 41.76 | 21.22 | 4.61 | 37.81 | 48.01 | 10.20 | 8.78 | 0.49 | -2.17 | 2.30 | 1.01 | 2.62 |
| | Left canter Right ASIS <i>rmsd</i> | 40.18 | 34.37 | 45.99 | 40.06 | 39.14 | 13.33 | 3.65 | 37.36 | 45.09 | 7.73 | 6.65 | 1.04 | -0.35 | 1.83 | 1.01 | 2.62 |
| | Walk delta P | 105.98 | 70.76 | 141.19 | 105.74 | 103.82 | 489.74 | 22.13 | 84.61 | 131.65 | 47.04 | 41.84 | 0.30 | -3.61 | 11.07 | 1.01 | 2.62 |
| | Trot delta P | 129.28 | 99.09 | 159.46 | 129.29 | 129.44 | 359.96 | 18.97 | 105.98 | 152.24 | 46.26 | 35.80 | -0.05 | 1.23 | 9.49 | 1.01 | 2.62 |
| | Left canter delta P | 127.18 | 111.37 | 142.98 | 126.99 | 125.53 | 98.67 | 9.93 | 116.99 | 140.67 | 23.68 | 18.53 | 0.93 | 1.57 | 4.97 | 1.01 | 2.62 |
| | Walk pitch ROM | 5.76 | 3.36 | 8.15 | 5.70 | 5.23 | 2.26 | 1.50 | 4.63 | 7.93 | 3.30 | 2.65 | 1.60 | 2.47 | 0.75 | 1.01 | 2.62 |
| | Trot pitch ROM | 9.19 | 6.77 | 11.60 | 9.23 | 9.57 | 2.31 | 1.52 | 7.03 | 10.58 | 3.55 | 2.74 | -1.36 | 2.41 | 0.76 | 1.01 | 2.62 |
| | Left canter pitch ROM | 11.72 | 7.14 | 16.30 | 11.71 | 11.68 | 8.29 | 2.88 | 8.60 | 14.92 | 6.32 | 5.52 | 0.05 | -3.24 | 1.44 | 1.01 | 2.62 |
| | Walk pelvis residual | 4.95 | -1.86 | 11.77 | 4.73 | 2.93 | 18.34 | 4.28 | 2.58 | 11.37 | 8.79 | 6.63 | 1.99 | 3.97 | 2.14 | 1.01 | 2.62 |
| | Trot pelvis residual | 4.78 | -3.24 | 12.80 | 4.54 | 2.61 | 25.40 | 5.04 | 1.61 | 12.31 | 10.70 | 8.04 | 1.95 | 3.84 | 2.52 | 1.01 | 2.62 |
| | Left canter pelvis residual | 7.29 | -1.73 | 16.31 | 7.05 | 5.11 | 32.15 | 5.67 | 3.34 | 15.62 | 12.28 | 9.70 | 1.76 | 3.13 | 2.83 | 1.01 | 2.62 |

Legend: ASIS: anterior superior iliac spine, PSIS: posterior superior iliac spine, *rmsd*: root mean square amplitude, ROM: range of motion. ROM reported in degrees, *rmsd* and delta P reported in millimetres.

C1.1.2 Normality tests

Table C1.2. Results of Shapiro-Wilk normality test for skin-affixed and trouser-affixed variables.

| | group | Shapiro-Wilk | | |
|------------------------------------|---------|--------------|----|-------|
| | | Statistic | df | Sig. |
| Walk Left PSIS <i>rmsd</i> | skin | 0.984 | 3 | 0.756 |
| | trouser | 0.844 | 4 | 0.208 |
| Walk Right PSIS <i>rmsd</i> | skin | 0.850 | 3 | 0.242 |
| | trouser | 0.982 | 4 | 0.912 |
| Walk Left ASIS <i>rmsd</i> | skin | 0.857 | 3 | 0.258 |
| | trouser | 0.937 | 4 | 0.636 |
| Walk Right ASIS <i>rmsd</i> | skin | 0.842 | 3 | 0.218 |
| | trouser | 0.941 | 4 | 0.661 |
| Trot Left PSIS <i>rmsd</i> | skin | 0.904 | 3 | 0.399 |
| | trouser | 0.981 | 4 | 0.909 |
| Trot Right PSIS <i>rmsd</i> | skin | 0.866 | 3 | 0.284 |
| | trouser | 0.868 | 4 | 0.290 |
| Trot Left ASIS <i>rmsd</i> | skin | 0.835 | 3 | 0.202 |
| | trouser | 0.981 | 4 | 0.907 |
| Trot Right ASIS <i>rmsd</i> | skin | 0.813 | 3 | 0.146 |
| | trouser | 0.946 | 4 | 0.689 |
| Left canter Left PSIS <i>rmsd</i> | skin | | | |
| | trouser | 0.948 | 4 | 0.701 |
| Left canter Right PSIS <i>rmsd</i> | skin | | | |
| | trouser | 0.936 | 4 | 0.630 |
| Left canter Left ASIS <i>rmsd</i> | skin | | | |
| | trouser | 0.947 | 4 | 0.700 |
| Left canter Right ASIS <i>rmsd</i> | skin | | | |
| | trouser | 0.864 | 4 | 0.273 |
| Walk delta P | skin | 0.759 | 3 | 0.020 |
| | trouser | 0.916 | 4 | 0.517 |
| Trot delta P | skin | 0.961 | 3 | 0.619 |
| | trouser | 0.980 | 4 | 0.901 |
| Left Canter delta P | skin | 0.976 | 3 | 0.704 |
| | trouser | 0.952 | 4 | 0.727 |
| Walk Pitch ROM | skin | 0.877 | 3 | 0.315 |
| | trouser | 0.837 | 4 | 0.187 |
| Trot Pitch ROM | skin | 0.797 | 3 | 0.107 |
| | trouser | 0.896 | 4 | 0.412 |
| Left Canter Pitch ROM | skin | 0.999 | 3 | 0.950 |
| | trouser | 0.951 | 4 | 0.723 |
| Walk Pelvis Residual | skin | 0.920 | 3 | 0.453 |
| | trouser | 0.669 | 4 | 0.005 |
| Trot Pelvis Residual | skin | 0.947 | 3 | 0.555 |
| | trouser | 0.711 | 4 | 0.016 |
| Left Canter Pelvis Residual | skin | 0.836 | 3 | 0.205 |
| | trouser | 0.796 | 4 | 0.096 |

Legend: ASIS: anterior superior iliac spine, PSIS: posterior superior iliac spine, *rmsd*: root mean square amplitude, ROM: range of motion, df: degrees of freedom, sig: statistical significance

The significance level is .050.

C1.1.3 Mann-Whitney U test outputs

Table C1.2. Results of Mann-Whitney U test outputs for *rmsd* variables.

| Null Hypothesis | U | Sig. | Decision |
|---|-------|-------|-----------------------------|
| The distribution of Walk Left PSIS <i>rmsd</i> is the same across categories of skin and trouser. | 6.00 | 0.686 | Retain the null hypothesis. |
| The distribution of Walk Right PSIS <i>rmsd</i> is the same across categories of skin and trouser. | 11.00 | 0.486 | Retain the null hypothesis. |
| The distribution of Walk Left ASIS <i>rmsd</i> is the same across categories of skin and trouser. | 9.00 | 1.000 | Retain the null hypothesis. |
| The distribution of Walk Right ASIS <i>rmsd</i> is the same across categories of skin and trouser. | 9.00 | 1.000 | Retain the null hypothesis. |
| The distribution of Trot Left PSIS <i>rmsd</i> is the same across categories of skin and trouser. | 4.00 | 0.343 | Retain the null hypothesis. |
| The distribution of Trot Right PSIS <i>rmsd</i> is the same across categories of skin and trouser. | 8.00 | 1.000 | Retain the null hypothesis. |
| The distribution of Trot Left ASIS <i>rmsd</i> is the same across categories of skin and trouser. | 15.00 | 0.057 | Retain the null hypothesis. |
| The distribution of Trot Right ASIS <i>rmsd</i> is the same across categories of skin and trouser. | 7.00 | 0.886 | Retain the null hypothesis. |
| The distribution of Left canter Left PSIS <i>rmsd</i> is the same across categories of skin and trouser. | 6.00 | 1.000 | Retain the null hypothesis. |
| The distribution of Left canter Right PSIS <i>rmsd</i> is the same across categories of skin and trouser. | 8.00 | 0.629 | Retain the null hypothesis. |
| The distribution of Left canter Left ASIS <i>rmsd</i> is the same across categories of skin and trouser. | 4.00 | 0.629 | Retain the null hypothesis. |
| The distribution of Left canter Right ASIS <i>rmsd</i> is the same across categories of skin and trouser. | 4.00 | 0.629 | Retain the null hypothesis. |

Legend: ASIS: anterior superior iliac spine, PSIS: posterior superior iliac spine, *rmsd*: root mean square amplitude, U: Mann-Whitney U statistic, Sig: statistical significance. Statistical significance set at $p < 0.05$.

Table C1.3. Results of Mann-Whitney U test outputs for delta P in walk, trot and left canter.

| Null Hypothesis | U | Sig. | Decision |
|--|-------|-------|-----------------------------|
| The distribution of Walk Delta P is the same across categories of skin and trouser. | 12.00 | 0.343 | Retain the null hypothesis. |
| The distribution of Trot Delta P is the same across categories of skin and trouser. | 9.00 | 1.00 | Retain the null hypothesis. |
| The distribution of Left Canter Delta P is the same across categories of skin and trouser. | 4.00 | 0.629 | Retain the null hypothesis. |

Legend: U: Mann-Whitney U statistic, Sig: statistical significance. Statistical significance set at $p < 0.05$.

Table C1.4. Results of Mann-Whitney U test outputs for pelvis residual in walk, trot and left canter.

| Null Hypothesis | U | Sig. | Decision |
|--|-------|-------|-----------------------------|
| The distribution of Walk Pelvis Residual is the same across categories of skin and trouser. | 10.00 | 0.686 | Retain the null hypothesis. |
| The distribution of Trot Pelvis Residual is the same across categories of skin and trouser. | 8.00 | 1.00 | Retain the null hypothesis. |
| The distribution of Left Canter Pelvis Residual is the same across categories of skin and trouser. | 10.00 | 0.229 | Retain the null hypothesis. |

Legend: U: Mann-Whitney U statistic, Sig: statistical significance. Statistical significance set at $p < 0.05$.

C1.1.4 Spearman's Correlation Test outputs

Table C1.5. Results of the Spearman's Correlation Test between the *rmsd* variables and body mass index.

| Variable | Body Mass Index | |
|--------------------------------|-------------------------|-----------------|
| | Correlation Coefficient | Sig. (2-tailed) |
| Walk L PSIS <i>rmsd</i> | -0.33 | 0.42 |
| Walk R PSIS <i>rmsd</i> | 0.19 | 0.65 |
| Walk L ASIS <i>rmsd</i> | 0.29 | 0.49 |
| Walk R ASIS <i>rmsd</i> | 0.45 | 0.26 |
| Trot L PSIS <i>rmsd</i> | -0.41 | 0.32 |
| Trot R PSIS <i>rmsd</i> | -0.43 | 0.29 |
| Trot L ASIS <i>rmsd</i> | 0.07 | 0.87 |
| Trot R ASIS <i>rmsd</i> | -0.07 | 0.87 |
| Left canter L PSIS <i>rmsd</i> | 0.32 | 0.48 |
| Left canter R PSIS <i>rmsd</i> | 0.50 | 0.25 |
| Left canter L ASIS <i>rmsd</i> | 0.50 | 0.25 |
| Left canter R ASIS <i>rmsd</i> | -0.43 | 0.34 |

Legend: ASIS: anterior superior iliac spine, PSIS: posterior superior iliac spine, *rmsd*: root mean square amplitude, Sig: statistical significance.

C1.2 Section 4.3

C1.2.1 Descriptive statistics

Table C1.6. Descriptive statistics for the circular mean of the simulator-pelvis and simulator-trunk continuous relative phase, and the simulator-pelvis and simulator-trunk discrete relative phase. Data given in degrees.

| | Statistic | | | | | | | | | | | | | Std. Error | | |
|----------------------|----------------------------------|-------------|-------------|-----------------|--------|----------|----------------|---------|---------|--------|---------------------|----------|----------|------------|----------|----------|
| | 95% Confidence Interval for Mean | | | 5% Trimmed Mean | Median | Variance | Std. Deviation | Minimum | Maximum | Range | Interquartile Range | Skewness | Kurtosis | Mean | Skewness | Kurtosis |
| | Mean | Lower Bound | Upper Bound | | | | | | | | | | | | | |
| Simulator-pelvis CRP | 10.79 | 9.23 | 12.34 | 10.56 | 10.29 | 16.07 | 4.01 | 5.52 | 20.75 | 15.23 | 5.90 | 0.80 | -0.06 | 0.76 | 0.44 | 0.86 |
| Simulator-trunk CRP | 21.89 | 17.43 | 26.36 | 21.15 | 17.95 | 132.48 | 11.51 | 5.68 | 53.12 | 47.44 | 12.76 | 1.17 | 0.94 | 2.18 | 0.44 | 0.86 |
| Simulator-pelvis DRP | 5.55 | 4.28 | 6.82 | 5.22 | 4.77 | 10.70 | 3.27 | 1.86 | 15.94 | 14.08 | 3.63 | 1.69 | 3.02 | 0.62 | 0.44 | 0.86 |
| Simulator-trunk DRP | 20.68 | 11.41 | 29.95 | 17.44 | 13.54 | 571.59 | 23.91 | 2.28 | 102.43 | 100.15 | 20.06 | 2.30 | 5.50 | 4.52 | 0.44 | 0.86 |

Legend: CRP: continuous relative phase, DRP: discrete relative phase.

C1.2.2 Normality tests

Table C1.7. Shapiro-Wilk tests for the circular mean of the simulator-pelvis and simulator-trunk continuous relative phase, and the simulator-pelvis and simulator-trunk discrete relative phase.

| | Statistic | df | Sig. |
|----------------------|-----------|-------|-------|
| Simulator-pelvis CRP | 0.926 | 28.00 | 0.049 |
| Simulator-trunk CRP | 0.892 | 28.00 | 0.007 |
| Simulator-pelvis DRP | 0.834 | 28.00 | 0.000 |
| Simulator-trunk DRP | 0.707 | 28.00 | 0.000 |

Legend: CRP: continuous relative phase, DRP: discrete relative phase, df: degrees of freedom, Sig: statistical significance.

C1.2.3 Pearson's correlation test outputs

Table C1.8. Pearson's correlation coefficients and statistical significance for the relationship between the circular mean of the simulator-pelvis and simulator-trunk continuous relative phase, and the simulator-pelvis and simulator-trunk discrete relative phase.

| | | Simulator- pelvis CRP | Simulator- pelvis DRP | Simulator- trunk CRP | Simulator- trunk DRP |
|----------------------|---------------------|--------------------------|--------------------------|-------------------------|-------------------------|
| Simulator-pelvis CRP | Pearson Correlation | 1.00 | | | |
| | Sig. (2-tailed) | - | | | |
| Simulator-pelvis DRP | Pearson Correlation | 0.194 | | | |
| | Sig. (2-tailed) | 0.322 | | | |
| Simulator-trunk CRP | Pearson Correlation | -0.166 | 0.283 | | |
| | Sig. (2-tailed) | 0.398 | 0.145 | | |
| Simulator-trunk DRP | Pearson Correlation | -0.010 | 0.308 | 0.611 | 1.00 |
| | Sig. (2-tailed) | 0.962 | 0.111 | 0.001 | - |

Legend: CRP: continuous relative phase, DRP: discrete relative phase, Sig: statistical significance.

C1.2.4 Paired t-test outputs

Table C1.8. Results of the paired *t*-tests between the circular mean of the continuous relative phase and discrete relative phase for the simulator-pelvis and simulator-trunk couplings.

| | | | | 95% Confidence Interval of the Difference | | | | |
|--|------|-------------------|--------------------|--|-------|----------|----|-----------------|
| | Mean | Std. Deviation | Std. Error Mean | Lower | Upper | <i>t</i> | df | Sig. (2-tailed) |
| Simulator-pelvis CRP Simulator-pelvis DRP | 5.27 | 4.66 | 0.88 | 3.43 | 7.04 | 5.95 | 27 | 0.000002 |
| Simulator-trunk CRP Simulator-trunk DRP | 1.21 | 19.17 | 3.62 | -6.22 | 8.65 | 0.34 | 27 | 0.74 |

Legend: CRP: continuous relative phase, DRP: discrete relative phase, *t*: *t*-statistic, Sig: statistical significance.

C2 – Chapter 5

C2.1 Descriptive statistics

Table C2.1. Descriptive statistics for the 35 riders' static and dynamic pelvic posture and pelvis pitch in simulated walk, trot, left canter, and right canter. Data given in degrees.

| | Statistic | | | | | | | | | | | | | Std. Error | | |
|-------------------|----------------------------------|-------------|-------------|------------------|--------|----------|----------------|---------|---------|--------|---------------------|----------|----------|------------|----------|----------|
| | 95% Confidence Interval for Mean | | | % Trimmed Median | Median | Variance | Std. Deviation | Minimum | Maximum | Range | Interquartile Range | Skewness | Kurtosis | Mean | Skewness | Kurtosis |
| | Mean | Lower Bound | Upper Bound | | | | | | | | | | | | | |
| Halt | -0.129 | -1.814 | 1.555 | -0.044 | 0.050 | 24.042 | 4.903 | -13.760 | 11.000 | 24.760 | 5.600 | -0.277 | 0.068 | 0.829 | 0.398 | 0.778 |
| Walk mean | -0.013 | -1.138 | 1.112 | -0.160 | -0.151 | 10.727 | 3.275 | -6.990 | 8.590 | 15.580 | 2.770 | 0.906 | 0.553 | 0.554 | 0.398 | 0.778 |
| Trot mean | 1.469 | 0.336 | 2.602 | 1.398 | 1.469 | 10.878 | 3.298 | -3.850 | 8.760 | 12.610 | 4.580 | 0.058 | -0.591 | 0.558 | 0.398 | 0.778 |
| Left canter mean | 1.803 | 0.497 | 3.110 | 1.618 | 1.809 | 14.468 | 3.804 | -4.360 | 13.530 | 17.890 | 4.530 | 0.818 | 0.407 | 0.643 | 0.398 | 0.778 |
| Right canter mean | 2.174 | 0.941 | 3.406 | 2.022 | 1.653 | 12.874 | 3.588 | -4.880 | 13.820 | 18.700 | 3.260 | 0.910 | 0.468 | 0.606 | 0.398 | 0.778 |
| Walk min | -2.850 | -3.776 | -1.924 | -2.940 | -2.998 | 7.261 | 2.695 | -8.240 | 5.530 | 13.770 | 2.910 | 0.468 | 1.906 | 0.455 | 0.398 | 0.778 |
| Walk max | 1.674 | 0.609 | 2.740 | 1.502 | 1.600 | 9.620 | 3.102 | -4.800 | 10.900 | 15.700 | 2.200 | 1.209 | 3.530 | 0.524 | 0.398 | 0.778 |
| Walk ROM | 4.534 | 3.989 | 5.079 | 4.452 | 4.200 | 2.516 | 1.586 | 1.900 | 9.000 | 7.100 | 2.500 | 0.835 | 0.472 | 0.268 | 0.398 | 0.778 |
| Trot min | -2.678 | -3.807 | -1.550 | -2.501 | -2.600 | 10.788 | 3.284 | -13.900 | 3.000 | 16.900 | 3.200 | -1.042 | 2.881 | 0.555 | 0.398 | 0.778 |
| Trot max | 4.577 | 3.582 | 5.572 | 4.615 | 5.100 | 8.392 | 2.897 | -0.900 | 9.200 | 10.100 | 4.000 | -0.263 | -0.744 | 0.490 | 0.398 | 0.778 |
| Trot ROM | 7.249 | 6.530 | 7.967 | 7.118 | 6.900 | 4.378 | 2.092 | 4.200 | 13.000 | 8.800 | 2.000 | 1.062 | 1.204 | 0.354 | 0.398 | 0.778 |
| Left canter min | -4.129 | -5.125 | -3.134 | -4.021 | -3.554 | 8.400 | 2.898 | -11.300 | 0.480 | 11.780 | 4.210 | -0.593 | -0.198 | 0.490 | 0.398 | 0.778 |
| Left canter max | 5.059 | 3.842 | 6.276 | 4.984 | 3.998 | 12.549 | 3.542 | -2.090 | 13.130 | 15.220 | 3.960 | 0.495 | 0.223 | 0.599 | 0.398 | 0.778 |
| Left canter ROM | 9.188 | 8.125 | 10.251 | 9.081 | 9.454 | 9.575 | 3.094 | 3.900 | 16.710 | 12.810 | 4.570 | 0.474 | -0.184 | 0.523 | 0.398 | 0.778 |
| Right canter min | -3.474 | -4.354 | -2.594 | -3.443 | -3.338 | 6.562 | 2.562 | -9.180 | 1.060 | 10.240 | 3.810 | -0.177 | -0.488 | 0.433 | 0.398 | 0.778 |
| Right canter max | 5.753 | 4.560 | 6.946 | 5.696 | 5.134 | 12.058 | 3.472 | -1.910 | 14.280 | 16.190 | 3.940 | 0.518 | 0.313 | 0.587 | 0.398 | 0.778 |
| Right canter ROM | 9.228 | 8.239 | 10.216 | 9.144 | 9.290 | 8.280 | 2.878 | 4.620 | 15.350 | 10.720 | 3.570 | 0.465 | -0.224 | 0.486 | 0.398 | 0.778 |

Legend: Min: minimum, Max: maximum, ROM: range of motion.

C2.2 Normality tests

Table C2.2. Results of the Shapiro-Wilk normality test and Levene's Test for homogeneity of variances on the pelvic pitch variables.

| | Shapiro-Wilk | | | Levene's Test | | | |
|-------------------------|--------------|----|-------|---------------|-----|-----|-------|
| | Statistic | df | Sig. | Statistic | df1 | df2 | Sig. |
| Halt posture | 0.931 | 35 | 0.052 | 0.685 | 2 | 32 | 0.511 |
| Mean walk pitch | 0.914 | 35 | 0.009 | 0.444 | 2 | 32 | 0.645 |
| Mean trot pitch | 0.917 | 35 | 0.046 | 0.756 | 2 | 32 | 0.478 |
| Mean left canter pitch | 0.953 | 35 | 0.014 | 1.239 | 2 | 32 | 0.303 |
| Mean right canter pitch | 0.941 | 35 | 0.054 | 1.843 | 2 | 32 | 0.175 |
| Walk min | 0.954 | 35 | 0.152 | | | | |
| Walk max | 0.861 | 35 | 0.408 | | | | |
| Walk ROM | 0.940 | 35 | 0.558 | | | | |
| Trot min | 0.931 | 35 | 0.060 | | | | |
| Trot max | 0.960 | 35 | 0.236 | | | | |
| Trot ROM | 0.983 | 35 | 0.127 | | | | |
| Left canter min | 0.962 | 35 | 0.257 | | | | |
| Left canter max | 0.958 | 35 | 0.199 | | | | |
| Left Canter ROM | 0.965 | 35 | 0.318 | | | | |
| Right canter min | 0.982 | 35 | 0.818 | | | | |
| Right canter max | 0.951 | 35 | 0.120 | | | | |
| Right canter ROM | 0.955 | 35 | 0.166 | | | | |

Legend: Min: minimum, Max: maximum, ROM: range of motion, df: degrees of freedom, sig: statistical significance.

C2.3 ANOVA output

Table C2.3. Results of the one-way ANOVA on the pelvic pitch variables.

| | | Test of Within Subject Effects | | | | | |
|--------------|-------------|--------------------------------|--------|-------------|-------|-------|---------------------|
| | | Type III Sum of Squares | df | Mean Square | F | Sig. | Partial Eta Squared |
| Gait | Huynh-Feldt | 157.100 | 1.890 | 83.138 | 4.500 | 0.017 | 0.123 |
| Gait*Level | Huynh-Feldt | 100.719 | 3.779 | 26.651 | 1.443 | 0.233 | 0.083 |
| Error (gait) | Huynh-Feldt | 1117.045 | 60.468 | 18.473 | | | |

Legend: df: degrees of freedom, F: F-statistic, Sig: Significance.

C2.3.1 Post-hoc t-tests

Table C2.4. Results of the Bonferroni-corrected post-hoc t-tests on the pelvic pitch variables.

| | | | | 95% Confidence Interval for Difference | | |
|--------------|-----------------|------------|-------|--|-------------|--------|
| | Mean Difference | Std. Error | Sig. | Lower Bound | Upper Bound | |
| Halt | Walk | -0.405 | 0.848 | 1.000 | -2.963 | 2.153 |
| | Trot | -1.870 | 0.958 | 0.597 | -4.758 | 1.018 |
| | Left Canter | -2.094 | 1.084 | 0.623 | -5.363 | 1.175 |
| | Right Canter | -2.415 | 0.984 | 0.198 | -5.383 | 0.553 |
| Walk | Halt | 0.405 | 0.848 | 1.000 | -2.153 | 2.963 |
| | Trot | -1.465 | 0.471 | 0.039 | -2.886 | -0.044 |
| | Left Canter | -1.689 | 0.487 | 0.015 | -3.157 | -0.222 |
| | Right Canter | -2.010 | 0.462 | 0.001 | -3.404 | -0.616 |
| Trot | Halt | 1.870 | 0.958 | 0.597 | -1.018 | 4.758 |
| | Walk | 1.465 | 0.471 | 0.039 | 0.044 | 2.886 |
| | Left Canter | -0.224 | 0.548 | 1.000 | -1.876 | 1.428 |
| | Right Canter | -0.545 | 0.607 | 1.000 | -2.375 | 1.285 |
| Left Canter | Halt | 2.094 | 1.084 | 0.623 | -1.175 | 5.363 |
| | Walk | 1.689 | 0.487 | 0.015 | 0.222 | 3.157 |
| | Trot | 0.224 | 0.548 | 1.000 | -1.428 | 1.876 |
| | Right Canter | -0.321 | 0.298 | 1.000 | -1.218 | 0.576 |
| Right Canter | Halt | 2.415 | 0.984 | 0.198 | -0.553 | 5.383 |
| | Walk | 2.010 | 0.462 | 0.001 | 0.616 | 3.404 |
| | Trot | 0.545 | 0.607 | 1.000 | -1.285 | 2.375 |
| | Left Canter | 0.321 | 0.298 | 1.000 | -0.576 | 1.218 |

Legend: Sig: Significance.

C2.4 Kruskal-Wallis test outputs

C2.4.1 Range of motion

Table C2.5. Results of the Kruskal-Wallis test outputs to compare halt posture categorised as anterior, neutral or posterior with the pelvic pitching range of motion.

| Null Hypothesis | Test statistic | Sig. | Decision |
|---|----------------|-------|-----------------------------|
| The distribution of Walk ROM is the same across categories of Halt Posture. | 5.09 | 0.085 | Retain the null hypothesis. |
| The distribution of Trot ROM is the same across categories of Halt Posture. | 5.16 | 0.572 | Retain the null hypothesis. |
| The distribution of Left canter ROM is the same across categories of Halt Posture. | 8.71 | 0.397 | Retain the null hypothesis. |
| The distribution of Right canter ROM is the same across categories of Halt Posture. | 2.93 | 0.557 | Retain the null hypothesis. |

Legend: U: Mann-Whitney U statistic, Sig: statistical significance. Statistical significance set at $p < 0.05$.

C2.4.2 Minimum pelvic tilt

Table C2.6. Results of the Kruskal-Wallis test outputs to compare halt posture categorised as anterior, neutral or posterior with the minimum pelvic pitch.

| Null Hypothesis | Test statistic | Sig. | Decision |
|---|----------------|-------|-----------------------------|
| The distribution of Walk ROM is the same across categories of Halt Posture. | 8.110 | 0.085 | Retain the null hypothesis. |
| The distribution of Trot ROM is the same across categories of Halt Posture. | 5.162 | 0.572 | Retain the null hypothesis. |
| The distribution of Left canter ROM is the same across categories of Halt Posture. | 8.713 | 0.397 | Retain the null hypothesis. |
| The distribution of Right canter ROM is the same across categories of Halt Posture. | 2.925 | 0.557 | Retain the null hypothesis. |

Legend: U: Mann-Whitney U statistic, Sig: statistical significance. Statistical significance set at $p < 0.05$.

C2.4.3 Maximum pelvic tilt

Table C2.6. Results of the Kruskal-Wallis test outputs to compare minimum and maximum pelvic tilt across the categories of competition level.

| Null Hypothesis | Test statistic | Sig. | Decision |
|--|----------------|-------|-----------------------------|
| The distribution of Walk minimum is the same across categories of competition level. | 2.516 | 0.284 | Retain the null hypothesis. |
| The distribution of Walk maximum is the same across categories of competition level. | 4.116 | 0.128 | Retain the null hypothesis. |
| The distribution of Trot minimum is the same across categories of competition level. | 0.141 | 0.932 | Retain the null hypothesis. |
| The distribution of Trot maximum is the same across categories of competition level. | 1.503 | 0.472 | Retain the null hypothesis. |
| The distribution of Left canter minimum is the same across categories of competition level. | 0.509 | 0.775 | Retain the null hypothesis |
| The distribution of Left canter maximum is the same across categories of competition level. | 1.753 | 0.416 | Retain the null hypothesis |
| The distribution of Right canter minimum is the same across categories of competition level. | 0.799 | 0.671 | Retain the null hypothesis |
| The distribution of Right canter maximum is the same across categories of competition level. | 8.108 | 0.017 | Reject the null hypothesis |

Legend: Sig: statistical significance. Statistical significance set at $p < 0.05$

Table C2.7. Results of the Bonferroni-corrected pairwise comparison of the competition level categories on the maximum pelvic tilt value in right canter.

| Pairwise comparison | Test Statistic | Std. Error | Std. Test Statistic | Sig. | Adj. Sig |
|-----------------------|----------------|------------|---------------------|-------|----------|
| Advanced-Intermediate | 0.711 | 4.32 | 0.165 | 0.869 | 1.00 |
| Advanced-Novice | 11.051 | 4.606 | 2.399 | 0.016 | 0.049 |
| Intermediate-Novice | 10.339 | 4.068 | 2.542 | 0.011 | 0.033 |

Legend: Sig: statistical significance. Adj. Sig: Bonferroni adjusted significance for multiple comparisons.

C2.5 Correlation test outputs

C2.5.1 Halt posture – mean pelvic tilt

Table C2.8. Results of the Pearson’s Product Moment test for correlation between the halt pelvic posture and the mean pelvic pitch in simulated medium walk, trot, left canter and right canter.

| | | Halt | Mean walk pitch | Mean trot pitch | Mean left canter pitch | Mean right canter pitch |
|-------------------------|---------------------|--------|-----------------|-----------------|------------------------|-------------------------|
| Halt | Pearson Correlation | 1 | | | | |
| | Sig. (2-tailed) | - | | | | |
| Mean walk pitch | Pearson Correlation | 0.253 | 1 | | | |
| | Sig. (2-tailed) | 0.143 | | | | |
| Mean trot pitch | Pearson Correlation | 0.066 | 0.676 | 1 | | |
| | Sig. (2-tailed) | 0.707 | 0.001 | | | |
| Mean left canter pitch | Pearson Correlation | -0.042 | 0.696 | 0.622 | 1 | |
| | Sig. (2-tailed) | 0.812 | 0.001 | 0.001 | | |
| Mean right canter pitch | Pearson Correlation | 0.131 | 0.685 | 0.485 | 0.893 | 1 |
| | Sig. (2-tailed) | 0.453 | 0.001 | 0.003 | 0.001 | - |

Legend: Sig: statistical significance.

C2.5.2 Halt pelvic tilt – range of motion

Table C2.9. Results of the Spearman’s Correlation test for correlation between the halt pelvic tilt and the minimum and maximum pelvic tilt values in each gait.

| | Halt pelvic tilt | |
|----------------------------|-------------------------|-----------------|
| | Correlation Coefficient | Sig. (2-tailed) |
| Walk minimum pitch | 0.00 | 0.983 |
| Walk maximum pitch | -0.10 | 0.582 |
| Trot minimum pitch | -0.06 | 0.745 |
| Trot maximum pitch | 0.05 | 0.778 |
| Left canter minimum pitch | 0.00 | 0.984 |
| Left canter maximum pitch | -0.08 | 0.651 |
| Right canter minimum pitch | -0.27 | 0.125 |
| Right canter maximum pitch | -0.27 | 0.117 |

Legend: Sig: statistical significance.

C2.5.3 Halt pelvic tilt – minimum and maximum pelvic tilt

Table C2.9. Results of the Spearman’s Correlation test for correlation between the halt pelvic tilt and the pelvis range of motion in each gait.

| | Halt pelvic tilt | |
|------------------|-------------------------|-----------------|
| | Correlation Coefficient | Sig. (2-tailed) |
| Walk ROM | -0.30 | 0.085 |
| Trot ROM | -0.10 | 0.572 |
| Left canter ROM | -0.15 | 0.397 |
| Right canter ROM | -0.10 | 0.557 |

Legend: Sig: statistical significance.

C3 – Chapter 7

C3.1 Descriptive statistics

Table C3.1. Descriptive statistics for the first three principal components of the continuous relative phase between the vertical displacement of the riding simulator and the pitch of the rider's pelvis.

| | | Statistic | | | | | | | | | | | | | Std. Error | | |
|---------------|-----|----------------------------------|-------------|-------------|-----------------|--------|----------|----------------|---------|---------|-------|---------------------|----------|----------|------------|----------|----------|
| | | 95% Confidence Interval for Mean | | | 5% Trimmed Mean | Median | Variance | Std. Deviation | Minimum | Maximum | Range | Interquartile Range | Skewness | Kurtosis | Mean | Skewness | Kurtosis |
| | | Mean | Lower bound | Upper bound | | | | | | | | | | | | | |
| Medium trot | PC1 | 0 | -1.01 | 1.01 | 0.14 | 0.96 | 101.92 | 10.10 | -45.01 | 30.25 | 75.26 | 10.95 | -0.56 | 2.92 | 0.51 | 0.12 | 0.25 |
| | PC2 | 0 | -0.39 | 0.39 | 0.00 | -0.33 | 15.62 | 3.95 | -14.09 | 20.48 | 34.57 | 4.44 | 0.29 | 2.16 | 0.20 | 0.12 | 0.25 |
| | PC3 | 0 | -0.35 | 0.35 | -0.04 | -0.09 | 12.59 | 3.55 | -11.00 | 14.50 | 25.50 | 4.58 | 0.19 | 0.97 | 0.18 | 0.12 | 0.25 |
| Extended trot | PC1 | 0 | -0.85 | 0.85 | -0.44 | -0.41 | 71.88 | 8.48 | -25.02 | 30.46 | 55.48 | 8.85 | 0.84 | 2.25 | 0.43 | 0.12 | 0.25 |
| | PC2 | 0 | -0.42 | 0.42 | 0.03 | 0.15 | 18.01 | 4.24 | -13.08 | 11.97 | 25.05 | 5.88 | -0.14 | -0.03 | 0.22 | 0.12 | 0.25 |
| | PC3 | 0 | -0.29 | 0.29 | -0.02 | 0.11 | 8.44 | 2.90 | -7.60 | 9.13 | 16.73 | 3.62 | 0.06 | 0.31 | 0.15 | 0.12 | 0.25 |

Legend: PC: principal component.

C3.2 Normality test

Table C3.2. Results of the Shapiro-Wilk normality test for the first three principal components of the continuous relative phase between the vertical displacement of the riding simulator and the pitch of the rider's pelvis.

| | | Shapiro-Wilk | | |
|---------------|-----|--------------|-----|-------|
| | | Statistic | df | Sig. |
| Medium trot | PC1 | 0.95 | 389 | 0.001 |
| | PC2 | 0.98 | 389 | 0.001 |
| | PC3 | 0.99 | 389 | 0.021 |
| Extended trot | PC1 | 0.94 | 389 | 0.001 |
| | PC2 | 1.00 | 389 | 0.043 |
| | PC3 | 0.99 | 389 | 0.050 |

Legend: PC: principal component, df: degrees of freedom, sig: statistical significance.

C3.3 Linear mixed model output

Table C3.3. Model dimension for the mixed model analyses of principal components in medium and extended trot.

| | | Number of Levels | Covariance Structure | Number of Parameters | Subject Variables |
|----------------|-------------------|------------------|----------------------|----------------------|-------------------|
| Fixed Effects | Intercept | 1 | | 1 | |
| | level | 2 | | 1 | |
| | cycle | 1 | | 1 | |
| | level * cycle | 2 | | 1 | |
| Random Effects | Intercept + cycle | 2 | Identity | 1 | ID |
| Residual | | | | 1 | |
| Total | | 8 | | 6 | |

Table C3.3. Model fit criteria for the mixed model analyses of principal components in medium and extended trot.

| | | Akaike's Information Criterion |
|---------------|-----|--------------------------------|
| Medium trot | PC1 | 2844.33 |
| | PC2 | 2101.88 |
| | PC3 | 1949.29 |
| Extended trot | PC1 | 2599.54 |
| | PC2 | 2072.68 |
| | PC3 | 1729.38 |

Legend: PC: principal component.

Table C3.4. Estimates of fixed effects for the first three principal components in medium and extended trot.

| | | Coefficient | SE | df | t | Sig. | |
|---------------|-----|---------------------|-------|------|--------|-------|-------|
| Medium trot | PC1 | Advanced | 1.64 | 1.63 | 367.99 | 1.01 | 0.314 |
| | | Intermediate | -3.26 | 2.03 | 364.01 | -1.61 | 0.109 |
| | | Cycle: Advanced | -0.18 | 0.36 | 123.17 | -0.51 | 0.613 |
| | | Cycle: Intermediate | 0.40 | 0.44 | 117.27 | 0.90 | 0.368 |
| | PC2 | Advanced | 0.42 | 0.61 | 368.93 | 0.70 | 0.486 |
| | | Intermediate | -0.34 | 0.76 | 367.04 | -0.45 | 0.656 |
| | | Cycle: Advanced | -0.43 | 0.13 | 100.81 | -0.30 | 0.762 |
| | | Cycle: Intermediate | 0.01 | 0.18 | 95.32 | 0.05 | 0.962 |
| | PC3 | Advanced | 0.46 | 0.49 | 375.91 | 0.09 | 0.926 |
| | | Intermediate | -0.13 | 0.61 | 375.29 | -0.21 | 0.834 |
| | | Cycle: Advanced | 0.05 | 0.14 | 65.04 | -0.32 | 0.703 |
| | | Cycle: Intermediate | -0.05 | 0.17 | 61.60 | -0.32 | 0.753 |
| Extended trot | PC1 | Advanced | 0.63 | 1.14 | 378.11 | 0.55 | 0.580 |
| | | Intermediate | 0.34 | 1.42 | 377.80 | 0.24 | 0.811 |
| | | Cycle: Advanced | -0.21 | 0.34 | 46.36 | -0.60 | 0.550 |
| | | Cycle: Intermediate | 0.04 | 0.43 | 44.03 | 0.10 | 0.917 |
| | PC2 | Advanced | 0.11 | 0.57 | 377.12 | 0.19 | 0.846 |
| | | Intermediate | -0.45 | 0.72 | 376.64 | -0.63 | 0.532 |
| | | Cycle: Advanced | 0.07 | 0.16 | 61.67 | 0.40 | 0.692 |
| | | Cycle: Intermediate | -0.05 | 0.21 | 58.49 | -0.26 | 0.793 |
| | PC3 | Advanced | -0.34 | 0.37 | 383.93 | -0.94 | 0.346 |
| | | Intermediate | 0.73 | 0.46 | 384.00 | 1.60 | 0.111 |
| | | Cycle: Advanced | 0.05 | 0.12 | 34.33 | 0.68 | 0.684 |
| | | Cycle: Intermediate | -0.09 | 0.15 | 32.88 | 0.55 | 0.553 |

Legend: PC: principal component, SE: standard error, df: degrees of freedom, t: t-statistic, Sig: statistical significance.

Table C3.4. Parameters of random effects of the cycle on the intercept and cycle by the subject for each model.

| | | | | | | 95% Confidence Interval | |
|---------------|-----|----------|------------|--------|------|-------------------------|-------------|
| | | Estimate | Std. Error | Wald Z | Sig. | Lower Bound | Upper Bound |
| Medium Trot | PC1 | 10.72 | 0.82 | 13.06 | 0.00 | 9.23 | 12.46 |
| | PC2 | 10.72 | 0.82 | 13.06 | 0.00 | 9.23 | 12.46 |
| | PC3 | 6.78 | 0.52 | 12.94 | 0.00 | 5.83 | 7.89 |
| Extended Trot | PC1 | 35.89 | 2.83 | 12.66 | 0.00 | 30.74 | 41.89 |
| | PC2 | 9.27 | 0.72 | 12.92 | 0.00 | 7.97 | 10.79 |
| | PC3 | 3.61 | 0.29 | 12.41 | 0.00 | 3.08 | 4.23 |

Legend: PC: principal component, Sig: statistical significance.

Appendix D: MATLAB script used to calculate CRP

```
function CRP_seg1seg2 = CRP(seg1,seg2,varargin)
%continuous relative phase calculated as per Lamb & Stockl (2014)
%assumption is that data is time and period normalised prior to use

%OUTPUT IS IN RADIANS

%specify number of strides to analyse CRP(seg1,seg2,strides)
%if no stride number specified, will run from the third valid stride

if nargin == 2
    for k = 2:size(seg1,2)
        seg1_h(:,k) = hilbert(seg1(:,k));
        seg2_h(:,k) = hilbert(seg2(:,k));
    end

    for k = 1:size(seg1,2)
        CRP_seg1seg2(:,k) = atan2(((imag(seg1_h(:,k)).*real(seg2_h(:,k)))-
(imag(seg2_h(:,k)).*real(seg1_h(:,k)))), ((real(seg1_h(:,k)).*real(seg2_h(:,
k)))+(imag(seg1_h(:,k)).*imag(seg2_h(:,k)))));
    end

else
    s = varargin{1}+2;
    if s-3 > size(seg1,2)
        error('number of strides specified exceeds max, number of total
strides used')
    end
    for k = 3:(size(seg1,2))
        seg1_h(:,k) = hilbert(seg1(:,k));
        seg2_h(:,k) = hilbert(seg2(:,k));
    end
    for k = 3:(size(seg1,2))
        CRP_seg1seg2(:,k) = atan2(((imag(seg1_h(:,k)).*real(seg2_h(:,k)))-
(imag(seg2_h(:,k)).*real(seg1_h(:,k)))), ((real(seg1_h(:,k)).*real(seg2_h(:,
k)))+(imag(seg1_h(:,k)).*imag(seg2_h(:,k)))));
    end

elseif s-3 < size(seg1,2)
    for k = 3:s
        seg1_h(:,k) = hilbert(seg1(:,k));
        seg2_h(:,k) = hilbert(seg2(:,k));
    end
    for k = 3:s
        CRP_seg1seg2(:,k) = atan2(((imag(seg1_h(:,k)).*real(seg2_h(:,k)))-
(imag(seg2_h(:,k)).*real(seg1_h(:,k)))), ((real(seg1_h(:,k)).*real(seg2_h(:,
k)))+(imag(seg1_h(:,k)).*imag(seg2_h(:,k)))));
    end
end

end
CRP_seg1seg2( :, all(~ CRP_seg1seg2,1) ) = [];
CRP_seg1seg2 = unwrap(CRP_seg1seg2);
end
```

Appendix E: Rider level, assessment rate (% of cycles in the same cluster) and cluster with the greatest assessment rate.

Rider level given as competition level, either British Dressage (BD) or Fédération Internationale Équestre (FEI).

| Rider | Highest competition level | Assessment Rate (%) | | Cluster with greatest assessment rate | |
|-------|---------------------------|---------------------|------------|---------------------------------------|------------|
| | | 3 clusters | 8 clusters | 3 clusters | 8 clusters |
| 1 | BD Novice | 60 | 40 | 1 | 8 |
| 2 | BD Elementary | 50 | 40 | 3 | 8 |
| 3 | BD Medium | 100 | 70 | 1 | 5 |
| 4 | FEI Intermediare I | 100 | 70 | 2 | 4 |
| 5 | BD Medium | 60 | 40 | 2 | 1 |
| 6 | FEI Intermediare I | 90 | 50 | 2 | 2 |
| 7 | BD Elementary | 100 | 100 | 1 | 4 |
| 8 | BD Novice | 72 | 14 | 2 | 1 |
| 9 | BD Novice | 90 | 90 | 3 | 7 |
| 10 | BD Elementary | 86 | 42 | 3 | 7 |
| 11 | BD Preliminary | 86 | 21 | 1 | 5 |
| 12 | FEI Prix St Georges | 70 | 70 | 2 | 6 |
| 13 | BD Elementary | 100 | 80 | 2 | 2 |
| 14 | BD Advanced Medium | 100 | 90 | 2 | 2 |
| 15 | BD Advanced Medium | 50 | 40 | 1 | 5 |
| 16 | BD Advanced | 70 | 60 | 2 | 6 |
| 17 | BD Advanced | 100 | 70 | 2 | 6 |
| 18 | BD Advanced Medium | 100 | 70 | 2 | 4 |
| 19 | BD Novice | 90 | 90 | 1 | 5 |
| 20 | BD Elementary | 90 | 40 | 1 | 6 |
| 21 | BD Advanced Medium | 100 | 100 | 1 | 5 |
| 22 | FEI Grand Prix | 100 | 80 | 2 | 4 |
| 23 | FEI Intermediare II | 100 | 100 | 2 | 2 |
| 24 | BD Advanced Medium | 60 | 40 | 2 | 1 |
| 25 | FEI Intermediare I | 60 | 40 | 1 | 8 |
| 26 | BD Medium | 100 | 70 | 2 | 6 |
| 27 | BD Advanced Medium | 60 | 70 | 2 | 6 |
| 28 | BD Advanced Medium | 60 | 40 | 2 | 5 |
| 29 | FEI Grand Prix | 90 | 60 | 2 | 1 |
| 30 | BD Elementary | 100 | 100 | 3 | 7 |
| 31 | FEI Prix St Georges | 100 | 80 | 2 | 4 |
| 32 | BD Novice | 100 | 70 | 2 | 2 |
| 33 | BD Novice | 100 | 60 | 2 | 4 |
| 34 | BD Advanced Medium | 100 | 60 | 2 | 2 |
| 35 | FEI Grand Prix | 100 | 60 | 2 | 2 |
| 36 | FEI Intermediare I | 100 | 100 | 2 | 2 |
| 37 | FEI Grand Prix | 100 | 50 | 2 | 2 |
| 38 | BD Advanced | 90 | 80 | 2 | 6 |
| 39 | BD Advanced | 100 | 50 | 2 | 2 |
| 40 | BD Medium | 100 | 24 | 2 | 2 |